

University of Alberta

An Investigation of a Pt-Pd Diesel Oxidation Catalyst

by

Milad Khosravi Hafshejani

A thesis submitted to the Faculty of Graduate Studies and Research
in partial fulfillment of the requirements for the degree of

Master of Science

in

Chemical Engineering

Department of Chemical and Materials Engineering

©Milad Khosravi Hafshejani

Spring 2013

Edmonton, Alberta

Permission is hereby granted to the University of Alberta Libraries to reproduce single copies of this thesis and to lend or sell such copies for private, scholarly or scientific research purposes only. Where the thesis is converted to, or otherwise made available in digital form, the University of Alberta will advise potential users of the thesis of these terms.

The author reserves all other publication and other rights in association with the copyright in the thesis and, except as herein before provided, neither the thesis nor any substantial portion thereof may be printed or otherwise reproduced in any material form whatsoever without the author's prior written permission.

*To my beloved mother, hear my thanks and gratitude along
with the flight of angels.*

Abstract

Global kinetic model for a Pt-Pd diesel oxidation catalyst (DOC) is proposed and validated. Experimental data was obtained using different concentrations of the artificial gas mixtures which were passed over a bimetallic catalyst. Previous works of Voltz [1], Pandya [2], Sola [3] and many others were used to propose a new model, which was validated using a MATLAB based solver and optimizer. A reasonable match between the experimental data and predicted values was seen for all experimental conditions except for the runs with CO, H₂, C₃H₆ and NO. Some fundamental observations were made in this case but further investigations are necessary to improve the model.

Acknowledgments

I would like to express my thanks to my supervisor, Prof. R.E. Hayes for his continuous support and understanding throughout my project. Under his supervision, I was given the freedom to pursue my research in my own way and I greatly appreciated that freedom.

My deepest gratitude and thanks go to my wife, Mitra for her support and love during the past few years. The past few years have been difficult and she had stuck by me through everything. Her support and encouragement was in the end what made this dissertation possible.

I would like to express my sincere appreciation and love to father, my brother, Reza and his wife, Fatemeh, whose love and support helped stabilizing my life after my mother death in 2009. To those my dearest friends: Ehsan, Keivan, Ghazaleh, Farshad, Mojtaba, Abolfazl, Javad, M. Tanhaemami, M. Seyydan, Kamran and many others, I shall always remain thankful.

I would like to acknowledge the Department of Chemical and Materials Engineering at University of Alberta for providing research opportunities. Financial support of Auto21 and the Natural Science and Engineering Research Council of Canada (NSERC) is also acknowledged.

I would like to express special thanks to A. Abedi and W. Epling at the University of Waterloo for providing experimental data.

Contents

1	INTRODUCTION	1
1.1	PROBLEM DEFINITION.....	2
1.2	RESEARCH OBJECTIVE	2
1.3	THESIS LAYOUT	2
2	BACKGROUND	3
2.1	AUTOMOTIVE EMISSIONS.....	3
2.2	LEGAL LEVEL OF EMISSIONS	3
2.3	EMISSION CONTROL.....	5
2.3.1	<i>Increasing Fuel Octane Number</i>	5
2.3.2	<i>Reducing Sulphur Content</i>	6
2.3.3	<i>Three Way Catalyst (TWC)</i>	6
2.3.4	<i>Exhaust Gas Recirculation (EGR)</i>	6
2.3.5	<i>Selective Catalytic Reduction (SCR)</i>	7
2.3.5.1	SCR by Ammonia (NH ₃).....	7
2.3.5.2	SCR by Hydrocarbon	8
2.3.6	<i>Diesel Particulate Filter (DPF)</i>	9
2.3.7	<i>Diesel Oxidation Catalyst (DOC)</i>	9
3	EXPERIMENTAL.....	11
3.1	CATALYST	11
3.2	EXPERIMENTAL PROCEDURE.....	12
3.3	EXPERIMENTAL PLAN	12
3.4	EXPERIMENTAL RESULTS.....	13
3.4.1	<i>CO, H₂ Oxidation</i>	13
3.4.2	<i>Propene Oxidation</i>	14
3.4.3	<i>NO Oxidation</i>	15
3.4.4	<i>CO, H₂ and Propene oxidation</i>	16
3.4.5	<i>NO and Propene Oxidation</i>	20
3.4.6	<i>NO and CO oxidation</i>	23
3.4.7	<i>Mixture of CO, H₂, C₃H₆ and NO Oxidation</i>	26
4	MODELLING	42
4.1	REACTOR MODELLING.....	42
4.2	KINETIC FORMULATION.....	45
4.3	PARAMETER ESTIMATION	53

5	RESULTS	57
5.1	MODELLING OF CO OXIDATION.....	57
5.2	MODELLING OF C ₃ H ₆ OXIDATION	60
5.3	MODELLING OF NO OXIDATION	62
5.4	MODELLING OF MIXTURE OF CO, H ₂ & C ₃ H ₆	73
5.5	MODELLING OF MIXTURE OF CO, H ₂ & NO.....	92
5.6	MODELLING OF MIXTURE OF C ₃ H ₆ & NO	131
5.6.1	<i>Kinetic and Mechanism of the reduction of NO_x by C₃H₆.....</i>	<i>152</i>
5.7	MODELLING OF MIXTURE OF CO, H ₂ , C ₃ H ₆ & NO.....	170
6	CONCLUSIONS AND FUTURE WORKS	187
7	REFERENCES.....	188

List of Tables

<i>Table 2-1: Tier 2 emission standards, Federal test procedure, g/mi, Intermediate life[11]</i>	5
<i>Table 2-2: Tier 2 emission standards, Federal test procedure, g/mi, Full useful life[11]</i>	5
<i>Table 3-1: Location of different thermocouples in the reactor</i>	11
<i>Table 3-2: Inlet concentration levels for CO, NO and C₃H₆</i>	12
<i>Table 3-3: CO, H₂ only experiments, inlet concentrations</i>	13
<i>Table 3-4: C₃H₆ only experiments, initial concentrations</i>	14
<i>Table 3-5: NO only experiments, initial concentrations</i>	15
<i>Table 3-6: CO, H₂ & Propene experiments, initial concentrations</i>	16
<i>Table 3-7: NO & Propene experiments, initial concentrations</i>	20
<i>Table 3-8: CO, H₂ & NO experiments, initial concentrations</i>	23
<i>Table 3-9: CO, H₂, Propene & NO experiments, initial concentrations</i>	27
<i>Table 4-1: k₁ to k₄, K₅ to K₁₀ and k₁₁ parameter description</i>	53
<i>Table 4-2: Genetic Algorithm parameters</i>	56
<i>Table 4-3: fmincon parameters</i>	56
<i>Table 5-1: CO, H₂ only experiments, initial concentrations</i>	57
<i>Table 5-2: Runs 1-3 individual optimization results</i>	57
<i>Table 5-3: Runs 1, 2b & 3 simultaneous optimization results</i>	59
<i>Table 5-4: Runs 2a, 2b & 3 simultaneous optimization results</i>	59
<i>Table 5-5: C₃H₆ only experiments, initial concentrations</i>	60
<i>Table 5-6: Runs 4-6 individual optimization results</i>	61
<i>Table 5-7: Runs 4a, 5 & 6 simultaneous optimization results</i>	62
<i>Table 5-8: NO only experiments, initial concentrations</i>	63
<i>Table 5-9: Runs 13-15 individual optimization results, Model 1</i>	64
<i>Table 5-10: Runs 13-15 individual optimization results, Model 2</i>	65
<i>Table 5-11: Runs 13-15 individual optimization results, Model 3</i>	66
<i>Table 5-12: Runs 13-15 individual optimization results, Model 4</i>	67
<i>Table 5-13: Runs 13-15 individual optimization results, Model 5</i>	68
<i>Table 5-14: Runs 13-15 simultaneous optimization results, Model 1</i>	69
<i>Table 5-15: Runs 13-15 simultaneous optimization results, Model 2</i>	70
<i>Table 5-16: Runs 13-15 simultaneous optimization results, Model 3</i>	71

<i>Table 5-17: Runs 13-15 simultaneous optimization results, Model 4</i>	72
<i>Table 5-18: Runs 13-15 simultaneous optimization results, Model 5</i>	73
<i>Table 5-19: CO, H₂ & Propene experiments, initial concentrations</i>	74
<i>Table 5-20: Runs 7-9 individual optimization results, Model 1</i>	75
<i>Table 5-21: Runs 10-12 individual optimization results, Model 1</i>	75
<i>Table 5-22: Runs 7-9 individual optimization results, Model 5</i>	80
<i>Table 5-23: Runs 10-12 individual optimization results, Model 5</i>	80
<i>Table 5-24: Runs 7-12 simultaneous optimization results, Model 1</i>	85
<i>Table 5-25: Runs 7-12 simultaneous optimization results, Model 5</i>	88
<i>Table 5-26: CO, H₂ & NO experiments, initial concentrations</i>	92
<i>Table 5-27: Runs 22-24 individual optimization results, Model 1</i>	93
<i>Table 5-28: Runs 25-27 individual optimization results, Model 1</i>	93
<i>Table 5-29: Runs 22-24 individual optimization results, Model 2</i>	97
<i>Table 5-30: Runs 25-27 individual optimization results, Model 2</i>	97
<i>Table 5-31: Runs 22-24 individual optimization results, Model 3</i>	101
<i>Table 5-32: Runs 25-27 individual optimization results, Model 3</i>	101
<i>Table 5-33: Runs 22-24 individual optimization results, Model 4</i>	105
<i>Table 5-34: Runs 25-27 individual optimization results, Model 4</i>	105
<i>Table 5-35: Runs 22-24 individual optimization results, Model 5</i>	109
<i>Table 5-36: Runs 25-27 individual optimization results, Model 5</i>	109
<i>Table 5-37: Runs 22-27 simultaneous optimization results, Model 1</i>	113
<i>Table 5-38: Runs 22-27 simultaneous optimization results, Model 2</i>	117
<i>Table 5-39: Runs 22-27 simultaneous optimization results, Model 3</i>	120
<i>Table 5-40: Runs 22-27 simultaneous optimization results, Model 4</i>	124
<i>Table 5-41: Runs 22-27 simultaneous optimization results, Model 5</i>	128
<i>Table 5-42: NO & Propene experiments, initial concentrations</i>	132
<i>Table 5-43: Runs 16-21 individual optimization results, Model 1</i>	133
<i>Table 5-44: Runs 16-21 individual optimization results, Model 2</i>	137
<i>Table 5-45: Runs 16-21 individual optimization results, Model 3</i>	141
<i>Table 5-46: Runs 16-21 individual optimization results, Model 4</i>	145
<i>Table 5-47: Runs 16-21 individual optimization results, Model 5</i>	149

<i>Table 5-48: Runs 16-21 simultaneous optimization results, Model 1</i>	<i>155</i>
<i>Table 5-49: Runs 16-21 simultaneous optimization results, Model 2</i>	<i>158</i>
<i>Table 5-50: Runs 16-21 simultaneous optimization results, Model 3</i>	<i>161</i>
<i>Table 5-51: Runs 16-21 simultaneous optimization results, Model 4</i>	<i>164</i>
<i>Table 5-52: Runs 16-21 simultaneous optimization results, Model 5</i>	<i>167</i>
<i>Table 5-53: CO, H₂, Propene & NO experiments, initial concentrations</i>	<i>171</i>
<i>Table 5-54: Runs 38, 39 & 53 individual optimization results, Model 5</i>	<i>177</i>
<i>Table 5-55: Runs 38, 39 & 53 individual optimization results, New Model 5</i>	<i>181</i>
<i>Table 5-56: Runs 38, 39 & 53 simultaneous optimization results, New Model 5.....</i>	<i>184</i>

List of Figures

<i>Figure 2-1: EGR or Exhaust Gas Recirculation[14]</i>	7
<i>Figure 2-2: SCR catalytic converter[14]</i>	8
<i>Figure 2-3: Monolithic diesel oxidation converter</i>	10
<i>Figure 3-1: Schematic of reactor assembly</i>	11
<i>Figure 3-2: CO ignition curves, Runs 1-3</i>	14
<i>Figure 3-3: C₃H₆ ignition curves, Runs 4-6</i>	15
<i>Figure 3-4: NO, NO_x & NO₂ - Ignition curves, Runs 13-15</i>	16
<i>Figure 3-5: CO & C₃H₆- Ignition curves, Run 7(a) & 7(b)</i>	17
<i>Figure 3-6: CO & C₃H₆- Ignition curves, Run 8</i>	17
<i>Figure 3-7: CO & C₃H₆- Ignition curves, Run 9</i>	18
<i>Figure 3-8: CO & C₃H₆- Ignition curves, Run 10</i>	18
<i>Figure 3-9: CO & C₃H₆- Ignition curves, Run 11</i>	19
<i>Figure 3-10: CO & C₃H₆- Ignition curves, Run 12</i>	19
<i>Figure 3-11: C₃H₆, NO, NO_x, NO₂ & N₂O - Ignition curves, Run 16</i>	20
<i>Figure 3-12: C₃H₆, NO, NO_x, NO₂ & N₂O - Ignition curves, Run 17</i>	21
<i>Figure 3-13: C₃H₆, NO, NO_x, NO₂ & N₂O - Ignition curves, Run 18</i>	21
<i>Figure 3-14: C₃H₆, NO, NO_x, NO₂ & N₂O - Ignition curves, Run 20</i>	22
<i>Figure 3-15: C₃H₆, NO, NO_x, NO₂ & N₂O - Ignition curves, Run 21</i>	22
<i>Figure 3-16: CO, NO, NO_x & NO₂ - Ignition curves, Run 22</i>	23
<i>Figure 3-17: CO, NO, NO_x & NO₂ - Ignition curves, Run 23</i>	24
<i>Figure 3-18: CO, NO, NO_x & NO₂ - Ignition curves, Run 24</i>	24
<i>Figure 3-19: CO, NO, NO_x & NO₂ - Ignition curve Run 25</i>	25
<i>Figure 3-20: CO, NO, NO_x & NO₂ - Ignition curve Run 26</i>	25
<i>Figure 3-21: CO, NO, NO_x & NO₂ - Ignition curve Run 27</i>	26
<i>Figure 3-22: CO, C₃H₆, NO, NO_x, NO₂ & N₂O - Ignition curve Run 28</i>	28
<i>Figure 3-23: CO, C₃H₆, NO, NO_x, NO₂ & N₂O - Ignition curve Run 29</i>	28
<i>Figure 3-24: CO, C₃H₆, NO, NO_x, NO₂ & N₂O - Ignition curve Run 30</i>	29
<i>Figure 3-25: CO, C₃H₆, NO, NO_x, NO₂ & N₂O - Ignition curve Run 31</i>	29
<i>Figure 3-26: CO, C₃H₆, NO, NO_x, NO₂ & N₂O - Ignition curve Run 32</i>	30
<i>Figure 3-27: CO, C₃H₆, NO, NO_x, NO₂ & N₂O - Ignition curve Run 33</i>	30

<i>Figure 3-28: CO, C₃H₆, NO, NO_x, NO₂ & N₂O - Ignition curve Run 34</i>	31
<i>Figure 3-29: CO, C₃H₆, NO, NO_x, NO₂ & N₂O - Ignition curve Run 35</i>	31
<i>Figure 3-30: CO, C₃H₆, NO, NO_x, NO₂ & N₂O - Ignition curve Run 36</i>	32
<i>Figure 3-31: CO, C₃H₆, NO, NO_x, NO₂ & N₂O - Ignition curve Run 37</i>	32
<i>Figure 3-32: CO, C₃H₆, NO, NO_x, NO₂ & N₂O - Ignition curve Run 38</i>	33
<i>Figure 3-33: CO, C₃H₆, NO, NO_x, NO₂ & N₂O - Ignition curve Run 39</i>	33
<i>Figure 3-34: CO, C₃H₆, NO, NO_x, NO₂ & N₂O - Ignition curve Run 40</i>	34
<i>Figure 3-35: CO, C₃H₆, NO, NO_x, NO₂ & N₂O - Ignition curve Run 41</i>	34
<i>Figure 3-36: CO, C₃H₆, NO, NO_x, NO₂ & N₂O - Ignition curve Run 42</i>	35
<i>Figure 3-37: CO, C₃H₆, NO, NO_x, NO₂ & N₂O - Ignition curve Run 43</i>	35
<i>Figure 3-38: CO, C₃H₆, NO, NO_x, NO₂ & N₂O - Ignition curve Run 44</i>	36
<i>Figure 3-39: CO, C₃H₆, NO, NO_x, NO₂ & N₂O - Ignition curve Run 45</i>	36
<i>Figure 3-40: CO, C₃H₆, NO, NO_x, NO₂ & N₂O - Ignition curve Run 46</i>	37
<i>Figure 3-41: CO, C₃H₆, NO, NO_x, NO₂ & N₂O - Ignition curve Run 47</i>	37
<i>Figure 3-42: CO, C₃H₆, NO, NO_x, NO₂ & N₂O - Ignition curve Run 48</i>	38
<i>Figure 3-43: CO, C₃H₆, NO, NO_x, NO₂ & N₂O - Ignition curve Run 49</i>	38
<i>Figure 3-44: CO, C₃H₆, NO, NO_x, NO₂ & N₂O - Ignition curve Run 50</i>	39
<i>Figure 3-45: CO, C₃H₆, NO, NO_x, NO₂ & N₂O - Ignition curve Run 51</i>	39
<i>Figure 3-46: CO, C₃H₆, NO, NO_x, NO₂ & N₂O - Ignition curve Run 52</i>	40
<i>Figure 3-47: CO, C₃H₆, NO, NO_x, NO₂ & N₂O - Ignition curve Run 53</i>	40
<i>Figure 3-48: CO, C₃H₆, NO, NO_x, NO₂ & N₂O - Ignition curve Run 54</i>	41
<i>Figure 5-1: Individual optimization result vs. Experimental data, Run 1-3</i>	58
<i>Figure 5-2: Simultaneous modelling result vs. Experimental data, Runs 1, 2b & 3</i>	59
<i>Figure 5-3: Simultaneous modelling result vs. Experimental data, Runs 2a, 2b & 3</i>	60
<i>Figure 5-4: Individual optimization result vs. Experimental data, Runs 4-6</i>	61
<i>Figure 5-5: Simultaneous modelling result vs. Experimental data, Runs 4a, 5 & 6</i>	62
<i>Figure 5-6: Individual optimization result vs. Experimental data, Runs 13-15, Model 1</i>	64
<i>Figure 5-7: Individual optimization result vs. Experimental data, Runs 13-15, Model 2</i>	65
<i>Figure 5-8: Individual optimization result vs. Experimental data, Runs 13-15, Model 3</i>	66
<i>Figure 5-9: Individual optimization result vs. Experimental data, Runs 13-15, Model 4</i>	67
<i>Figure 5-10: Individual optimization result vs. Experimental data, Runs 13-15, Model 5</i>	68

<i>Figure 5-11: Simultaneous optimization result vs. Experimental data, Runs 13-15, Model 1.....</i>	69
<i>Figure 5-12: Simultaneous optimization result vs. Experimental data, Runs 13-15, Model 2.....</i>	70
<i>Figure 5-13: Simultaneous optimization result vs. Experimental data, Runs 13-15, Model 3.....</i>	71
<i>Figure 5-14: Simultaneous optimization result vs. Experimental data, Runs 13-15, Model 4.....</i>	72
<i>Figure 5-15: Simultaneous optimization result vs. Experimental data, Runs 13-15, Model 5.....</i>	73
<i>Figure 5-16: Individual optimization result vs. Experimental data, Run 7a, Model 1.....</i>	76
<i>Figure 5-17: Individual optimization result vs. Experimental data, Run 7b, Model 1.....</i>	76
<i>Figure 5-18: Individual optimization result vs. Experimental data, Run 8, Model 1.....</i>	77
<i>Figure 5-19: Individual optimization result vs. Experimental data, Run 9, Model 1.....</i>	77
<i>Figure 5-20: Individual optimization result vs. Experimental data, Run 10, Model 1.....</i>	78
<i>Figure 5-21: Individual optimization result vs. Experimental data, Run 11, Model 1.....</i>	78
<i>Figure 5-22: Individual optimization result vs. Experimental data, Run 12, Model 1.....</i>	79
<i>Figure 5-23: Individual optimization result vs. Experimental data, Run 7a, Model 5.....</i>	81
<i>Figure 5-24: Individual optimization result vs. Experimental data, Run 7b, Model 5.....</i>	81
<i>Figure 5-25: Individual optimization result vs. Experimental data, Run 8, Model 5.....</i>	82
<i>Figure 5-26: Individual optimization result vs. Experimental data, Run 9, Model 5.....</i>	82
<i>Figure 5-27: Individual optimization result vs. Experimental data, Run 10, Model 5.....</i>	83
<i>Figure 5-28: Individual optimization result vs. Experimental data, Run 11, Model 5.....</i>	83
<i>Figure 5-29: Individual optimization result vs. Experimental data, Run 12, Model 5.....</i>	84
<i>Figure 5-30: Simultaneous optimization result vs. Experimental data, Run 7a, Model 1.....</i>	85
<i>Figure 5-31: Simultaneous optimization result vs. Experimental data, Run 8, Model 1.....</i>	86
<i>Figure 5-32: Simultaneous optimization result vs. Experimental data, Run 9, Model 1.....</i>	86
<i>Figure 5-33: Simultaneous optimization result vs. Experimental data, Run 10, Model 1.....</i>	87
<i>Figure 5-34: Simultaneous optimization result vs. Experimental data, Run 11, Model 1.....</i>	87
<i>Figure 5-35: Simultaneous optimization result vs. Experimental data, Run 12, Model 1.....</i>	88
<i>Figure 5-36: Simultaneous optimization result vs. Experimental data, Run 7b, Model 5.....</i>	89
<i>Figure 5-37: Simultaneous optimization result vs. Experimental data, Run 8, Model 5.....</i>	89
<i>Figure 5-38: Simultaneous optimization result vs. Experimental data, Run 9, Model 5.....</i>	90
<i>Figure 5-39: Simultaneous optimization result vs. Experimental data, Run 10, Model 5.....</i>	90
<i>Figure 5-40: Simultaneous optimization result vs. Experimental data, Run 11, Model 5.....</i>	91
<i>Figure 5-41: Simultaneous optimization result vs. Experimental data, Run 12, Model 5.....</i>	91

<i>Figure 5-42: Individual optimization result vs. Experimental data, Run 22, Model 1</i>	94
<i>Figure 5-43: Individual optimization result vs. Experimental data, Run 23, Model 1</i>	94
<i>Figure 5-44: Individual optimization result vs. Experimental data, Run 24, Model 1</i>	95
<i>Figure 5-45: Individual optimization result vs. Experimental data, Run 25, Model 1</i>	95
<i>Figure 5-46: Individual optimization result vs. Experimental data, Run 26, Model 1</i>	96
<i>Figure 5-47: Individual optimization result vs. Experimental data, Run 27, Model 1</i>	96
<i>Figure 5-48: Individual optimization result vs. Experimental data, Run 22, Model 2</i>	98
<i>Figure 5-49: Individual optimization result vs. Experimental data, Run 23, Model 2</i>	98
<i>Figure 5-50: Individual optimization result vs. Experimental data, Run 24, Model 2</i>	99
<i>Figure 5-51: Individual optimization result vs. Experimental data, Run 25, Model 2</i>	99
<i>Figure 5-52: Individual optimization result vs. Experimental data, Run 26, Model 2</i>	100
<i>Figure 5-53: Individual optimization result vs. Experimental data, Run 27, Model 2</i>	100
<i>Figure 5-54: Individual optimization result vs. Experimental data, Run 22, Model 3</i>	102
<i>Figure 5-55: Individual optimization result vs. Experimental data, Run 23, Model 3</i>	102
<i>Figure 5-56: Individual optimization result vs. Experimental data, Run 24, Model 3</i>	103
<i>Figure 5-57: Individual optimization result vs. Experimental data, Run 25, Model 3</i>	103
<i>Figure 5-58: Individual optimization result vs. Experimental data, Run 26, Model 3</i>	104
<i>Figure 5-59: Individual optimization result vs. Experimental data, Run 27, Model 3</i>	104
<i>Figure 5-60: Individual optimization result vs. Experimental data, Run 22, Model 4</i>	106
<i>Figure 5-61: Individual optimization result vs. Experimental data, Run 23, Model 4</i>	106
<i>Figure 5-62: Individual optimization result vs. Experimental data, Run 24, Model 4</i>	107
<i>Figure 5-63: Individual optimization result vs. Experimental data, Run 25, Model 4</i>	107
<i>Figure 5-64: Individual optimization result vs. Experimental data, Run 26, Model 4</i>	108
<i>Figure 5-65: Individual optimization result vs. Experimental data, Run 27, Model 4</i>	108
<i>Figure 5-66: Individual optimization result vs. Experimental data, Run 22, Model 5</i>	110
<i>Figure 5-67: Individual optimization result vs. Experimental data, Run 23, Model 5</i>	110
<i>Figure 5-68: Individual optimization result vs. Experimental data, Run 24, Model 5</i>	111
<i>Figure 5-69: Individual optimization result vs. Experimental data, Run 25, Model 5</i>	111
<i>Figure 5-70: Individual optimization result vs. Experimental data, Run 26, Model 5</i>	112
<i>Figure 5-71: Individual optimization result vs. Experimental data, Run 27, Model 5</i>	112
<i>Figure 5-72: Simultaneous optimization result vs. Experimental data, Run 22, Model 1</i>	113

<i>Figure 5-73: Simultaneous optimization result vs. Experimental data, Run 23, Model 1.....</i>	<i>114</i>
<i>Figure 5-74: Simultaneous optimization result vs. Experimental data, Run 24, Model 1.....</i>	<i>114</i>
<i>Figure 5-75: Simultaneous optimization result vs. Experimental data, Run 25, Model 1.....</i>	<i>115</i>
<i>Figure 5-76: Simultaneous optimization result vs. Experimental data, Run 26, Model 1.....</i>	<i>115</i>
<i>Figure 5-77: Simultaneous optimization result vs. Experimental data, Run 27, Model 1.....</i>	<i>116</i>
<i>Figure 5-78: Simultaneous optimization result vs. Experimental data, Run 22, Model 2.....</i>	<i>117</i>
<i>Figure 5-79: Simultaneous optimization result vs. Experimental data, Run 23, Model 2.....</i>	<i>118</i>
<i>Figure 5-80: Simultaneous optimization result vs. Experimental data, Run 24, Model 2.....</i>	<i>118</i>
<i>Figure 5-81: Simultaneous optimization result vs. Experimental data, Run 25, Model 2.....</i>	<i>119</i>
<i>Figure 5-82: Simultaneous optimization result vs. Experimental data, Run 26, Model 2.....</i>	<i>119</i>
<i>Figure 5-83: Simultaneous optimization result vs. Experimental data, Run 27, Model 2.....</i>	<i>120</i>
<i>Figure 5-84: Simultaneous optimization result vs. Experimental data, Run 22, Model 3.....</i>	<i>121</i>
<i>Figure 5-85: Simultaneous optimization result vs. Experimental data, Run 23, Model 3.....</i>	<i>121</i>
<i>Figure 5-86: Simultaneous optimization result vs. Experimental data, Run 24, Model 3.....</i>	<i>122</i>
<i>Figure 5-87: Simultaneous optimization result vs. Experimental data, Run 25, Model 3.....</i>	<i>122</i>
<i>Figure 5-88: Simultaneous optimization result vs. Experimental data, Run 26, Model 3.....</i>	<i>123</i>
<i>Figure 5-89: Simultaneous optimization result vs. Experimental data, Run 27, Model 3.....</i>	<i>123</i>
<i>Figure 5-90: Simultaneous optimization result vs. Experimental data, Run 22, Model 4.....</i>	<i>124</i>
<i>Figure 5-91: Simultaneous optimization result vs. Experimental data, Run 23, Model 4.....</i>	<i>125</i>
<i>Figure 5-92: Simultaneous optimization result vs. Experimental data, Run 24, Model 4.....</i>	<i>125</i>
<i>Figure 5-93: Simultaneous optimization result vs. Experimental data, Run 25, Model 4.....</i>	<i>126</i>
<i>Figure 5-94: Simultaneous optimization result vs. Experimental data, Run 26, Model 4.....</i>	<i>126</i>
<i>Figure 5-95: Simultaneous optimization result vs. Experimental data, Run 27, Model 4.....</i>	<i>127</i>
<i>Figure 5-96: Simultaneous optimization result vs. Experimental data, Run 22, Model 5.....</i>	<i>128</i>
<i>Figure 5-97: Simultaneous optimization result vs. Experimental data, Run 23, Model 5.....</i>	<i>129</i>
<i>Figure 5-98: Simultaneous optimization result vs. Experimental data, Run 24, Model 5.....</i>	<i>129</i>
<i>Figure 5-99: Simultaneous optimization result vs. Experimental data, Run 25, Model 5.....</i>	<i>130</i>
<i>Figure 5-100: Simultaneous optimization result vs. Experimental data, Run 26, Model 5.....</i>	<i>130</i>
<i>Figure 5-101: Simultaneous optimization result vs. Experimental data, Run 27, Model 5.....</i>	<i>131</i>
<i>Figure 5-102: Individual optimization result vs. Experimental data, Run 16, Model 1.....</i>	<i>133</i>
<i>Figure 5-103: Individual optimization result vs. Experimental data, Run 17, Model 1.....</i>	<i>134</i>

<i>Figure 5-104: Individual optimization result vs. Experimental data, Run 18, Model 1.....</i>	<i>134</i>
<i>Figure 5-105: Individual optimization result vs. Experimental data, Run 20, Model 1.....</i>	<i>135</i>
<i>Figure 5-106: Individual optimization result vs. Experimental data, Run 21, Model 1.....</i>	<i>135</i>
<i>Figure 5-107: Individual optimization result vs. Experimental data, Run 16, Model 2.....</i>	<i>137</i>
<i>Figure 5-108: Individual optimization result vs. Experimental data, Run 17, Model 2.....</i>	<i>138</i>
<i>Figure 5-109: Individual optimization result vs. Experimental data, Run 18, Model 2.....</i>	<i>138</i>
<i>Figure 5-110: Individual optimization result vs. Experimental data, Run 20, Model 2.....</i>	<i>139</i>
<i>Figure 5-111: Individual optimization result vs. Experimental data, Run 21, Model 2.....</i>	<i>139</i>
<i>Figure 5-112: Individual optimization result vs. Experimental data, Run 16, Model 3.....</i>	<i>141</i>
<i>Figure 5-113: Individual optimization result vs. Experimental data, Run 17, Model 3.....</i>	<i>142</i>
<i>Figure 5-114: Individual optimization result vs. Experimental data, Run 18, Model 3.....</i>	<i>142</i>
<i>Figure 5-115: Individual optimization result vs. Experimental data, Run 20, Model 3.....</i>	<i>143</i>
<i>Figure 5-116: Individual optimization result vs. Experimental data, Run 21, Model 3.....</i>	<i>143</i>
<i>Figure 5-117: Individual optimization result vs. Experimental data, Run 16, Model 4.....</i>	<i>145</i>
<i>Figure 5-118: Individual optimization result vs. Experimental data, Run 17, Model 4.....</i>	<i>146</i>
<i>Figure 5-119: Individual optimization result vs. Experimental data, Run 18, Model 4.....</i>	<i>146</i>
<i>Figure 5-120: Individual optimization result vs. Experimental data, Run 20, Model 4.....</i>	<i>147</i>
<i>Figure 5-121: Individual optimization result vs. Experimental data, Run 21, Model 4.....</i>	<i>147</i>
<i>Figure 5-122: Individual optimization result vs. Experimental data, Run 16, Model 5.....</i>	<i>149</i>
<i>Figure 5-123: Individual optimization result vs. Experimental data, Run 17, Model 5.....</i>	<i>150</i>
<i>Figure 5-124: Individual optimization result vs. Experimental data, Run 18, Model 5.....</i>	<i>150</i>
<i>Figure 5-125: Individual optimization result vs. Experimental data, Run 20, Model 5.....</i>	<i>151</i>
<i>Figure 5-126: Individual optimization result vs. Experimental data, Run 21 Model 5.....</i>	<i>151</i>
<i>Figure 5-127: Oxidation and reduction of the catalyst surface</i>	<i>153</i>
<i>Figure 5-128: Simultaneous optimization result vs. Experimental data, Run 16, Model 1.....</i>	<i>155</i>
<i>Figure 5-129: Simultaneous optimization result vs. Experimental data, Run 17, Model 1.....</i>	<i>156</i>
<i>Figure 5-130: Simultaneous optimization result vs. Experimental data, Run 18, Model 1.....</i>	<i>156</i>
<i>Figure 5-131: Simultaneous optimization result vs. Experimental data, Run 20, Model 1.....</i>	<i>157</i>
<i>Figure 5-132: Simultaneous optimization result vs. Experimental data, Run 21, Model 1.....</i>	<i>157</i>
<i>Figure 5-133: Simultaneous optimization result vs. Experimental data, Run 16, Model 2.....</i>	<i>158</i>
<i>Figure 5-134: Simultaneous optimization result vs. Experimental data, Run 17, Model 2.....</i>	<i>159</i>

<i>Figure 5-135: Simultaneous optimization result vs. Experimental data, Run 18, Model 2.....</i>	<i>159</i>
<i>Figure 5-136: Simultaneous optimization result vs. Experimental data, Run 20, Model 2.....</i>	<i>160</i>
<i>Figure 5-137: Simultaneous optimization result vs. Experimental data, Run 21, Model 2.....</i>	<i>160</i>
<i>Figure 5-138: Simultaneous optimization result vs. Experimental data, Run 16, Model 3.....</i>	<i>161</i>
<i>Figure 5-139: Simultaneous optimization result vs. Experimental data, Run 17, Model 3.....</i>	<i>162</i>
<i>Figure 5-140: Simultaneous optimization result vs. Experimental data, Run 18, Model 3.....</i>	<i>162</i>
<i>Figure 5-141: Simultaneous optimization result vs. Experimental data, Run 20, Model 3.....</i>	<i>163</i>
<i>Figure 5-142: Simultaneous optimization result vs. Experimental data, Run 21, Model 3.....</i>	<i>163</i>
<i>Figure 5-143: Simultaneous optimization result vs. Experimental data, Run 16, Model 4.....</i>	<i>164</i>
<i>Figure 5-144: Simultaneous optimization result vs. Experimental data, Run 17, Model 4.....</i>	<i>165</i>
<i>Figure 5-145: Simultaneous optimization result vs. Experimental data, Run 18, Model 4.....</i>	<i>165</i>
<i>Figure 5-146: Simultaneous optimization result vs. Experimental data, Run 20, Model 4.....</i>	<i>166</i>
<i>Figure 5-147: Simultaneous optimization result vs. Experimental data, Run 21, Model 4.....</i>	<i>166</i>
<i>Figure 5-148: Simultaneous optimization result vs. Experimental data, Run 16, Model 5.....</i>	<i>167</i>
<i>Figure 5-149: Simultaneous optimization result vs. Experimental data, Run 17, Model 5.....</i>	<i>168</i>
<i>Figure 5-150: Simultaneous optimization result vs. Experimental data, Run 18, Model 5.....</i>	<i>168</i>
<i>Figure 5-151: Simultaneous optimization result vs. Experimental data, Run 20, Model 5.....</i>	<i>169</i>
<i>Figure 5-152: Simultaneous optimization result vs. Experimental data, Run 21, Model 5.....</i>	<i>169</i>
<i>Figure 5-153: CO, C₃H₆, NO, NO_x, NO₂ & N₂O - Ignition curve Run 46.....</i>	<i>172</i>
<i>Figure 5-154: CO, C₃H₆, NO, NO_x, NO₂ & N₂O - Ignition curve Run 42.....</i>	<i>172</i>
<i>Figure 5-155: Ignition curves comparison, Run 18 vs. Run 42</i>	<i>173</i>
<i>Figure 5-156: C₃H₆ Ignition curves comparison, Run 34 vs. Run 35</i>	<i>174</i>
<i>Figure 5-157: C₃H₆ Ignition curves comparison, Run 28 vs. Run 30</i>	<i>175</i>
<i>Figure 5-158: C₃H₆ Ignition curves comparison, Run 28 vs. Run 32</i>	<i>176</i>
<i>Figure 5-159: Individual optimization result vs. Experimental data, Run 38 Model 5.....</i>	<i>178</i>
<i>Figure 5-160: Individual optimization result vs. Experimental data, Run 39 Model 5.....</i>	<i>178</i>
<i>Figure 5-161: Individual optimization result vs. Experimental data, Run 53 Model 5.....</i>	<i>179</i>
<i>Figure 5-162: Individual optimization result vs. Experimental data, Run 38 New Model 5.....</i>	<i>182</i>
<i>Figure 5-163: Individual optimization result vs. Experimental data, Run 39 New Model 5.....</i>	<i>182</i>
<i>Figure 5-164: Individual optimization result vs. Experimental data, Run 53 New Model 5.....</i>	<i>183</i>
<i>Figure 5-165: Simultaneous optimization result vs. Experimental data, Run 38, New Model 5 .</i>	<i>185</i>

Figure 5-166: Simultaneous optimization result vs. Experimental data, Run 39, New Model 5 . 185

Figure 5-167: Simultaneous optimization result vs. Experimental data, Run 53, New Model 5 . 186

List of Symbols

Symbol	Unit	Description
LB	-	Lower Bond
HB	-	Higher Bond
F	mol/s	Molar flow
C	mol/m ³	Concentration
$CPSI$	units/in ²	Channels per square inch
STP	-	Standard conditions for temperature and pressure
u_m	m/s	Mean velocity
C_f	mol/m ³	Bulk molar concentration
Y_j	-	Mole fraction of species j
$(-R_j)$	mol/m ² .s	Rate of disappearance of species j
Z	m	Length of reactor
V_{wc}	m ³	Washcoat volume
V_c	m ³	Channel volume
D_{wc}	m	Diameter of circular cylinder before washcoat
D_H	m	Diameter of circular cylinder after washcoat
O_i	-	Objective function of the optimization
X_{exp}	-	Experimental data
X_{pred}	-	Predicted data
k_i	mol ⁽¹⁻ⁿ⁾ .m ³⁽ⁿ⁻¹⁾ .s ⁻¹	Kinetic constant/ Rate coefficient for a reaction of order “n”
A_i	mol ⁽¹⁻ⁿ⁾ .m ³⁽ⁿ⁻¹⁾ .s ⁻¹	Pre-exponential factor of the Arrhenius equation for the kinetic constant i
E_i	J/mol	Activation energy for the kinetic constant for the kinetic constant i
R_g	J/(mol.K)	Gas constant
T	K	Temperature
K_j	mol ⁽¹⁻ⁿ⁾ .m ³⁽ⁿ⁻¹⁾ .s ⁻¹	Adsorption equilibrium constant/Rate coefficient for a reaction of order “n”
B_j	mol ⁽¹⁻ⁿ⁾ .m ³⁽ⁿ⁻¹⁾ .s ⁻¹	Pre-exponential factor of the Arrhenius equation for the adsorption constant j
H_j	J/mol	Activation energy for the kinetic constant for the adsorption constant j
B	-	Equilibrium term
P	Bar	Pressure
K_{eq}	-	Equilibrium constant

1 Introduction

The continuously increasing number of automobiles and corresponding vehicle pollutants are a major concern. In the past 60 years the number of vehicles on the road has increased more than 1650% [4, 5]. In Canada, automotive sources are responsible for 59% of CO emission and 53% of NO_x emissions [6]. Different emissions can cause various problems for us. CO₂, N₂O and CH₄ are green house gases whilst CO, NO_x, O₃ and SO₂ can damage both the environment and the human body seriously. Many researches on NO_x effects showed that NO_x consumes atmospheric oxygen and can cause acidic rain. On the other hand, it can increase the probability of bacterial and viral infection of the lung. Lung malfunction and changes of its metabolism with NO_x has also been reported [7, 8].

These concerns have led to much research to discover methods to eliminate these emissions.

The main method used to eliminate harmful exhaust gas emissions is catalytic converters. There are many different types of catalytic converters, but in all of them the main idea is to convert emissions from engine exhaust gas into less harmful compounds via chemical reaction.

The three way catalytic converter (TWC) is the most popular and effective converter for stoichiometric gasoline engines. It works under stoichiometric air to fuel ratio condition, and oxidizes CO and hydrocarbon and reduces NO_x content of the exhaust gas at the same time. In lean burn engines like diesel engines, because of the presence of excess oxygen, reduction of the NO_x is not possible with a three way converters, so other types of converters must be used in this case. For lean burn engines, two types of converters are used in series. In the first converter, called the Diesel Oxidation Converter (DOC), CO and hydrocarbons are oxidized to CO₂ and H₂O. Some of the NO is oxidized to NO₂. In addition, some N₂O may be formed, and some of the NO may be converted to N₂ on a

reaction with hydrocarbons. Following the DOC, another converter is used to reduce the NO and NO₂ to nitrogen. The focus of this work is the DOC

1.1 Problem Definition

Diesel oxidation converters consist of a honey comb monolith support which is covered with a washcoat, e.g. γ -Al₂O₃ that contains small particles of precious metals like Pt, Pd or Rh or combination of them. To aid in the design of catalytic systems, computer simulation can be very helpful. These simulations require kinetic models for the catalyst system in question. These models are specific to the catalyst formulation. In previous researches, Sola [3] proposed several models for Pt/Al₂O₃ diesel oxidation converters which work relatively well for Pt catalyst in various conditions.

1.2 Research Objective

The focus of this project was to find a kinetic model that can fit to experimental results from a Pt-Pd/Al₂O₃ catalyst, and predict how the system behaves in various conditions. Sola's model was used as a base for the research, and modifications are proposed to improve it. Experimental results were provided by researchers at the University of Waterloo.

1.3 Thesis Layout

After this brief introduction, additional background of this research is presented, which includes emission production, emission regulations and current methods that are being used to eliminate the emissions. After that, the experimental procedure and results are included. In the next chapter modelling methodology and parameter estimation procedures are discussed, which is followed by detailed modelling results and discussion.

2 Background

2.1 Automotive Emissions

The emission type and amount depend on the engine operating conditions. For example, CO generation depends on the air to fuel ratio (AFR). Air to fuel ratio is defined as the mass of air divided by the mass of fuel in the air-fuel mixture at any given moment. Moving from rich condition i.e. condition that AFR is low, to stoichiometric condition and then lean condition i.e. condition that AFR is high, will decrease the amount of CO emission from the engine.

Higher engine operational temperature can cause more NO_x production. This can be inhibited by circulating portion of exhaust gas into engine chamber which decrease temperature of combustion due to dilatation of fuel-air composite.

In some cases, in gasoline engines, the flame cannot penetrate into small fractures or seams in combustion chamber of engines. As a result, unburned hydrocarbon particles which are trapped in there, will be emitted in the exhaust gas as air pollution [9].

To decrease pollutants from engines, governments have established regulations which define maximum allowable level of emissions for different types of engines. Strict regulations also established for quality of fuel that is used in automotive engines such as the sulphur content of diesel fuel.

2.2 Legal Level of Emissions

The United States first established regulations for automotive emissions in 1975. Japan, Europe, Australia and other countries later established such regulations. Today US and European instructions are the most important and are becoming stricter every day.

In all of these legislations, emissions are measured over an engine test procedure, which simulates real driving condition in a repeatable condition. Regulations also provide a standard method to measure the pollutants.

According to U.S. and European standards, the following limitations are applied:

- CO content
- Total Hydrocarbon (HC) content in Europe and non-methane hydrocarbon content in U.S.
- NO_x content.
- Particulate matter (PM) content[10]

In Canada, regulations for railway locomotives, aircrafts and commercial marine vessels are published by Transport Canada, whilst Environment Canada is responsible for other internal combustion engines regulations.

Today, regulations for light duty vehicles (LDV) are based on two sets of standards, Tier 1 and Tier 2; which the U.S. Environment Protection Agency (EPA) stated in the Clean AIR ACT Amendments (CAAA) in 1990 and can be found in Table 2-1 and Table 2-2.

Tier 1 standards apply to all new light duty vehicles. This regulation is based on the weight of vehicles, and consists of two different standards, one for light LDV and the other one for heavy LDV.

The Tier 2 regulation has stricter emission limits and can be applied to all LDV plus medium duty passenger vehicles (MDPV). In Tier 2 standards, every engine has to meet the same limits regardless of its weight or fuel.

Tier 2 standard is divided into 8 sub certificates called “Bins”. All vehicles have to pass at least one of these 8 limits. In addition, all LDV and MDPV sold by each manufacturer since 2009 have to meet the average of 0.07 g/mi for NO_x emission [11].

Table 2-1: Tier 2 emission standards, Federal test procedure, g/mi, Intermediate life[11]

Bin No.	Intermediate life (5 years / 50,000 mi)				
	NMOG *	CO	NO _x	PM	HCHO
8	0.100 (0.125)	3.4	0.14	-	0.015
7	0.075	3.4	0.11	-	0.015
6	0.075	3.4	0.08	-	0.015
5	0.075	3.4	0.05	-	0.015
4	-	-	-	-	-
3	-	-	-	-	-
2	-	-	-	-	-
1	-	-	-	-	-

* Only for Diesel fueled vehicles

Table 2-2: Tier 2 emission standards, Federal test procedure, g/mi, Full useful life[11]

Bin No.	Full useful life				
	NMOG*	CO	NO _x	PM	HCHO
8	0.125 (0.156)	4.2	0.2	0.02	0.018
7	0.09	4.2	0.15	0.02	0.018
6	0.09	4.2	0.1	0.01	0.018
5	0.09	4.2	0.07	0.01	0.018
4	0.07	2.1	0.04	0.01	0.011
3	0.055	2.1	0.03	0.01	0.011
2	0.01	2.1	0.02	0.01	0.004
1	0	0	0	0	0

* Only for Diesel fueled vehicles

2.3 Emission Control

Automotive industries have taken different actions to reduce exhaust emissions. Changes made to engine design and fuel composition to reduce emission production, whilst after treatment methods have been developed a lot to capture emissions or convert them into less harmful components. The following paragraphs are a summary of the most important changes that have been made.

2.3.1 Increasing Fuel Octane Number

Higher octane fuels can withstand more pressure before ignition in the combustion chamber. This can decrease knocking effect of engine which is caused by chamber walls resonance. Knocking effect increases coke formation and produces more unburned hydrocarbon. Normal spark ignition gasoline

engines have good performance using high octane fuel (85 to 100). Using higher octane fuel leads to higher compression ratio in engine that improves engine performance and power, and reduces hydrocarbon in the exhaust gas [12].

2.3.2 Reducing Sulphur Content

Reducing the sulphur content of fuel can significantly reduce SO₂ emissions. Desulphurization methods can be applied to both gasoline and diesel fuel. Currently gasoline sulphur content is about 500 ppmw and there is 0.1 to 0.03 wt% sulphur in diesel fuel. Canadian oil producers are trying to decrease sulphur content of fuel by desulphurization of crude oil at refining stages [12].

2.3.3 Three Way Catalyst (TWC)

In spark ignition (SI) engines, one of the most popular ways to eliminate emissions is using three way catalysts. Three way converter works under stoichiometric condition to oxidize CO and HC and reduce NO_x simultaneously. To maintain proper air fuel ratio, oxygen sensors placed in the engine manifold transmit feed back to the engine control system to regulate the air fuel ratio at engine inlet. Efficiency of this system is about 80% and can provide 95% effectiveness [9].

2.3.4 Exhaust Gas Recirculation (EGR)

NO_x is one of the most difficult emissions to control. The Rate of NO_x formation is related to combustion chamber temperature. Increasing temperature can cause high amount of NO_x formation. Exhaust gas recirculation (EGR) is an approach to decrease combustion zone temperature by recirculation a portion of the exhaust gas into the intake manifold and mixing it with fuel and air mixture. Although EGR can lower the engine power and its efficiency by 5 to 10%, EGR can reduce NO_x formation by 50%. Another approach for decreasing temperature is to increase the concentration of residual gas (exhaust gas remaining in chamber after stroke) [12]. However there is a tradeoff between temperature reduction and particulate matter production. Decreasing the chamber temperature leads to

formation of more particular matter (PM) [13]. A schematic diagram of EGR system can be found in Figure 2-1.

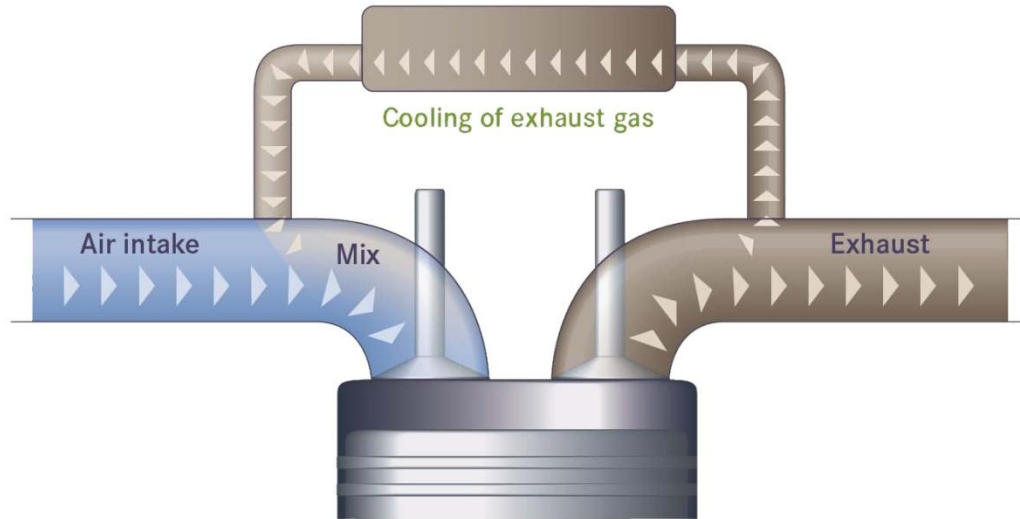


Figure 2-1: EGR or Exhaust Gas Recirculation[14]

2.3.5 Selective Catalytic Reduction (SCR)

Selective catalytic reduction (SCR) is one method that can be used to reduce NO_x emissions from lean burn (e.g. Diesel) engines. It is important to use high quality fuel in engines with SCR since SCR catalysts are highly sensitive to metal and sulphur, and can easily deactivate [15].

2.3.5.1 SCR by Ammonia (NH_3)

The use of ammonia to eliminate NO_x has been widely commercialized. Today a lot of power generation plants are using this method to reduce NO_x emission in their exhaust gas. For automotive engines, systems have been designed to convert urea to NH_3 and then use ammonia to eliminate NO_x .

In this method, ammonia reacts with NO_x over a suitable catalyst at a temperature between 320 to 400 °C (depending on sulphur content of fuel) to produce N_2 and H_2O . A 1:1 ratio for NO/NO_2 gives the best performance of SCR.



As mentioned before, in automotive adopted SCR systems, urea is used as primary reactant instead of NH_3 since it is easier to store and transport urea than NH_3 [15]. After injection, urea reacts with water to produce ammonia.



Figure 2-2 illustrates a schematic diagram for Ammonia SCR system.

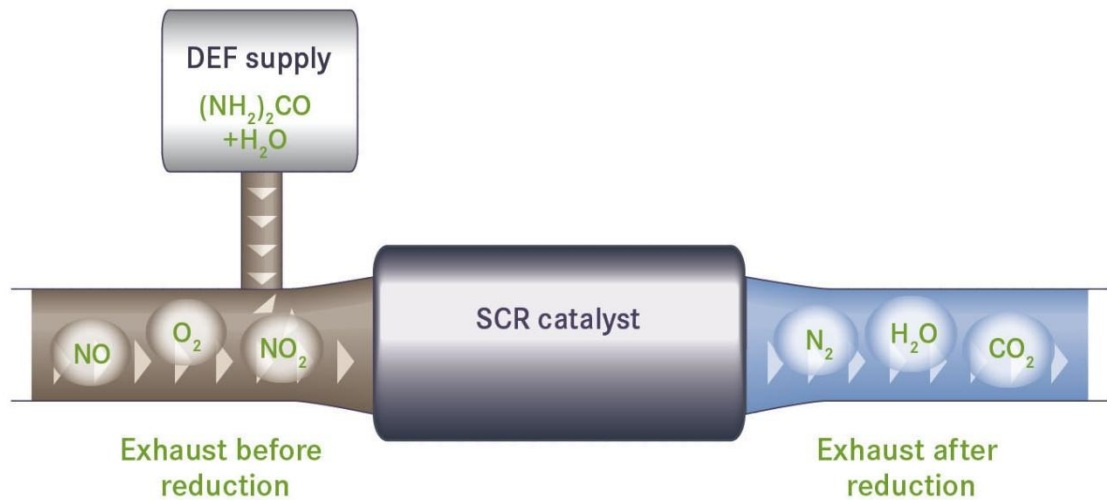


Figure 2-2: SCR catalytic converter[14]

2.3.5.2 SCR by Hydrocarbon

NO_x reduction to N_2 by hydrocarbon is a smart approach to eliminate NO_x from exhaust gas for both stationary and automotive sources. This method was pioneered by early work of Iwamoto [16] and Armour [17]. The temperature window for this method is narrow, and NO/NO_2 ratio does not have a significant

effect on overall performance. We can choose CH₄ as a good candidate to reduce NO_x to N₂ as following reactions:



This reaction happens over Co-ZSM-5 at 400 °C [18].

Some limitations in using hydrocarbon SCR method promoted development of similar methods called NO_x trap. 90 to 95% of total NO_x content in diesel exhaust gas is consisted of NO which can easily be oxidized to NO₂ while engine operates in lean condition. Then NO₂ is stored by trapping agents as follow [19]:



These nitrates are thermodynamically unstable at high temperature, surplus fuel or breakdown to NO or NO₂ [20, 21].



Once the engine switched to rich condition; HC, CO or H₂ reduce NO_x to N₂ [19, 22].

2.3.6 Diesel Particulate Filter (DPF)

This device is used to capture particulate matter from diesel exhaust gas. DPF consists of a honeycomb monolith which works as filter to trap PM and let the rest of the exhaust gas leave freely. This structure needs to be regenerated periodically. Oxygen regeneration requires high temperature, around 600 °C. Regeneration of DPF by NO₂ is possible at temperature of 275 °C which is significantly lower than the previous one, but it is still hard to achieve this temperature in light duty diesel engines. Injection of fuel into DPF can oxidize the soot captured at relatively low temperature [19, 22].

2.3.7 Diesel Oxidation Catalyst (DOC)

We have discussed methods for capturing PM and NO_x elimination in the previous sections. There are two more things to take care of:

- CO and HC elimination
- NO/NO₂ ratio adjustment

Diesel Oxidation Catalyst (DOC) is a honeycomb monolith catalyst which is primarily used to oxidize CO and hydrocarbon residual, and to regulate NO/NO₂ ratio in exhaust gas that can be used as inlet in the SCR section. This converter also consists of a washcoated monolith substrate with a precious metal catalyst. Cordierite is the most common monolith since it has low porosity and high strength. High surface area Silica, Aluminum and zeolite based materials are used as washcoat. Most of the time, one or combination of two or more of Rh, Pt and Pd is dispersed on washcoat as catalyst [19, 22]. Schematic diagram for a diesel oxidation catalyst can be found in Figure 2-3.

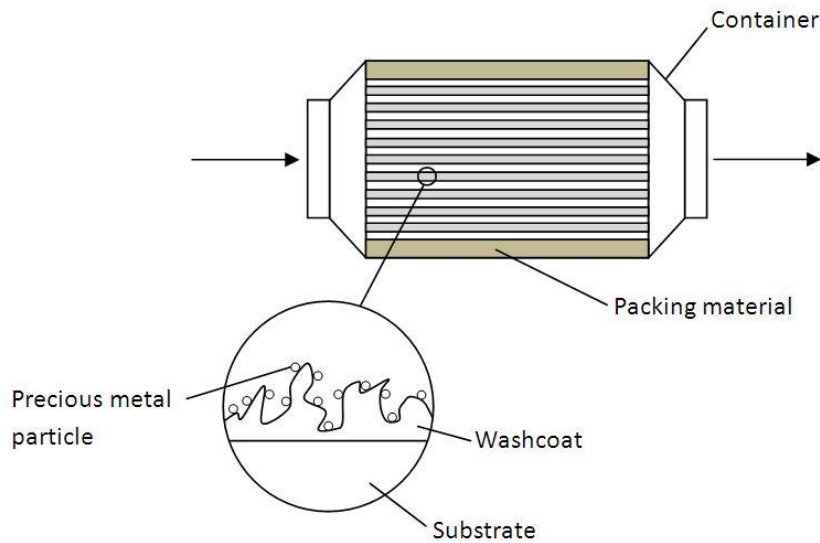


Figure 2-3: Monolithic diesel oxidation converter

3 Experimental

This chapter presents the experimental results that are used as the basis for this work. The experiments were performed by A.Abedi at the University of Waterloo. First our catalyst characterizations were presented followed by experimental procedures and plans and finally results were categorized and presented.

3.1 Catalyst

The catalyst sample was a pre-aged Pt:Pd monolith was diesel oxidation catalyst that was prepared by Umicore AG on 400 CPSI (Cells per square inch) substrate with square channels. Al₂O₃ was selected as the washcoat. Overall amount of catalyst load was 95 g/ft³ with Pt/Pd ratio of 4 to 1. A 0.9” (2.29 cm) diameter core with length of 2.4” (6.10 cm) was cut from a full size converter so the overall reactor volume was 25 cm³. Catalyst was wrapped in 3M insulation material, inserted into a horizontal quartz tube and then placed into a Lindberg Minimate temperature controlled furnace. Six K type thermocouples were placed at various positions along the catalyst length. The locations of the thermocouples are given in Table 3-1 and can be seen in Figure 3-1 schematically:

Table 3-1: Location of different thermocouples in the reactor

Thermocouple	Location
CH0	Upstream
CH1	0 cm, Middle
CH2	2 cm, Top
CH3	2 cm, Middle
CH4	2 cm, Bottom
CH5	4 cm, Middle
CH6	6 cm, Middle

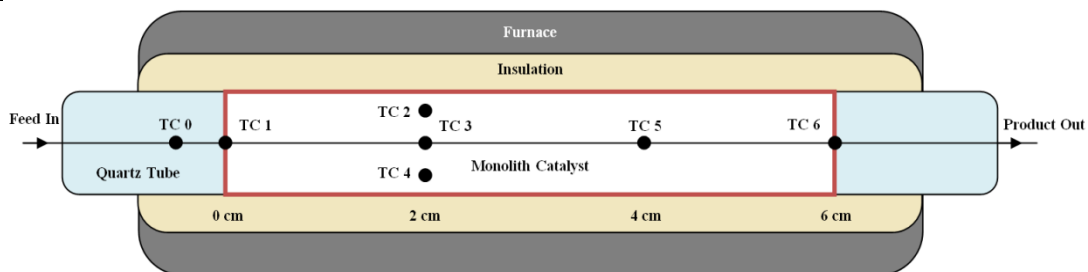


Figure 3-1: Schematic of reactor assembly

3.2 Experimental Procedure

The input stream was initially fed into the reactor at a temperature below 80 °C to avoid reaction before ramping. The reactor temperature was programmed to increase at 3 °C per minute. After oxidation completion, the reactor was cooled down to below 80 °C. Input stream base consisted of 10% O₂, 10% H₂O, 10% CO₂, 300 ppm or 1% He. In each experiment, an appropriate combination of CO, H₂, C₃H₆ and NO was added to this base. The balance of the mixture was N₂. Total gas flow was 9.34 L/Min which gave a space velocity equal to 20520 h⁻¹ at STP.

A MultiGas 2030 FTIR analyzer (MKS) and an HPR20 mass spectrometer (MS) were used to analyze the outlet gas. Experiments with pure N₂ were performed to obtain the temperature difference in radial direction and back and front of the catalyst. It was observed that the temperature difference between front and back thermocouples was less than 4 °C and the radial difference was less than 5 °C which occurred at high temperatures.

3.3 Experimental Plan

For each component we defined three level of concentration, called low, medium and high. The concentrations of the three primary reactants corresponding to these designations are shown in Table 3-2.

Table 3-2: Inlet concentration levels for CO, NO and C₃H₆

Component	Low Concentration	Medium Concentration	High Concentration
CO	500 ppm	1000 ppm	2000 ppm
C ₃ H ₆	250 ppm	500 ppm	750 ppm
NO	150 ppm	300 ppm	600 ppm

H₂ concentration specified at 1/3 of the CO concentration. Only ignition curves were done, and not the extinction curves. Some experiments were repeated to make sure that results were reproducible. First each component at different concentration was fed into reactor. Then combinations of two species were used

as inlet stream, and finally all three species at different concentration were mixed together and fed into the reactor.

Our colleagues at the University of Waterloo reported a huge amount of data, consisting of concentration of each species in exhaust gas measured every second, while the temperature was ramped from around 300 °C to around 600 °C. Since we need to use these data to fit our theoretical model into experimental results, more data points means more demand for calculation resources. So there is a tradeoff between experimental result trend accuracy and resources needed for analyzing them. Our data reduction method was to take points every delta conversion of the order 5% or a temperature change of 5 °C, whichever is smaller. This reduction gave sufficient data for modelling without requiring huge computational resources.

3.4 Experimental Results

3.4.1 CO, H₂ Oxidation

In the first three experiments, the inlet gas consisted of base and CO, H₂ complex at different concentrations. Initial concentration and ignition curves for these three experiments are shown in Table 3-3 and Figure 3-2.

Table 3-3: CO, H₂ only experiments, inlet concentrations

Run	CO, ppm	H ₂ , ppm
1	500	167
2(a)	1000	333
2(b)	1000	333
2(c)	1000	0
3	2000	666

Hydrogen conversion is not shown in the graph, but it is known that H₂ reacts shortly after the CO is converted. Comparing graphs shows us that CO has a self-inhibition effect, that is, increasing CO concentration increased the light off temperature.

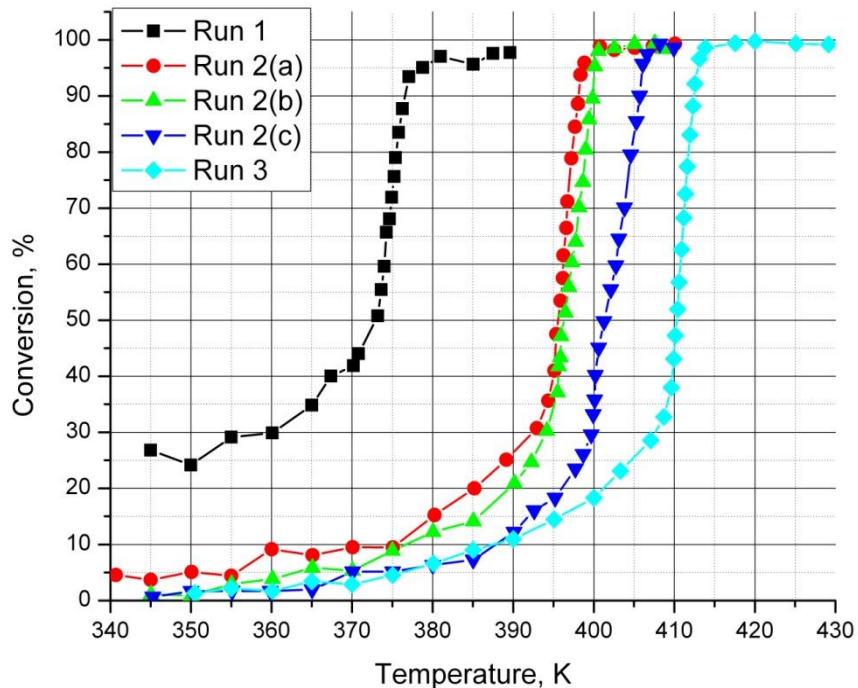


Figure 3-2: CO ignition curves, Runs 1-3

It is clear that H_2 enhanced CO oxidation by decreasing light off temperature.

3.4.2 Propene Oxidation

The next experiments were performed with propene as the sole reactant. Table 3-4 gives the initial concentrations, while the ignition curves are shown in Figure 3-3.

Table 3-4: C_3H_6 only experiments, initial concentrations

Run	C_3H_6 , ppm
4(a)	250
4(b)	250
5	500
6	750

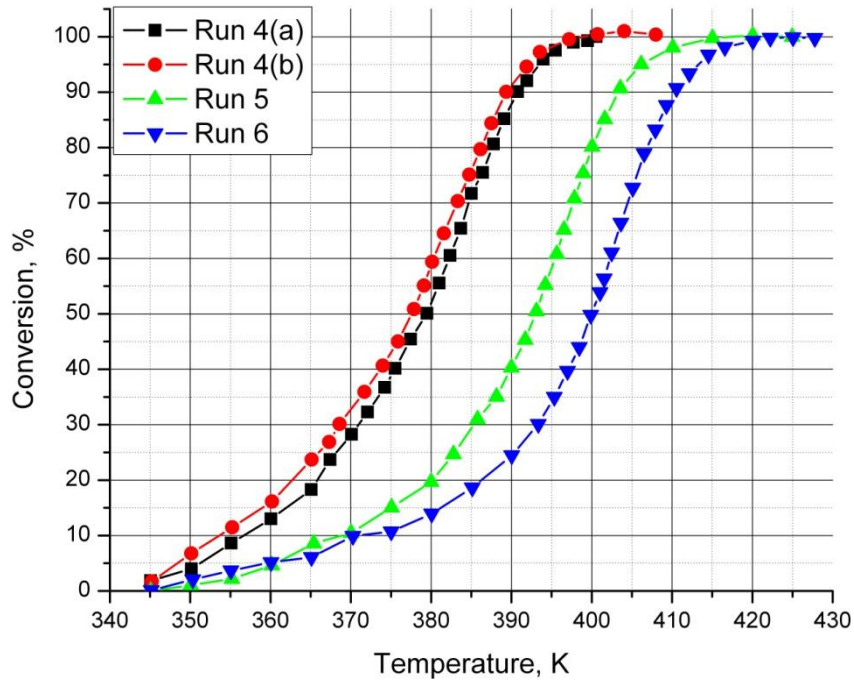


Figure 3-3: C₃H₆ ignition curves, Runs 4-6

Again, self inhibition effect for propene is observed. Increasing propene concentration increased light off temperature but the correlation between light off change and propene change is not linear.

3.4.3 NO Oxidation

In this set of experiments, the only reactant was NO, with inlet concentrations given in Table 3-5. Figures 3-4 shows the ignition curves obtained for each run. In each case, the total conversion of NO is shown.

Table 3-5: NO only experiments, initial concentrations

Run	NO, ppm
13	150
14	300
15	600

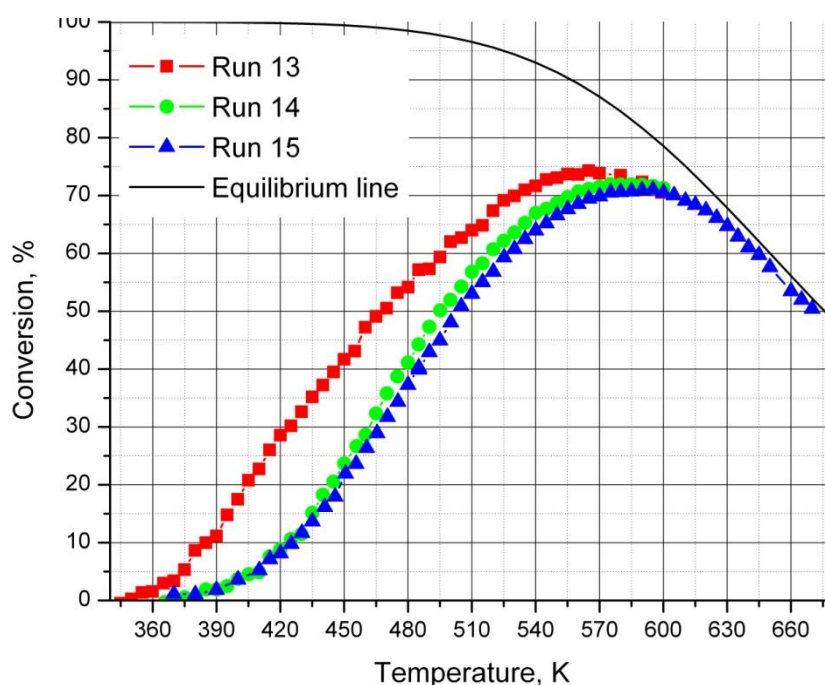


Figure 3-4: NO, NO_x & NO₂ - Ignition curves, Runs 13-15

NO shows self inhibition by pushing light off temperature to right when NO concentration increased. The conversion of NO to NO₂ is limited by equilibrium at higher temperatures. The equilibrium line is also shown in Figure 3-4.

3.4.4 CO, H₂ and Propene oxidation

The next set of results was obtained with a mixture of CO/H₂ and propene as reactants, as shown in Table 3-6. The results of the six experiments are given in Figure 3-5 to Figure 3-10.

Table 3-6: CO, H₂ & Propene experiments, initial concentrations

Run	CO, ppm	H ₂ , ppm	C ₃ H ₆ , ppm
7(a)	500	167	250
7(b)	500	167	250
8	1000	333	250
9	2000	666	250
10	1000	333	500
11	1000	333	750
12	2000	666	500

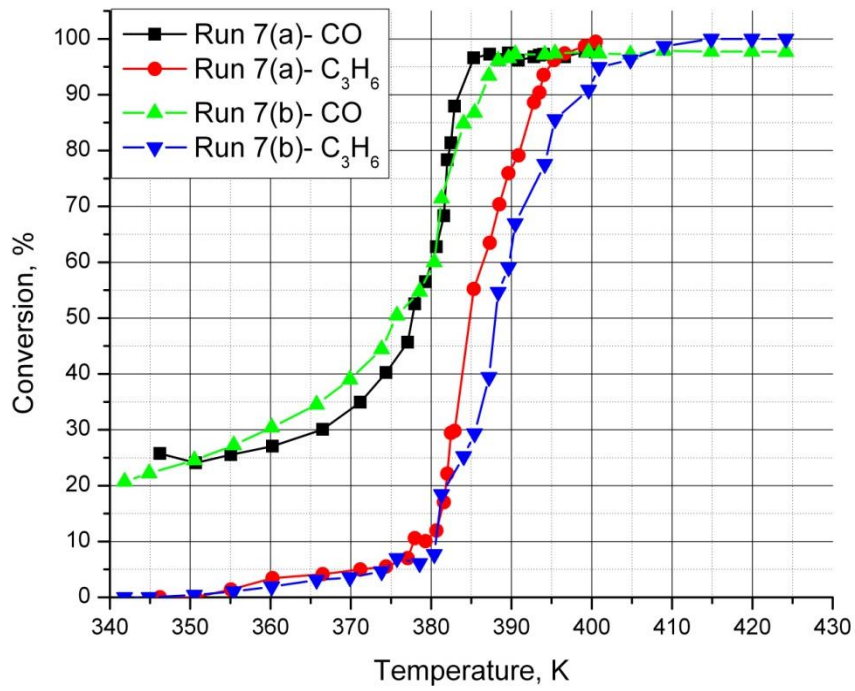


Figure 3-5: CO & C₃H₆- Ignition curves, Run 7(a) & 7(b)

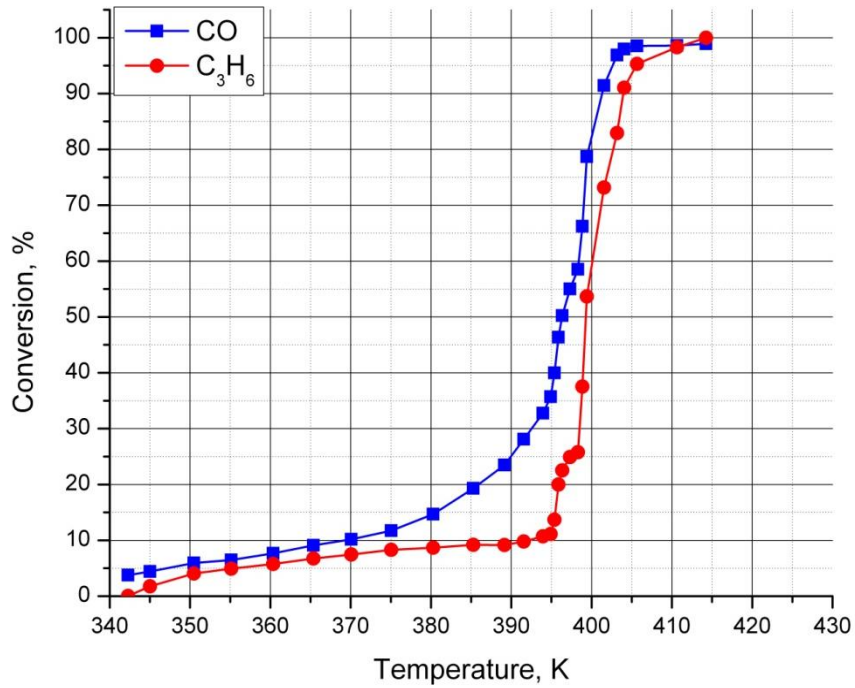


Figure 3-6: CO & C₃H₆- Ignition curves, Run 8

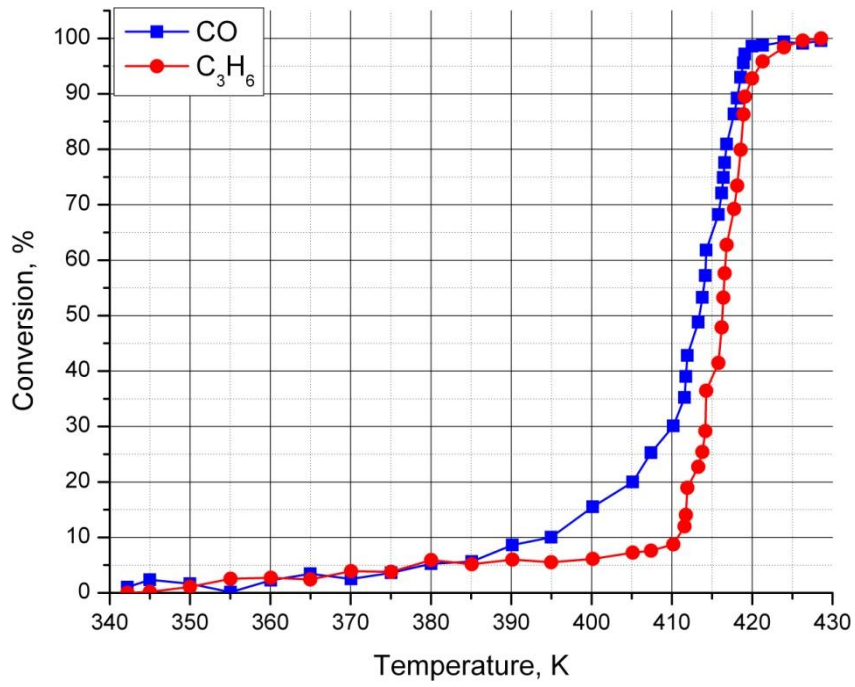


Figure 3-7: CO & C₃H₆- Ignition curves, Run 9

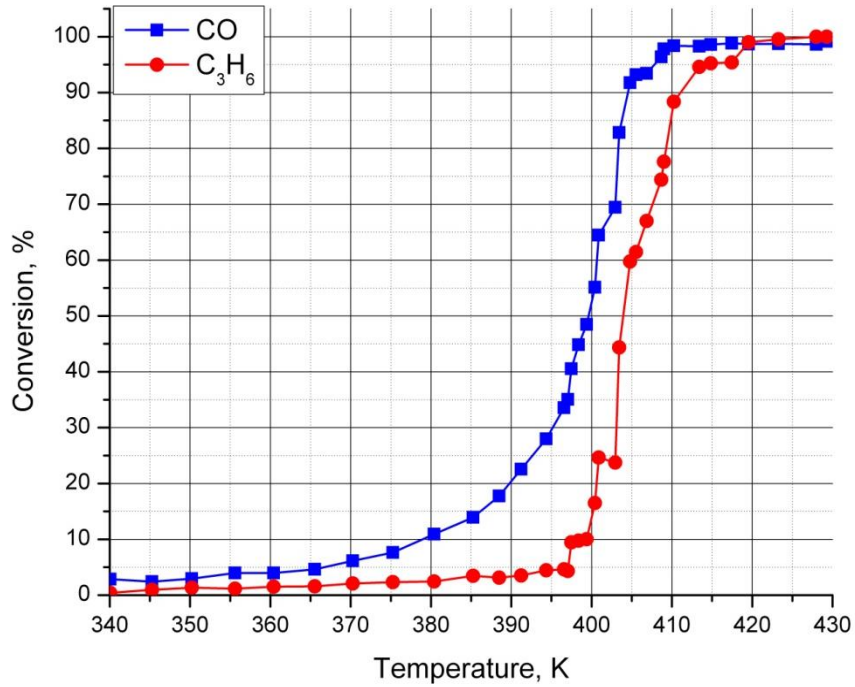


Figure 3-8: CO & C₃H₆- Ignition curves, Run 10

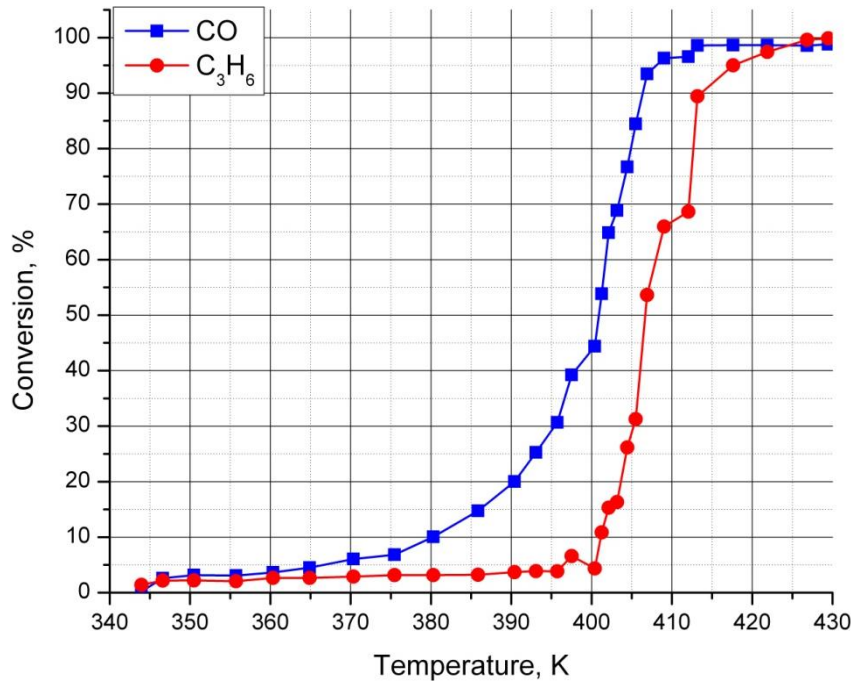


Figure 3-9: CO & C₃H₆- Ignition curves, Run 11

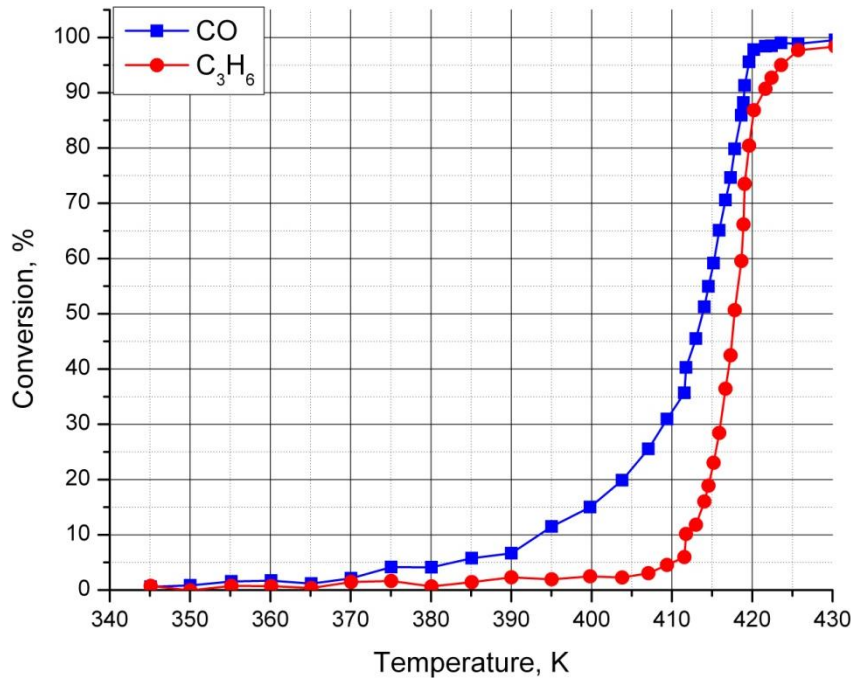


Figure 3-10: CO & C₃H₆- Ignition curves, Run 12

From these figures it is seen that the presence of CO inhibits the oxidation of C_3H_6 , and the presence of C_3H_6 inhibits the oxidation of CO.

3.4.5 NO and Propene Oxidation

The next set of results presented are for the case of NO and C_3H_6 as reactants. Table 3-7 gives the feed concentrations, whilst Figure 3-11 to Figure 3-15 illustrate the ignition curves. Each figure shows the conversion of C_3H_6 , the conversion of NO, the conversion of NO_x , and the conversion of NO to N_2O and NO_2 .

Table 3-7: NO & Propene experiments, initial concentrations

Run	Propene, ppm	NO, ppm
16	500	150
17	500	300
18	500	600
20	750	300
21	750	600

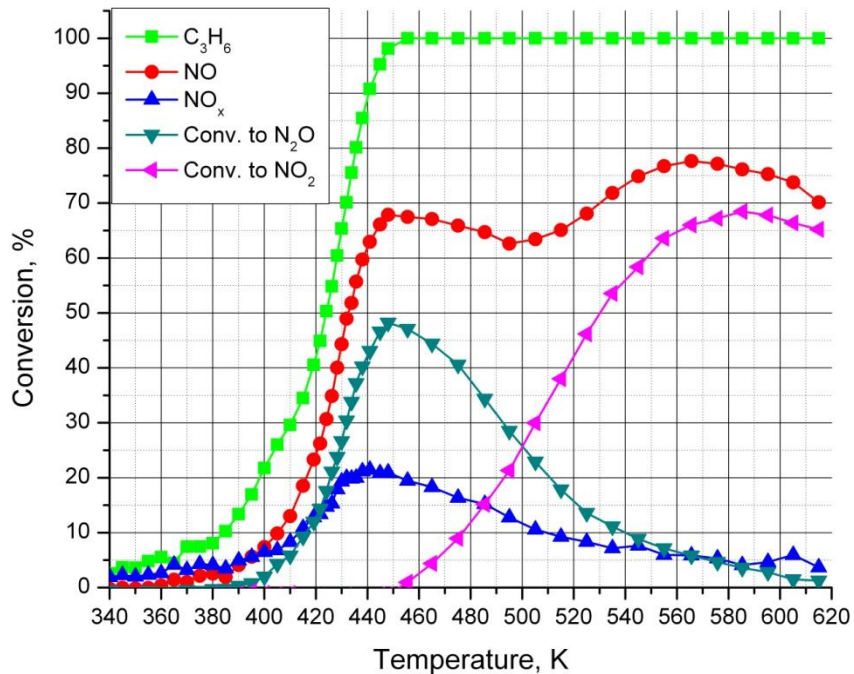


Figure 3-11: C_3H_6 , NO, NO_x , NO_2 & N_2O - Ignition curves, Run 16

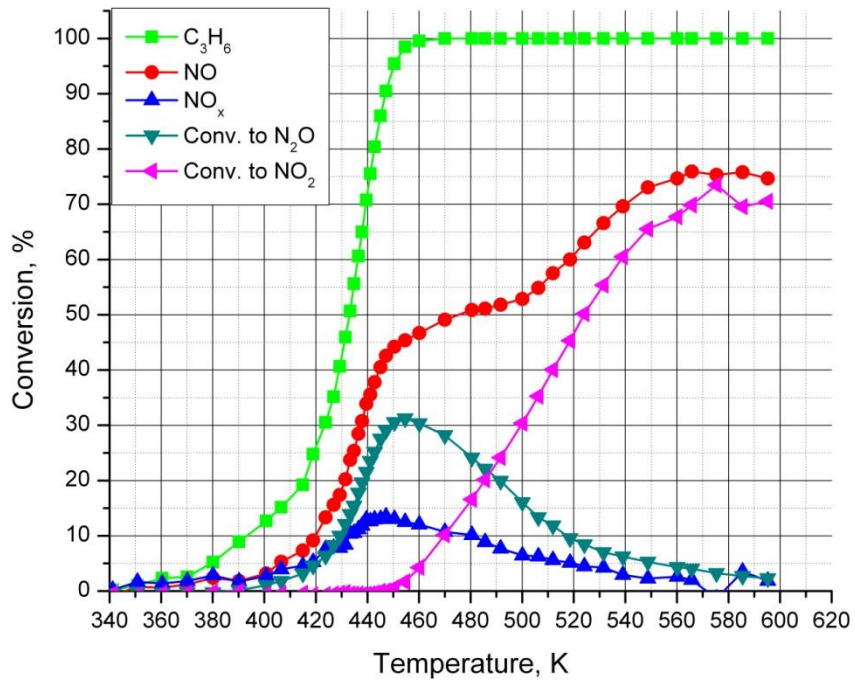


Figure 3-12: C_3H_6 , NO, NO_x , NO_2 & N_2O - Ignition curves, Run 17

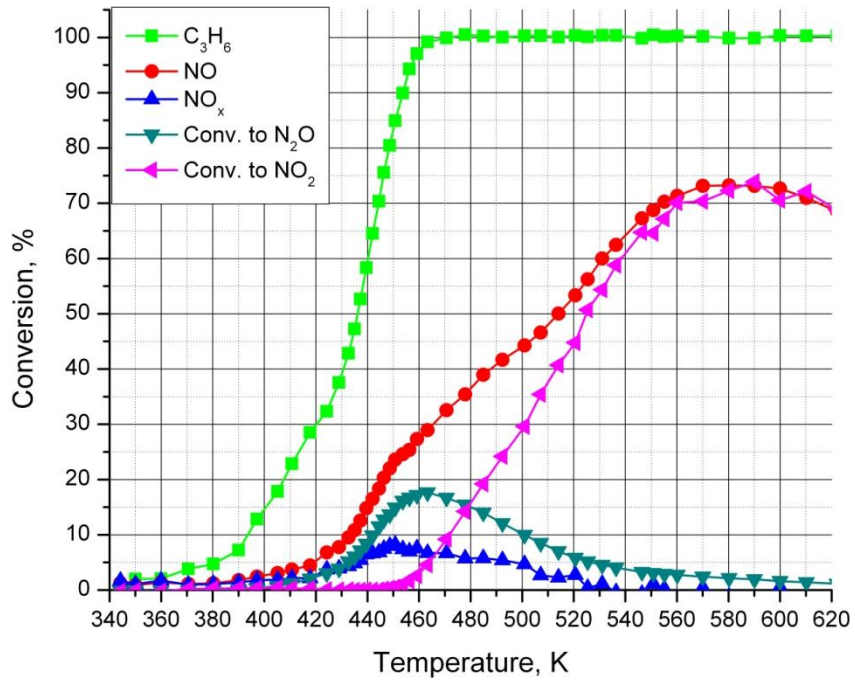


Figure 3-13: C_3H_6 , NO, NO_x , NO_2 & N_2O - Ignition curves, Run 18

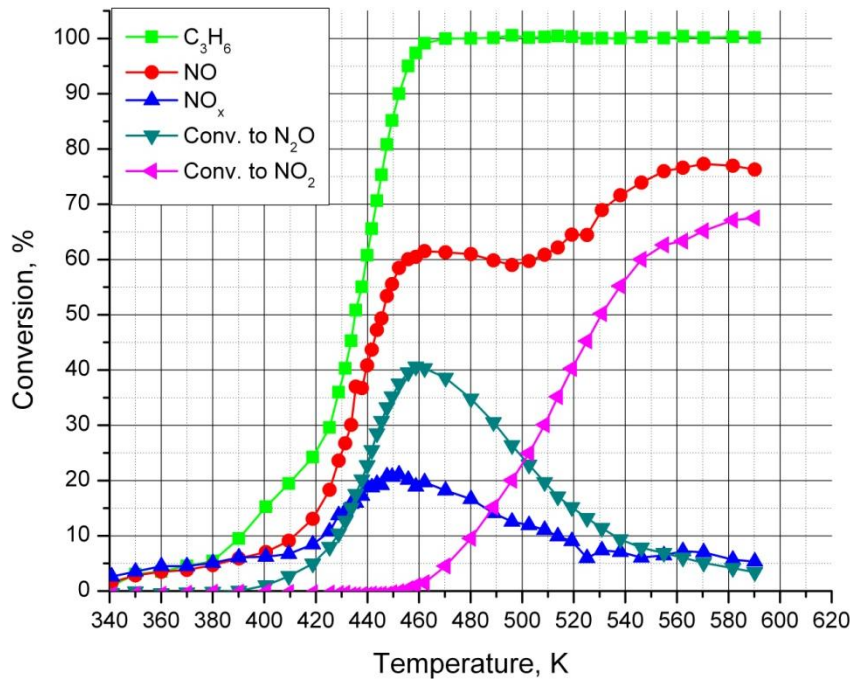


Figure 3-14: C₃H₆, NO, NO_x, NO₂ & N₂O - Ignition curves, Run 20

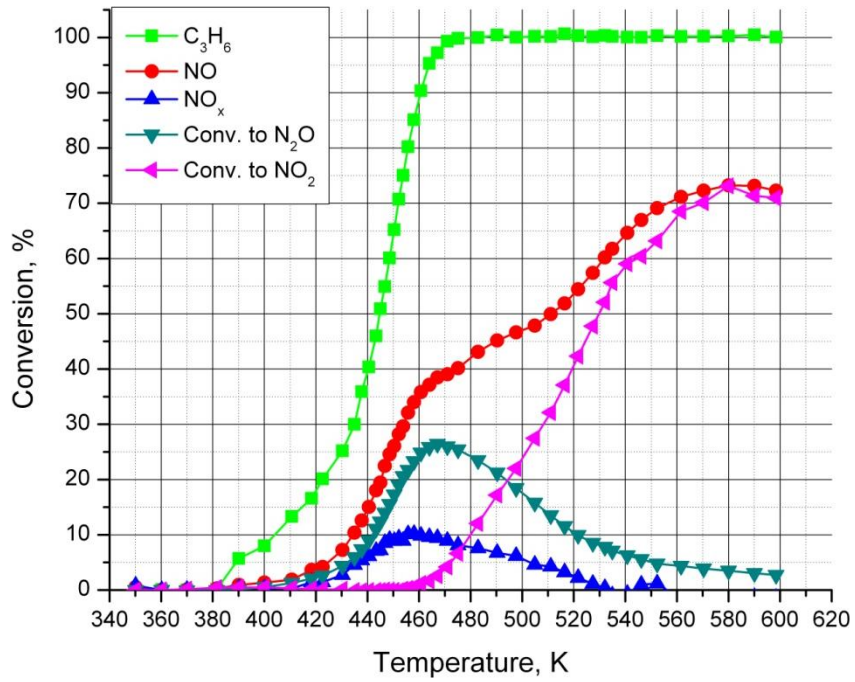


Figure 3-15: C₃H₆, NO, NO_x, NO₂ & N₂O - Ignition curves, Run 21

It is clear that the reactions of NO in the presence of propene are more complicated than reactions with NO alone. At low temperature the NO can react with hydrocarbon to produce N₂ and N₂O, while at high temperature NO is more likely to react with oxygen and produce NO₂.

3.4.6 NO and CO oxidation

Table 3-8 shows the feed concentrations for the next set of experiments, which used CO/H₂ and NO as reactants. Again the conversion of CO and NO are given in Figure 3-16 to Figure 3-21. No N₂O formation was observed.

Table 3-8: CO, H₂ & NO experiments, initial concentrations

Run	CO, ppm	H ₂ , ppm	NO, ppm
22	1000	333	150
23	1000	333	300
24	1000	333	600
25	500	167	300
26	2000	666	300
27	500	167	600

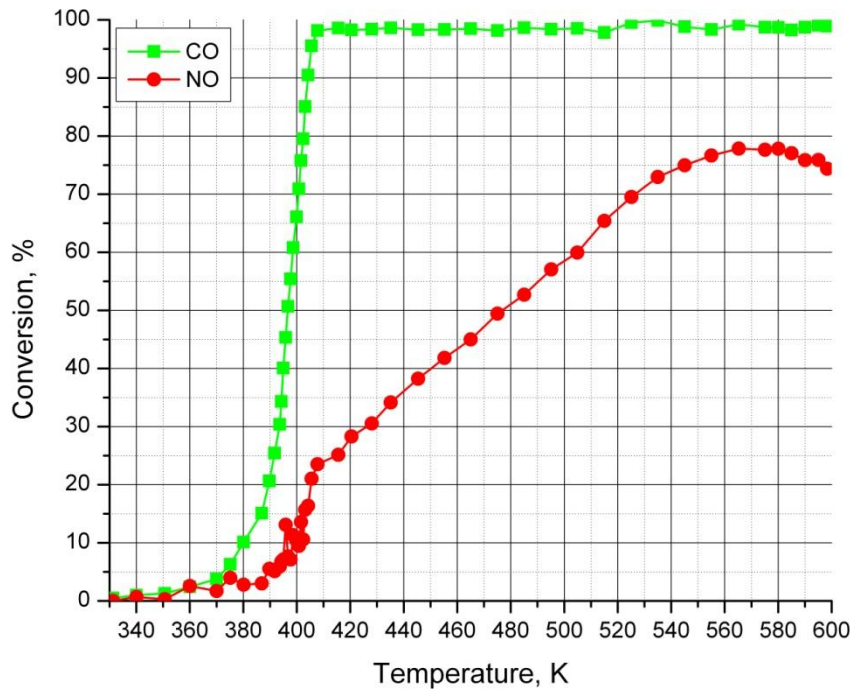


Figure 3-16: CO, NO, NO_x & NO₂ - Ignition curves, Run 22

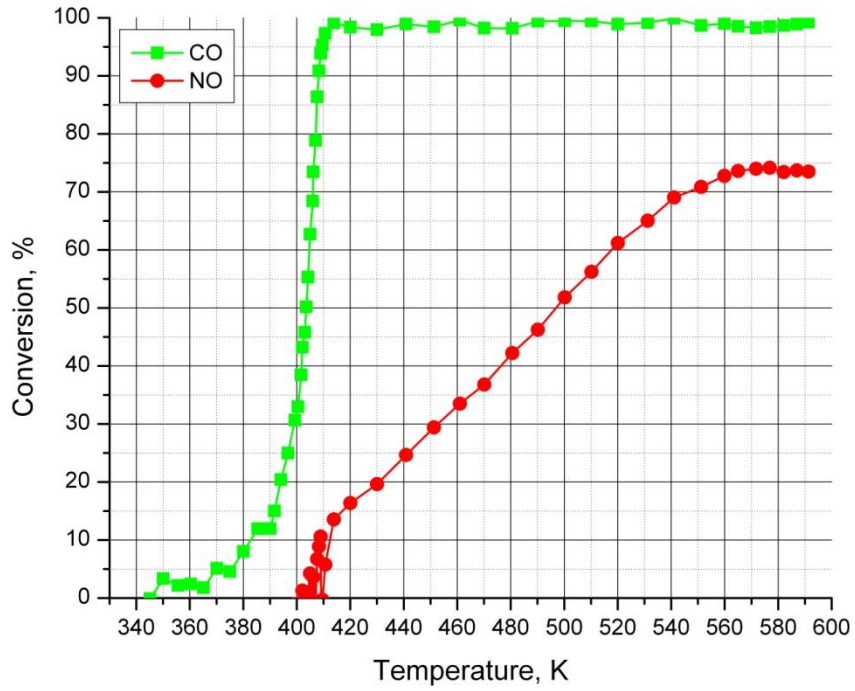


Figure 3-17: CO, NO, NO_x & NO₂ - Ignition curves, Run 23

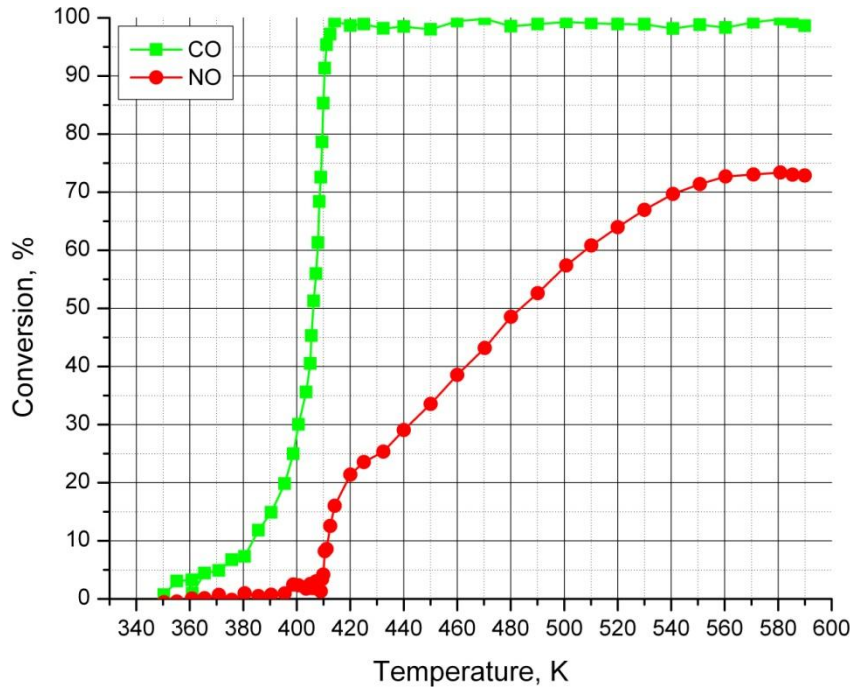


Figure 3-18: CO, NO, NO_x & NO₂ - Ignition curves, Run 24

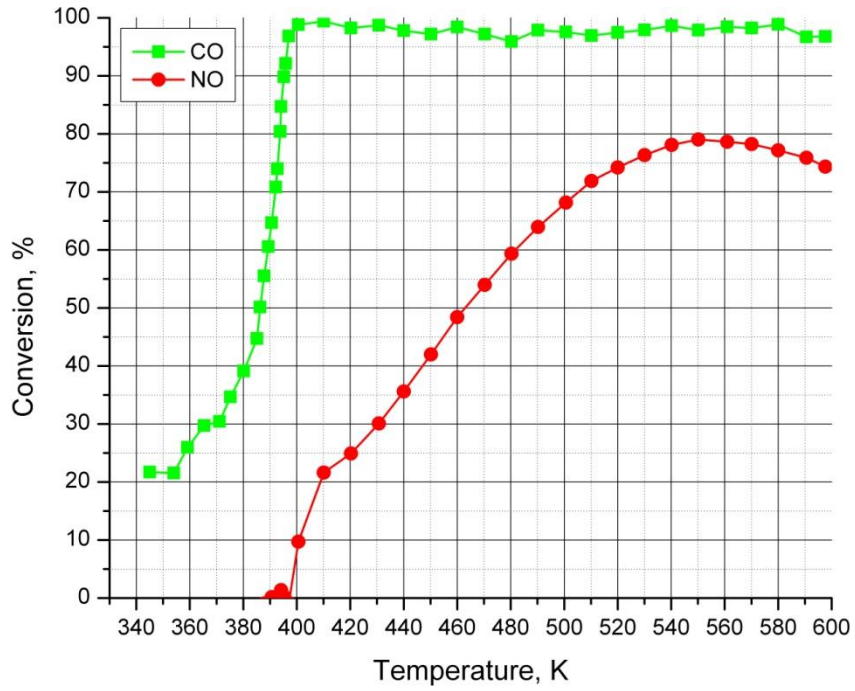


Figure 3-19: CO, NO, NO_x & NO₂ - Ignition curve Run 25

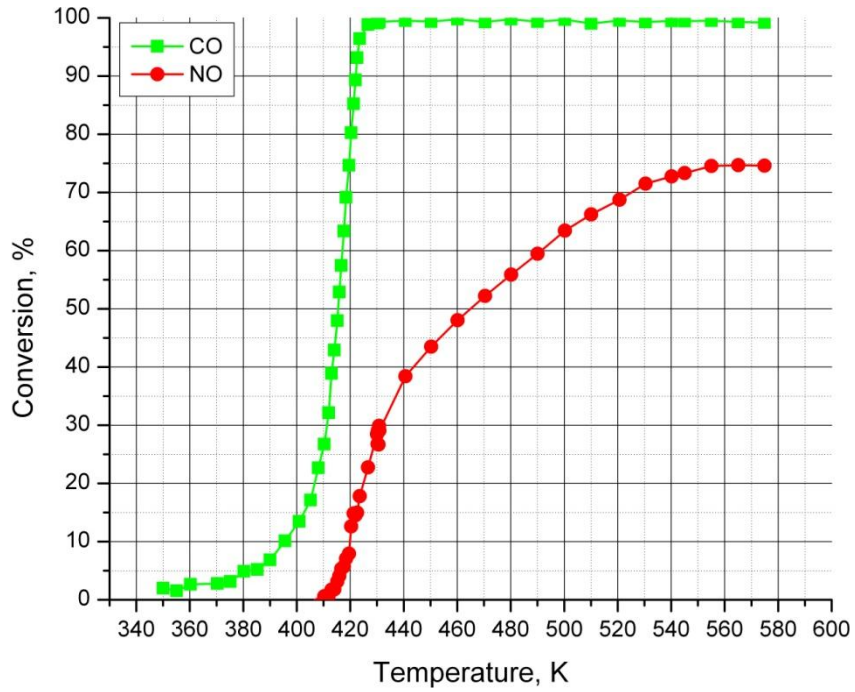


Figure 3-20: CO, NO, NO_x & NO₂ - Ignition curve Run 26

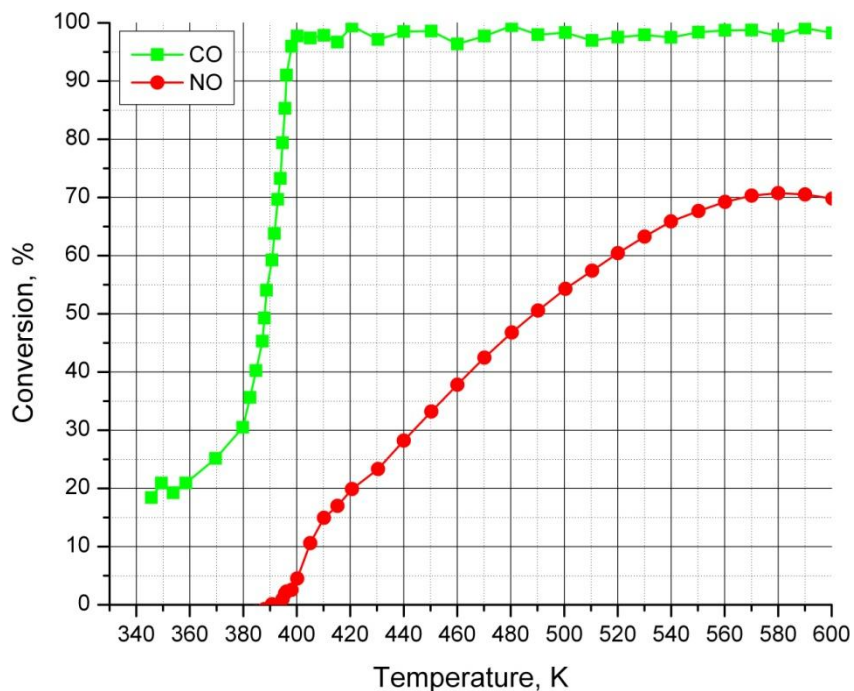


Figure 3-21: CO, NO, NO_x & NO₂ - Ignition curve Run 27

3.4.7 Mixture of CO, H₂, C₃H₆ and NO Oxidation

The final 27 experiments represent a full factorial analysis of all 3 reactants, CO/H₂, NO and C₃H₆, at low, medium and high concentrations. Table 3-9 gives the feed concentrations for these runs. The ignition curves are presented in Figure 3-22 to Figure 3-48. Each graph shows the conversion of CO and C₃H₆. The reactions involving NO are presented as total conversion of NO, conversion of NO to NO₂, conversion of NO to N₂O, and total NO_x conversion (i.e. conversion of NO_x to N₂).

It is seen that some reduction of NO_x occurs by reaction with C₃H₆, and that significant amounts of N₂O are formed. Furthermore, it is observed that under some conditions, the ignition curve for C₃H₆ is not smooth but rather exhibits a two step shape.

Table 3-9: CO, H₂, Propene & NO experiments, initial concentrations

Run	CO [ppm]	H2 [ppm]	Propene [ppm]	NO [ppm]
28	500	167	250	150
29	2000	666	250	150
30	500	167	750	150
31	2000	666	750	150
32	500	167	250	600
33	2000	666	250	600
34	500	167	750	600
35	2000	666	750	600
36	1000	333	250	150
37	1000	333	250	600
38	1000	333	750	150
39	1000	333	750	600
40	500	167	500	150
41	2000	666	500	150
42	500	167	500	600
43	2000	666	500	600
44	500	167	250	300
45	2000	666	250	300
46	500	167	750	300
47	2000	666	750	300
48	1000	333	500	150
49	1000	333	250	300
50	500	167	500	300
51	1000	333	500	300
52	2000	666	500	300
53	1000	333	750	300
54	1000	333	500	600

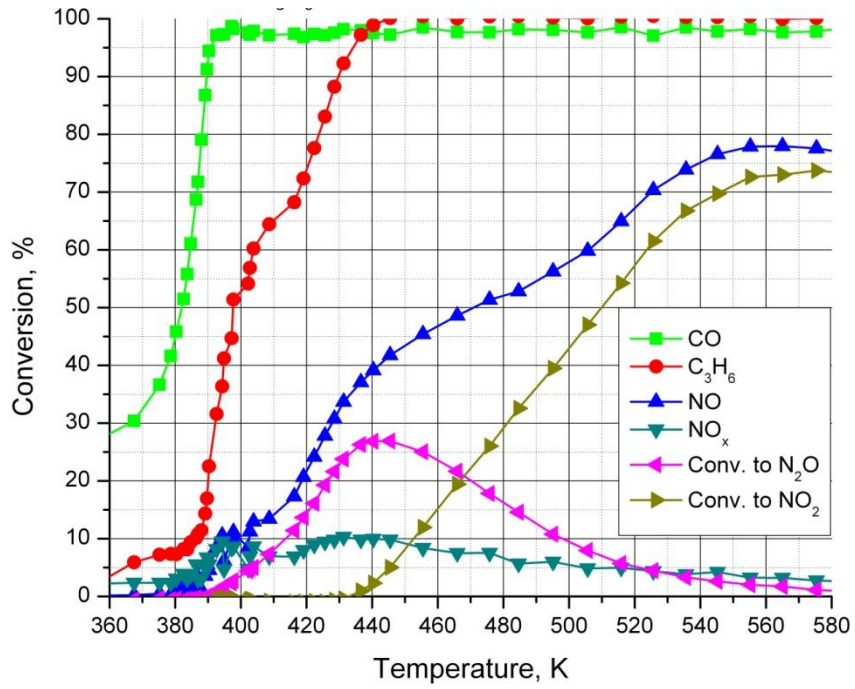


Figure 3-22: CO, C₃H₆, NO, NO_x, NO₂ & N₂O - Ignition curve Run 28

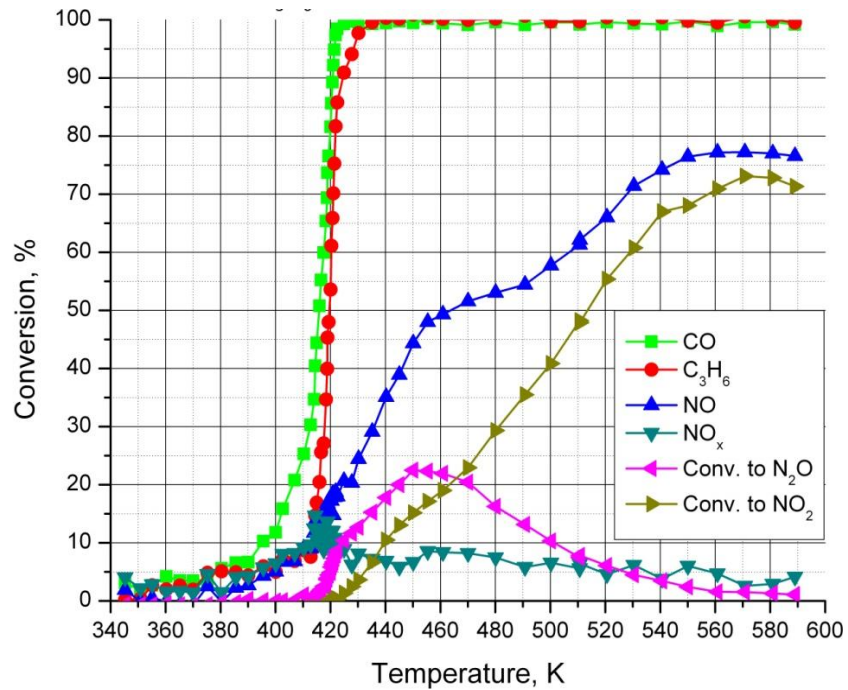


Figure 3-23: CO, C₃H₆, NO, NO_x, NO₂ & N₂O - Ignition curve Run 29

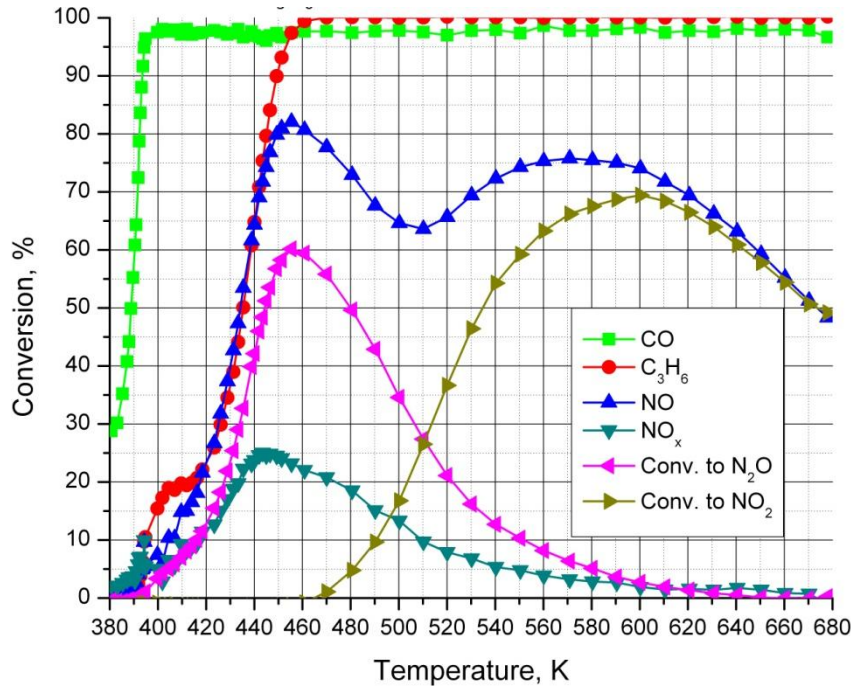


Figure 3-24: CO, C₃H₆, NO, NO_x, NO₂ & N₂O - Ignition curve Run 30

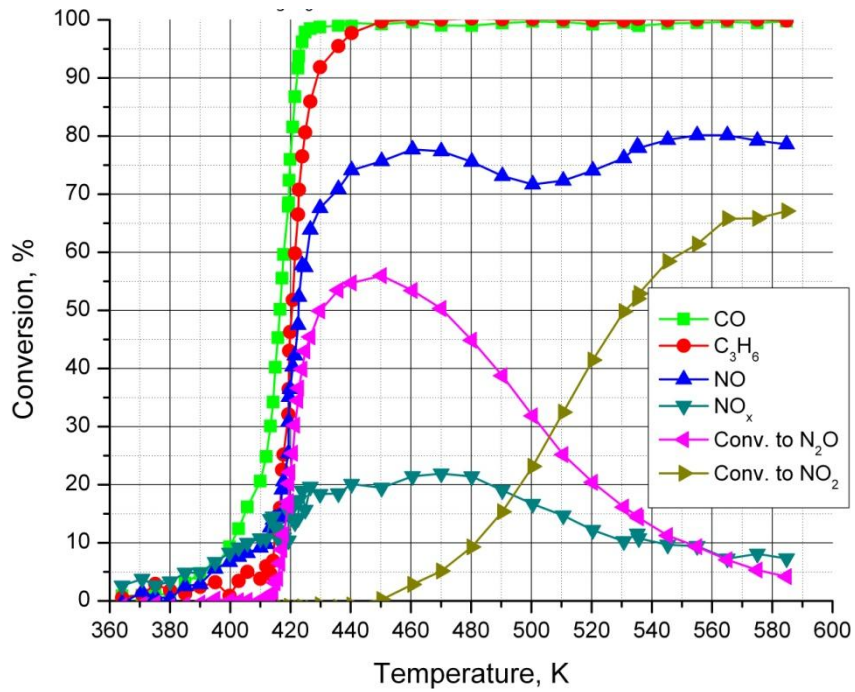


Figure 3-25: CO, C₃H₆, NO, NO_x, NO₂ & N₂O - Ignition curve Run 31

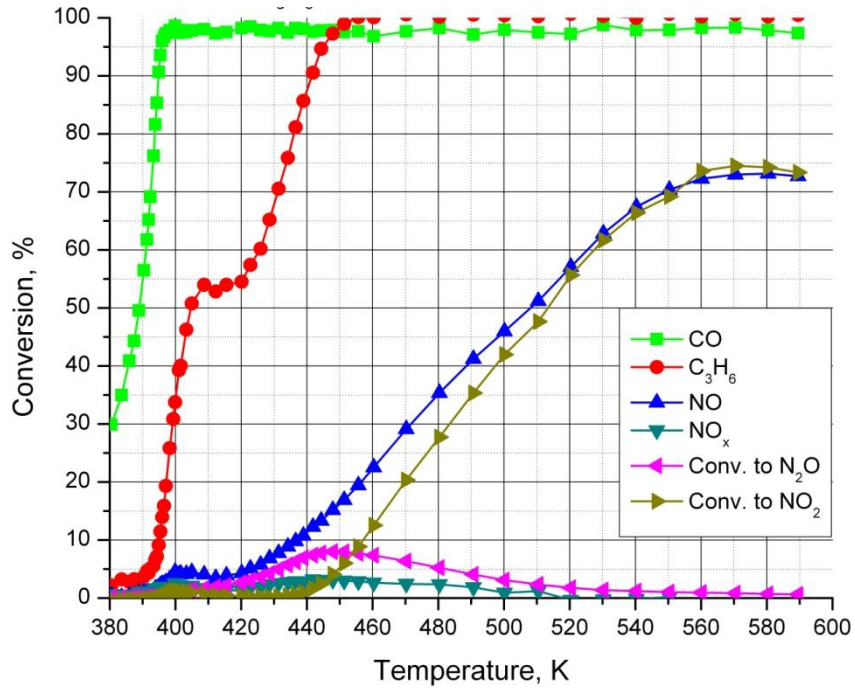


Figure 3-26: CO, C₃H₆, NO, NO_x, NO₂ & N₂O - Ignition curve Run 32

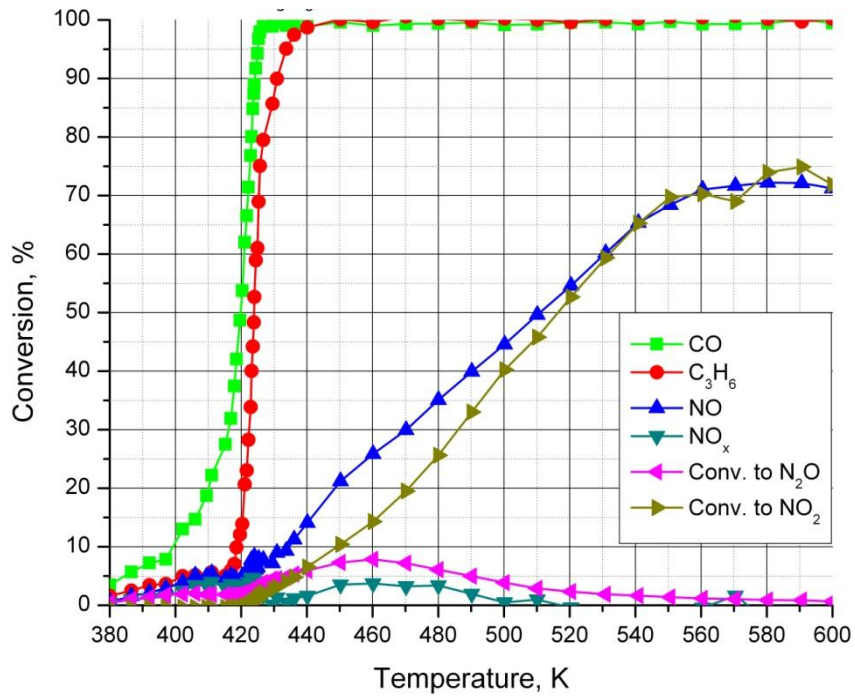


Figure 3-27: CO, C₃H₆, NO, NO_x, NO₂ & N₂O - Ignition curve Run 33

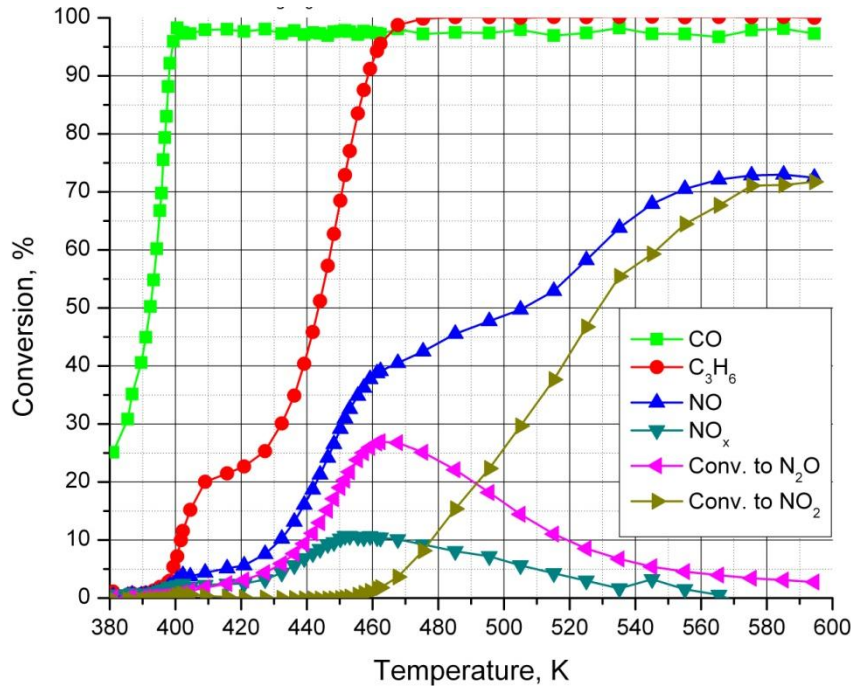


Figure 3-28: CO, C₃H₆, NO, NO_x, NO₂ & N₂O - Ignition curve Run 34

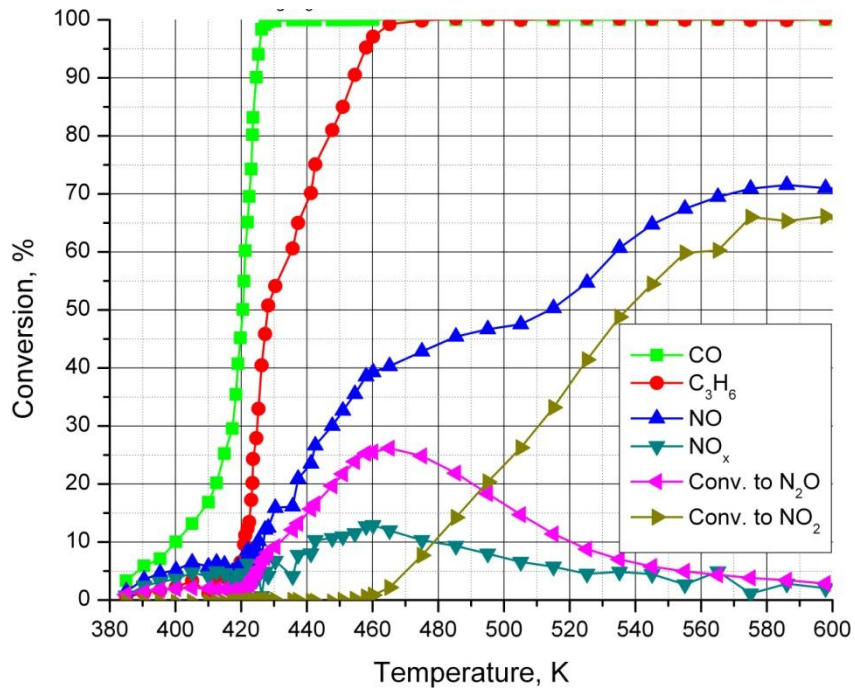


Figure 3-29: CO, C₃H₆, NO, NO_x, NO₂ & N₂O - Ignition curve Run 35

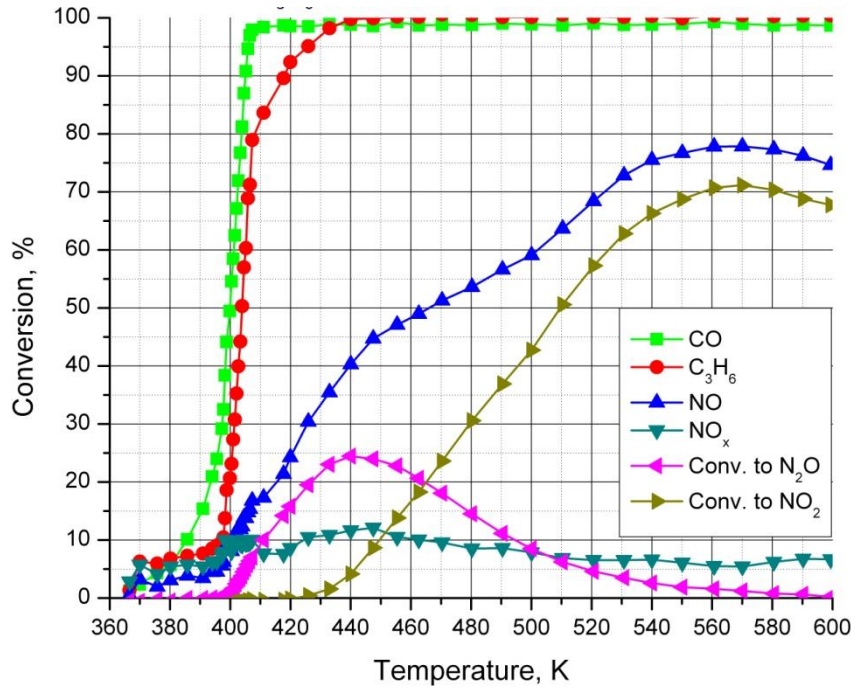


Figure 3-30: CO, C₃H₆, NO, NO_x, NO₂ & N₂O - Ignition curve Run 36

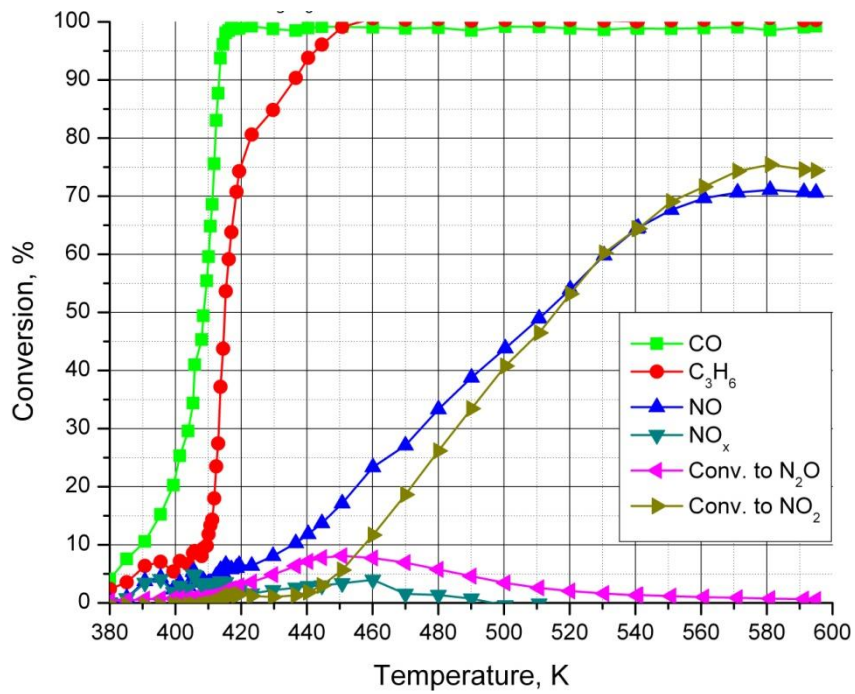


Figure 3-31: CO, C₃H₆, NO, NO_x, NO₂ & N₂O - Ignition curve Run 37

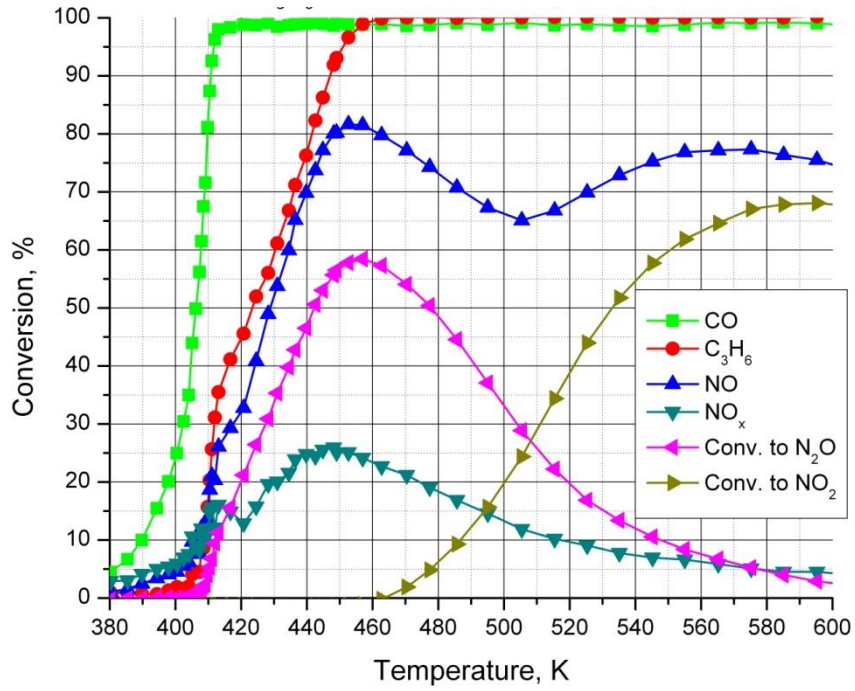


Figure 3-32: CO, C₃H₆, NO, NO_x, NO₂ & N₂O - Ignition curve Run 38

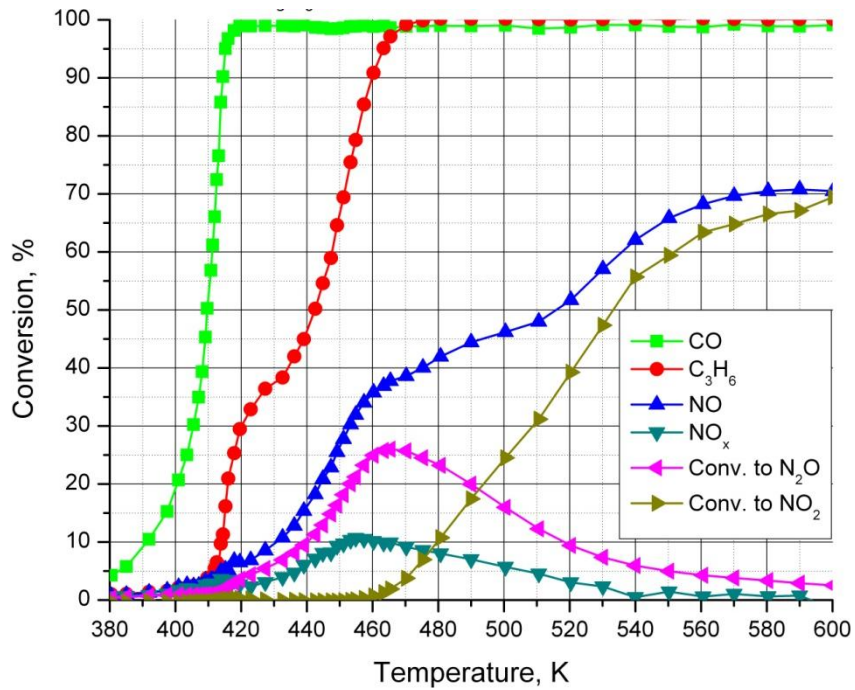


Figure 3-33: CO, C₃H₆, NO, NO_x, NO₂ & N₂O - Ignition curve Run 39

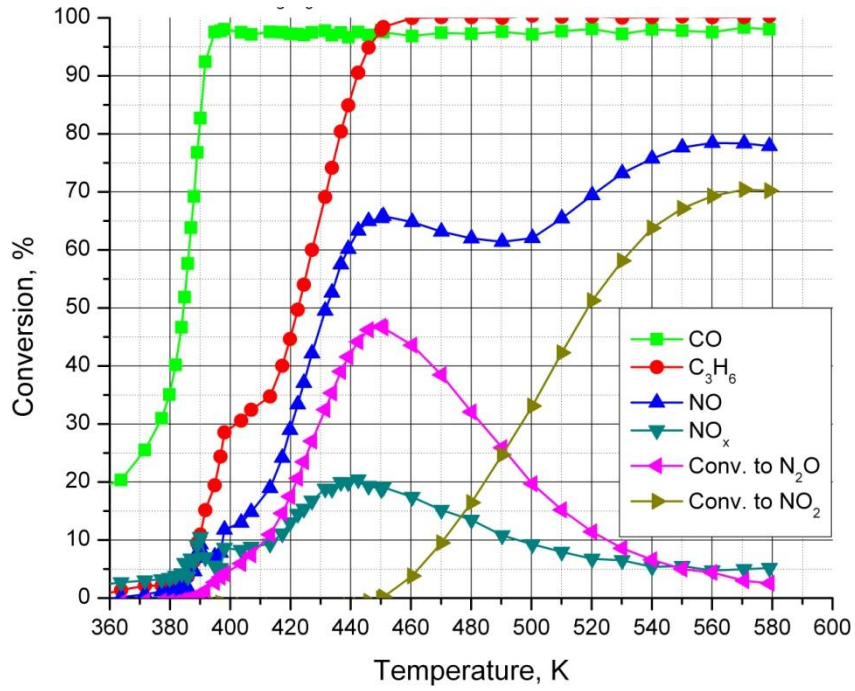


Figure 3-34: CO, C₃H₆, NO, NO_x, NO₂ & N₂O - Ignition curve Run 40

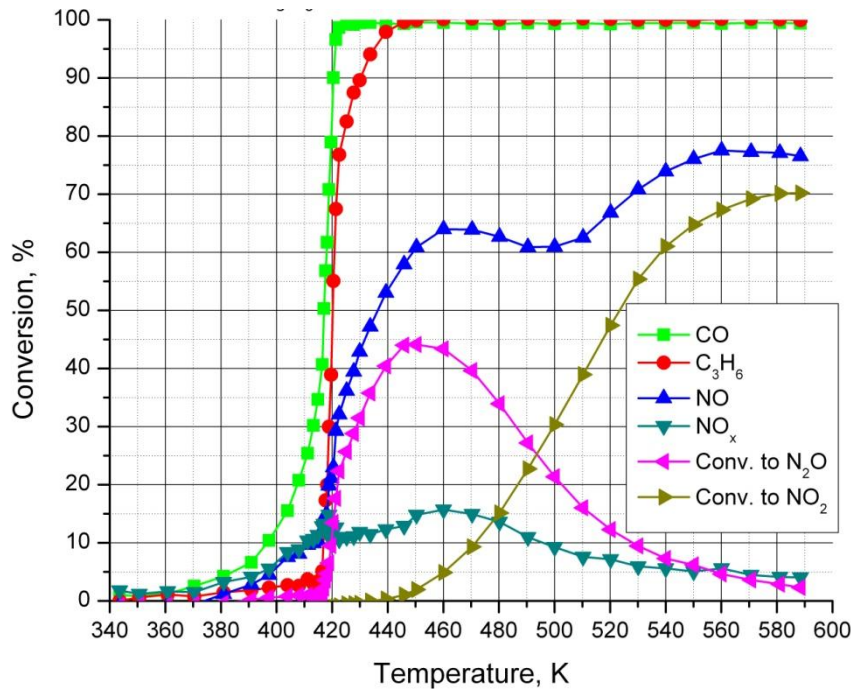


Figure 3-35: CO, C₃H₆, NO, NO_x, NO₂ & N₂O - Ignition curve Run 41

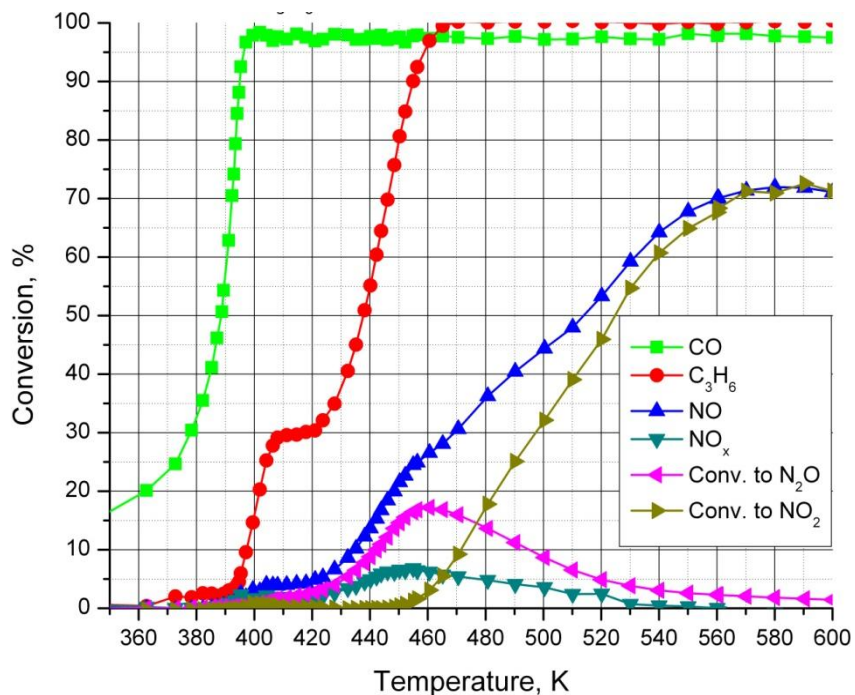


Figure 3-36: CO, C₃H₆, NO, NO_x, NO₂ & N₂O - Ignition curve Run 42

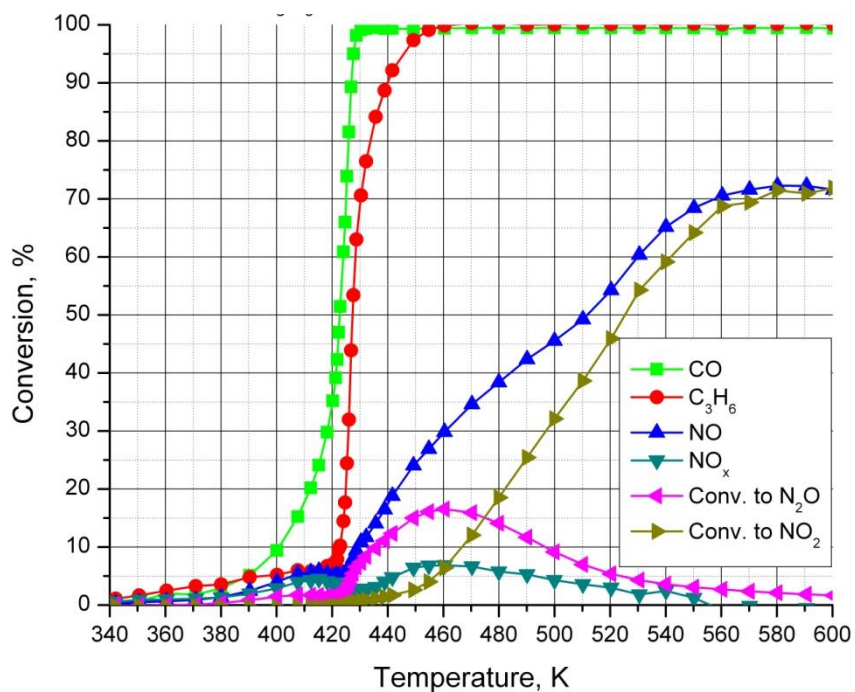


Figure 3-37: CO, C₃H₆, NO, NO_x, NO₂ & N₂O - Ignition curve Run 43

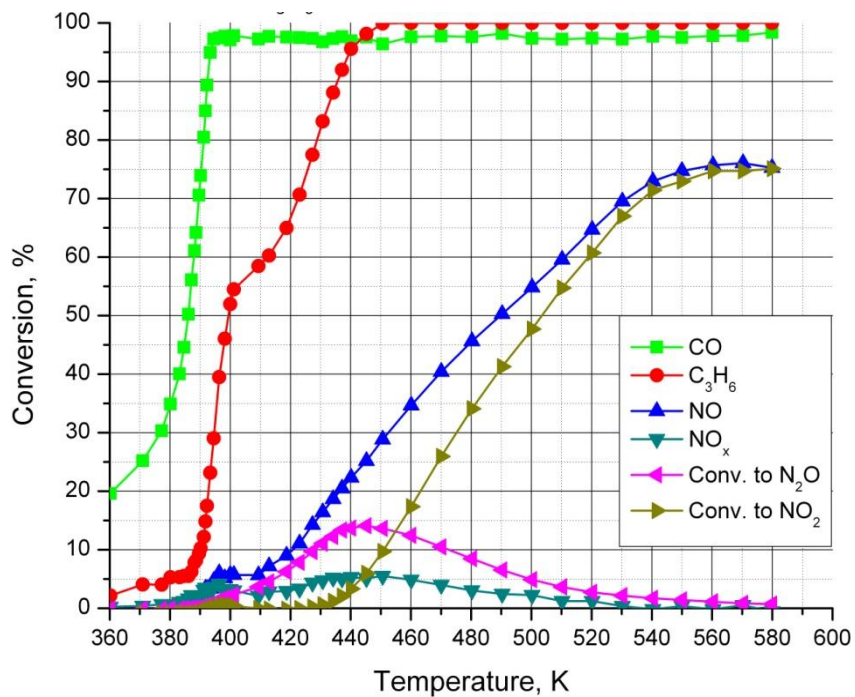


Figure 3-38: CO, C₃H₆, NO, NO_x, NO₂ & N₂O - Ignition curve Run 44

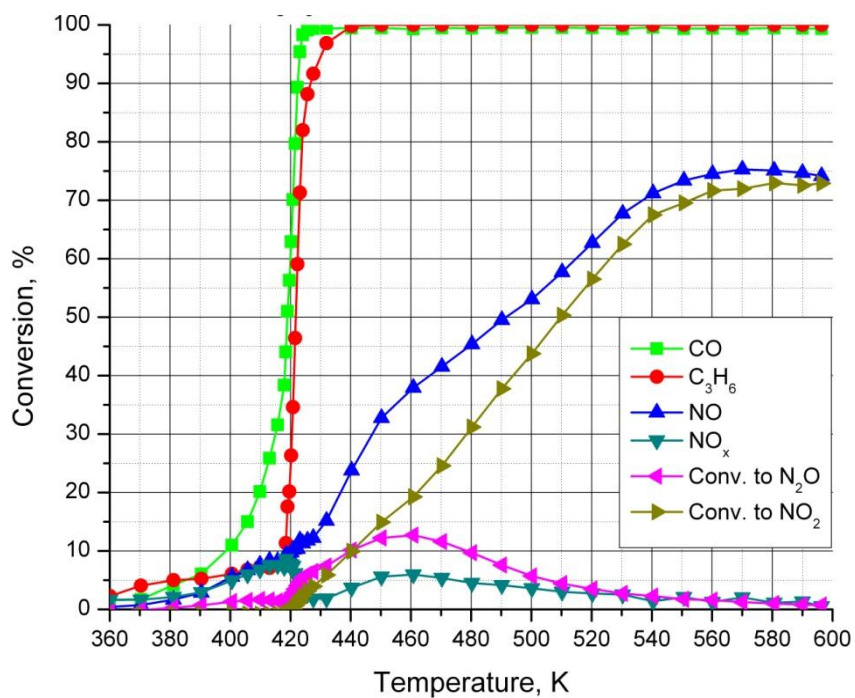


Figure 3-39: CO, C₃H₆, NO, NO_x, NO₂ & N₂O - Ignition curve Run 45

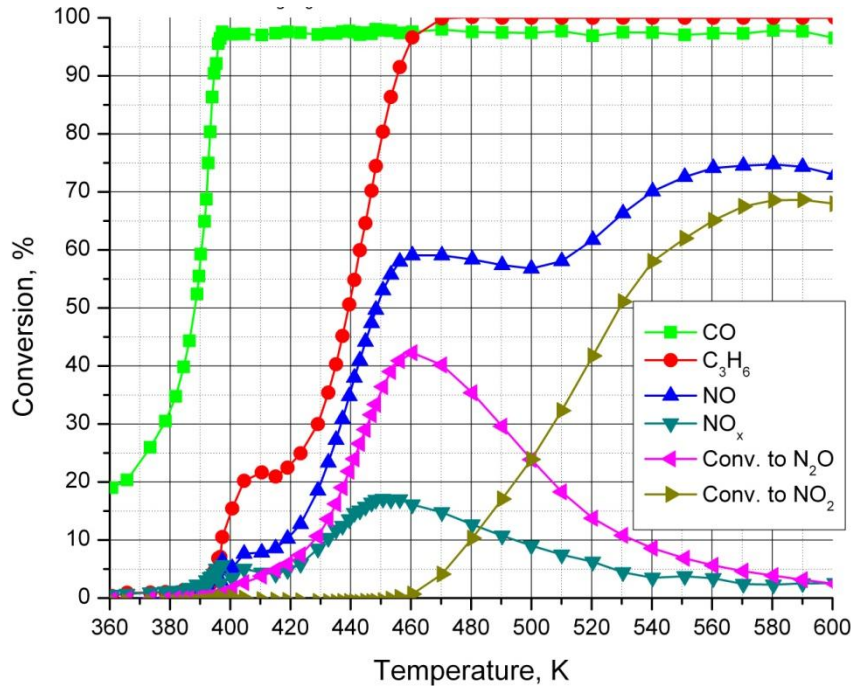


Figure 3-40: CO, C₃H₆, NO, NO_x, NO₂ & N₂O - Ignition curve Run 46

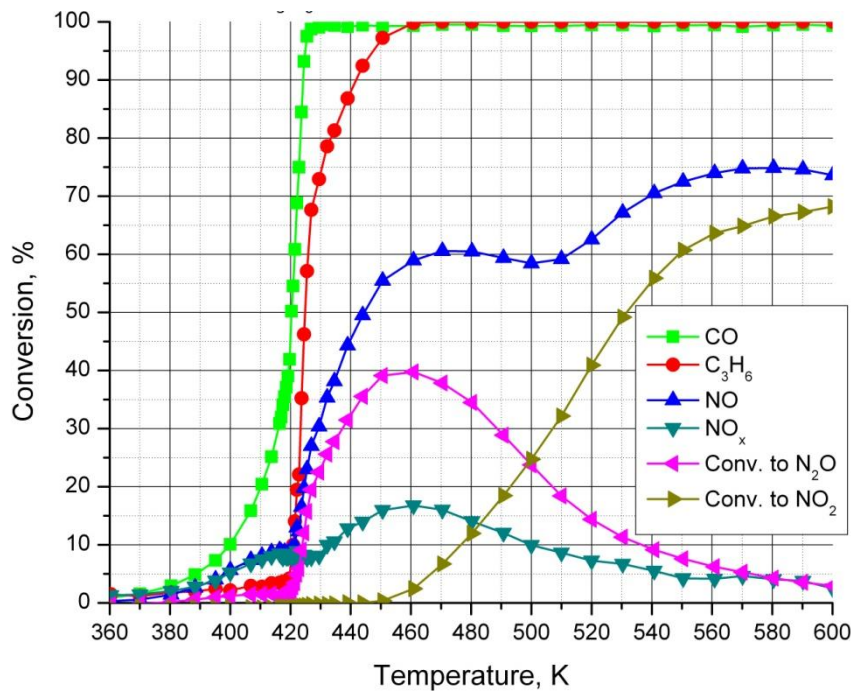


Figure 3-41: CO, C₃H₆, NO, NO_x, NO₂ & N₂O - Ignition curve Run 47

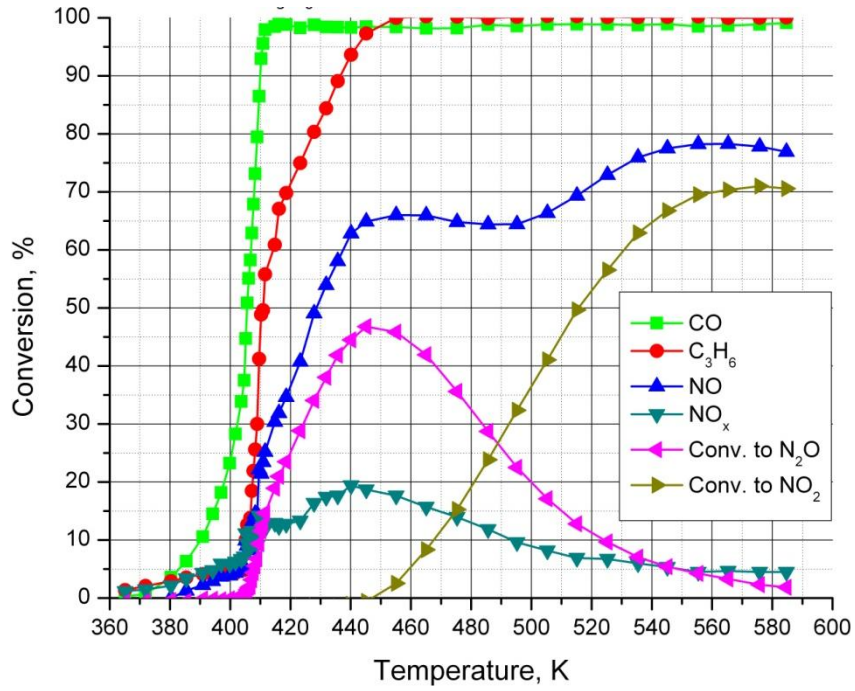


Figure 3-42: CO, C₃H₆, NO, NO_x, NO₂ & N₂O - Ignition curve Run 48

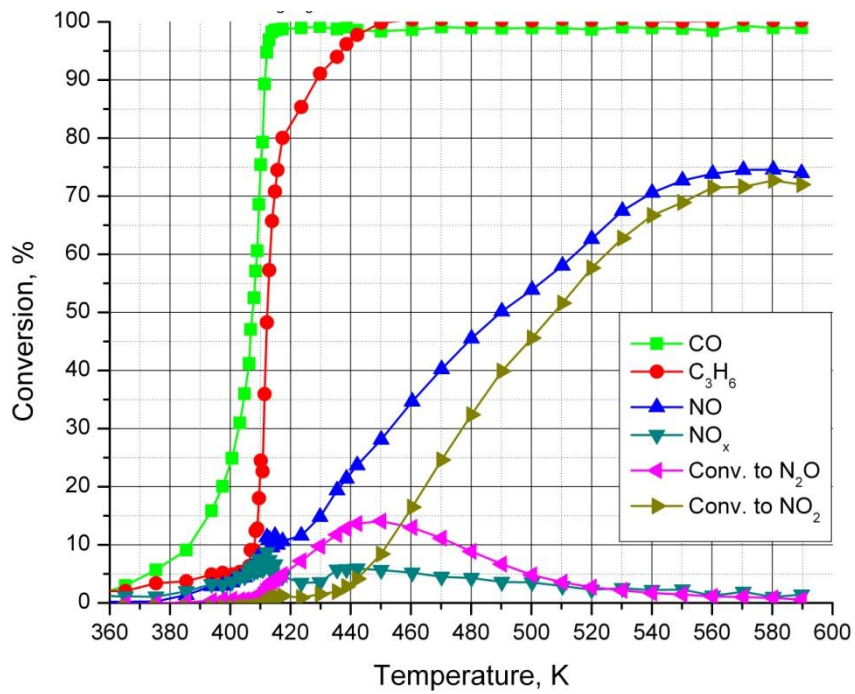


Figure 3-43: CO, C₃H₆, NO, NO_x, NO₂ & N₂O - Ignition curve Run 49

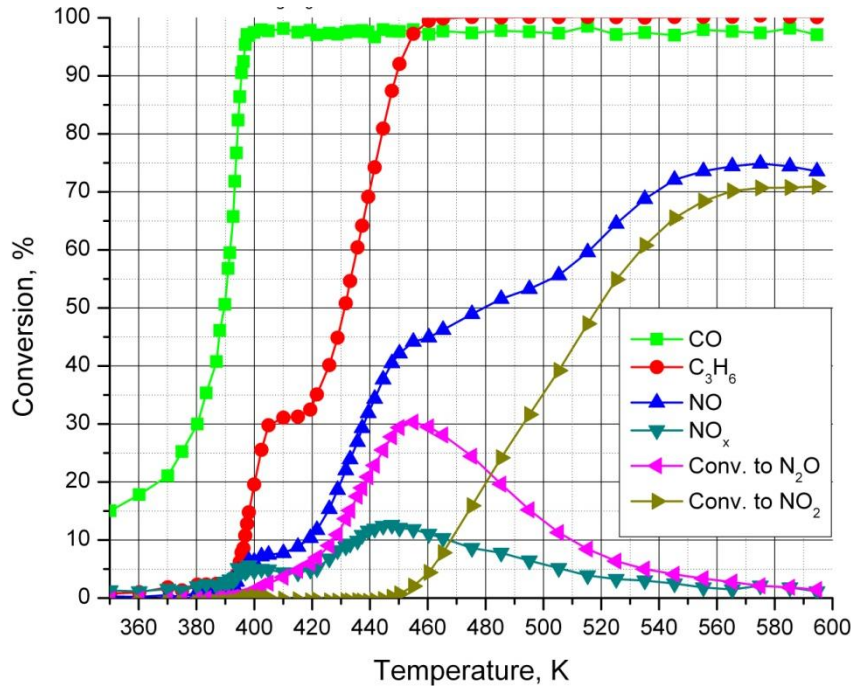


Figure 3-44: CO, C₃H₆, NO, NO_x, NO₂ & N₂O - Ignition curve Run 50

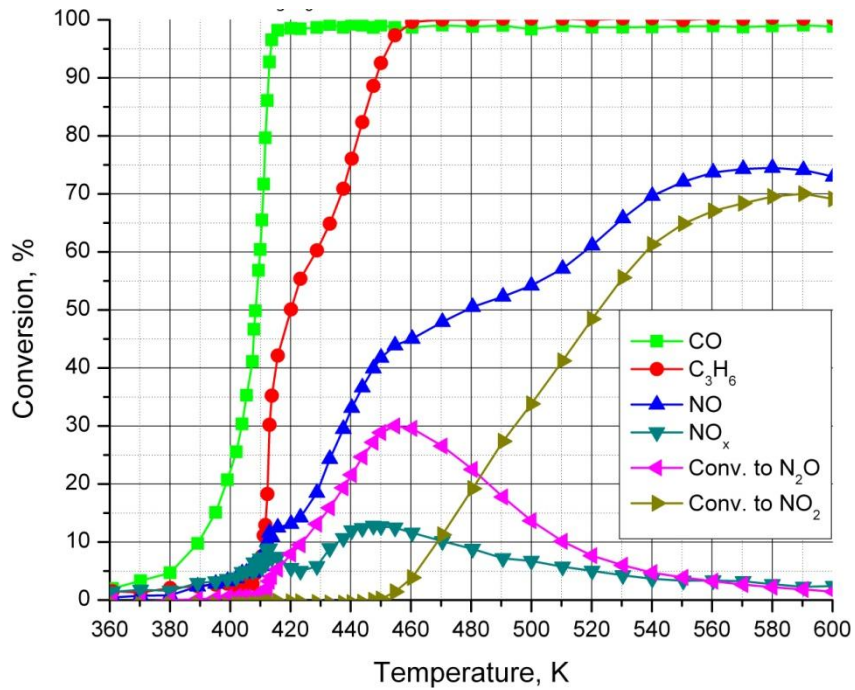


Figure 3-45: CO, C₃H₆, NO, NO_x, NO₂ & N₂O - Ignition curve Run 51

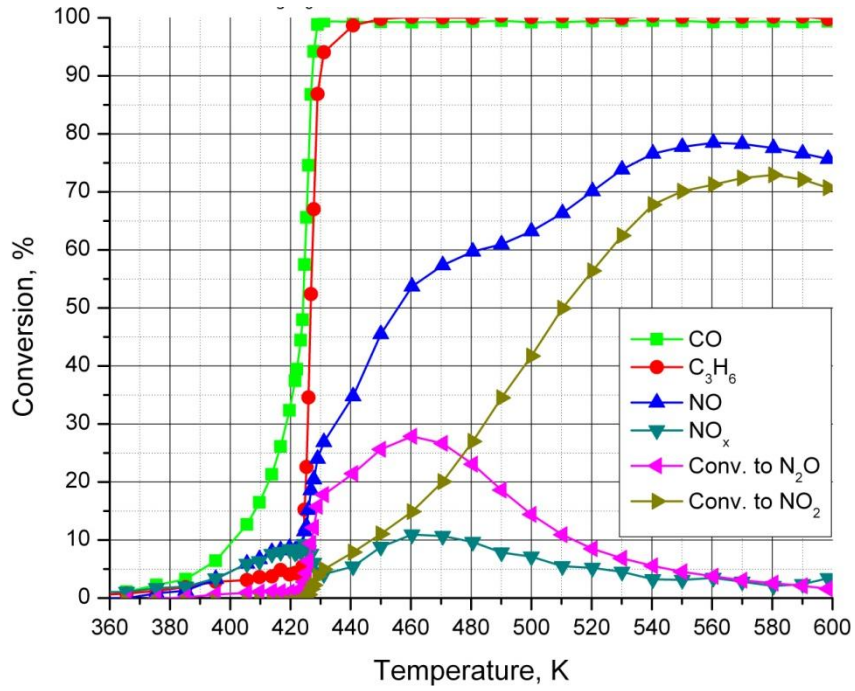


Figure 3-46: CO, C₃H₆, NO, NO_x, NO₂ & N₂O - Ignition curve Run 52

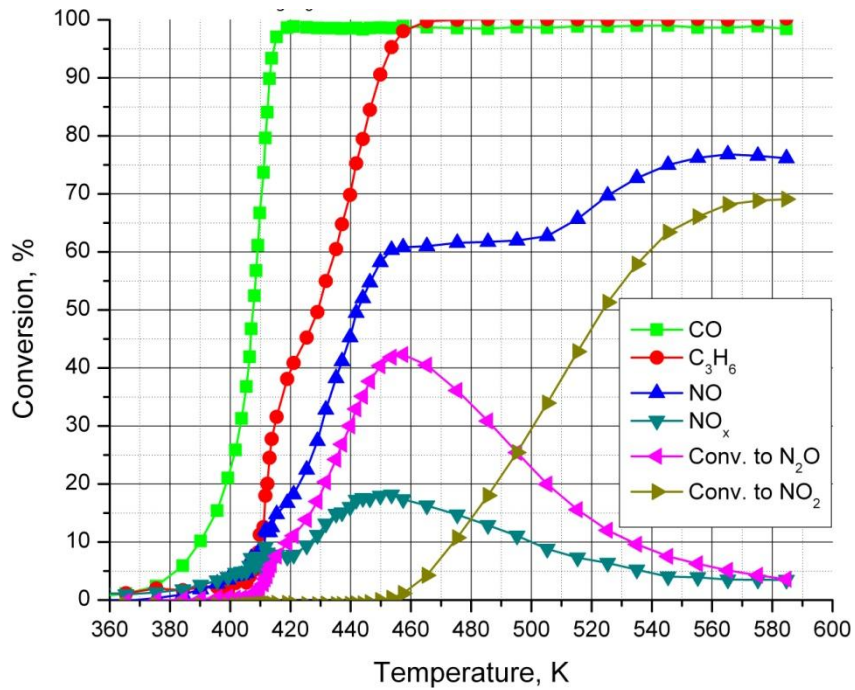


Figure 3-47: CO, C₃H₆, NO, NO_x, NO₂ & N₂O - Ignition curve Run 53

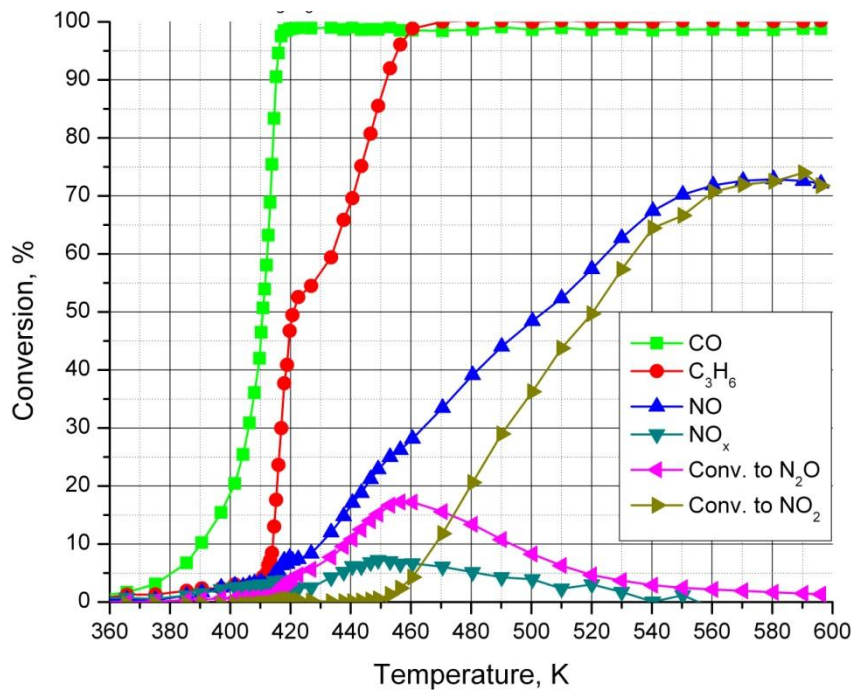


Figure 3-48: CO, C₃H₆, NO, NO_x, NO₂ & N₂O - Ignition curve Run 54

4 Modelling

4.1 Reactor Modelling

The main goal of this thesis was to develop and validate a kinetic model for the Pt-Pd diesel oxidation catalyst.

The validation of a proposed kinetic model requires the optimization of the parameters in it, which in turn requires an efficient and realistic reactor model, which can be coupled to an optimization routine. Because a very large number of reactor simulations must be performed during the optimization process, it is essential that the model execute very rapidly. To achieve the higher execution speed, some loss in physical realism must be accepted.

The catalyst used in this work consists of a washcoated monolith. There are different mathematical ways to model a monolith reactor. In single channel model (SCM), we assume that all channels in a monolith behave exactly the same so we can model just one channel. A single channel model was selected for this work.

Another important decision that we should make is to select modelling dimension. In one dimensional modeling which is simplest way of monolith modeling, we ignore radial or angular gradients of the parameters and consider all gradients only in axial direction. A two dimensional model considers axial and radial gradients but neglects angular possible changes in parameters. Finally in a 3 dimensional model, every possible gradients including axial, radial or angular should be considered. It is clear that increasing dimension of model can increase the accuracy of the model but at the same time this will increase dramatically execution time. More calculation means more demand for computational resources and will increase time required for doing such calculations. On the other hand, the difference between 1D and 2D or 3D models may not be significant. Researchers compared 1D and 2D models for simple experimental data and showed that the difference between 1D and 2D model in predicting temperature was just about 2 °C[23, 24]. Computational time for 1D models can be as low as,

or lower than $1/10^{\text{th}}$ time needed for 2D models, while a single iteration in 3D model can take more than 6 hours. We need a fast model which can be used in parameter optimization problem.

For the mole and energy balance equations, we have two choices:

1) Heterogeneous Model

We have to write separate mole and heat balance equations for solid phase (washcoat) and gas phase (reactants and products) and couple these two by mass and heat transfer coefficients.

2) Pseudo-homogenous Model

Solid and gas phase concentrations and temperatures are assumed to be the same.

The difference between heterogeneous and pseudo-homogeneous models depends on the reaction conditions. For conditions close to steady state, the observed differences between fluid and solid temperature and concentration may be small. However, regardless of the difference, it was felt that the improved performance of the pseudo-homogenous model was sufficient justification for its use.

The internal diffusion resistance was not included in the reactor model, again for reason of execution time. Therefore, it must be emphasized that the kinetic parameters represent a combination of kinetic constants and heat and mass transfer coefficients.

The flow in the channel was assumed to be plug flow. This assumption results in the conservation equations being first order ODE, or initial value problems. This gives the most efficient model.

A mole balance equation must be solved for every species in the reactor. Furthermore an energy balance equation must also be solved. However, for the reactor system used in this investigation, it was not possible to solve the energy balance. The reactor was located inside a furnace, and the heating rates are not

known. However, the linear temperature profile along the reactor was measured at four points along the axis. Therefore, the following methodology was adapted. For each reactor simulation, the experimentally measured temperatures were imposed in the reactor. Temperatures between the four measured points were determined by linear interpolation. The gas phase was then assumed to be in steady state with the imposed temperature profile. The modeled ignition curves are thus pseudo steady state curves. For the relatively slow temperature ramps used in this work, this methodology is not unreasonable.

The pseudo-homogenous plug flow reactor model mole balance equation can be written for species i as:

$$-\frac{\partial F_i}{\partial V_c} = (-R_i)_{V_c} \quad (4-1)$$

In equation 4-1 the reaction rate is based on the channel volume (V_c). Assume that the channel is a right circular cylinder of diameter D_H surrounded by an annular ring of washcoat with an outside diameter D_{wc} . The ratio of washcoat volume V_{wc} to the channel volume is then given by:

$$\frac{V_{wc}}{V_c} = \frac{D_{wc}^2 - D_H^2}{D_H^2} \quad (4-2)$$

The mole balance equation with the reaction rate expressed in terms of washcoat volume is:

$$-\frac{dF_i}{dV_c} = (-R_i)_{V_{wc}} \frac{D_{wc}^2 - D_H^2}{D_H^2} \quad (4-3)$$

We can express molar flow rate in terms of velocity and concentration:

$$-u_m C_f \frac{dY_i}{dz} = (-R_i)_{V_{wc}} \frac{D_{wc}^2 - D_H^2}{D_H^2} \quad (4-4)$$

Here u_m is the mean velocity and C_f is the total molar concentration given by the ideal gas law. Writing equation 4-3 explicitly in terms of derivatives and using the ideal gas law to calculate u_m and C_f gives us the following equation:

$$-\frac{dY_i}{dz} = (-R_i)_{V_{wc}} \frac{D_{wc}^2 - D_H^2}{D_H^2} \left(\frac{R_g T_{ref}}{P} \right) \left(\frac{1}{u_{m,ref}} \right) \quad (4-5)$$

Temperature at reference state is 298 K, P is taken as 101.325 KPa and the value for R_g is 8.314 J/(mol.K). Washcoat thickness is 51.9 microns. Inlet velocity at 298 K is 0.6117 m/s. Substituting these numbers in equation 4-5 gives us following equation for any species i .

$$-\frac{dY_i}{dz} = 7.688 \times 10^{-3} (-R_i)_{V_{wc}} \quad (4-6)$$

We measured concentration for five different species during the experiments, so we have to solve following five ODE simultaneously to calculate the concentration of each species as a function of distance from the inlet of the reactor. The equations are:

$$\frac{dY_{CO}}{dz} = -7.688 \times 10^{-3} (-R_{CO}) \quad (4-7)$$

$$\frac{dY_{C_3H_6}}{dz} = -7.688 \times 10^{-3} \left\{ (-R_{C_3H_6}) + \frac{1}{2} (-R_{NO})_{r1} + \frac{1}{2} (-R_{NO})_{r2} + (-R_{NO_2})_{r3} \right\} \quad (4-8)$$

$$\frac{dY_{NO}}{dz} = -7.688 \times 10^{-3} \left\{ (-R_{NO}) + (-R_{NO})_{r1} + (-R_{NO})_{r2} - (-R_{NO_2})_{r3} \right\} \quad (4-9)$$

$$\frac{dY_{NO_2}}{dz} = 7.688 \times 10^{-3} \left\{ (-R_{NO}) - (-R_{NO_2})_{r3} \right\} \quad (4-10)$$

$$\frac{dY_{N_2O}}{dz} = 7.688 \times 10^{-3} \left\{ \frac{1}{2} (-R_{NO})_{r2} \right\} \quad (4-11)$$

4.2 Kinetic Formulation

For each reaction term it is necessary to have a rate model.

There are two different approaches for modelling catalytic converters:

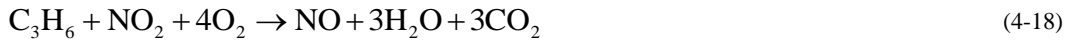
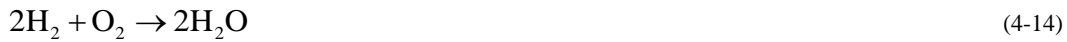
1) Mechanistic Model

This model contains lot of details regarding what is really happening on the surface of the catalyst and attempts to simulate exact chemical reactions over the catalyst surface.

2) Global Model

In this model, we just consider overall reactions happening on the surface regardless of what are the molecular steps of such reactions. This model is more empirical than a mechanistic model.

In this study we used the global modelling approach. The overall reactions can be written as:



In the following sections we introduce models that we used. Each model contains different parameters, which are defined in Arrhenius form:

$$k_i = A \exp\left(\frac{-E}{R_g T}\right) \quad (4-19)$$

$$K_i = B \exp\left(\frac{-H}{R_g T}\right) \quad (4-20)$$

Lower case k parameters represent kinetic constants while capital K parameters represent adsorption inhibition constants. To increase optimizer stability and speed, and to decrease data ranges for the pre-exponential factors, we changed definition of parameters a little bit as follows:

$$k_i = \exp\left(A_i - \frac{E_i}{R_g} \left[\frac{1}{T} - \frac{1}{450}\right]\right) \quad (4-21)$$

$$K_i = \exp\left(B_i - \frac{H_i}{R_g} \left[\frac{1}{T} - \frac{1}{450}\right]\right) \quad (4-22)$$

Sola [3] proposed five different models for the reactions of equations 4-7 to 4-11 for a platinum diesel oxidation catalyst. These models were used as a starting point for this study to see if they were valid for platinum – palladium catalyst. Following is a summary of the models proposed by Sola.

Each model has an equation for the oxidation of CO and C₃H₆. These equations are similar to those suggested by Voltz et al.[1]. The model for H₂ oxidation (not shown) is the same form as for CO oxidation, and uses the same constant values. The models for the oxidation of NO were inspired by various literature sources. The model for the reduction of NO by C₃H₆ was inspired by the work of Ansell et al. [25] and Pandya [2]. For each major model proposed, a variation was added that included the reduction of NO₂ to NO by C₃H₆. This rate was arbitrarily set to be 10 times faster than the rate of reduction of NO to N₂.

Model C_{1a}:

Oxidation of CO:

$$(-R_{\text{CO}}) = \frac{k_1 Y_{\text{CO}} Y_{\text{O}_2}}{T(1 + K_5 Y_{\text{CO}} + K_6 Y_{\text{C}_3\text{H}_6})^2 \left(1 + K_7 (Y_{\text{CO}} Y_{\text{C}_3\text{H}_6})^2\right) (1 + K_8 Y_{\text{NO}})} \quad (4-23)$$

Oxidation of propene:

$$(-R_{\text{C}_3\text{H}_6}) = \frac{k_3 Y_{\text{C}_3\text{H}_6} Y_{\text{O}_2}}{T(1 + K_5 Y_{\text{CO}} + K_6 Y_{\text{C}_3\text{H}_6})^2 \left(1 + K_7 (Y_{\text{CO}} Y_{\text{C}_3\text{H}_6})^2\right) (1 + K_8 Y_{\text{NO}})} \quad (4-24)$$

Oxidation of NO:

$$(-R_{\text{NO}}) = \frac{k_4 Y_{\text{NO}} Y_{\text{O}_2}^{0.5} [1 - \beta]}{T(1 + K_5 Y_{\text{CO}} + K_6 Y_{\text{C}_3\text{H}_6})^2 \left(1 + K_7 (Y_{\text{CO}} Y_{\text{C}_3\text{H}_6})^2\right) (1 + K_8 Y_{\text{NO}})} \quad (4-25)$$

$$\beta = \left[\frac{1}{K_{\text{eq}}} \frac{1}{\sqrt{P}} \frac{Y_{\text{NO}_2}}{Y_{\text{NO}} (Y_{\text{O}_2})^{0.5}} \right] \quad (4-26)$$

$$K_{\text{eq}} = \exp\left(5.045 + \frac{6.344 \times 10^3}{T} - 2.3 \ln(T) + 3.031 \times 10^{-3} T - 8.281 \times 10^{-7} T^2 + 1.142 \times 10^{-10} T^3\right) \quad (4-27)$$

Reduction of NO to N₂:

$$(-R_{\text{NO}})_{\text{r1}} = \frac{(-R_{\text{C}_3\text{H}_6}) k_2 Y_{\text{NO}}}{(1 + K_9 Y_{\text{O}_2})} \quad (4-28)$$

Reduction of NO to N₂O:

$$(-R_{\text{NO}})_{\text{r2}} = \frac{(-R_{\text{C}_3\text{H}_6}) k_{11} Y_{\text{NO}}}{(1 + K_9 Y_{\text{O}_2})} \quad (4-29)$$

Model C_{1b}: An equation for reduction of NO₂ by hydrocarbon was added to the original model.

$$(-R_{\text{NO}_2})_{\text{r3}} = \frac{(-R_{\text{C}_3\text{H}_6}) 10 k_2 Y_{\text{NO}_2}}{(1 + K_9 Y_{\text{O}_2})} \quad (4-30)$$

Model C_{2a}:

Oxidation of CO:

$$(-R_{\text{CO}}) = \frac{k_1 Y_{\text{CO}} Y_{\text{O}_2}}{T(1 + K_5 Y_{\text{CO}} + K_6 Y_{\text{C}_3\text{H}_6})^2 \left(1 + K_7 (Y_{\text{CO}} Y_{\text{C}_3\text{H}_6})^2\right) (1 + K_8 Y_{\text{NO}})} \quad (4-31)$$

Oxidation of propene:

$$(-R_{\text{C}_3\text{H}_6}) = \frac{k_3 Y_{\text{C}_3\text{H}_6} Y_{\text{O}_2}}{T(1 + K_5 Y_{\text{CO}} + K_6 Y_{\text{C}_3\text{H}_6})^2 \left(1 + K_7 (Y_{\text{CO}} Y_{\text{C}_3\text{H}_6})^2\right) (1 + K_8 Y_{\text{NO}})} \quad (4-32)$$

Oxidation of NO:

$$(-R_{\text{NO}}) = \frac{k_4 Y_{\text{NO}} Y_{\text{O}_2} [1 - \beta]}{T(1 + K_5 Y_{\text{CO}} + K_6 Y_{\text{C}_3\text{H}_6})^2 \left(1 + K_7 (Y_{\text{CO}} Y_{\text{C}_3\text{H}_6})^2\right) (Y_{\text{NO}} + K_{10} Y_{\text{NO}_2})} \quad (4-33)$$

$$\beta = \left[\frac{1}{K_{\text{eq}}} \frac{1}{\sqrt{P}} \frac{Y_{\text{NO}_2}}{Y_{\text{NO}} (Y_{\text{O}_2})^{0.5}} \right] \quad (4-34)$$

$$K_{\text{eq}} = \exp\left(5.045 + \frac{6.344 \times 10^3}{T} - 2.3 \ln(T) + 3.031 \times 10^{-3} T - 8.281 \times 10^{-7} T^2 + 1.142 \times 10^{-10} T^3\right) \quad (4-35)$$

Reduction of NO to N₂:

$$(-R_{\text{NO}})_{\text{r1}} = \frac{(-R_{\text{C}_3\text{H}_6}) k_2 Y_{\text{NO}}}{(1 + K_9 Y_{\text{O}_2})} \quad (4-36)$$

Reduction of NO to N₂O:

$$(-R_{\text{NO}})_{\text{r2}} = \frac{(-R_{\text{C}_3\text{H}_6}) k_{11} Y_{\text{NO}}}{(1 + K_9 Y_{\text{O}_2})} \quad (4-37)$$

Model C_{2b}: An equation for reduction of NO₂ by hydrocarbon was added to the original model.

$$(-R_{\text{NO}_2})_{\text{r3}} = \frac{(-R_{\text{C}_3\text{H}_6}) 10 k_2 Y_{\text{NO}_2}}{(1 + K_9 Y_{\text{O}_2})} \quad (4-38)$$

Model C_{3a}:

Oxidation of CO:

$$(-R_{\text{CO}}) = \frac{k_1 Y_{\text{CO}} Y_{\text{O}_2}}{T(1 + K_5 Y_{\text{CO}} + K_6 Y_{\text{C}_3\text{H}_6})^2 \left(1 + K_7 (Y_{\text{CO}} Y_{\text{C}_3\text{H}_6})^2\right) (1 + K_8 Y_{\text{NO}})} \quad (4-39)$$

Oxidation of propene:

$$(-R_{\text{C}_3\text{H}_6}) = \frac{k_3 Y_{\text{C}_3\text{H}_6} Y_{\text{O}_2}}{T(1 + K_5 Y_{\text{CO}} + K_6 Y_{\text{C}_3\text{H}_6})^2 \left(1 + K_7 (Y_{\text{CO}} Y_{\text{C}_3\text{H}_6})^2\right) (1 + K_8 Y_{\text{NO}})} \quad (4-40)$$

Oxidation of NO:

$$(-R_{\text{NO}}) = \frac{k_4 Y_{\text{O}_2}^{0.5} [1 - \beta^2]}{T(1 + K_5 Y_{\text{CO}} + K_6 Y_{\text{C}_3\text{H}_6})^2 \left(1 + K_7 (Y_{\text{CO}} Y_{\text{C}_3\text{H}_6})^2\right) \left(1 + K_8 Y_{\text{NO}} + K_{10} \frac{Y_{\text{NO}_2}}{Y_{\text{NO}}}\right)} \quad (4-41)$$

$$\beta = \left[\frac{1}{K_{\text{eq}}} \frac{1}{\sqrt{P}} \frac{Y_{\text{NO}_2}}{Y_{\text{NO}} (Y_{\text{O}_2})^{0.5}} \right] \quad (4-42)$$

$$K_{\text{eq}} = \exp\left(5.045 + \frac{6.344 \times 10^3}{T} - 2.3 \ln(T) + 3.031 \times 10^{-3} T - 8.281 \times 10^{-7} T^2 + 1.142 \times 10^{-10} T^3\right) \quad (4-43)$$

Reduction of NO to N₂:

$$(-R_{\text{NO}})_{\text{r1}} = \frac{(-R_{\text{C}_3\text{H}_6}) k_2 Y_{\text{NO}}}{(1 + K_9 Y_{\text{O}_2})} \quad (4-44)$$

Reduction of NO to N₂O:

$$(-R_{\text{NO}})_{\text{r2}} = \frac{(-R_{\text{C}_3\text{H}_6}) k_{11} Y_{\text{NO}}}{(1 + K_9 Y_{\text{O}_2})} \quad (4-45)$$

Model C_{3b}: An equation for reduction of NO₂ by hydrocarbon was added to the original model.

$$(-R_{\text{NO}_2})_{\text{r3}} = \frac{(-R_{\text{C}_3\text{H}_6}) 10 k_2 Y_{\text{NO}_2}}{(1 + K_9 Y_{\text{O}_2})} \quad (4-46)$$

Model C_{4a}:

Oxidation of CO:

$$(-R_{\text{CO}}) = \frac{k_1 Y_{\text{CO}} Y_{\text{O}_2}}{T(1 + K_5 Y_{\text{CO}} + K_6 Y_{\text{C}_3\text{H}_6})^2 \left(1 + K_7 (Y_{\text{CO}} Y_{\text{C}_3\text{H}_6})^2\right) (1 + K_8 Y_{\text{NO}})} \quad (4-47)$$

Oxidation of propene:

$$(-R_{\text{C}_3\text{H}_6}) = \frac{k_3 Y_{\text{C}_3\text{H}_6} Y_{\text{O}_2}}{T(1 + K_5 Y_{\text{CO}} + K_6 Y_{\text{C}_3\text{H}_6})^2 \left(1 + K_7 (Y_{\text{CO}} Y_{\text{C}_3\text{H}_6})^2\right) (1 + K_8 Y_{\text{NO}})} \quad (4-48)$$

Oxidation of NO:

$$(-R_{\text{NO}}) = \frac{k_4 Y_{\text{O}_2}^{0.5} [1 - \beta]}{T(1 + K_5 Y_{\text{CO}} + K_6 Y_{\text{C}_3\text{H}_6})^2 \left(1 + K_7 (Y_{\text{CO}} Y_{\text{C}_3\text{H}_6})^2\right) \left(1 + K_8 Y_{\text{NO}} + K_{10} \frac{Y_{\text{NO}_2}}{Y_{\text{NO}}}\right)} \quad (4-49)$$

$$\beta = \left[\frac{1}{K_{\text{eq}}} \frac{1}{\sqrt{P}} \frac{Y_{\text{NO}_2}}{Y_{\text{NO}} (Y_{\text{O}_2})^{0.5}} \right] \quad (4-50)$$

$$K_{\text{eq}} = \exp\left(5.045 + \frac{6.344 \times 10^3}{T} - 2.3 \ln(T) + 3.031 \times 10^{-3} T - 8.281 \times 10^{-7} T^2 + 1.142 \times 10^{-10} T^3\right) \quad (4-51)$$

Reduction of NO to N₂:

$$(-R_{\text{NO}})_{r1} = \frac{(-R_{\text{C}_3\text{H}_6}) k_2 Y_{\text{NO}}}{(1 + K_9 Y_{\text{O}_2})} \quad (4-52)$$

Reduction of NO to N₂O:

$$(-R_{\text{NO}})_{r2} = \frac{(-R_{\text{C}_3\text{H}_6}) k_{11} Y_{\text{NO}}}{(1 + K_9 Y_{\text{O}_2})} \quad (4-53)$$

Model C_{4b}: An equation for reduction of NO₂ by hydrocarbon was added to the original model.

$$(-R_{\text{NO}_2})_{r3} = \frac{(-R_{\text{C}_3\text{H}_6}) 10 k_2 Y_{\text{NO}_2}}{(1 + K_9 Y_{\text{O}_2})} \quad (4-54)$$

Model C_{5a}:

Oxidation of CO:

$$(-R_{\text{CO}}) = \frac{k_1 Y_{\text{CO}} Y_{\text{O}_2}}{T(1 + K_5 Y_{\text{CO}} + K_6 Y_{\text{C}_3\text{H}_6} + K_8 Y_{\text{NO}})^2} \quad (4-55)$$

Oxidation of propene:

$$(-R_{\text{C}_3\text{H}_6}) = \frac{k_3 Y_{\text{C}_3\text{H}_6} Y_{\text{O}_2}}{T(1 + K_5 Y_{\text{CO}} + K_6 Y_{\text{C}_3\text{H}_6} + K_8 Y_{\text{NO}})^2} \quad (4-56)$$

Oxidation of NO:

$$(-R_{\text{NO}}) = \frac{k_4 Y_{\text{NO}} Y_{\text{O}_2}^{0.5} [1 - \beta]}{T(1 + K_5 Y_{\text{CO}} + K_6 Y_{\text{C}_3\text{H}_6} + K_8 Y_{\text{NO}} + K_{10} Y_{\text{NO}_2})^2} \quad (4-57)$$

$$\beta = \left[\frac{1}{K_{\text{eq}}} \frac{1}{\sqrt{P}} \frac{Y_{\text{NO}_2}}{Y_{\text{NO}} (Y_{\text{O}_2})^{0.5}} \right] \quad (4-58)$$

$$K_{\text{eq}} = \exp\left(5.045 + \frac{6.344 \times 10^3}{T} - 2.3 \ln(T) + 3.031 \times 10^{-3} T - 8.281 \times 10^{-7} T^2 + 1.142 \times 10^{-10} T^3\right) \quad (4-59)$$

Reduction of NO to N₂:

$$(-R_{\text{NO}})_{\text{r1}} = \frac{(-R_{\text{C}_3\text{H}_6}) k_2 Y_{\text{NO}}}{(1 + K_9 Y_{\text{O}_2})} \quad (4-60)$$

Reduction of NO to N₂O:

$$(-R_{\text{NO}})_{\text{r2}} = \frac{(-R_{\text{C}_3\text{H}_6}) k_{11} Y_{\text{NO}}}{(1 + K_9 Y_{\text{O}_2})} \quad (4-61)$$

Model C_{5b}: An equation for reduction of NO₂ by hydrocarbon was added to the original model.

$$(-R_{\text{NO}_2})_{\text{r3}} = \frac{(-R_{\text{C}_3\text{H}_6}) 10 k_2 Y_{\text{NO}_2}}{(1 + K_9 Y_{\text{O}_2})} \quad (4-62)$$

Description for each parameter used in these models is available in Table 4-1.

Table 4-1: k_1 to k_4 , K_5 to K_{10} and k_{11} parameter description

Parameter		Description of Parameter
k_1	A_1	pre-exponential factor, CO oxidation rate constant
	E_1	activation energy, CO oxidation rate constant
k_2	A_2	pre-exponential factor, NO reduction rate constant (N_2)
	E_2	activation energy, NO reduction rate constant (N_2)
k_3	A_3	pre-exponential factor, C_3H_6 oxidation rate constant
	E_3	activation energy, C_3H_6 oxidation rate constant
k_4	A_4	pre-exponential factor, NO oxidation rate constant
	E_4	activation energy, NO oxidation rate constant
K_5	B_5	pre-exponential factor, CO adsorption inhibition term
	H_5	activation energy, CO adsorption inhibition term
K_6	B_6	pre-exponential factor, C_3H_6 adsorption inhibition term
	H_6	activation energy, C_3H_6 adsorption inhibition term
K_7	B_7	pre-exponential factor, CO/ C_3H_6 mixture adsorption inhibition term
	H_7	activation energy, CO/ C_3H_6 mixture adsorption inhibition term
K_8	B_8	pre-exponential factor, NO adsorption inhibition term
	H_8	activation energy, NO adsorption inhibition term
K_9	B_9	pre-exponential factor, O_2 adsorption inhibition term
	H_9	activation energy, O_2 adsorption inhibition term
K_{10}	B_{10}	pre-exponential factor, NO_2 adsorption inhibition term
	H_{10}	activation energy, NO_2 adsorption inhibition term
k_{11}	A_{11}	pre-exponential factor, NO reduction rate constant (N_2O)
	E_{11}	activation energy, NO reduction rate constant (N_2O)

4.3 Parameter Estimation

The principal objective of this research was to find a global kinetic model for the Pt-Pd diesel oxidation catalyst. To fit our models to experimental data, we have to have an efficient optimizer that can scan the whole range of data for each parameter, and then to find the best combination for parameters which gives the minimum error between experimental data and modelling results.

At first it is necessary to define the objective function and then to minimize it using the proper optimization procedure. At first, a set of parameters and a model have to be selected. We used a MATLAB code to solve the appropriate

differential equations simultaneously. Because computation time was important, NAG toolbox solver, “d02ej” was used to solve stiff differential equations, which is almost two times faster than regular MATLAB solvers (e.g. ode15s or ode45).

This gives the mole fraction of each species as a function of temperature. The fractional conversions are defined as follows:

$$\text{CO:} \quad X_{\text{CO}} = \frac{(Y_{\text{CO}})_0 - (Y_{\text{CO}})_f}{(Y_{\text{CO}})_0} \quad (4-63)$$

$$\text{C}_3\text{H}_6: \quad X_{\text{C}_3\text{H}_6} = \frac{(Y_{\text{C}_3\text{H}_6})_0 - (Y_{\text{C}_3\text{H}_6})_f}{(Y_{\text{C}_3\text{H}_6})_0} \quad (4-64)$$

$$\text{NO:} \quad X_{\text{NO}} = \frac{(Y_{\text{NO}})_0 - (Y_{\text{NO}})_f}{(Y_{\text{NO}})_0} \quad (4-65)$$

$$\text{NO to NO}_2: \quad X_{\text{NO}_2} = \frac{(Y_{\text{NO}_2})_f}{(Y_{\text{NO}})_0} \quad (4-66)$$

$$\text{NO to N}_2\text{O:} \quad X_{\text{N}_2\text{O}} = \frac{2(Y_{\text{N}_2\text{O}})_f}{(Y_{\text{NO}})_0} \quad (4-67)$$

$$\text{Total NO}_x: \quad X_{\text{NO}_x} = \frac{(Y_{\text{NO}})_0 - [(Y_{\text{NO}})_f + 2(Y_{\text{N}_2\text{O}})_f + (Y_{\text{NO}_2})_f]}{(Y_{\text{NO}})_0} \quad (4-68)$$

Fractional conversions were calculated for both experimental data and modelling results. Minimum square rule was applied to them using the following equations:

$$\text{CO:} \quad O_{\text{CO}} = \frac{1}{n} \sum_{i=1}^n [(X_{\text{CO}})_{\text{pred}} - (X_{\text{CO}})_{\text{exp}}]^2 \quad (4-69)$$

$$\text{C}_3\text{H}_6: \quad O_{\text{C}_3\text{H}_6} = \frac{1}{n} \sum_{i=1}^n [(X_{\text{C}_3\text{H}_6})_{\text{pred}} - (X_{\text{C}_3\text{H}_6})_{\text{exp}}]^2 \quad (4-70)$$

$$\text{Total NO: } O_{\text{NO}} = \frac{1}{n} \sum_{i=1}^n \left[(X_{\text{NO}})_{\text{pred}} - (X_{\text{NO}})_{\text{exp}} \right]^2 \quad (4-71)$$

$$\text{NO to NO}_2: O_{\text{NO}_2} = \frac{1}{n} \sum_{i=1}^n \left[(X_{\text{NO}_2})_{\text{pred}} - (X_{\text{NO}_2})_{\text{exp}} \right]^2 \quad (4-72)$$

$$\text{NO to N}_2\text{O: } O_{\text{N}_2\text{O}} = \frac{1}{n} \sum_{i=1}^n \left[(X_{\text{N}_2\text{O}})_{\text{pred}} - (X_{\text{N}_2\text{O}})_{\text{exp}} \right]^2 \quad (4-73)$$

$$\text{Total NO}_x: O_{\text{NO}_x} = \frac{1}{n} \sum_{i=1}^n \left[(X_{\text{NO}_x})_{\text{pred}} - (X_{\text{NO}_x})_{\text{exp}} \right]^2 \quad (4-74)$$

The total objective function is the sum of all of the above equations except for the total NO. Thus:

$$O_{\text{Total}} = O_{\text{CO}} + O_{\text{C}_3\text{H}_6} + O_{\text{NO}_x} + O_{\text{N}_2\text{O}} + O_{\text{NO}_2} \quad (4-75)$$

An optimization procedure is required to minimize the objective function. Sola used a General Pattern Search (GPS) algorithm. The GPS is a gradient free method, thus computation of the gradients is not necessary. This method can thus be easily coupled to “black box” solvers. In the case where the solver returns an invalid result e.g. division by zero, the optimizer can simply discard the result and continue without halting [3].

Though GPS is a very powerful algorithm to find a global minimum, it has some drawbacks for this problem. There are 22 different parameters and parameters ranges in our problem are so wide that the GPS was very time consuming.

We decided to use one of the MATLAB predefined algorithms called fmincon. fmincon is a gradient based algorithm which attempts to find a constrained minimum of a scalar multivariable function starting at an initial point [26]. Providing a reasonable initial point for fmincon can significantly increase accuracy of the results. fmincon can trap into local minima easily if the initial

point is not wisely chosen. So we have to find a good way to determine an initial point that will lead to a good solution.

Genetic Algorithm (GA) was used as a preliminary optimizer to locate reasonable initial points to start `fmincon`.

The GA is a non-gradient method which can be used for solving both constrained and unconstrained problems. Basically, it works based on *biological evolution* theory. At each step, GA uses a pair of current population as parents to produce children for next generation. Over successive generations, the population evolves toward an optimal solution. There are three main rules which GA uses to produce the next generation from current populations:

- *Selection rules*: Procedures for selecting parents.
- *Crossover rules*: Procedures for combining two parents to form children.
- *Mutation rules*: Procedures for applying random changes to individual parents to form children [27].

We used GA to scan whole data ranges to find best initial value for `fmincon`. This initial value was used by `fmincon` to find global minimum for our objective function. Combining these two methods gave better results in comparison with GPS algorithm. Determined parameters in both `fmincon` and GA for MATLAB users can be found in Table 4-2 and Table 4-3.

Table 4-2: Genetic Algorithm parameters

EliteCount	5
CrossoverFraction	0.3
PopulationSize	80
Generations	70
StallGenLimit	30
TolFun	1e-10

Table 4-3: `fmincon` parameters

Algorithm	Interior Point
TolFun	1e-10
TolX	1e-18
TolCon	1e-2
FinDiffType	central
MaxFunEval	20000

5 Results

In this chapter, modelling results for different experiments are presented. Following the methodology of Sola, both individual experiments and sets of experiments were optimized. It is expected that it is easier to fit single experiments; however, it is necessary to have a single set of parameters that can fit all experiments if a general model is to be developed.

5.1 Modelling of CO Oxidation

In the first five experiments, the only reacting compounds are CO and H₂. Although we have 5 different models, for experiments with CO only, models are the same. We have to optimize only k₁ and K₅ in this case. Initial concentrations for these runs are available in Table 5-1.

Table 5-1: CO, H₂ only experiments, initial concentrations

Run	CO, ppm	H ₂ , ppm
1	500	167
2(a)	1000	333
2(b)	1000	333
2(c)	1000	0
3	2000	666

Oxidation of CO:

$$(-R_{\text{CO}}) = \frac{k_1 Y_{\text{CO}} Y_{\text{O}_2}}{T(1 + K_5 Y_{\text{CO}})^2} \quad (5-1)$$

Following are the results for CO only oxidation case when each experiment was optimized separately. The parameter values are presented in Table 5-2 and the experimental and predicted conversions are given in Figure 5-1.

Table 5-2: Runs 1-3 individual optimization results

Parameter		LB	HB	Run 1	Run 2(a)	Run 2(b)	Run 2(c)	Run 3
k ₁	A ₁	0	30	19.8	24.7	20.4	28.1	21.3
	E ₁	20000	150000	22560	114664	62296	143996	50325
K ₅	B ₅	0	30	6.66	8.87	3.77	8.80	5.82
	H ₅	-150000	0	-44731	-17806	-120772	-74607	-108183
Cumulative Residual				78	26	16	84	27

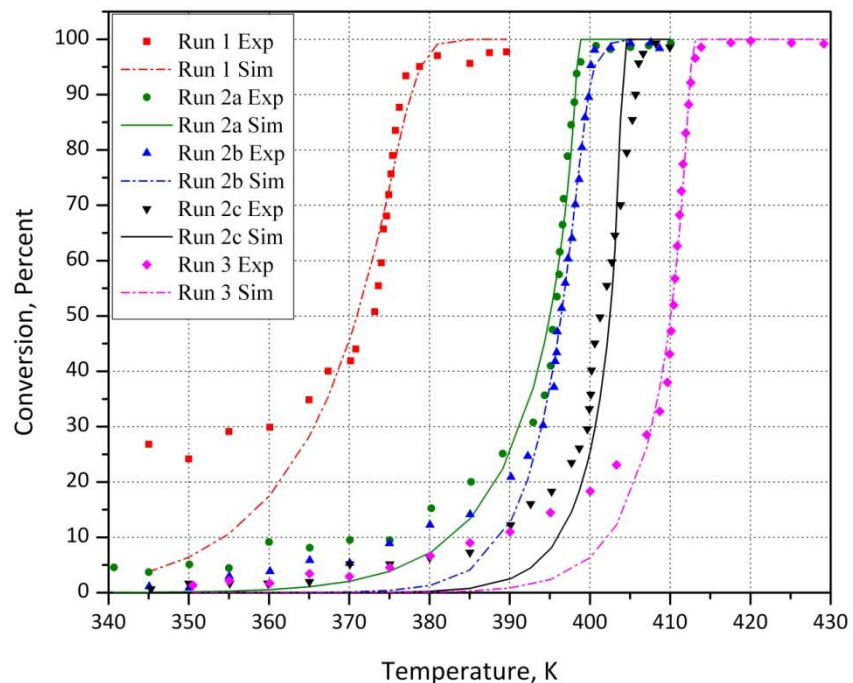


Figure 5-1: Individual optimization result vs. Experimental data, Run 1-3

Generally, it is seen that the fits are reasonable, although the initial portion of the curve is not reproduced well. This is particularly true for the experiment with the lowest concentration, 500 ppm. Experiments 2(a) and 2(b) were the same, and experiment 2(c) did not contain hydrogen. Therefore, the next step was to optimize experiments 1, 2(b) and 3 simultaneously. The results are shown in Table 5-3 and Figure 5-2.

Table 5-3: Runs 1, 2b & 3 simultaneous optimization results

Parameter	LB	HB	Run 1	Run 2(b)	Run 3
k_1	A_1	0	30	19.6	
	E_1	20000	150000	20132	
K_5	B_5	0	30	7.11	
	H_5	-150000	0	-36285	
Cumulative Residual			114	255	202

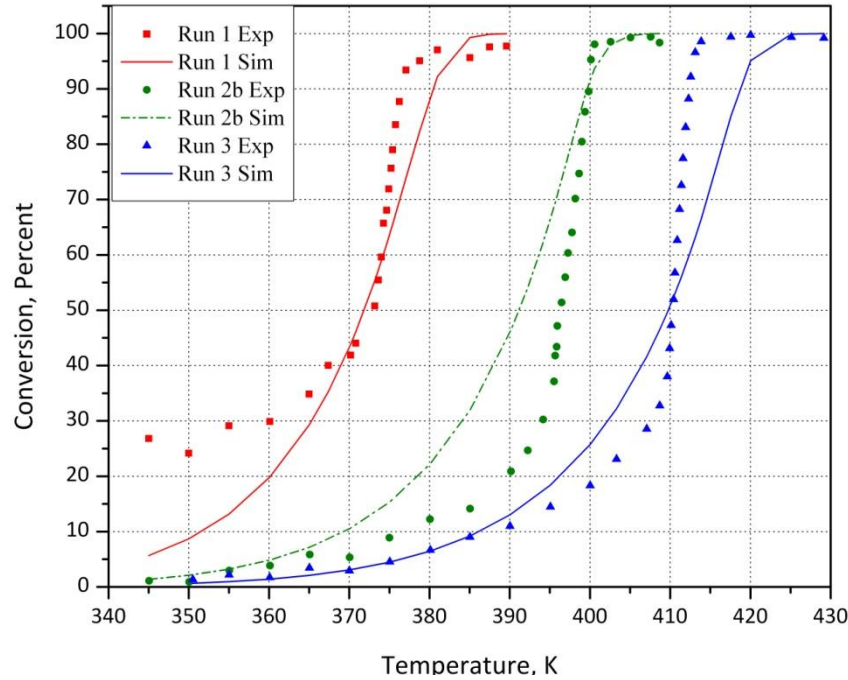


Figure 5-2: Simultaneous modelling result vs. Experimental data, Runs 1, 2b & 3

The low concentration run tends to weight the results, and a closer match can be obtained by fitting experiments 2(a), 2(b) and 3 simultaneously. These results are presented in Table 5-4 and Figure 5-3.

Table 5-4: Runs 2a, 2b & 3 simultaneous optimization results

Parameter	LB	HB	Run 2(a)	Run 2(b)	Run 3
k_1	A_1	0	30	25.2	
	E_1	20000	150000	93762	
K_5	B_5	0	30	9.62	
	H_5	-150000	0	-16966	
Cumulative Residual			59	41	33

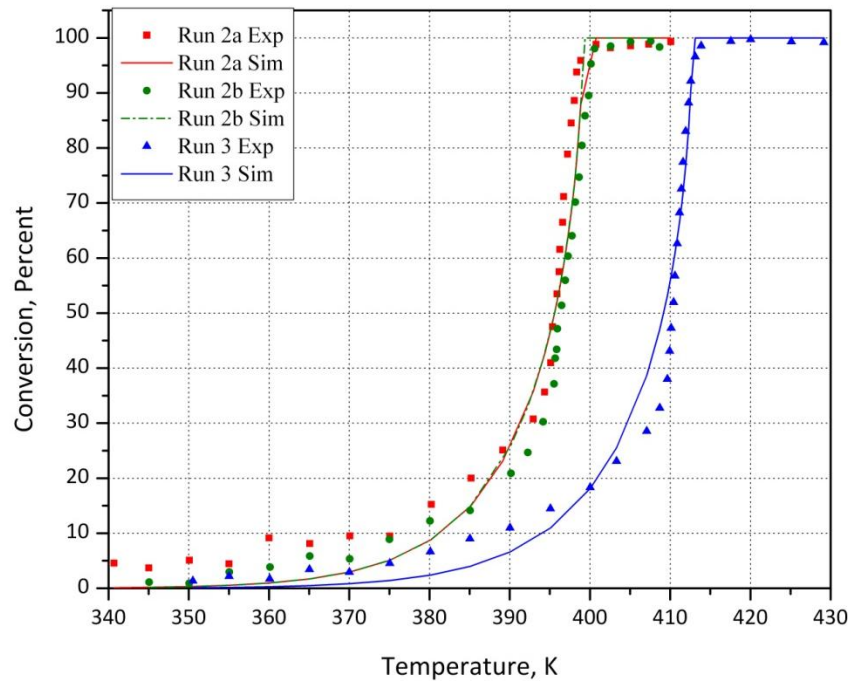


Figure 5-3: Simultaneous modelling result vs. Experimental data, Runs 2a, 2b & 3

With these results, it is seen that the model can predict CO oxidation very well at higher concentrations, although there is still some discrepancy for the initial part of the curve.

5.2 Modelling of C₃H₆ Oxidation

The next step was to optimize the experiments with propene only in the feed. Table 5-5 presents the initial concentration of the suitable experiments.

Table 5-6 and Figure 5-4 present the results for the individual optimization of each curve. It is seen that the fit is very good in each case and the residual is low.

Table 5-5: C₃H₆ only experiments, initial concentrations

Run	C ₃ H ₆ , ppm
4(a)	250
4(b)	250
5	500
6	750

Oxidation of propene:

$$(-R_{C_3H_6}) = \frac{k_3 Y_{C_3H_6} Y_{O_2}}{T(1 + K_6 Y_{C_3H_6})^2} \quad (5-2)$$

Table 5-6: Runs 4-6 individual optimization results

Parameter	LB	HB	Run 4(a)	Run 4(b)	Run 5	Run 6	
k_3	A_3	0	30	21.3	19.6	20.4	19.9
	E_3	20000	150000	114685	55868	97823	122031
K_6	B_6	0	30	1.04	6.87	7.27	5.53
	H_6	-150000	0	-29840	-31117	-5428	-3.30
Cumulative Residual			2.5	2.9	1.3	5.2	

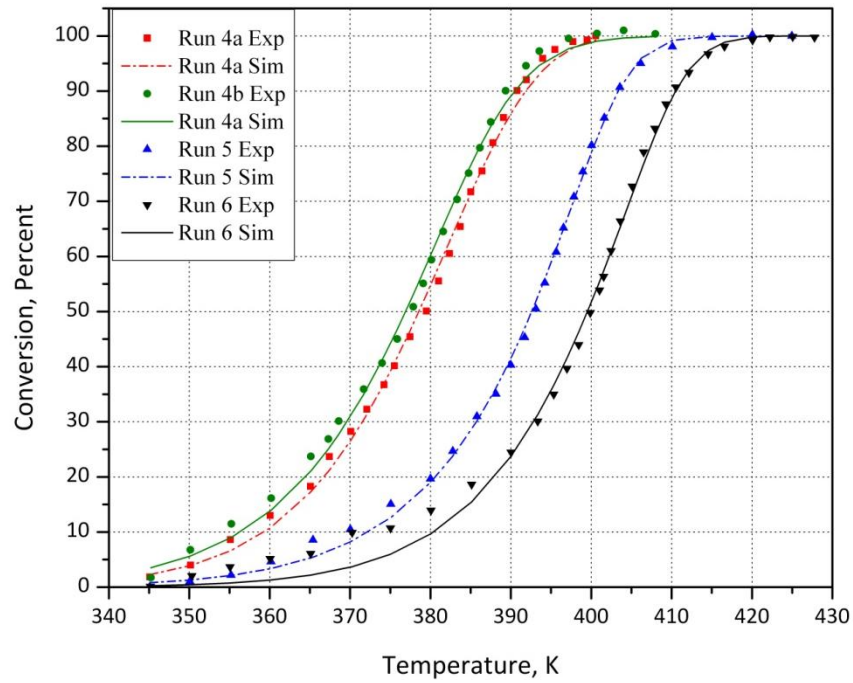


Figure 5-4: Individual optimization result vs. Experimental data, Runs 4-6

When experiments 4(a), 5 and 6 were optimize simultaneously, the results shown in

Table 5-7 and Figure 5-5 were obtained. It is clear in this case that the model works well.

Table 5-7: Runs 4a, 5 & 6 simultaneous optimization results

Parameter	LB	HB	Run 4(a)	Run 5	Run 6
k ₃	A ₃	0	30	20.3	
	E ₃	20000	150000	72151	
K ₆	B ₆	0	30	8.01	
	H ₆	-150000	0	-8886	
Cumulative Residual			2.5	4.9	5.9

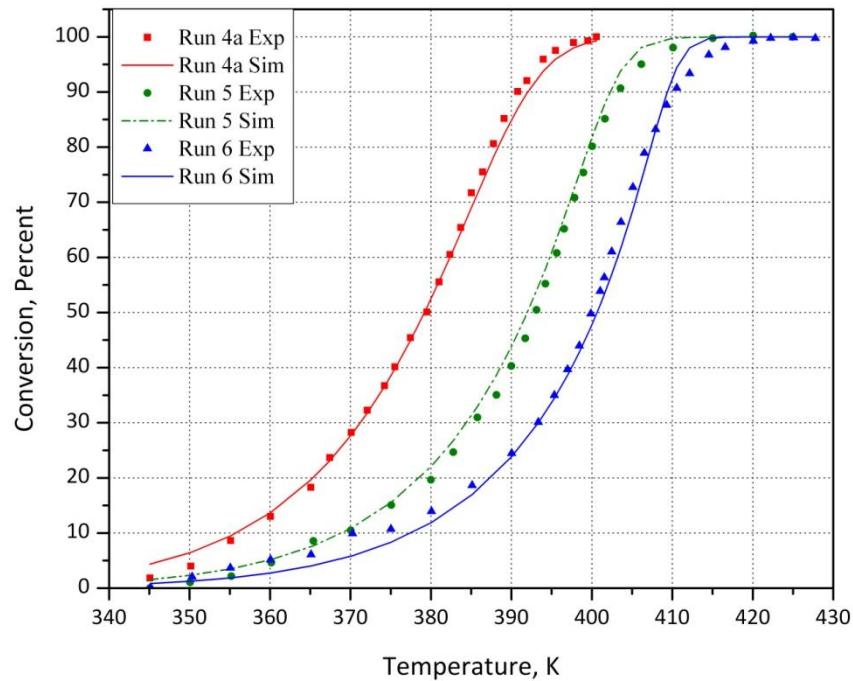


Figure 5-5: Simultaneous modelling result vs. Experimental data, Runs 4a, 5 & 6

5.3 Modelling of NO Oxidation

Experiments 13, 14 and 15 have only NO as a reactant. We have five models to consider in this case.

Model C₁, Oxidation of NO:

$$(-R_{NO}) = \frac{k_4 Y_{NO} Y_{O_2}^{0.5} [1 - \beta]}{T(1 + K_8 Y_{NO})} \quad (5-3)$$

Model C₂, Oxidation of NO:

$$(-R_{\text{NO}}) = \frac{k_4 Y_{\text{NO}} Y_{\text{O}_2} [1 - \beta]}{T(Y_{\text{NO}} + K_{10} Y_{\text{NO}_2})} \quad (5-4)$$

Model C₃, Oxidation of NO:

$$(-R_{\text{NO}}) = \frac{k_4 Y_{\text{O}_2}^{0.5} [1 - \beta^2]}{T\left(1 + K_8 Y_{\text{NO}} + K_{10} \frac{Y_{\text{NO}_2}}{Y_{\text{NO}}}\right)} \quad (5-5)$$

Model C₄, Oxidation of NO:

$$(-R_{\text{NO}}) = \frac{k_4 Y_{\text{O}_2}^{0.5} [1 - \beta]}{T\left(1 + K_8 Y_{\text{NO}} + K_{10} \frac{Y_{\text{NO}_2}}{Y_{\text{NO}}}\right)} \quad (5-6)$$

Model C₅, Oxidation of NO:

$$(-R_{\text{NO}}) = \frac{k_4 Y_{\text{NO}} Y_{\text{O}_2}^{0.5} [1 - \beta]}{T(1 + K_8 Y_{\text{NO}} + K_{10} Y_{\text{NO}_2})^2} \quad (5-7)$$

As with the CO and C₃H₆ experiments, each of the three experiments was fit individually for all of the five models. Initial concentrations are shown in Table 5-8, whilst the results are shown in Table 5-9 to Table 5-13 and Figure 5-6 to Figure 5-10.

Table 5-8: NO only experiments, initial concentrations

Run	NO, ppm
13	150
14	300
15	600

Table 5-9: Runs 13-15 individual optimization results, Model 1

Parameter		LB	HB	Run 13	Run 14	Run 15
k_4	A_3	0	30	14.3	14.1	14.0
	E_3	20000	150000	21697	26558	27673
K_8	B_6	0	30	6.72	7.94	7.41
	H_6	-150000	0	-76079	-62711	-52449
Cumulative Residual				0.48	0.21	1.2

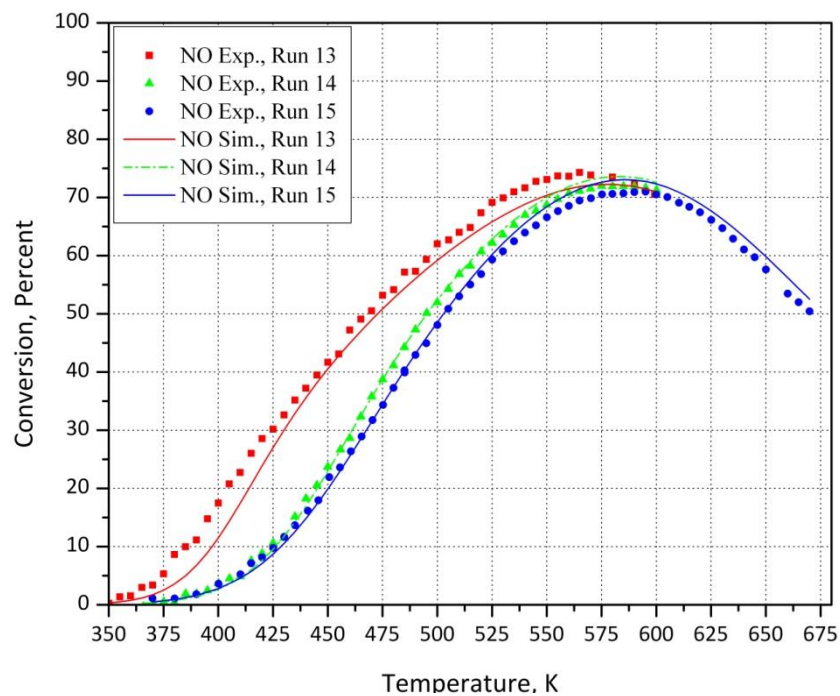


Figure 5-6: Individual optimization result vs. Experimental data, Runs 13-15, Model 1

Table 5-10: Runs 13-15 individual optimization results, Model 2

Parameter		LB	HB	Run 13	Run 14	Run 15
k_4	A_3	0	30	7.02	6.99	7.60
	E_3	20000	150000	38880	18557	19947
K_{10}	B_{10}	0	30	1.52	1.56	1.84
	H_{10}	-150000	0	-1.26	-137095	-124999
Cumulative Residual				17	0.22	1.3

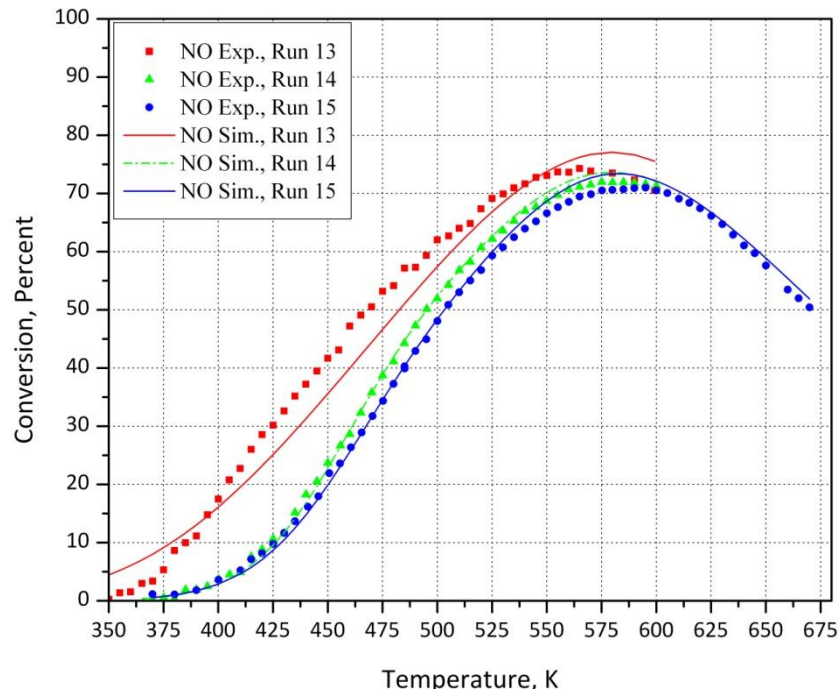


Figure 5-7: Individual optimization result vs. Experimental data, Runs 13-15, Model 2

Table 5-11: Runs 13-15 individual optimization results, Model 3

Parameter		LB	HB	Run 13	Run 14	Run 15
k_4	A_3	0	30	23.6	13.8	15.0
	E_3	20000	150000	10482	12651	10705
K_8	B_6	0	30	26.1	16.6	16.6
	H_6	-150000	0	-59414	-49892	-42631
K_{10}	B_{10}	0	30	19.1	8.75	9.02
	H_{10}	-150000	0	-16483	-14424	-12727
Cumulative Residual				1.7	0.64	1.6

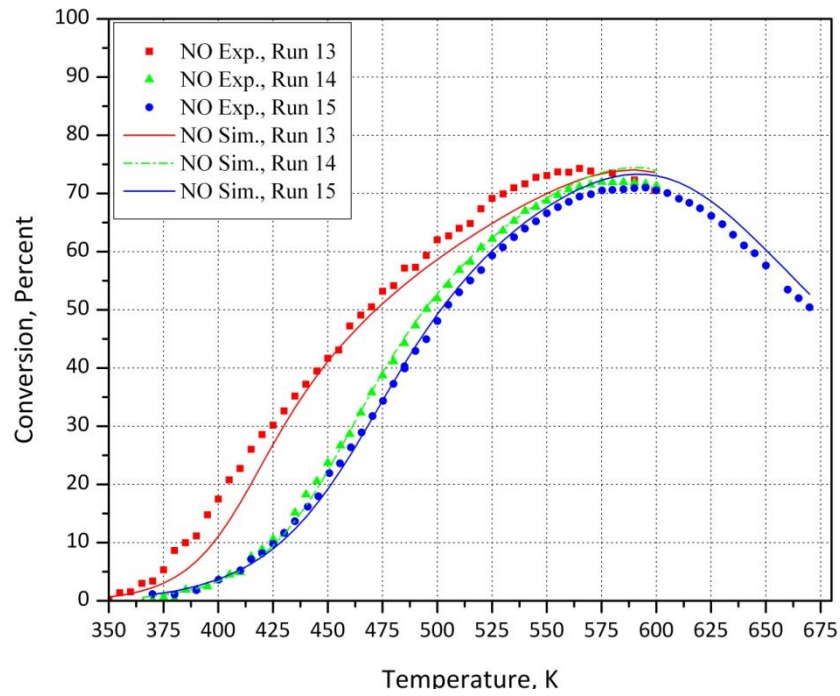


Figure 5-8: Individual optimization result vs. Experimental data, Runs 13-15, Model 3

Table 5-12: Runs 13-15 individual optimization results, Model 4

Parameter	LB	HB	Run 13	Run 14	Run 15	
k_4	A_3	0	30	22.8	15.9	15.1
	E_3	20000	150000	31955	16984	16421
K_8	B_6	0	30	8.80	18.5	16.6
	H_6	-150000	0	-11353	-51857	-44344
K_{10}	B_{10}	0	30	19.1	11.2	9.75
	H_{10}	-150000	0	-18067	-19958	-20585
Cumulative Residual			29	0.32	1.3	

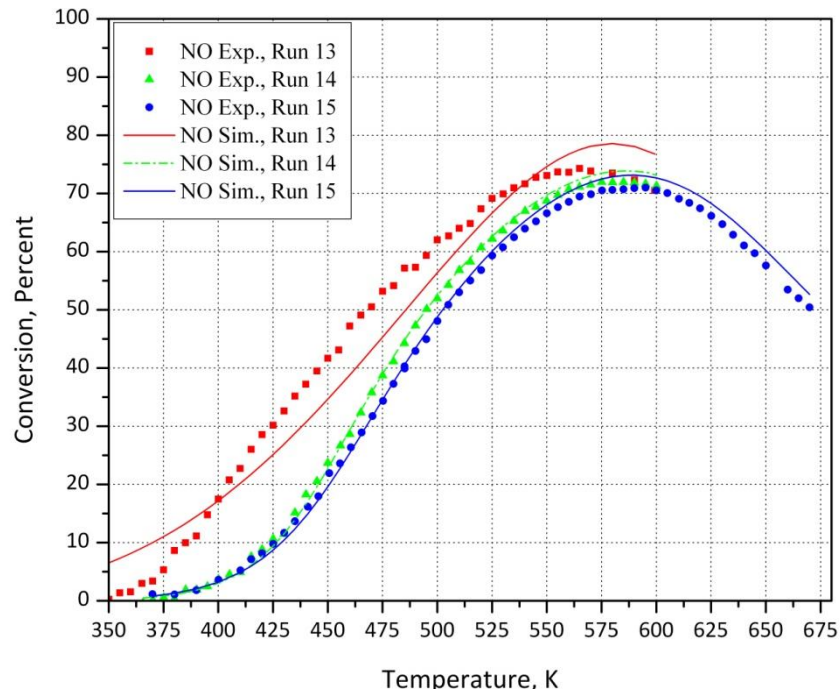


Figure 5-9: Individual optimization result vs. Experimental data, Runs 13-15, Model 4

Table 5-13: Runs 13-15 individual optimization results, Model 5

Parameter		LB	HB	Run 13	Run 14	Run 15
k_4	A_3	0	30	14.5	19.2	20.7
	E_3	20000	150000	18983	15614	14581
K_8	B_6	0	30	5.96	10.7	11.0
	H_6	-150000	0	-72204	-31734	-25395
K_{10}	B_{10}	0	30	7.98	11.4	11.4
	H_{10}	-150000	0	-48123	-11799	-10343
Cumulative Residual				0.37	0.27	1.3

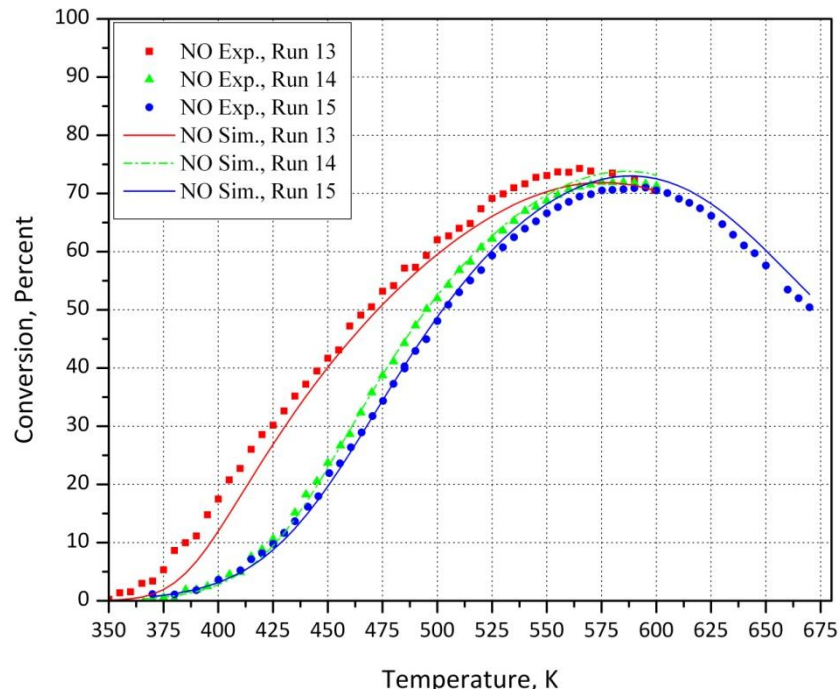


Figure 5-10: Individual optimization result vs. Experimental data, Runs 13-15, Model 5

Table 5-14 to Table 5-18 and Figure 5-11 to Figure 5-15 are presenting results for modelling of all three experiments together with each of the different models.

Table 5-14: Runs 13-15 simultaneous optimization results, Model 1

Parameter		LB	HB	Run 13	Run 14	Run 15
k_4	A_3	0	30	14.5		
	E_3	20000	150000	19359		
K_8	B_6	0	30	8.40		
	H_6	-150000	0	-44844		
Cumulative Residual				7.2	8.7	2.7

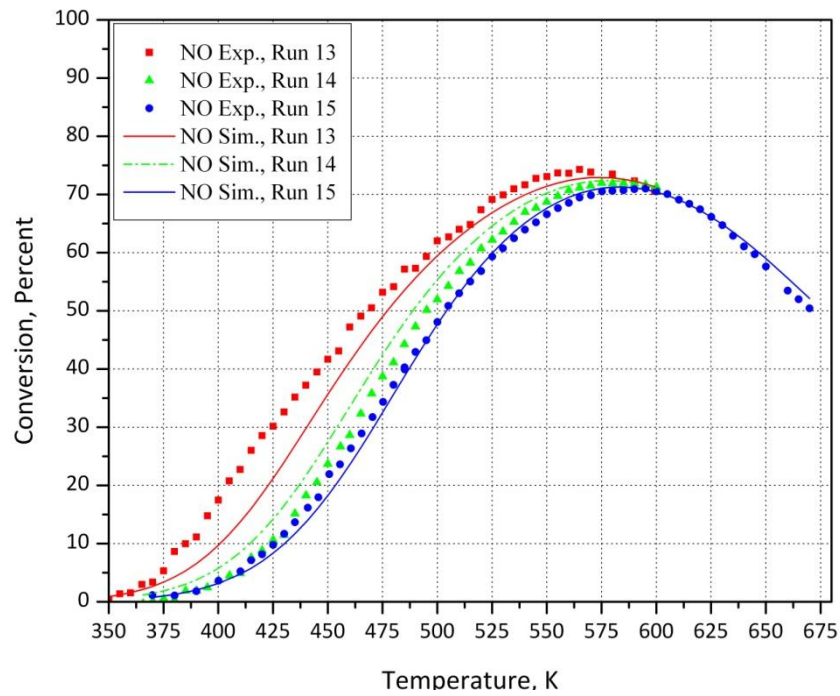


Figure 5-11: Simultaneous optimization result vs. Experimental data, Runs 13-15, Model 1

Table 5-15: Runs 13-15 simultaneous optimization results, Model 2

Parameter	LB	HB	Run 13	Run 14	Run 15
k_4	A_3	0	30	18.1	
	E_3	20000	150000	29030	
K_{10}	B_{10}	0	30	13.4	
	H_{10}	-150000	0	-33835	
Cumulative Residual			55	23	36

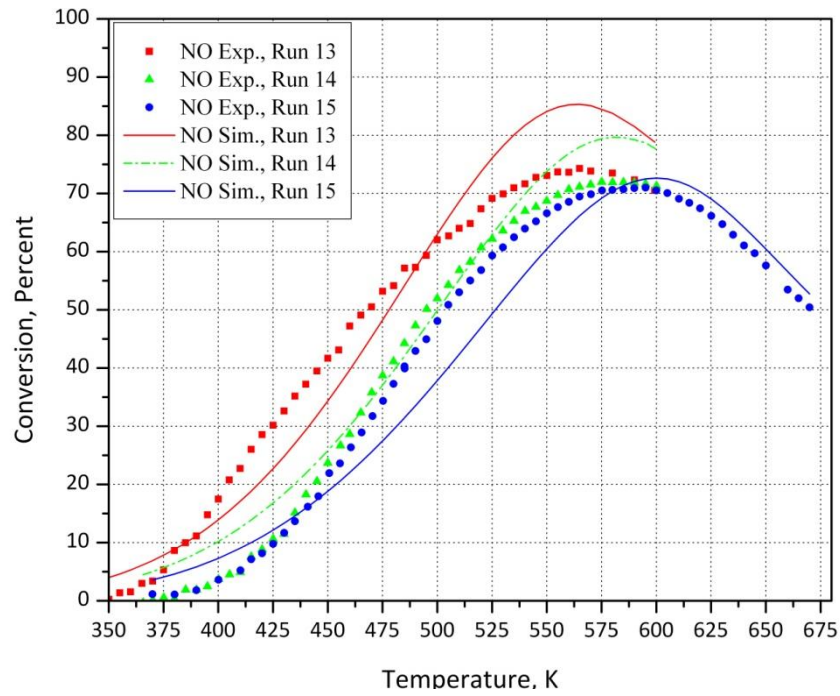


Figure 5-12: Simultaneous optimization result vs. Experimental data, Runs 13-15, Model 2

Table 5-16: Runs 13-15 simultaneous optimization results, Model 3

Parameter	LB	HB	Run 13	Run 14	Run 15
k_4	A_3	0	30	28.0	
	E_3	20000	150000	28003	
K_8	B_6	0	30	28.5	
	H_6	-150000	0	-104341	
K_{10}	B_{10}	0	30	24.0	
	H_{10}	-150000	0	-22913	
Cumulative Residual			46	13	42

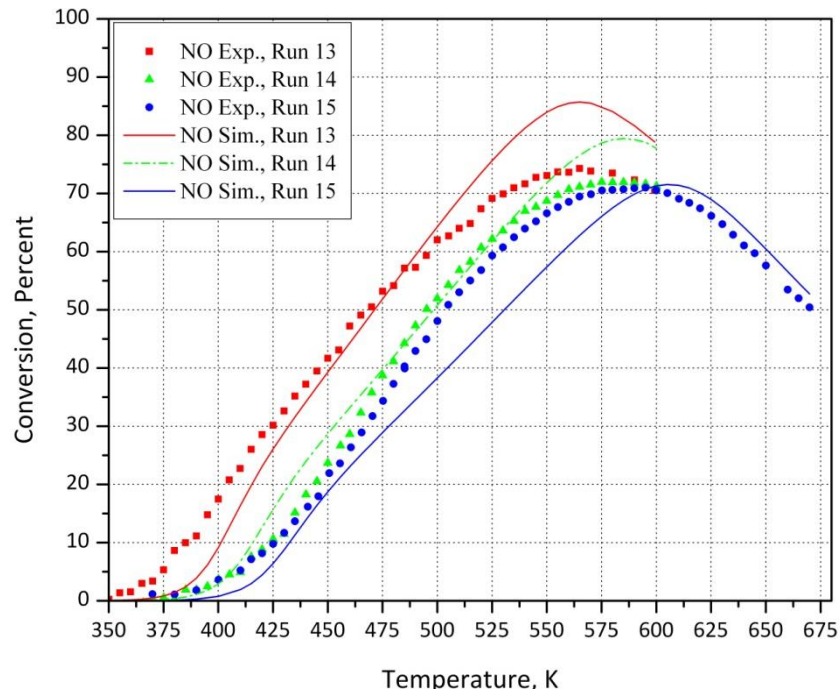


Figure 5-13: Simultaneous optimization result vs. Experimental data, Runs 13-15, Model 3

Table 5-17: Runs 13-15 simultaneous optimization results, Model 4

Parameter	LB	HB	Run 13	Run 14	Run 15
k_4	A_3	0	30	27.8	
	E_3	20000	150000	35300	
K_8	B_6	0	30	28.2	
	H_6	-150000	0	-96503	
K_{10}	B_{10}	0	30	23.8	
	H_{10}	-150000	0	-19346	
Cumulative Residual			41	10	37

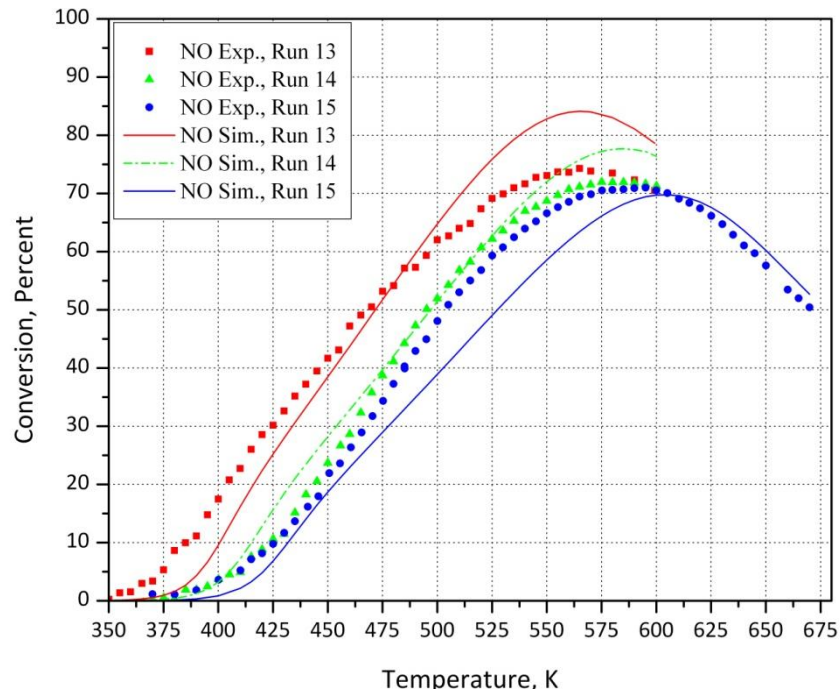


Figure 5-14: Simultaneous optimization result vs. Experimental data, Runs 13-15, Model 4

Table 5-18: Runs 13-15 simultaneous optimization results, Model 5

Parameter	LB	HB	Run 13	Run 14	Run 15
k_4	A_3	0	30	14.5	
	E_3	20000	150000	20132	
K_8	B_6	0	30	7.28	
	H_6	-150000	0	-41960	
K_{10}	B_{10}	0	30	7.06	
	H_{10}	-150000	0	-48909	
Cumulative Residual			5.4	8.6	3.1

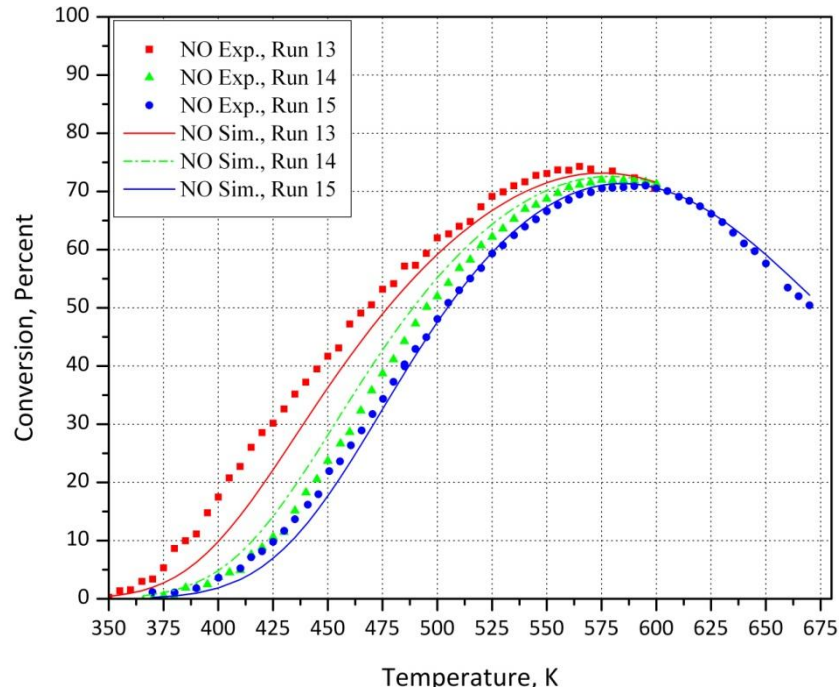


Figure 5-15: Simultaneous optimization result vs. Experimental data, Runs 13-15, Model 5

From the plots and results, it can be inferred that the best result was obtained with the Model 5, followed very close by Model 1. It is seen that despite other three models, these two models can capture the NO ignition curve at low initial concentration reasonably well.

5.4 Modelling of Mixture of CO, H₂ & C₃H₆

Having considered the experiments with only a single reactant, experiments with combinations of reactants are now presented. In the first instance, experiments 7 to 12 are considered, in which combinations of CO/H₂ and C₃H₆ were used.

Because the NO mole fraction in the inlet gas was zero, there is no difference between oxidation in the first 4 models, but model 5 is different because of the different hydrocarbon reaction rate equation. So we have to apply two models to the results of the different experiments. Initial concentrations for these experiments are available in Table 5-19, whilst the results for the individual optimization of each experiment with the different models can be found in Table 5-20 to Table 5-23 and Figure 5-16 to Figure 5-29.

Table 5-19: CO, H2 & Propene experiments, initial concentrations

Run	CO, ppm	H ₂ , ppm	C ₃ H ₆ , ppm
7(a)	500	167	250
7(b)	500	167	250
8	1000	333	250
9	2000	666	250
10	1000	333	500
11	1000	333	750
12	2000	666	500

Model C₁, Oxidation of CO:

$$(-R_{CO}) = \frac{k_1 Y_{CO} Y_{O_2}}{T(1 + K_5 Y_{CO} + K_6 Y_{C_3H_6})^2 (1 + K_7 (Y_{CO} Y_{C_3H_6})^2)} \quad (5-8)$$

Model C₁, Oxidation of propene:

$$(-R_{C_3H_6}) = \frac{k_3 Y_{C_3H_6} Y_{O_2}}{T(1 + K_5 Y_{CO} + K_6 Y_{C_3H_6})^2 (1 + K_7 (Y_{CO} Y_{C_3H_6})^2)} \quad (5-9)$$

Table 5-20: Runs 7-9 individual optimization results, Model 1

Parameter		LB	HB	Run 7a	Run 7b	Run 8	Run 9
k ₁	A ₁	0	30	24.4	22.7	23.2	20.2
	E ₁	20000	150000	118024	83315	35067	73330
k ₃	A ₃	0	30	23.2	20.4	25.7	21.1
	E ₃	20000	150000	127381	75199	131914	149999
K ₅	B ₅	0	30	8.27	8.76	8.52	6.63
	H ₅	-150000	0	-1075	-5.67	-33067	-16761
K ₆	B ₆	0	30	8.80	7.60	9.18	5.81
	H ₆	-150000	0	-102	-9970	-44320	-80221
K ₇	B ₇	0	30	14.2	3.83	14.8	28.8
	H ₇	-150000	0	-75598	-68767	-74767	-33173
Model 1	CO Residual			81	72	18	7.4
	C ₃ H ₆ Residual			28	12	37	9.4
	Cumulative Residual			109	84	55	16

Table 5-21: Runs 10-12 individual optimization results, Model 1

Parameter		LB	HB	Run 10	Run 11	Run 12
k ₁	A ₁	0	30	22.4	24.1	25.5
	E ₁	20000	150000	20658	124110	97278
k ₃	A ₃	0	30	21.1	19.3	23.9
	E ₃	20000	150000	20818	21961	82411
K ₅	B ₅	0	30	2.21	7.01	1.15
	H ₅	-150000	0	-32174	-55379	-125642
K ₆	B ₆	0	30	9.62	7.69	8.98
	H ₆	-150000	0	-253	-22431	-108219
K ₇	B ₇	0	30	27	3.3	0.12
	H ₇	-150000	0	-100647	-8376	-75948
Model 1	CO Residual			9.6	32	43
	C ₃ H ₆ Residual			17	15	13
	Cumulative Residual			27	48	56

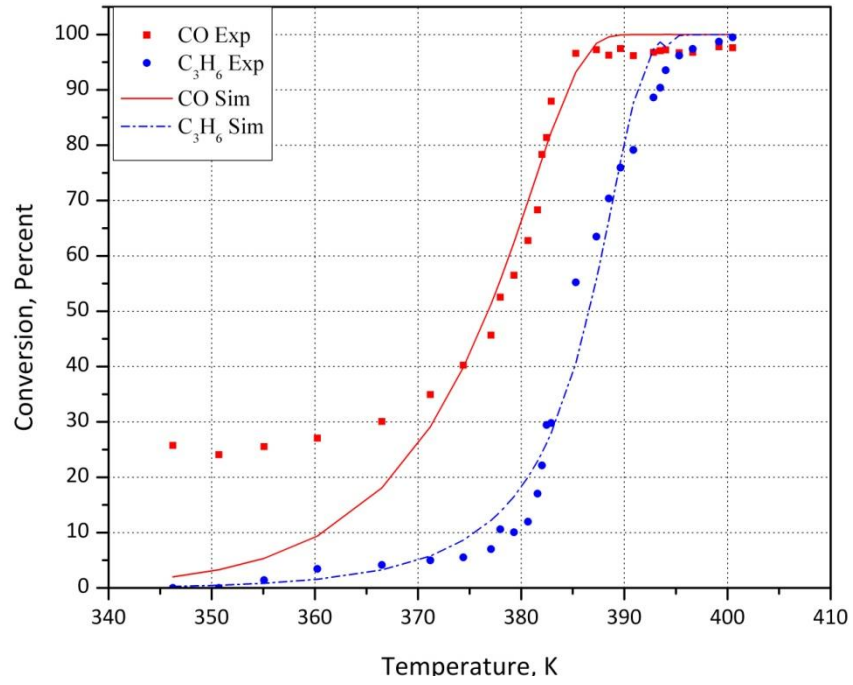


Figure 5-16: Individual optimization result vs. Experimental data, Run 7a, Model 1

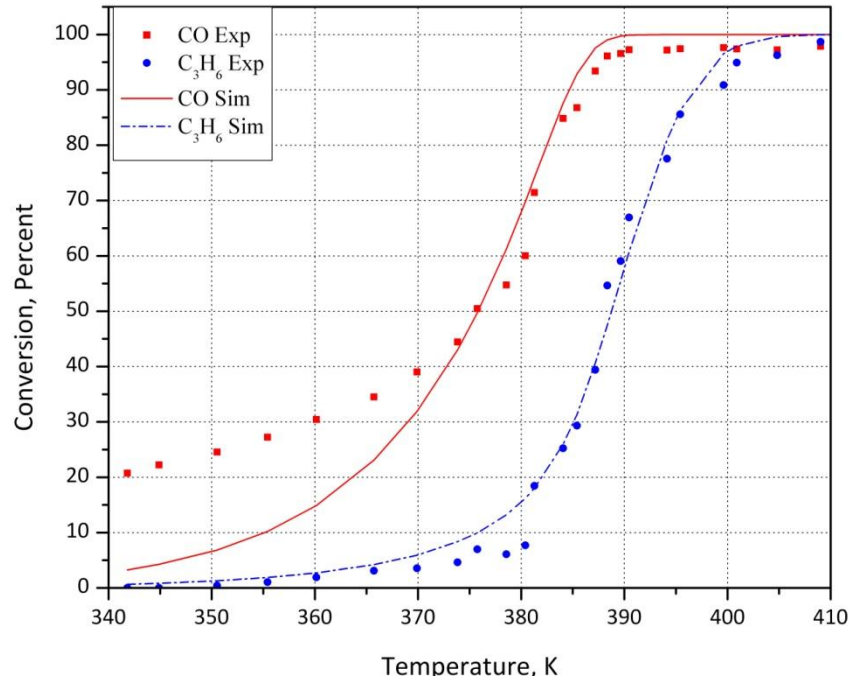


Figure 5-17: Individual optimization result vs. Experimental data, Run 7b, Model 1

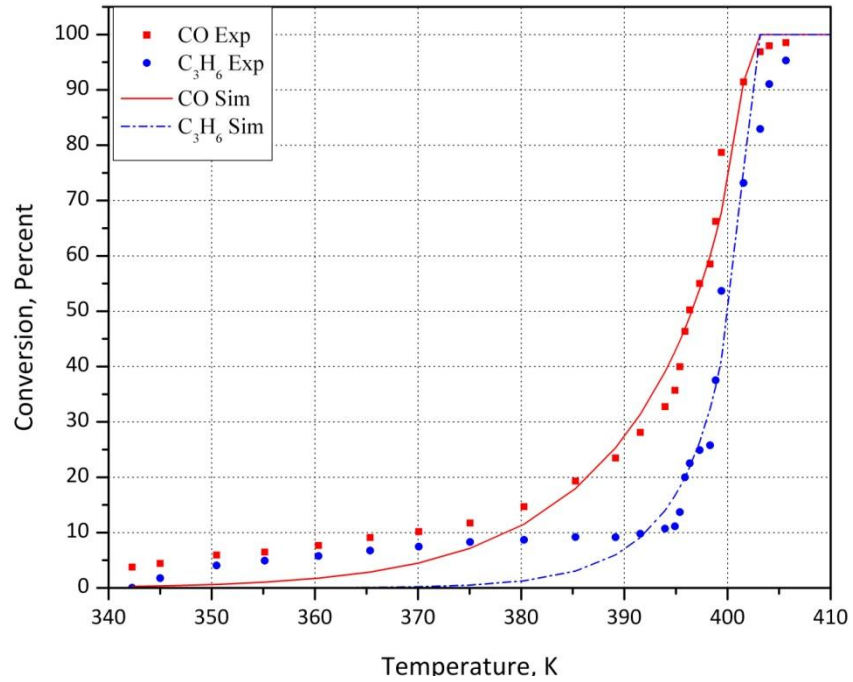


Figure 5-18: Individual optimization result vs. Experimental data, Run 8, Model 1

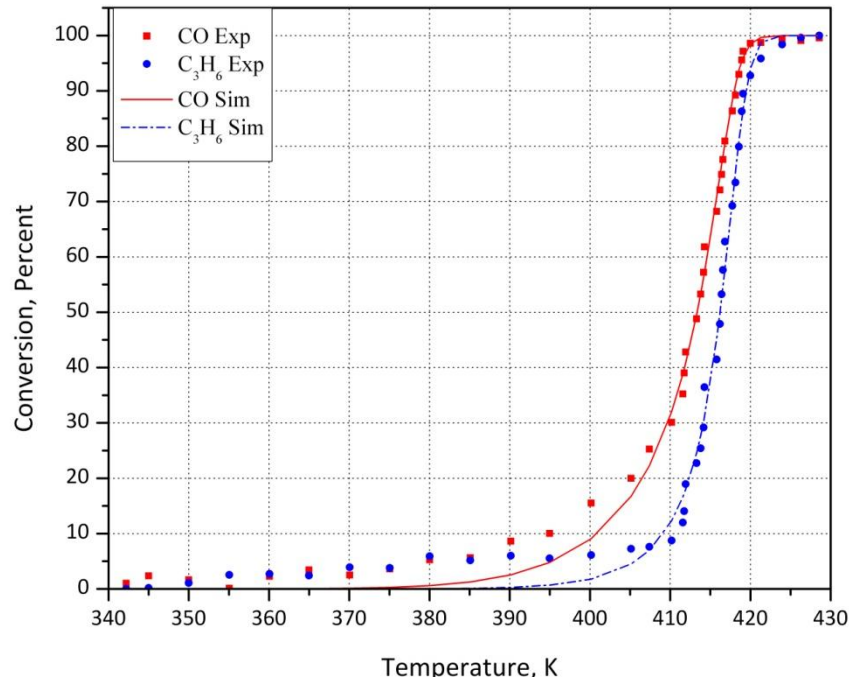


Figure 5-19: Individual optimization result vs. Experimental data, Run 9, Model 1

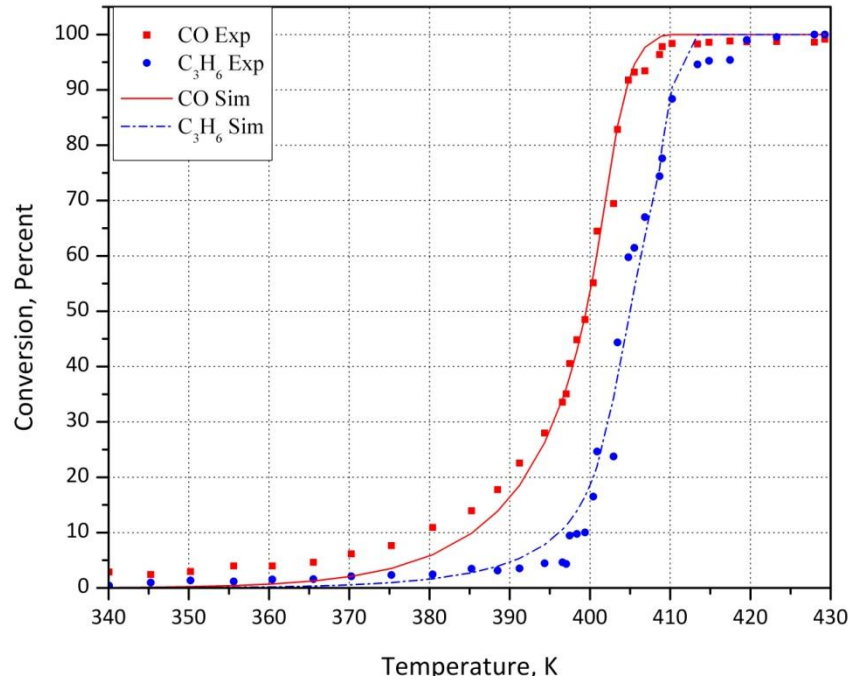


Figure 5-20: Individual optimization result vs. Experimental data, Run 10, Model 1

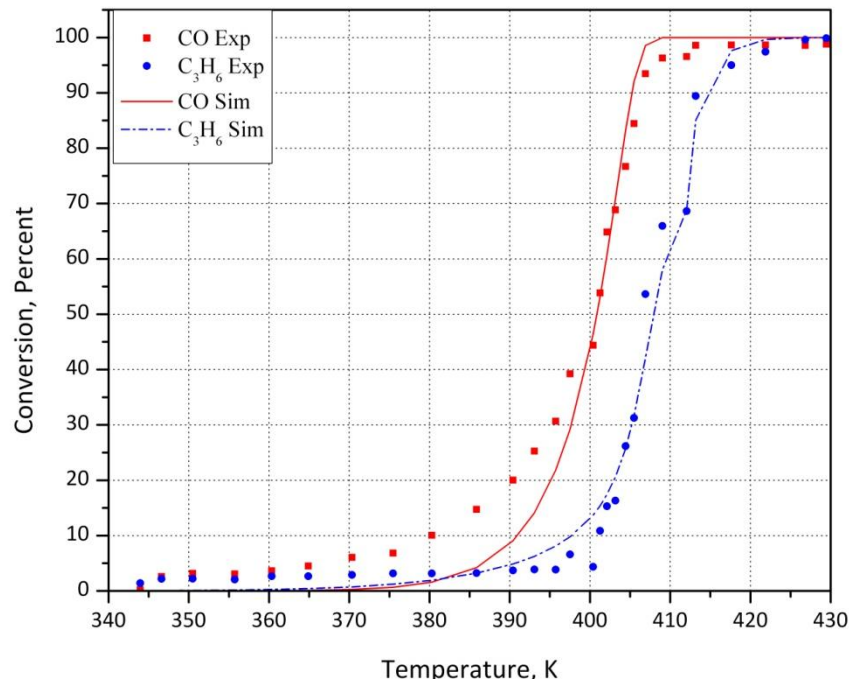


Figure 5-21: Individual optimization result vs. Experimental data, Run 11, Model 1

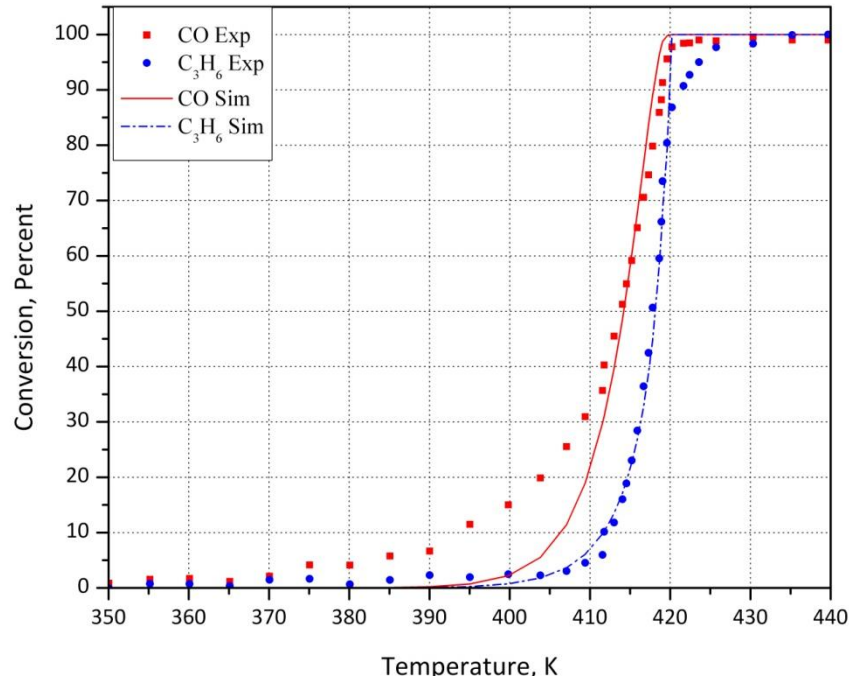


Figure 5-22: Individual optimization result vs. Experimental data, Run 12, Model 1

Model C₅, Oxidation of CO:

$$(-R_{\text{CO}}) = \frac{k_1 Y_{\text{CO}} Y_{\text{O}_2}}{T(1 + K_5 Y_{\text{CO}} + K_6 Y_{\text{C}_3\text{H}_6})^2} \quad (5-10)$$

Model C₅, Oxidation of propene:

$$(-R_{\text{C}_3\text{H}_6}) = \frac{k_3 Y_{\text{C}_3\text{H}_6} Y_{\text{O}_2}}{T(1 + K_5 Y_{\text{CO}} + K_6 Y_{\text{C}_3\text{H}_6})^2} \quad (5-11)$$

Table 5-22: Runs 7-9 individual optimization results, Model 5

Parameter		LB	HB	Run 7a	Run 7b	Run 8	Run 9
k ₁	A ₁	0	30	21.6	28.0	22.1	21.8
	E ₁	20000	150000	44457	33167	107264	87558
k ₃	A ₃	0	30	19.5	29.4	22.6	21.8
	E ₃	20000	150000	38951	101485	147447	123836
K ₅	B ₅	0	30	9.06	12.1	5.64	5.17
	H ₅	-150000	0	-9768	-6404	-61415	-75312
K ₆	B ₆	0	30	3.95	12.6	8.18	9.03
	H ₆	-150000	0	-8353	-6898	-822	-48372
Model 5	CO Residual			40	19	29	8.7
	C ₃ H ₆ Residual			19	39	25	15
	Cumulative Residual			59	59	55	23

Table 5-23: Runs 10-12 individual optimization results, Model 5

Parameter		LB	HB	Run 10	Run 11	Run 12
k ₁	A ₁	0	30	29.2	21.5	20.0
	E ₁	20000	150000	88417	76466	24518
k ₃	A ₃	0	30	19.2	20.1	21.4
	E ₃	20000	150000	57296	84023	145002
K ₅	B ₅	0	30	10.9	4.13	6.86
	H ₅	-150000	0	-44167	-69676	-59323
K ₆	B ₆	0	30	5.03	6.66	3.23
	H ₆	-150000	0	-63869	-57096	-41709
Model 5	CO Residual			58	12	3.1
	C ₃ H ₆ Residual			48	30	6.3
	Cumulative Residual			107	43	9.5

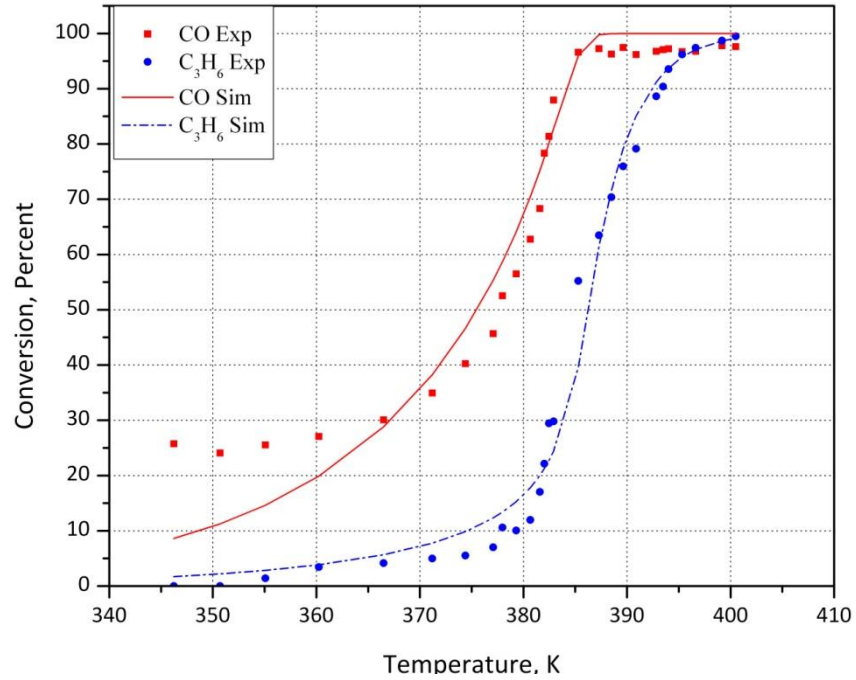


Figure 5-23: Individual optimization result vs. Experimental data, Run 7a, Model 5

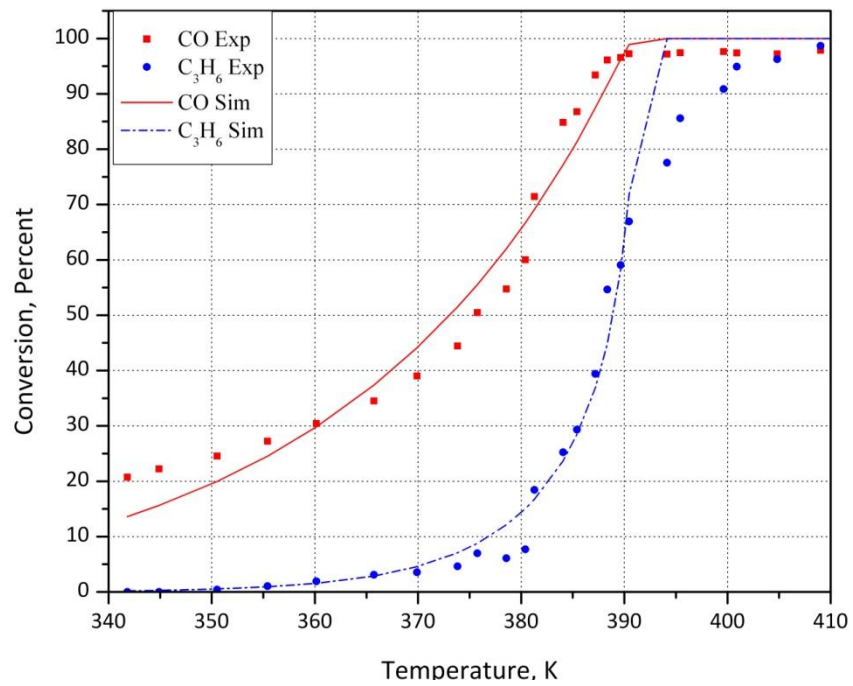


Figure 5-24: Individual optimization result vs. Experimental data, Run 7b, Model 5

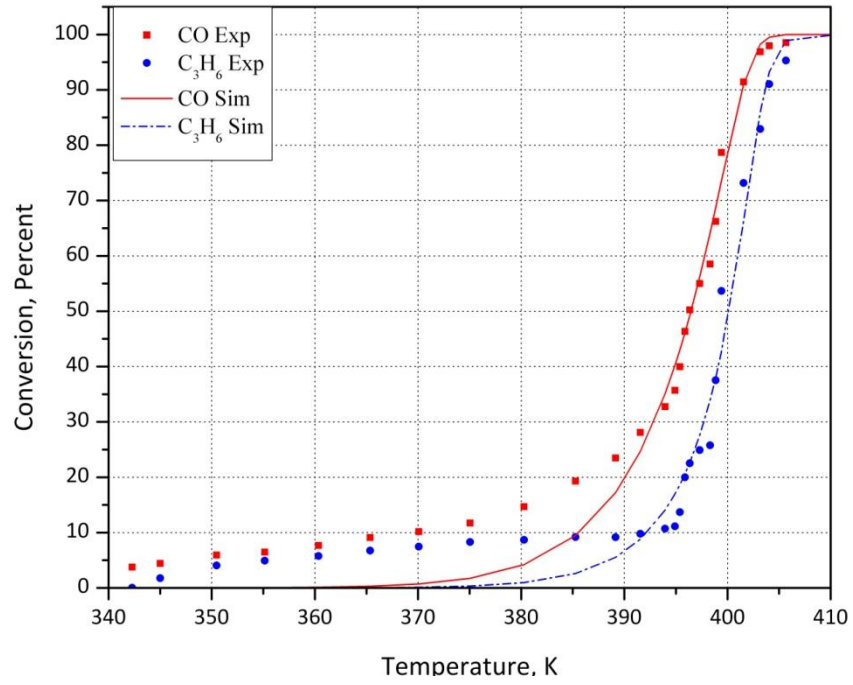


Figure 5-25: Individual optimization result vs. Experimental data, Run 8, Model 5

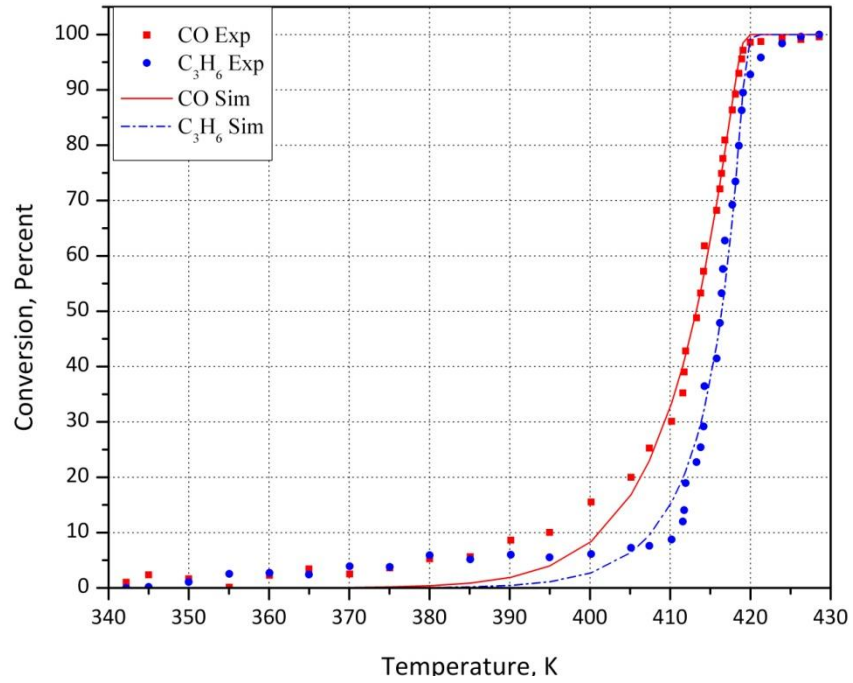


Figure 5-26: Individual optimization result vs. Experimental data, Run 9, Model 5

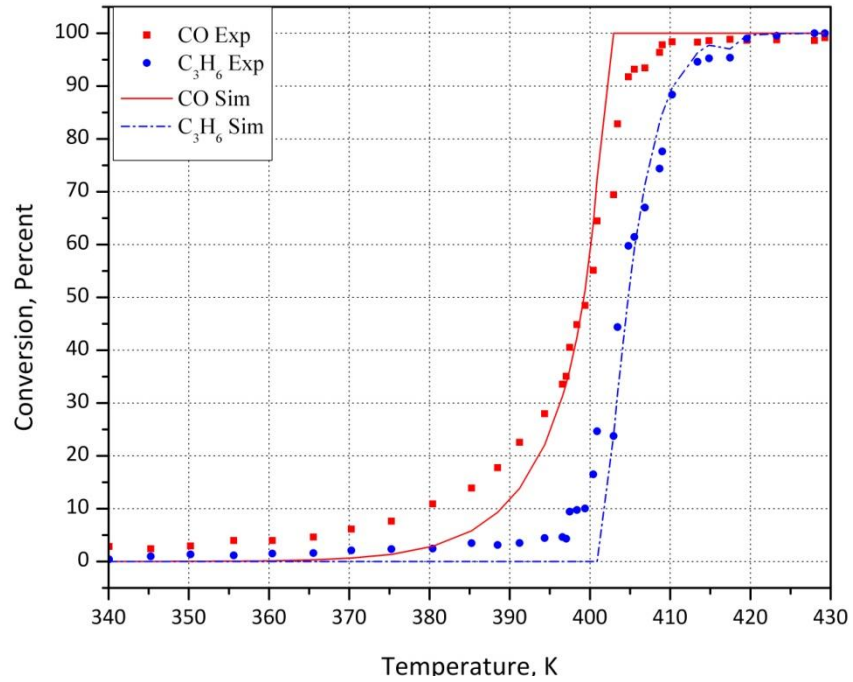


Figure 5-27: Individual optimization result vs. Experimental data, Run 10, Model 5

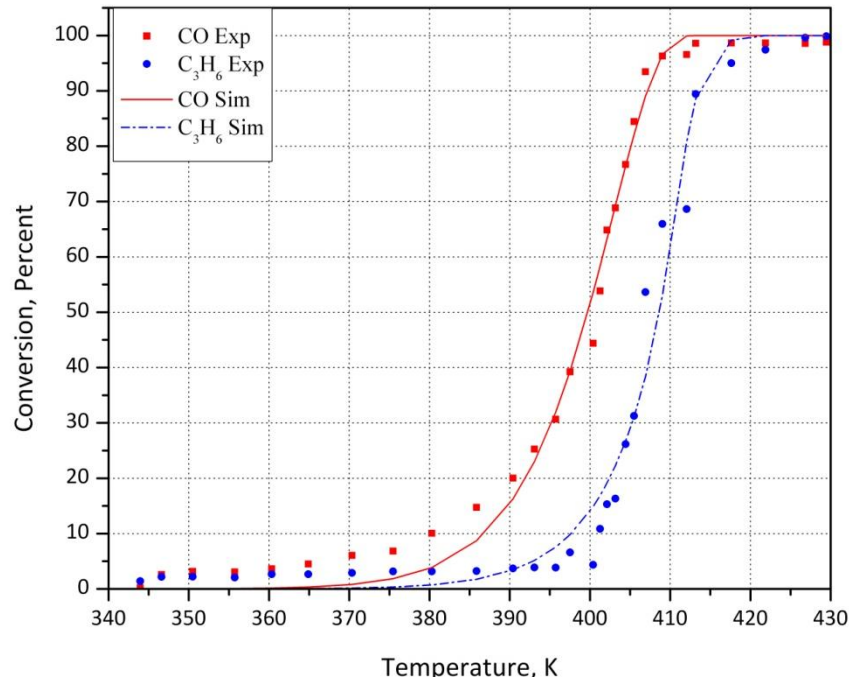


Figure 5-28: Individual optimization result vs. Experimental data, Run 11, Model 5

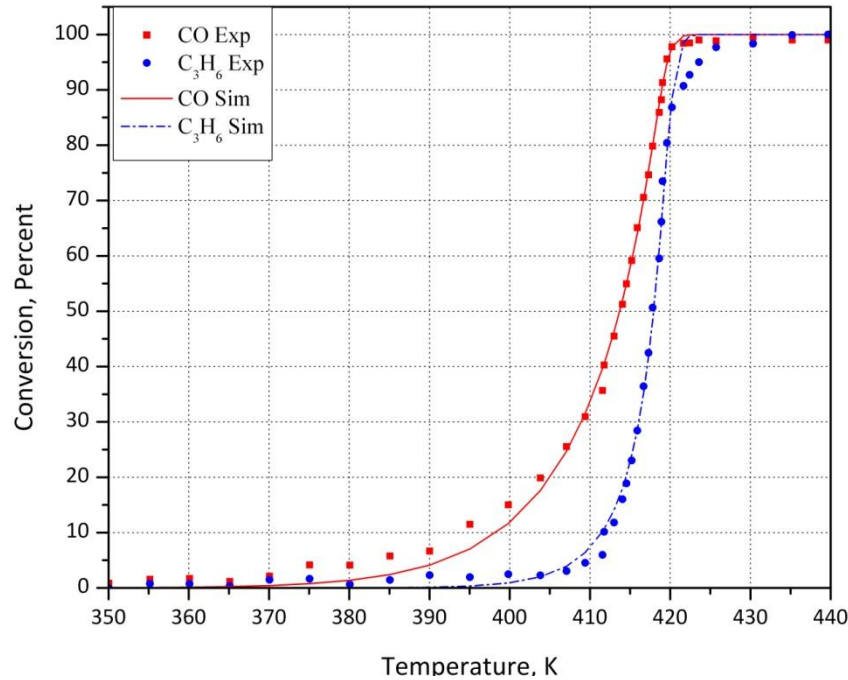


Figure 5-29: Individual optimization result vs. Experimental data, Run 12, Model 5

It is seen that both models are able to capture most of the details of the experiment in this case, although the low conversion portion of the CO oxidation curve is not captured well. Model 5 seems to be better than Model 1 in this regard.

Now it is time to see if we can find a set of parameters which can be used to predict behaviours of the system at different initial condition. Table 5-24 to Table 5-25 and Figure 5-30 to Figure 5-41 are presenting the results of simultaneous optimization of different experiments with model 1 and 5:

Table 5-24: Runs 7-12 simultaneous optimization results, Model 1

Parameter		LB	HB	Run 7(a)	Run 8	Run 9	Run 10	Run 11	Run 12
k ₁	A ₁	0	30	20.9					
	E ₁	20000	150000	21679					
k ₃	A ₃	0	30	20.9					
	E ₃	20000	150000	61194					
K ₅	B ₅	0	30	7.79					
	H ₅	-150000	0	-39119					
K ₆	B ₆	0	30	7.30					
	H ₆	-150000	0	-24197					
K ₇	B ₇	0	30	17.8					
	H ₇	-150000	0	-84444					
Model 1	CO Residual			75	43.	31	35	16	14
	C ₃ H ₆ Residual			45	54	22	64	61	50
	Cumulative Residual			120	97	54	100	78	65

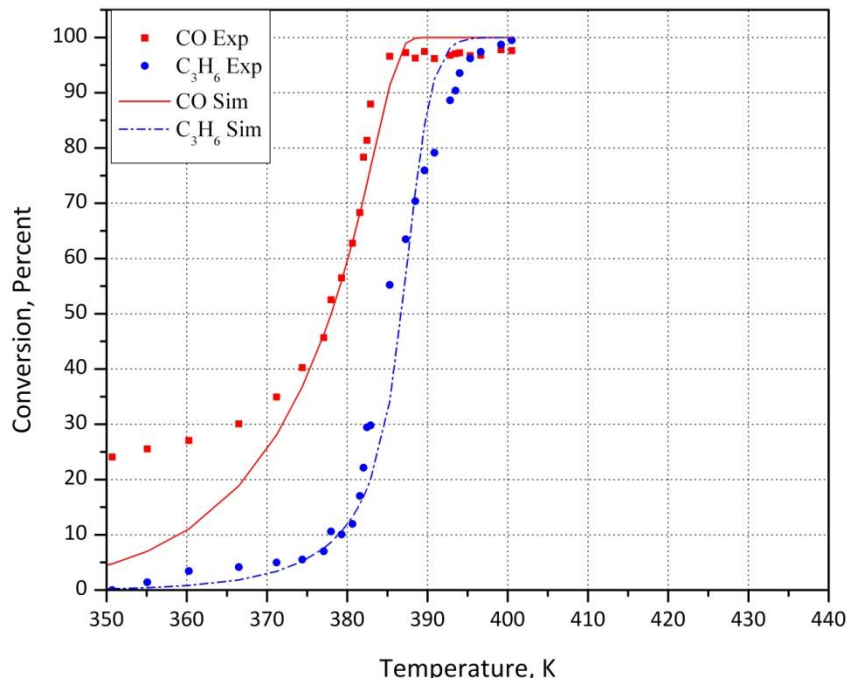


Figure 5-30: Simultaneous optimization result vs. Experimental data, Run 7a, Model 1

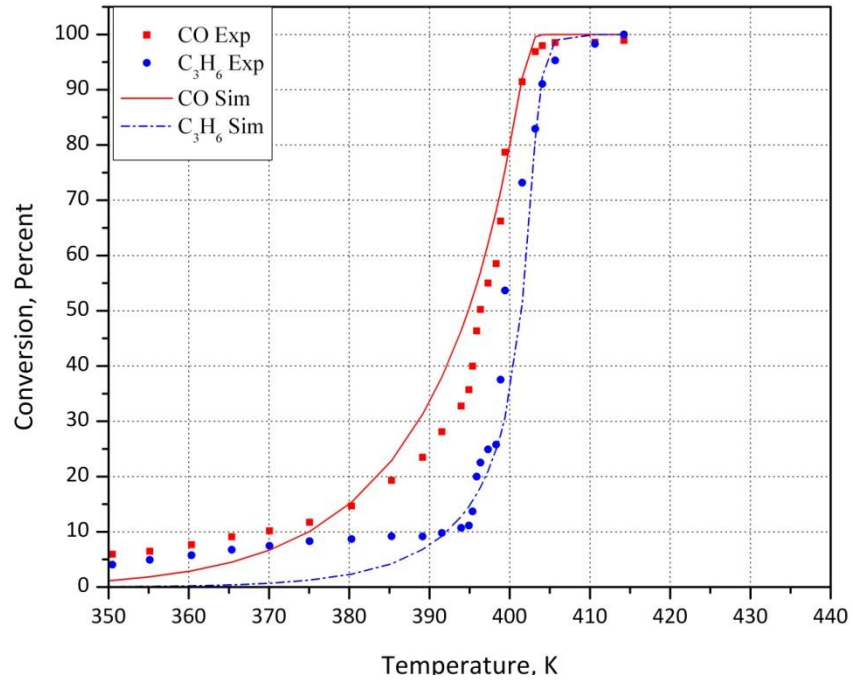


Figure 5-31: Simultaneous optimization result vs. Experimental data, Run 8, Model 1

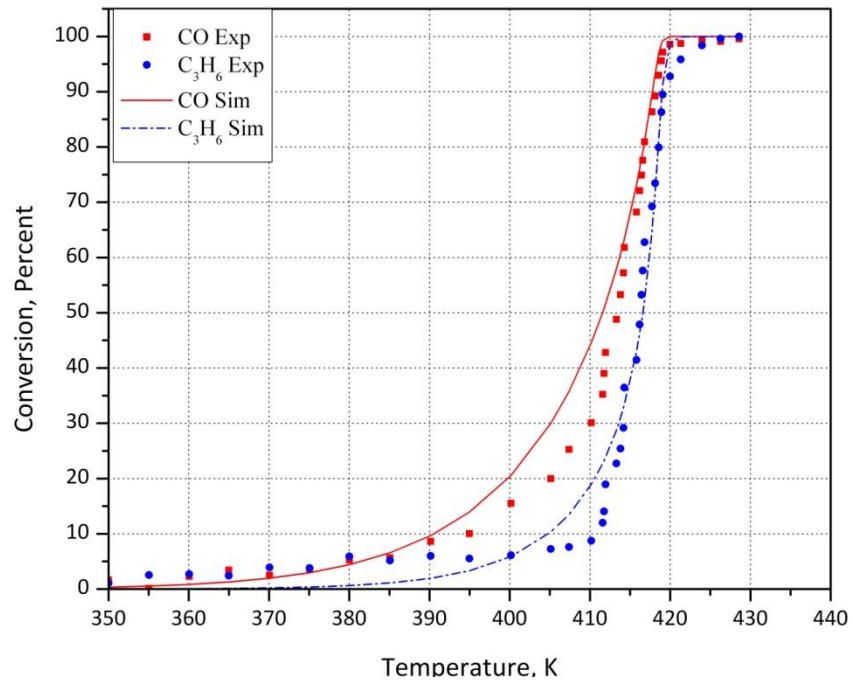


Figure 5-32: Simultaneous optimization result vs. Experimental data, Run 9, Model 1

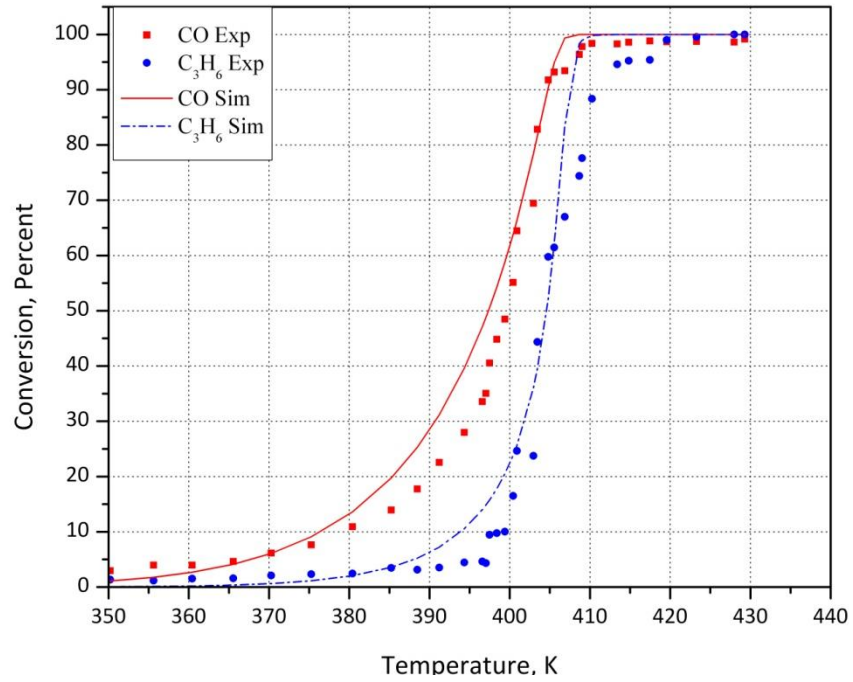


Figure 5-33: Simultaneous optimization result vs. Experimental data, Run 10, Model 1

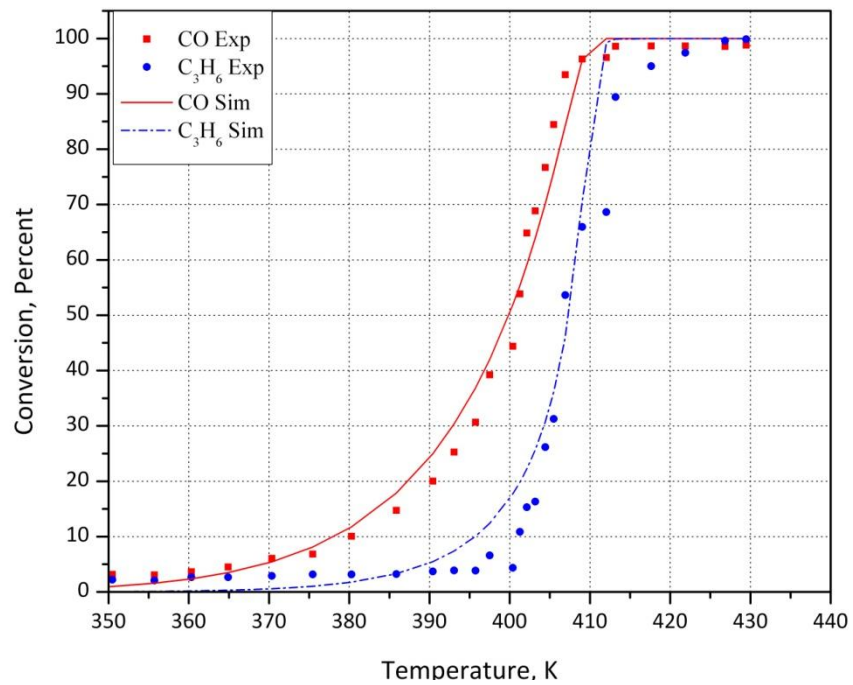


Figure 5-34: Simultaneous optimization result vs. Experimental data, Run 11, Model 1

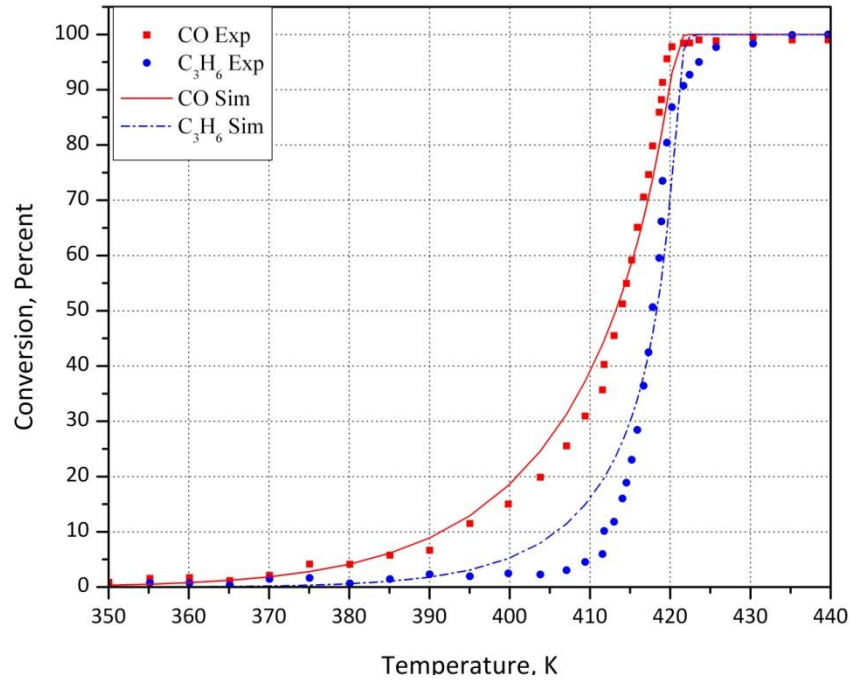


Figure 5-35: Simultaneous optimization result vs. Experimental data, Run 12, Model 1

Table 5-25: Runs 7-12 simultaneous optimization results, Model 5

Parameter	LB	HB	Run 7(b)	Run 8	Run 9	Run 10	Run 11	Run 12
k_1	A_1	0	30	21.9				
	E_1	20000	150000	54852				
k_3	A_3	0	30	22.1				
	E_3	20000	150000	102626				
K_5	B_5	0	30	8.36				
	H_5	-150000	0	-18803				
K_6	B_6	0	30	7.51				
	H_6	-150000	0	-16641				
Model 5	CO Residual		92	41	26	29	17	12
	C_3H_6 Residual		29	73	25	65	60	39
	Cumulative Residual		122	114	51	95	78	52

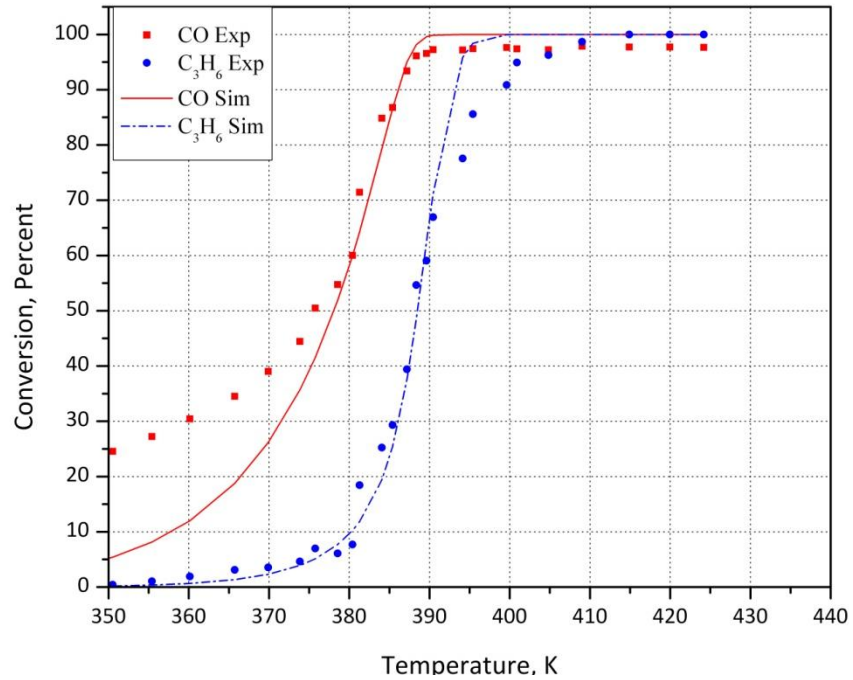


Figure 5-36: Simultaneous optimization result vs. Experimental data, Run 7b, Model 5

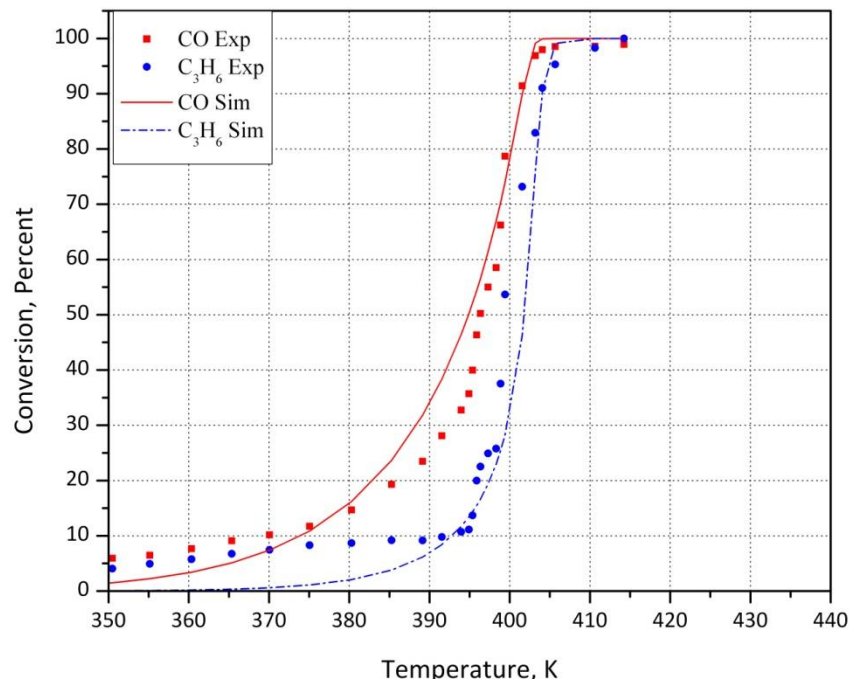


Figure 5-37: Simultaneous optimization result vs. Experimental data, Run 8, Model 5

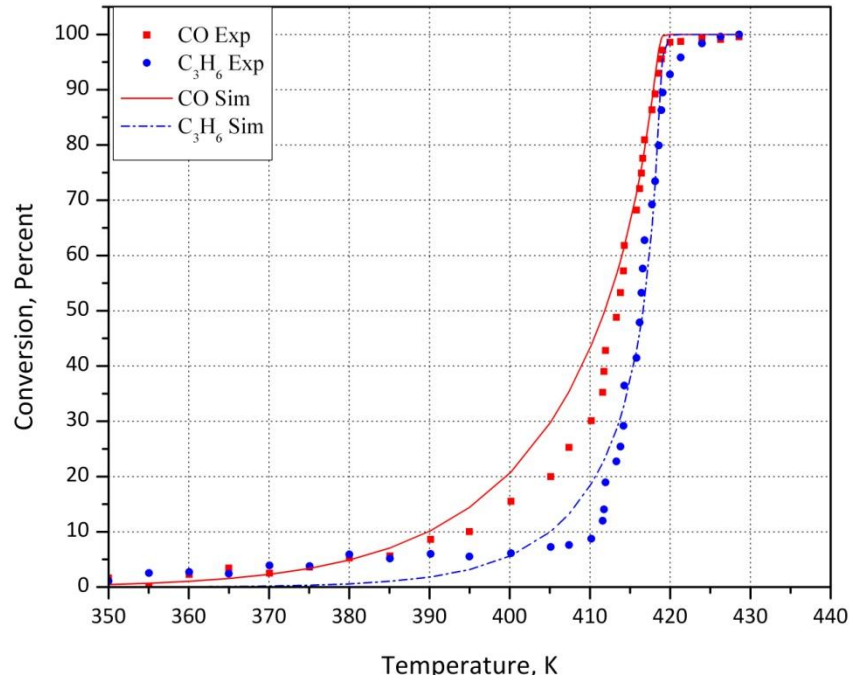


Figure 5-38: Simultaneous optimization result vs. Experimental data, Run 9, Model 5

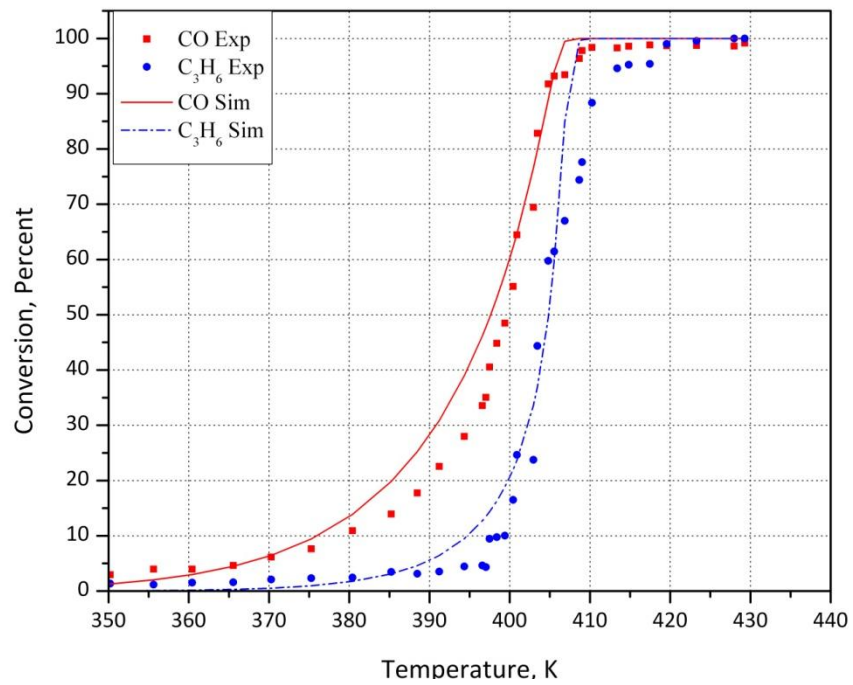


Figure 5-39: Simultaneous optimization result vs. Experimental data, Run 10, Model 5

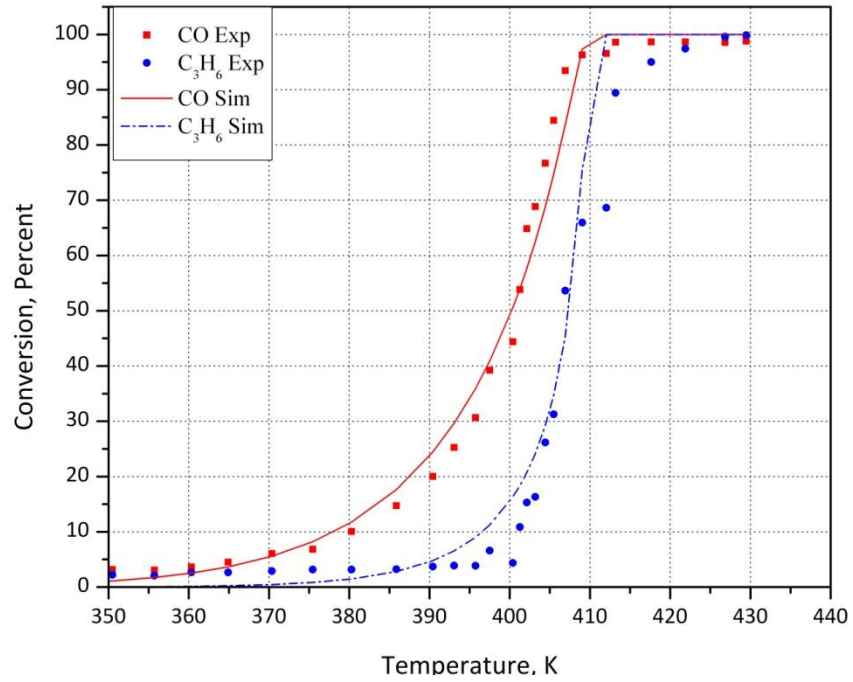


Figure 5-40: Simultaneous optimization result vs. Experimental data, Run 11, Model 5

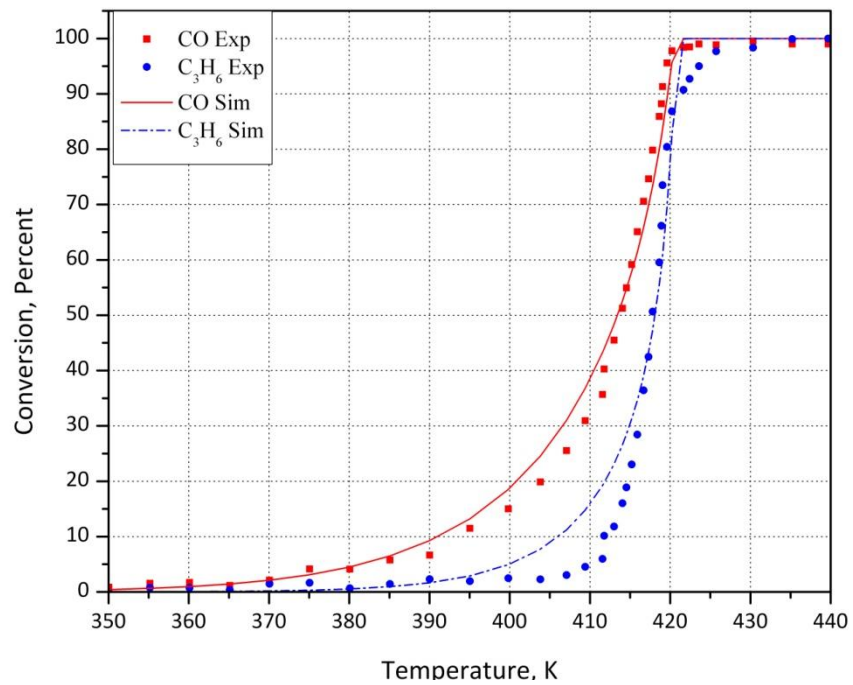


Figure 5-41: Simultaneous optimization result vs. Experimental data, Run 12, Model 5

Although both these two models can capture most of the details of the ignition curves, but Model 5 works slightly better than Model 1. It is also seen that both models have problem capturing the low conversion part of the CO oxidation curves in experiments with low CO concentration.

5.5 Modelling of Mixture of CO, H₂ & NO

In experiments 22 to 27, the inlet gas contained of CO, H₂ and NO. So, five different models can be tested. Initial concentrations for these experiments can be found in Table 5-26.

Table 5-26: CO, H₂ & NO experiments, initial concentrations

Run	CO, ppm	H ₂ , ppm	NO, ppm
22	1000	333	150
23	1000	333	300
24	1000	333	600
25	500	167	300
26	2000	666	300
27	500	167	600

The results for individual optimization of each experiment with each of the different models can be found in Table 5-27 to Table 5-36 and Figure 5-42 to Figure 5-71.

Model C₁, Oxidation of CO:

$$(-R_{CO}) = \frac{k_1 Y_{CO} Y_{O_2}}{T(1 + K_5 Y_{CO})^2 (1 + K_8 Y_{NO})} \quad (5-12)$$

Model C₁, Oxidation of NO:

$$(-R_{NO}) = \frac{k_4 Y_{NO} Y_{O_2}^{0.5} [1 - \beta]}{T(1 + K_5 Y_{CO})^2 (1 + K_8 Y_{NO})} \quad (5-13)$$

Table 5-27: Runs 22-24 individual optimization results, Model 1

Parameter		LB	HB	Run 22	Run 23	Run 24
k ₁	A ₁	0	30	19.8	20.8	21.3
	E ₁	20000	150000	43563	55707	26448
k ₄	A ₄	0	30	14.1	14.0	14.2
	E ₄	0	150000	26313	31918	28013
K ₅	B ₅	0	30	6.40	7.29	8.07
	H ₅	-150000	0	-49970	-44216	-49088
K ₈	B ₈	0	30	4.05	5.86	4.54
	H ₈	-150000	0	-53213	-10601	-8182
Model 1	CO Residual			2.9	3.7	4.8
	NO Residual			2.8	1.7	2.4
	Cumulative Residual			5.7	5.4	7.2

Table 5-28: Runs 25-27 individual optimization results, Model 1

Parameter		LB	HB	Run 25	Run 26	Run 27
k ₁	A ₁	0	30	21.3	20.1	19.5
	E ₁	20000	150000	77248	89073	38833
k ₄	A ₄	0	30	14.5	14.5	13.9
	E ₄	0	150000	31403	22558	32330
K ₅	B ₅	0	30	8.56	6.85	7.58
	H ₅	-150000	0	-1.98	-28889	-24238
K ₈	B ₈	0	30	6.55	3.33	0.60
	H ₈	-150000	0	-0.001	-44012	-63512
Model 1	CO Residual			38	2.5	31
	NO Residual			5.5	4.1	4.4
	Cumulative Residual			43.5	6.6	35.4

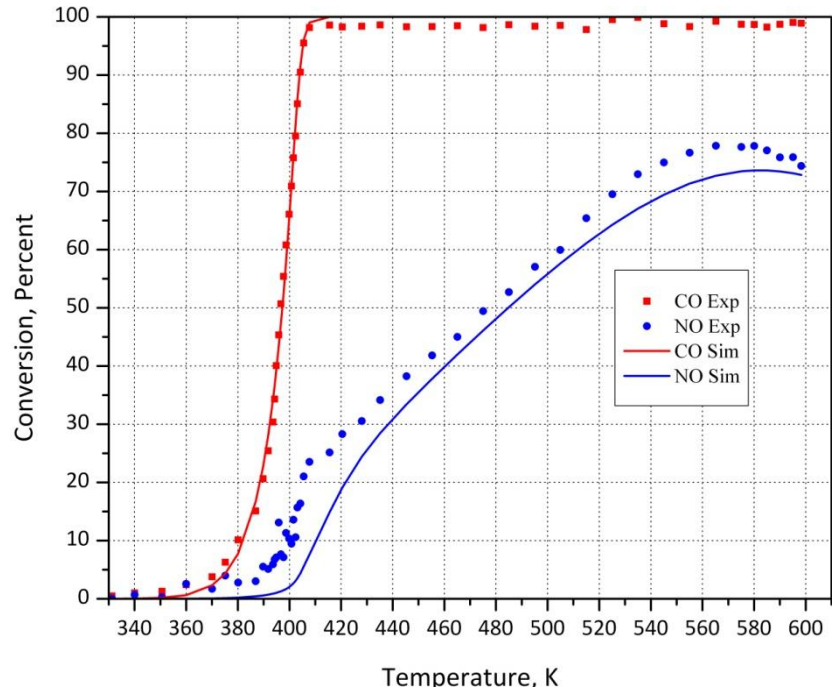


Figure 5-42: Individual optimization result vs. Experimental data, Run 22, Model 1

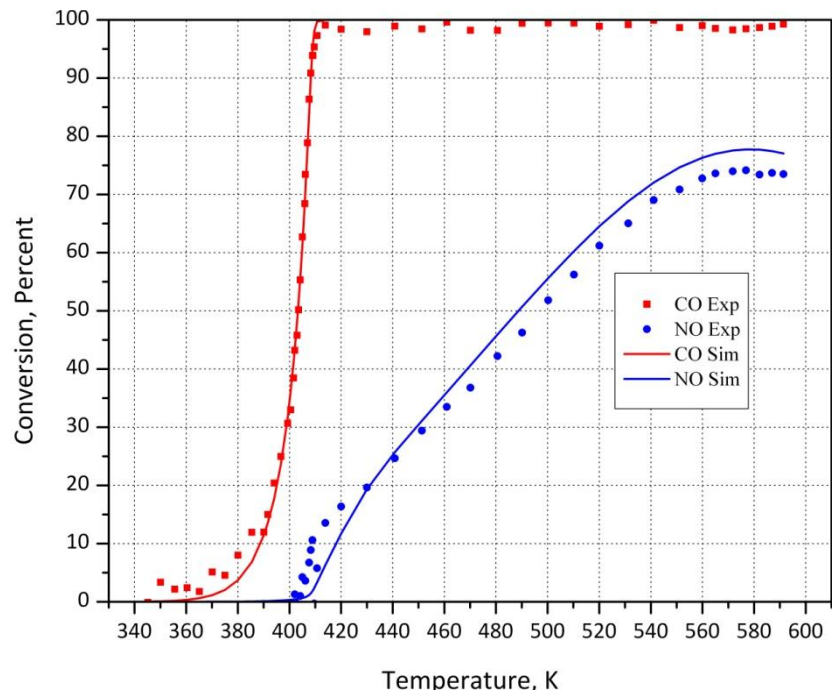


Figure 5-43: Individual optimization result vs. Experimental data, Run 23, Model 1

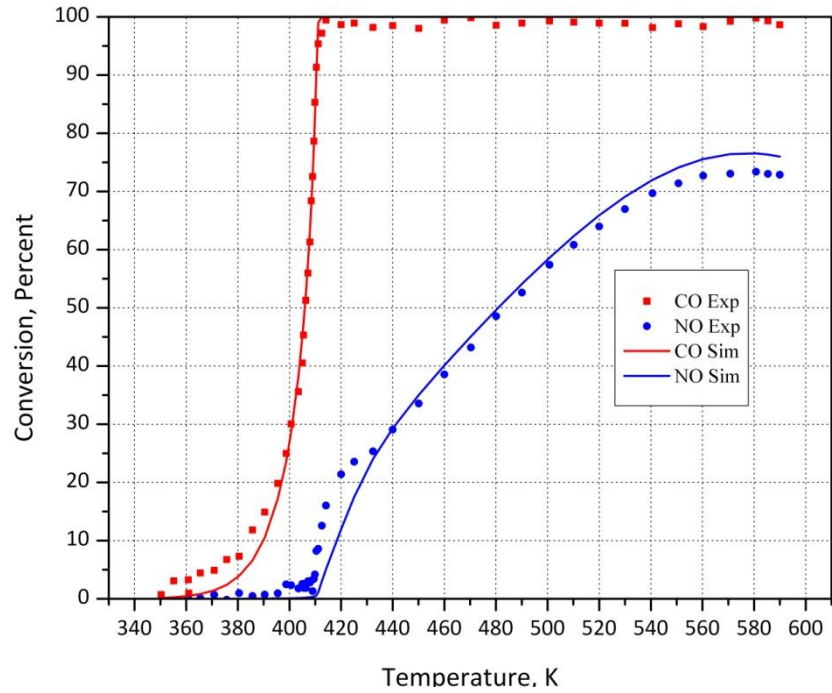


Figure 5-44: Individual optimization result vs. Experimental data, Run 24, Model 1

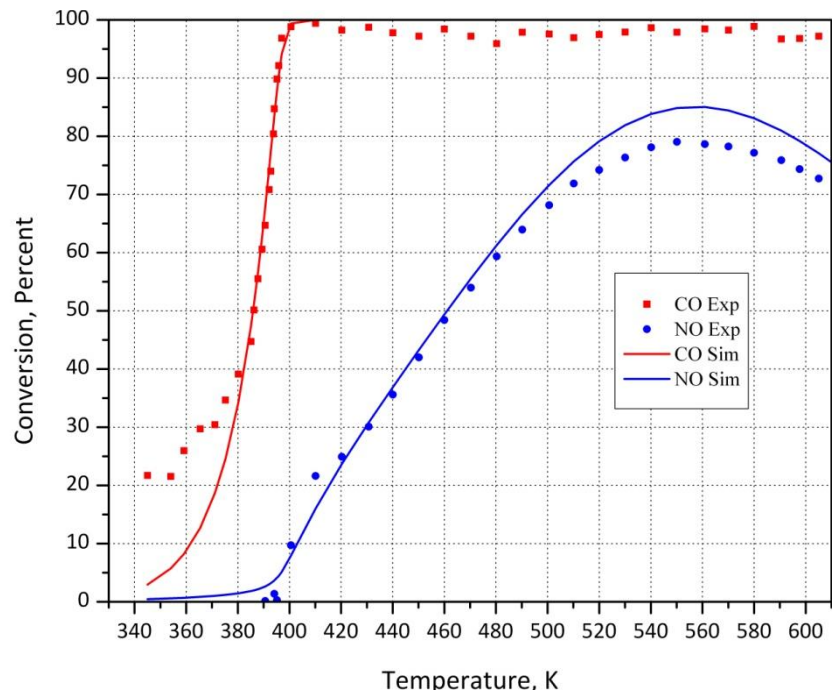


Figure 5-45: Individual optimization result vs. Experimental data, Run 25, Model 1

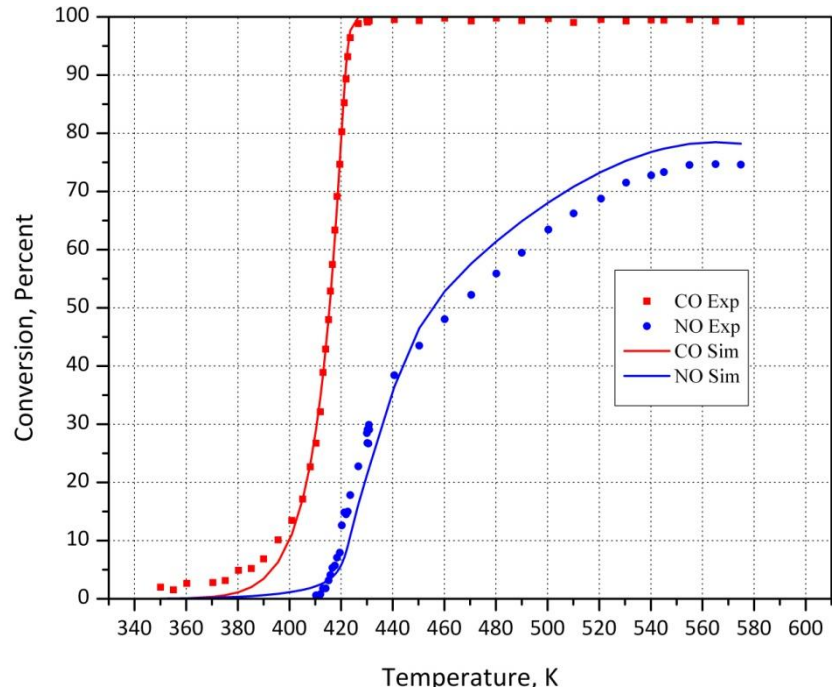


Figure 5-46: Individual optimization result vs. Experimental data, Run 26, Model 1

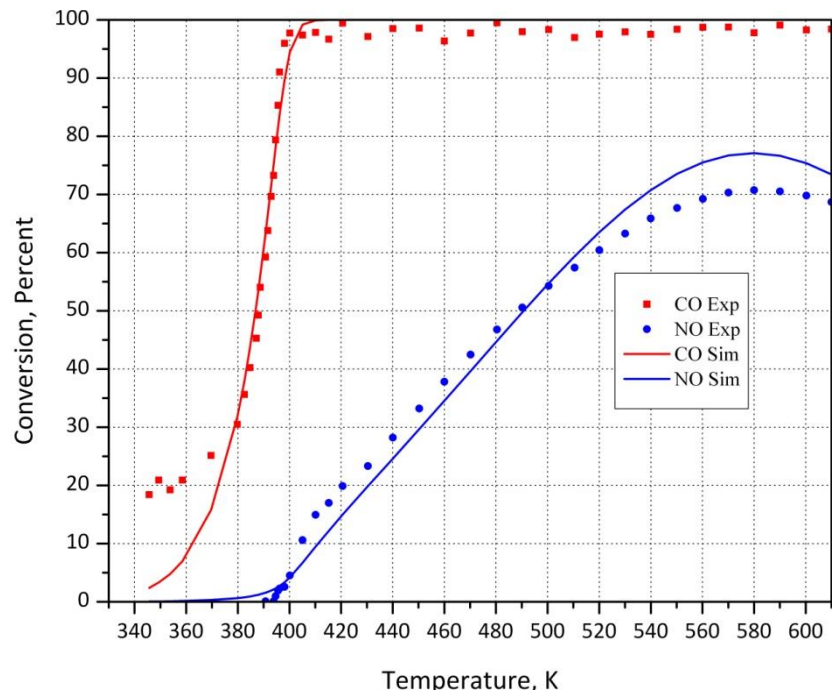


Figure 5-47: Individual optimization result vs. Experimental data, Run 27, Model 1

Model C₂, Oxidation of CO:

$$(-R_{CO}) = \frac{k_1 Y_{CO} Y_{O_2}}{T(1 + K_5 Y_{CO})^2 (1 + K_8 Y_{NO})} \quad (5-14)$$

Model C₂, Oxidation of NO:

$$(-R_{NO}) = \frac{k_4 Y_{NO} Y_{O_2} [1 - \beta]}{T(1 + K_5 Y_{CO})^2 (Y_{NO} + K_{10} Y_{NO_2})} \quad (5-15)$$

Table 5-29: Runs 22-24 individual optimization results, Model 2

Parameter		LB	HB	Run 22	Run 23	Run 24
k ₁	A ₁	0	30	19.7	29.6	29.9
	E ₁	20000	150000	24649	62696	97151
k ₄	A ₄	0	30	6.65	13.3	23.9
	E ₄	0	150000	14142	60400	44887
K ₅	B ₅	0	30	6.79	12.8	11.8
	H ₅	-150000	0	-47408	-11887	-18813
K ₈	B ₈	0	30	4.59	2.33	8.22
	H ₈	-150000	0	-72638	-115203	-0.04
K ₁₀	B ₁₀	0	30	0.56	8.38	17.8
	H ₁₀	-150000	0	-52028	-0.000	-5947
Model 2	CO Residual			3.4	7.4	12
	NO Residual			2.5	2.3	1.4
	Cumulative Residual			5.9	9.7	13.4

Table 5-30: Runs 25-27 individual optimization results, Model 2

Parameter		LB	HB	Run 25	Run 26	Run 27
k ₁	A ₁	0	30	25.3	19.2	18.5
	E ₁	20000	150000	25194	88918	36145
k ₄	A ₄	0	30	10.6	23.3	7.99
	E ₄	0	150000	17517	61970	43244
K ₅	B ₅	0	30	11.9	4.22	4.17
	H ₅	-150000	0	-4729	-113518	-86828
K ₈	B ₈	0	30	6.06	2.09	0.54
	H ₈	-150000	0	-2142	-3020	-20836
K ₁₀	B ₁₀	0	30	4.16	17.9	1.33
	H ₁₀	-150000	0	-26848	-2024	-1.2E-05
Model 2	CO Residual			9.4	12	54
	NO Residual			1.9	28	7.6
	Cumulative Residual			11.3	40	61.6

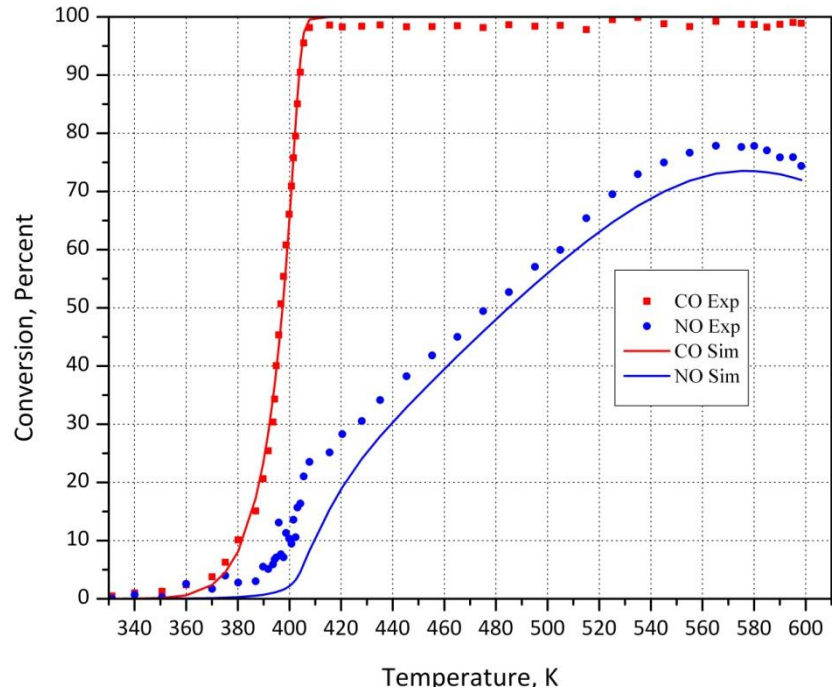


Figure 5-48: Individual optimization result vs. Experimental data, Run 22, Model 2

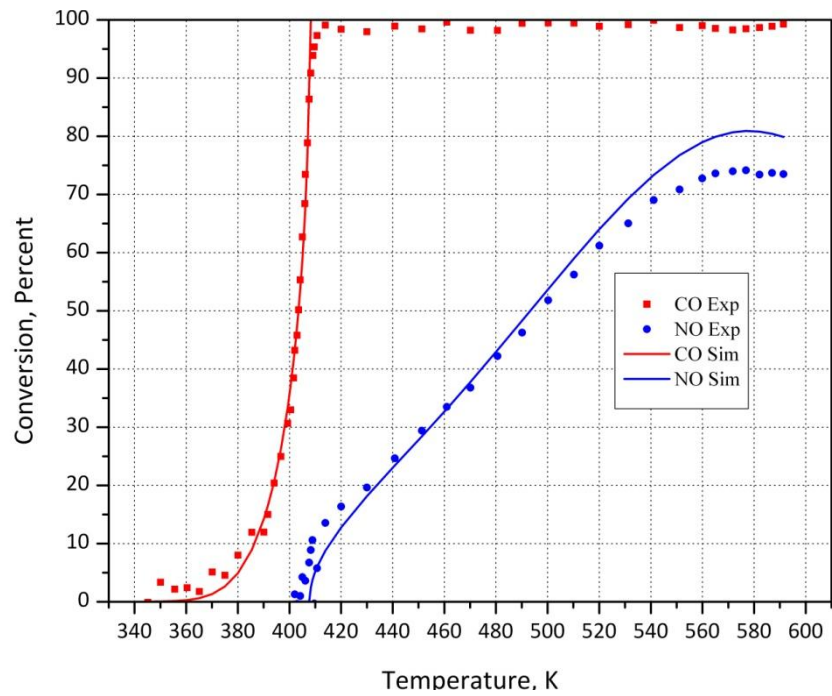


Figure 5-49: Individual optimization result vs. Experimental data, Run 23, Model 2

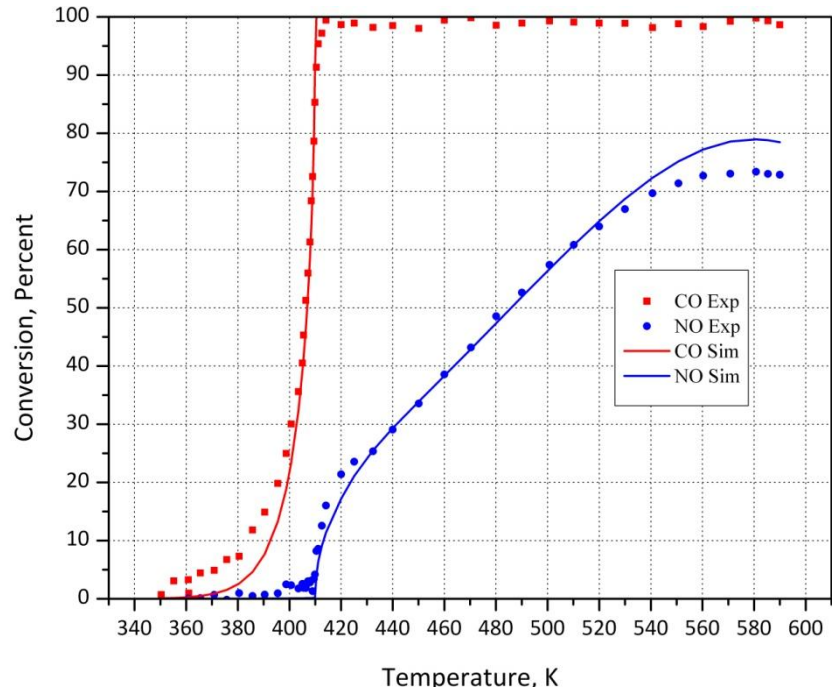


Figure 5-50: Individual optimization result vs. Experimental data, Run 24, Model 2

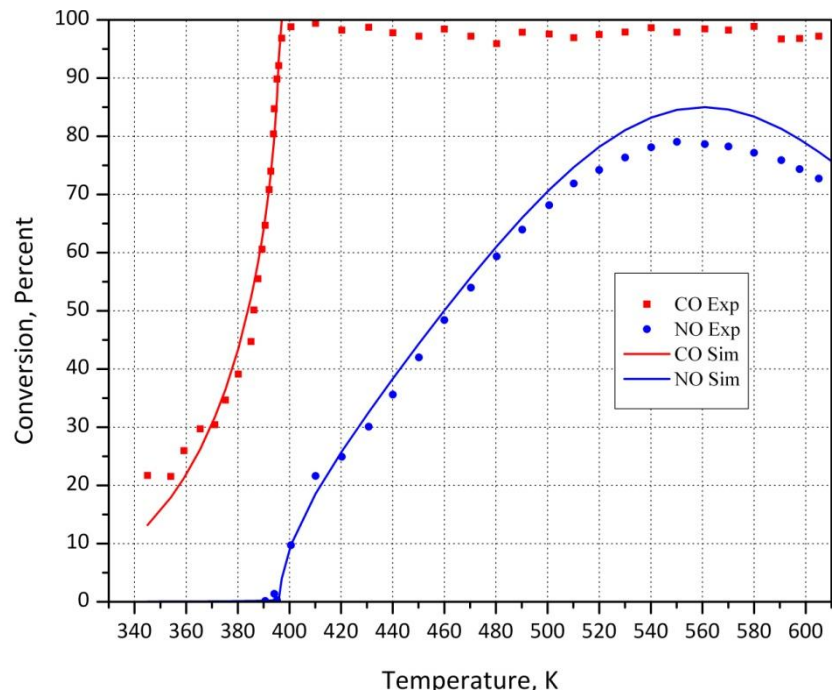


Figure 5-51: Individual optimization result vs. Experimental data, Run 25, Model 2

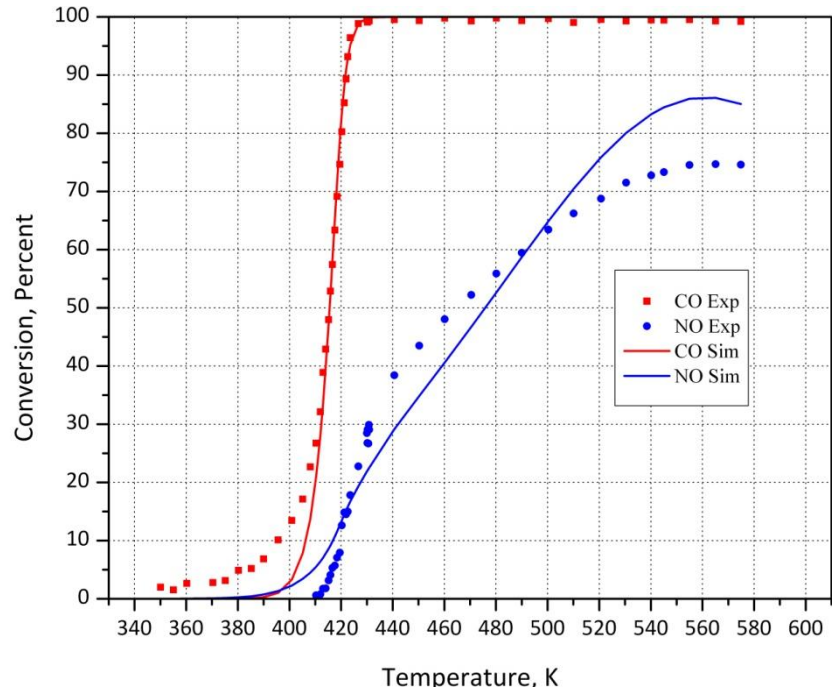


Figure 5-52: Individual optimization result vs. Experimental data, Run 26, Model 2

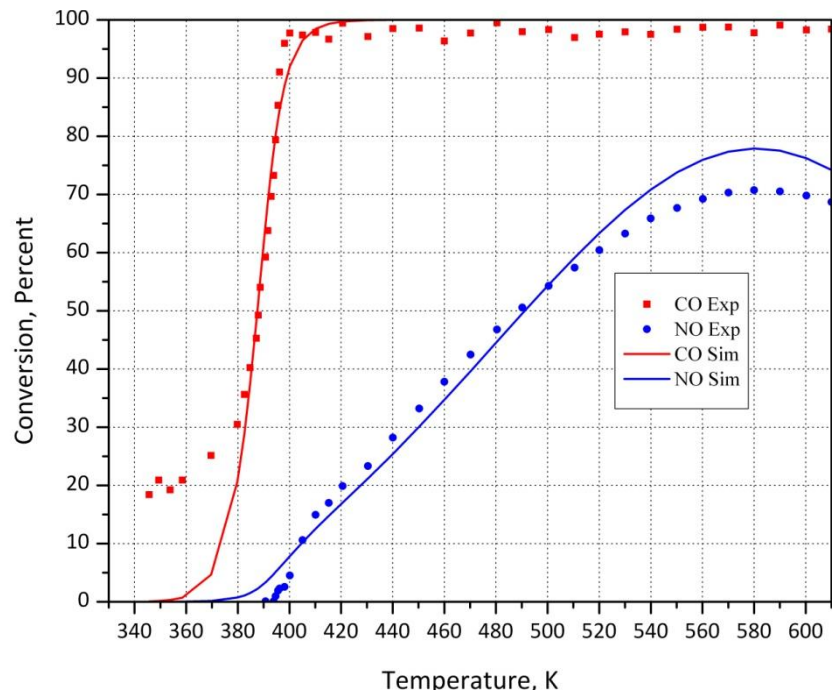


Figure 5-53: Individual optimization result vs. Experimental data, Run 27, Model 2

Model C₃, Oxidation of CO:

$$(-R_{CO}) = \frac{k_1 Y_{CO} Y_{O_2}}{T(1 + K_5 Y_{CO})^2 (1 + K_8 Y_{NO})} \quad (5-16)$$

Model C₃, Oxidation of NO:

$$(-R_{NO}) = \frac{k_4 Y_{O_2}^{0.5} [1 - \beta^2]}{T(1 + K_5 Y_{CO})^2 \left(1 + K_8 Y_{NO} + K_{10} \frac{Y_{NO_2}}{Y_{NO}} \right)} \quad (5-17)$$

Table 5-31: Runs 22-24 individual optimization results, Model 3

Parameter		LB	HB	Run 22	Run 23	Run 24
k ₁	A ₁	0	30	28.5	23.7	24.1
	E ₁	20000	150000	63607	147436	148106
k ₄	A ₄	0	30	13.7	7.92	18.6
	E ₄	0	150000	30704	49763	58084
K ₅	B ₅	0	30	4.18	3.88	4.15
	H ₅	-150000	0	-10407	-44308	-100692
K ₈	B ₈	0	30	14.4	8.41	9.97
	H ₈	-150000	0	-136200	-96094	-15522
K ₁₀	B ₁₀	0	30	9.96	3.76	14.1
	H ₁₀	-150000	0	-6797	-0.011	-5675
Model 3	CO Residual			3.1	12	26
	NO Residual			5.6	4.1	26
	Cumulative Residual			8.7	16.1	52

Table 5-32: Runs 25-27 individual optimization results, Model 3

Parameter		LB	HB	Run 25	Run 26	Run 27
k ₁	A ₁	0	30	24.4	27.8	29.9
	E ₁	20000	150000	34950	37281	49271
k ₄	A ₄	0	30	11.5	15.3	23.3
	E ₄	0	150000	44595	30305	13110
K ₅	B ₅	0	30	9.28	5.01	6.65
	H ₅	-150000	0	-538	-19050	-34475
K ₈	B ₈	0	30	11.7	15.7	18.0
	H ₈	-150000	0	-10021	-144006	-310
K ₁₀	B ₁₀	0	30	6.29	10.2	18.7
	H ₁₀	-150000	0	-390	-4756	-43311
Model 3	CO Residual			16	4.4	37
	NO Residual			5.8	2.7	17
	Cumulative Residual			21.8	7.1	54

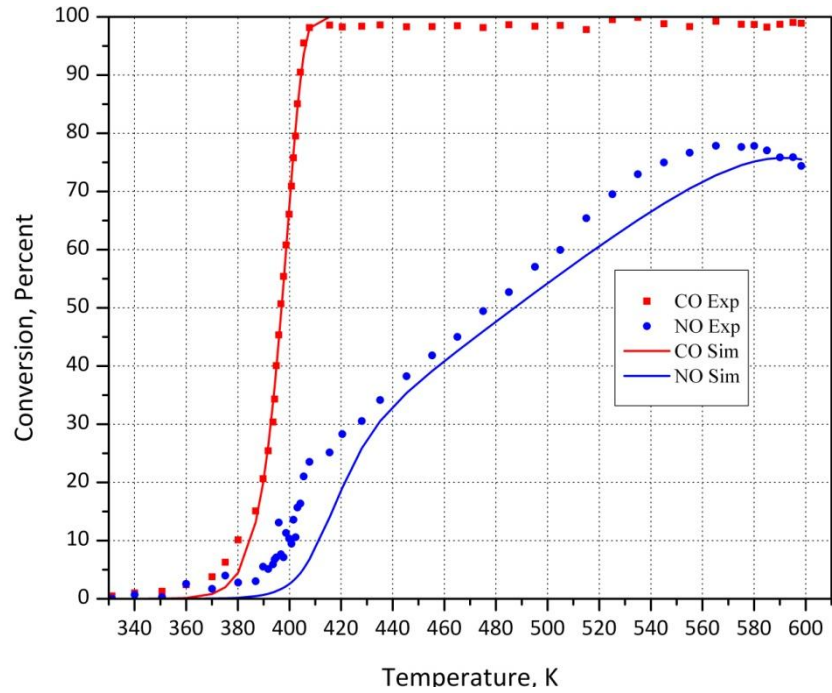


Figure 5-54: Individual optimization result vs. Experimental data, Run 22, Model 3

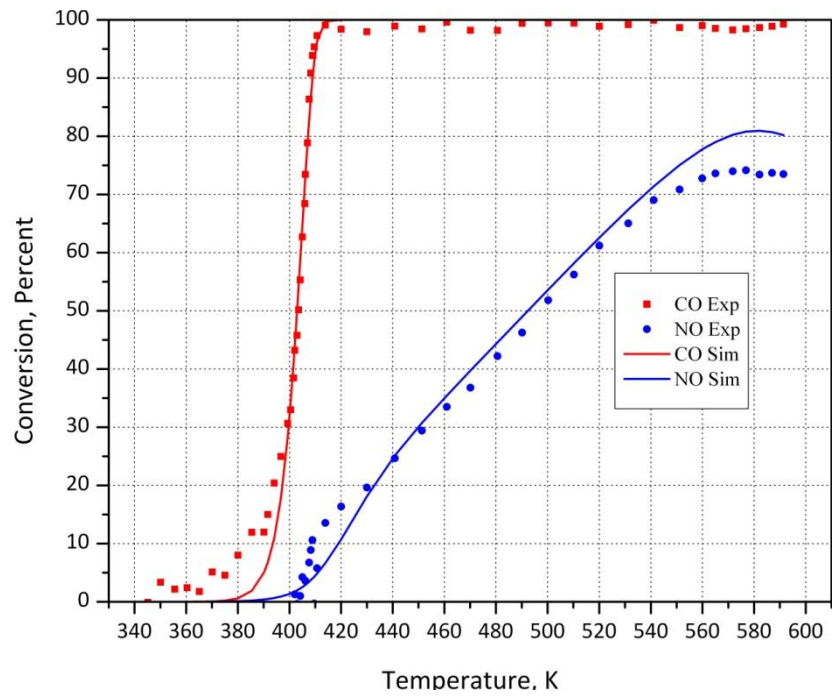


Figure 5-55: Individual optimization result vs. Experimental data, Run 23, Model 3

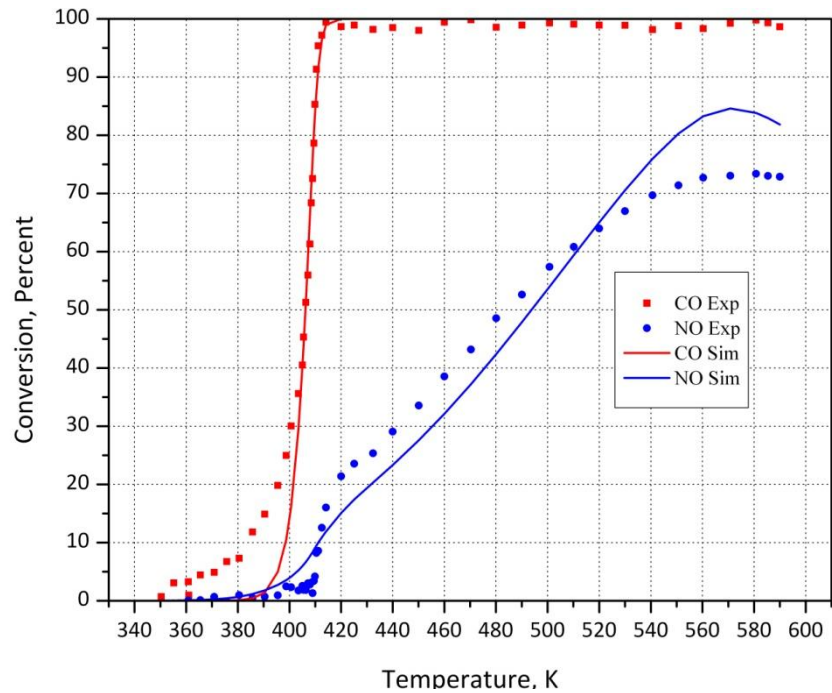


Figure 5-56: Individual optimization result vs. Experimental data, Run 24, Model 3

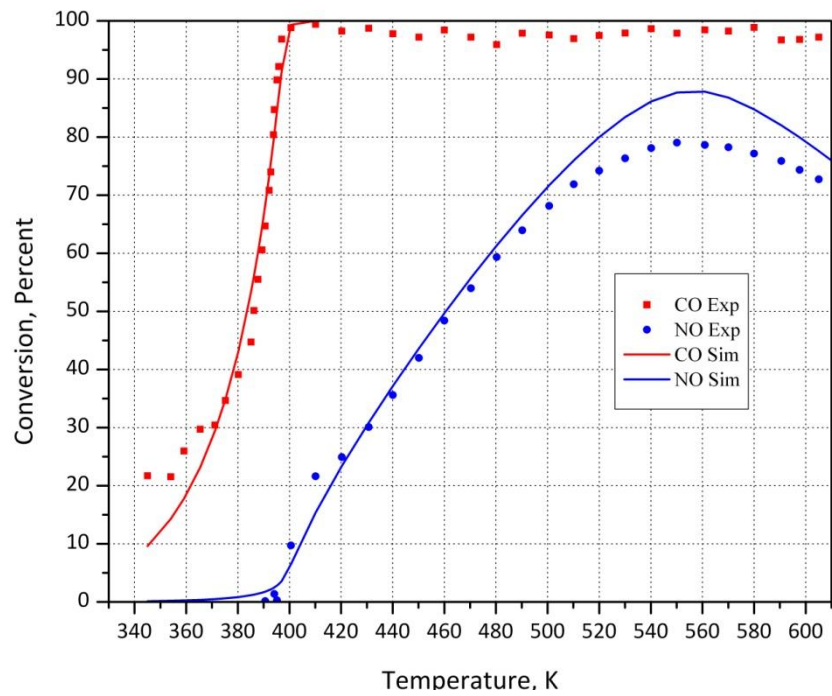


Figure 5-57: Individual optimization result vs. Experimental data, Run 25, Model 3

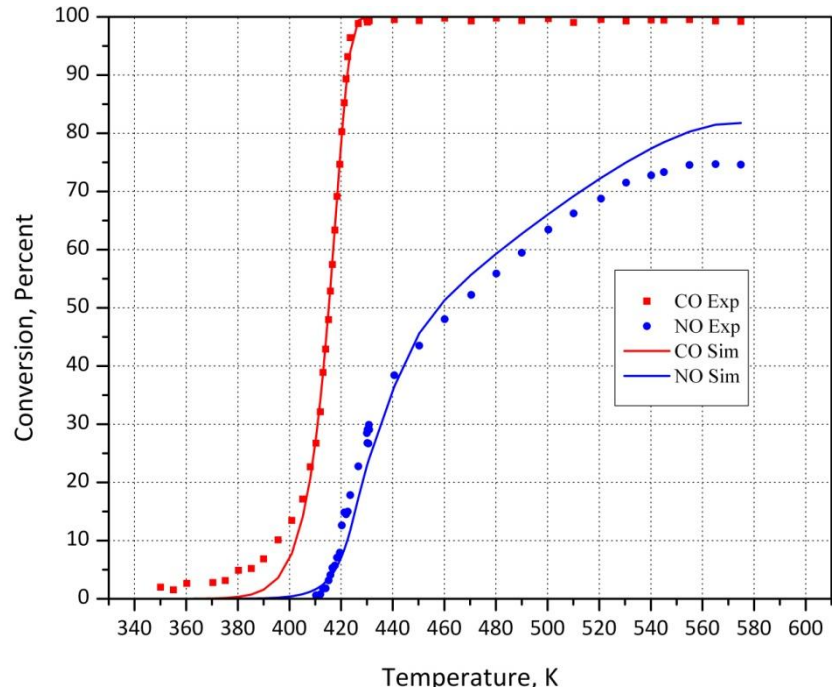


Figure 5-58: Individual optimization result vs. Experimental data, Run 26, Model 3

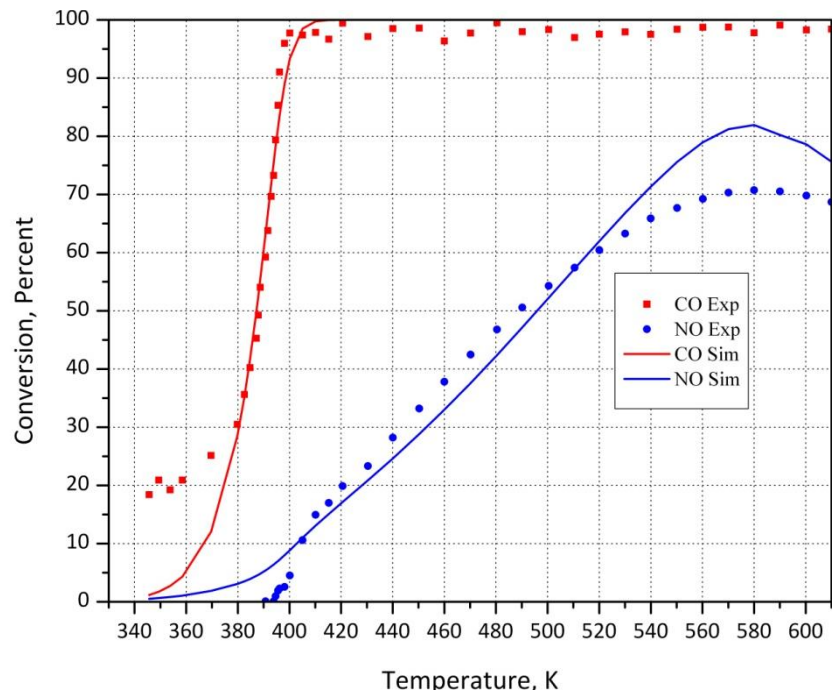


Figure 5-59: Individual optimization result vs. Experimental data, Run 27, Model 3

Model C₄, Oxidation of CO:

$$(-R_{CO}) = \frac{k_1 Y_{CO} Y_{O_2}}{T(1 + K_5 Y_{CO})^2 (1 + K_8 Y_{NO})} \quad (5-18)$$

Model C₄, Oxidation of NO:

$$(-R_{NO}) = \frac{k_4 Y_{O_2}^{0.5} [1 - \beta]}{T(1 + K_5 Y_{CO})^2 \left(1 + K_8 Y_{NO} + K_{10} \frac{Y_{NO_2}}{Y_{NO}} \right)} \quad (5-19)$$

Table 5-33: Runs 22-24 individual optimization results, Model 4

Parameter		LB	HB	Run 22	Run 23	Run 24
k ₁	A ₁	0	30	19.5	20.2	21.6
	E ₁	20000	150000	24814	29144	22966
k ₄	A ₄	0	30	6.71	6.15	8.11
	E ₄	0	150000	16377	20827	3656
K ₅	B ₅	0	30	6.74	6.91	8.14
	H ₅	-150000	0	-47263	-58783	-48892
K ₈	B ₈	0	30	4.32	6.16	6.62
	H ₈	-150000	0	-59110	-15062	-4098
K ₁₀	B ₁₀	0	30	3.85	0.931	2.75
	H ₁₀	-150000	0	-63606	-35578	-55847
Model 4	CO Residual			4.2	3.8	4.7
	NO Residual			41	1.0	0.70
	Cumulative Residual			45.2	4.8	5.4

Table 5-34: Runs 25-27 individual optimization results, Model 4

Parameter		LB	HB	Run 25	Run 26	Run 27
k ₁	A ₁	0	30	22.9	20.0	29.1
	E ₁	20000	150000	20048.	98014	117729
k ₄	A ₄	0	30	11.2	8.49	21.2
	E ₄	0	150000	53952	57944	26294
K ₅	B ₅	0	30	4.73	5.13	6.98
	H ₅	-150000	0	-4.96	-78911	-0.018
K ₈	B ₈	0	30	11.4	7.73	14.0
	H ₈	-150000	0	-64500	-0.015	-31785
K ₁₀	B ₁₀	0	30	6.32	3.98	16.9
	H ₁₀	-150000	0	-389	-0.016	-38398
Model 4	CO Residual			42	9.1	51
	NO Residual			8.1	18	23
	Cumulative Residual			50.1	27.1	74

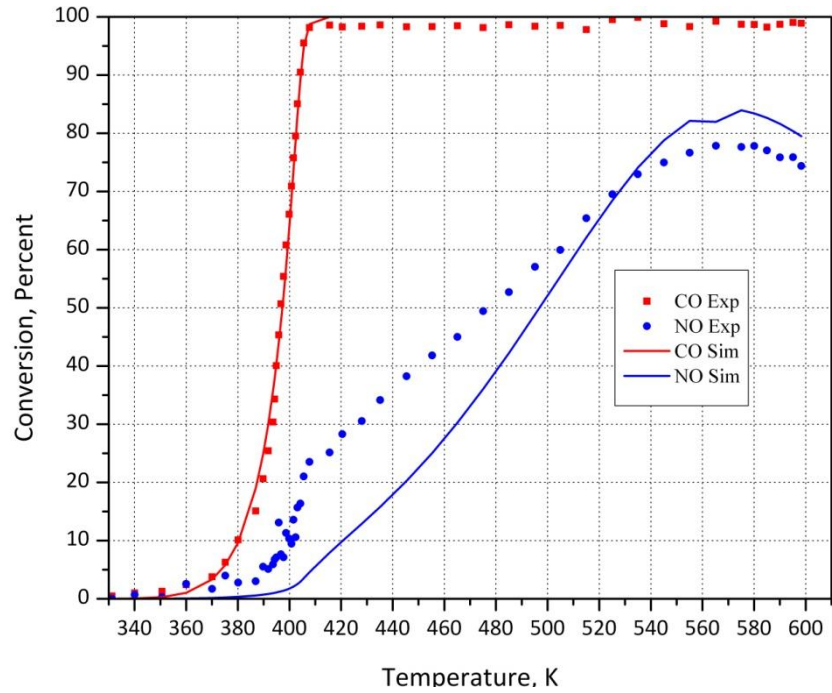


Figure 5-60: Individual optimization result vs. Experimental data, Run 22, Model 4

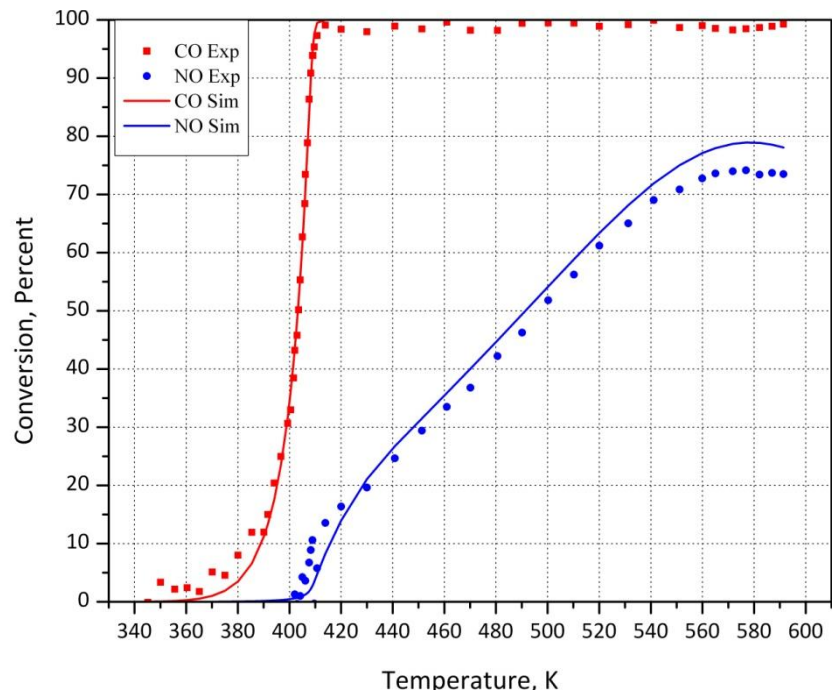


Figure 5-61: Individual optimization result vs. Experimental data, Run 23, Model 4

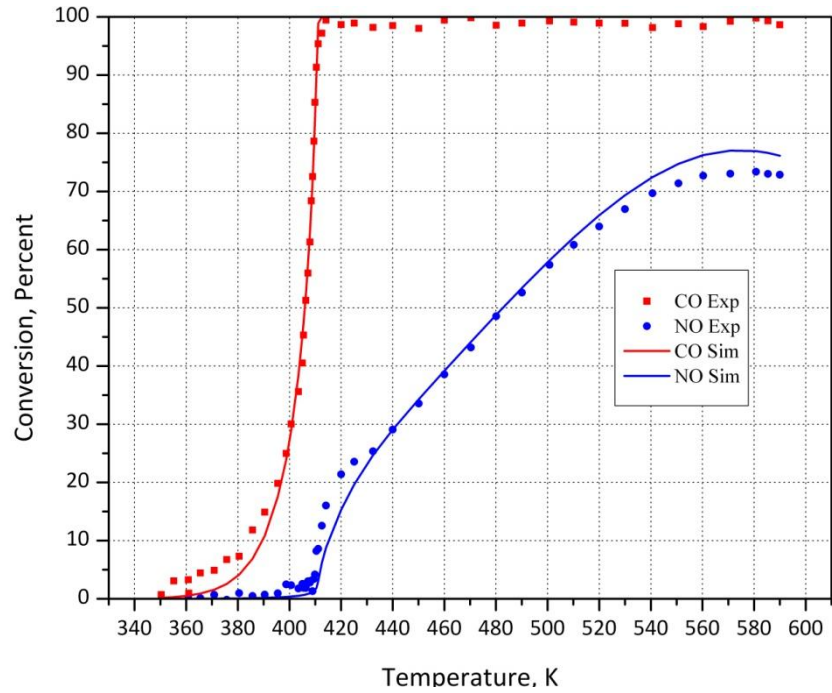


Figure 5-62: Individual optimization result vs. Experimental data, Run 24, Model 4

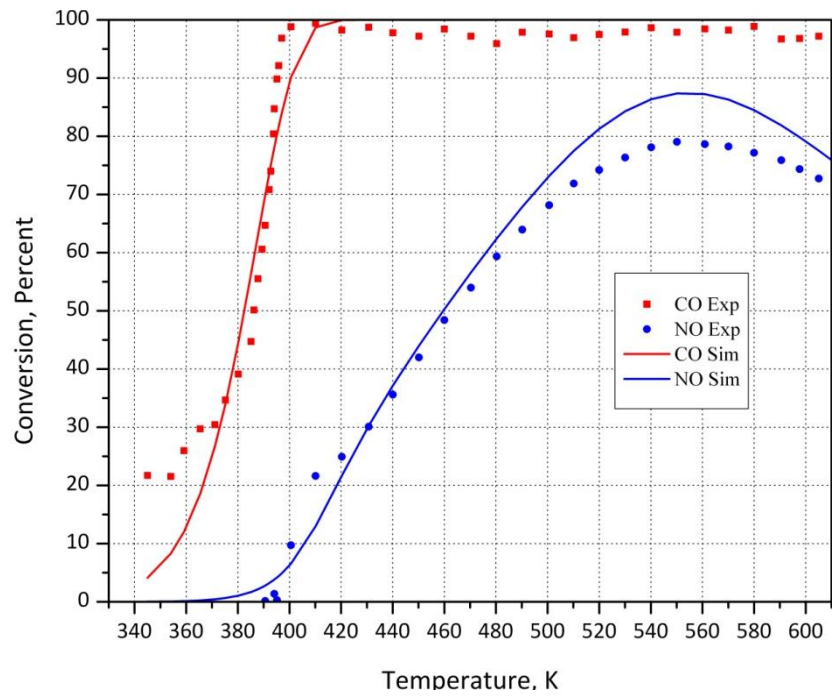


Figure 5-63: Individual optimization result vs. Experimental data, Run 25, Model 4

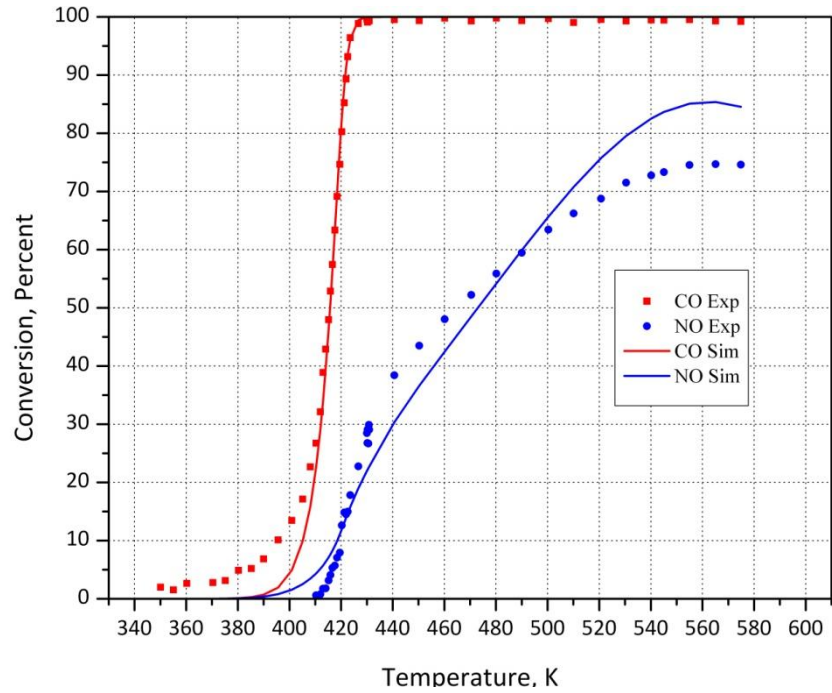


Figure 5-64: Individual optimization result vs. Experimental data, Run 26, Model 4

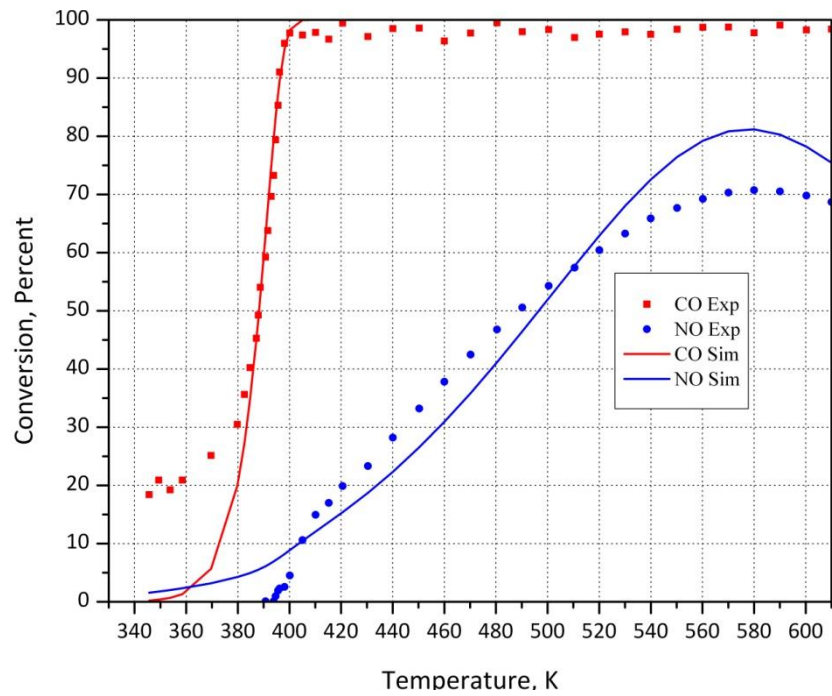


Figure 5-65: Individual optimization result vs. Experimental data, Run 27, Model 4

Model C₅, Oxidation of CO:

$$(-R_{CO}) = \frac{k_1 Y_{CO} Y_{O_2}}{T(1 + K_5 Y_{CO} + K_8 Y_{NO})^2} \quad (5-20)$$

Model C₅, Oxidation of NO:

$$(-R_{NO}) = \frac{k_4 Y_{NO} Y_{O_2}^{0.5} [1 - \beta]}{T(1 + K_5 Y_{CO} + K_8 Y_{NO} + K_{10} Y_{NO_2})^2} \quad (5-21)$$

Table 5-35: Runs 22-24 individual optimization results, Model 5

Parameter		LB	HB	Run 22	Run 23	Run 24
k ₁	A ₁	0	30	29.8	20.7	28.1
	E ₁	20000	150000	74877	53851	43540
k ₄	A ₄	0	30	24.0	14.4	18.1
	E ₄	0	150000	21728	34529	70983
K ₅	B ₅	0	30	11.7	7.26	10.8
	H ₅	-150000	0	-23666	-46152	-70770
K ₈	B ₈	0	30	9.34	3.78	6.11
	H ₈	-150000	0	-121039	-32362	-94811
K ₁₀	B ₁₀	0	30	15.4	8.67	10.9
	H ₁₀	-150000	0	-22746	-18063	-0.010
Model 5	CO Residual			33	3.7	35
	NO Residual			9.0	1.1	2.0
	Cumulative Residual			42	4.8	37

Table 5-36: Runs 25-27 individual optimization results, Model 5

Parameter		LB	HB	Run 25	Run 26	Run 27
k ₁	A ₁	0	30	29.9	29.0	18.3
	E ₁	20000	150000	51017	144507	23882
k ₄	A ₄	0	30	26.0	22.7	13.9
	E ₄	0	150000	55995	40672	32662
K ₅	B ₅	0	30	12.5	4.15	5.05
	H ₅	-150000	0	-4465	-32335	-74676
K ₈	B ₈	0	30	13.6	11.0	0.98
	H ₈	-150000	0	-1987	-100615	-24238
K ₁₀	B ₁₀	0	30	14.8	13.3	3.31
	H ₁₀	-150000	0	-6629	-2771	-157
Model 5	CO Residual			36	28	50
	NO Residual			22	2.4	5.3
	Cumulative Residual			58	30.4	55.3

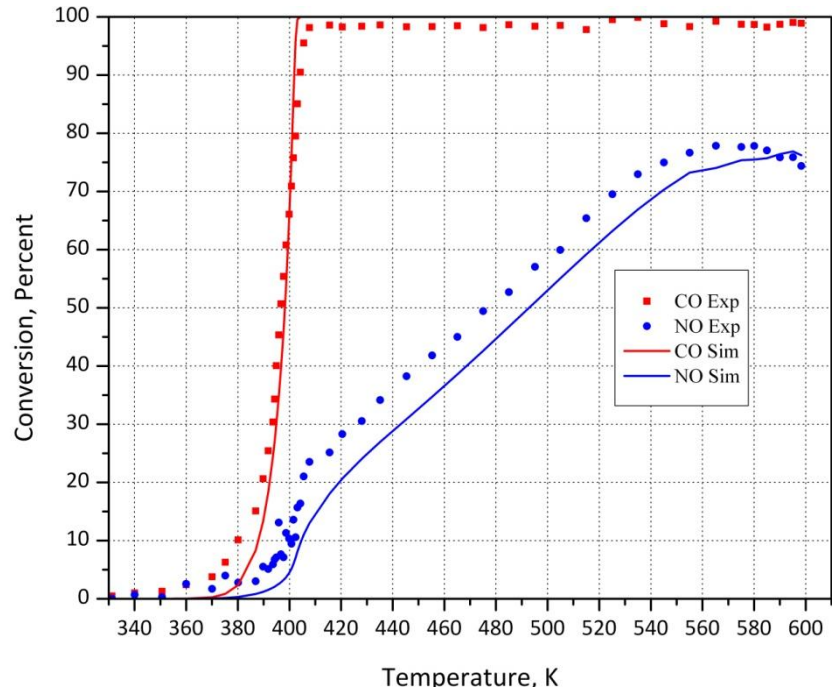


Figure 5-66: Individual optimization result vs. Experimental data, Run 22, Model 5

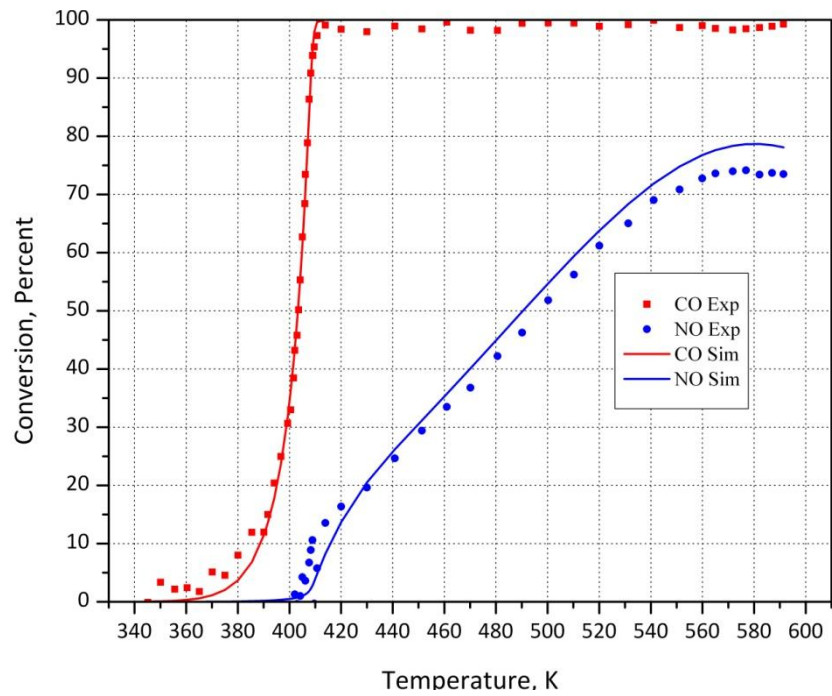


Figure 5-67: Individual optimization result vs. Experimental data, Run 23, Model 5

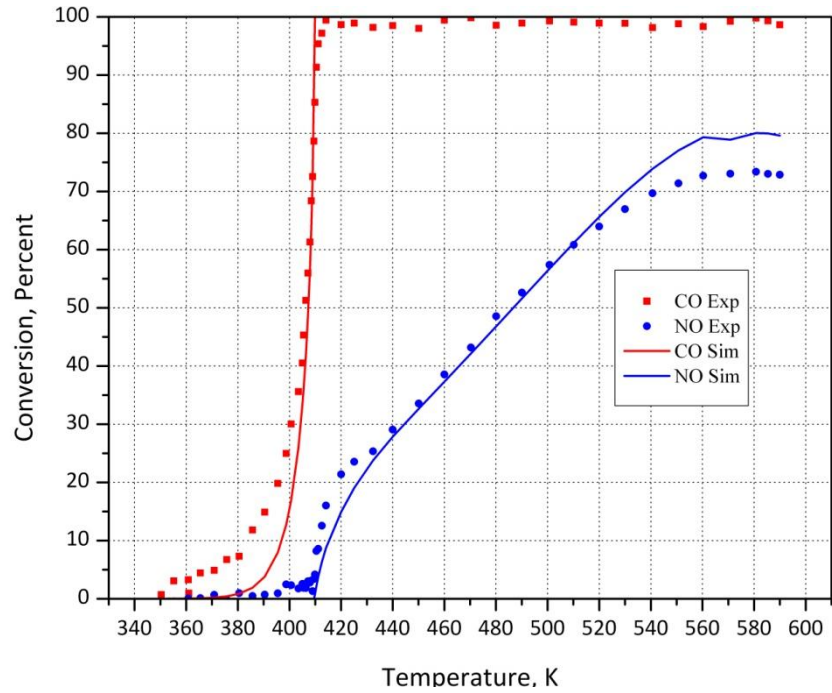


Figure 5-68: Individual optimization result vs. Experimental data, Run 24, Model 5

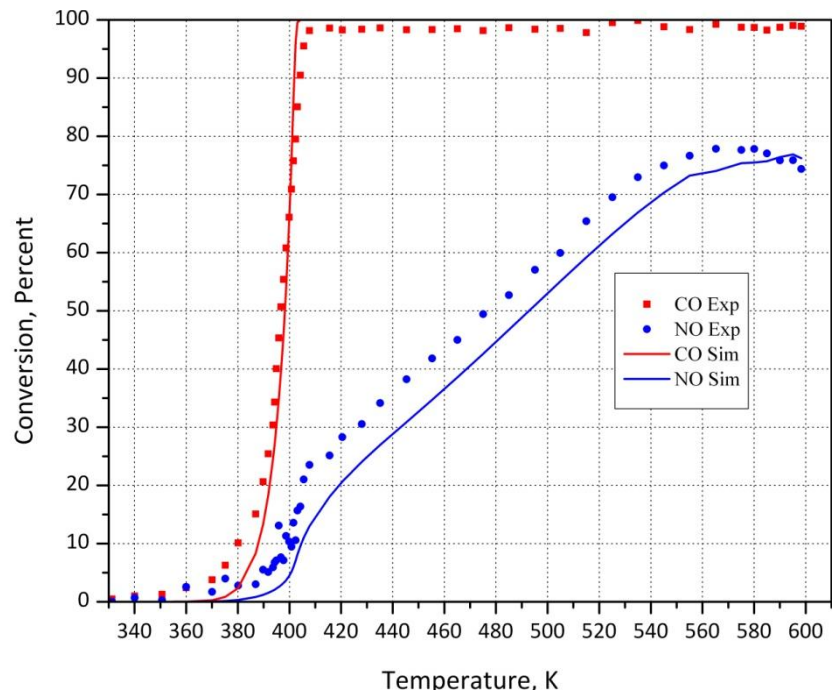


Figure 5-69: Individual optimization result vs. Experimental data, Run 25, Model 5

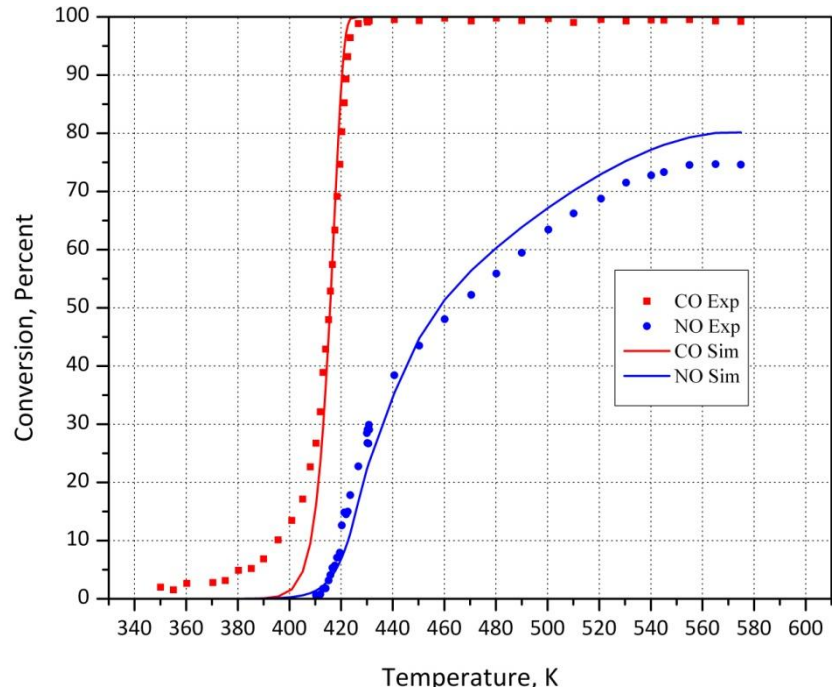


Figure 5-70: Individual optimization result vs. Experimental data, Run 26, Model 5

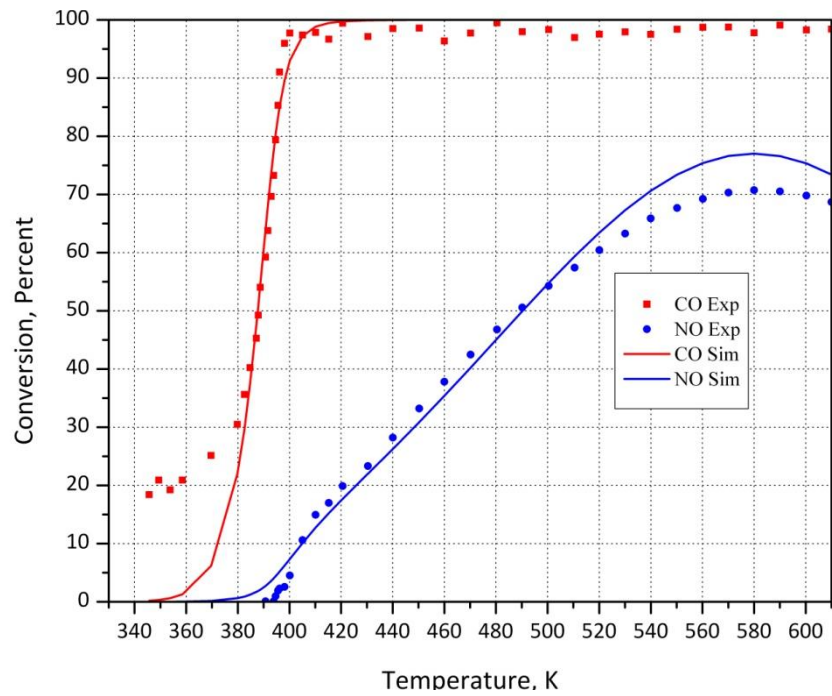


Figure 5-71: Individual optimization result vs. Experimental data, Run 27, Model 5

For each model, All different experiments were selected to be optimized simultaneously to find a set of parameters for each model and use them as general correlation for NO and CO oxidation modelling. Table 5-37 to Table 5-41 and Figure 5-72 to Figure 5-101 are presenting the results.

Table 5-37: Runs 22-27 simultaneous optimization results, Model 1

Parameter		LB	HB	Run 22	Run 23	Run 24	Run 25	Run 26	Run 27
k ₁	A ₁	0	30	20.2					
	E ₁	20000	150000	42275					
k ₄	A ₄	0	30	14.3					
	E ₄	0	150000	25965					
K ₅	B ₅	0	30	7.26					
	H ₅	-150000	0	-34807					
K ₈	B ₈	0	30	6.38					
	H ₈	-150000	0	-21033					
Model 1	CO Residual			33	25	19	69	3.4	57
	NO Residual			12.2	9.7	3.3	29	45	3.6
	Cumulative Residual			45.2	34.7	22.3	98	48.4	60.6

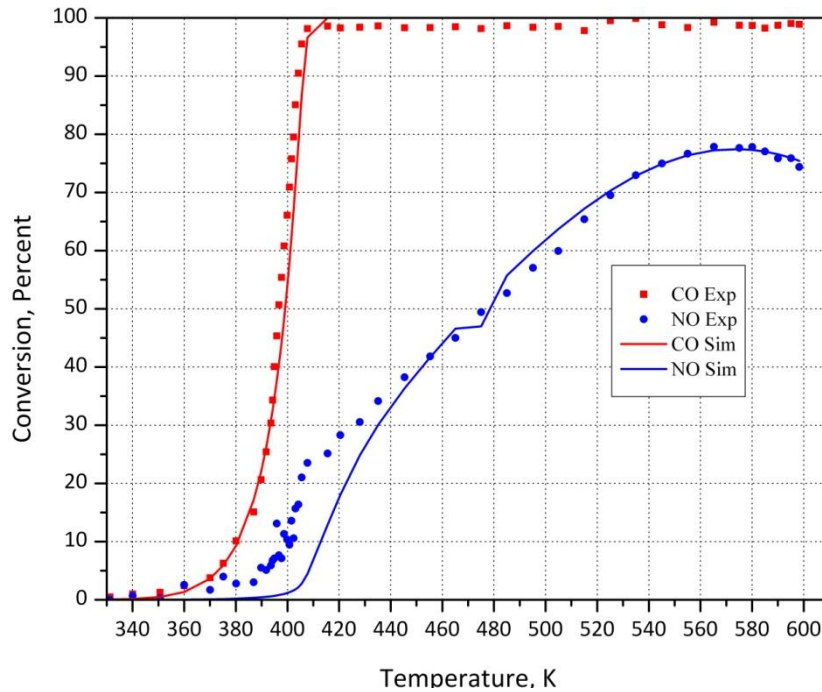


Figure 5-72: Simultaneous optimization result vs. Experimental data, Run 22, Model 1

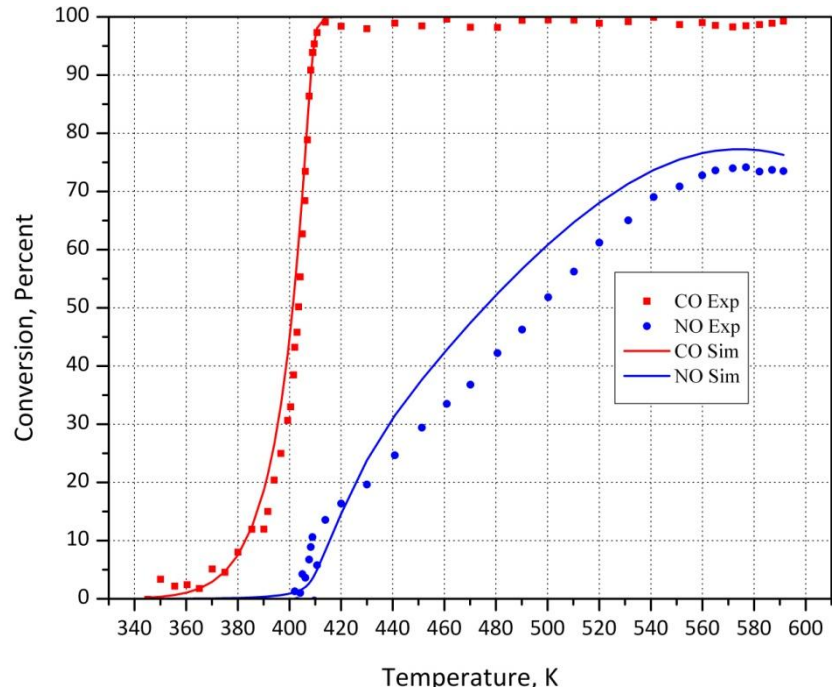


Figure 5-73: Simultaneous optimization result vs. Experimental data, Run 23, Model 1

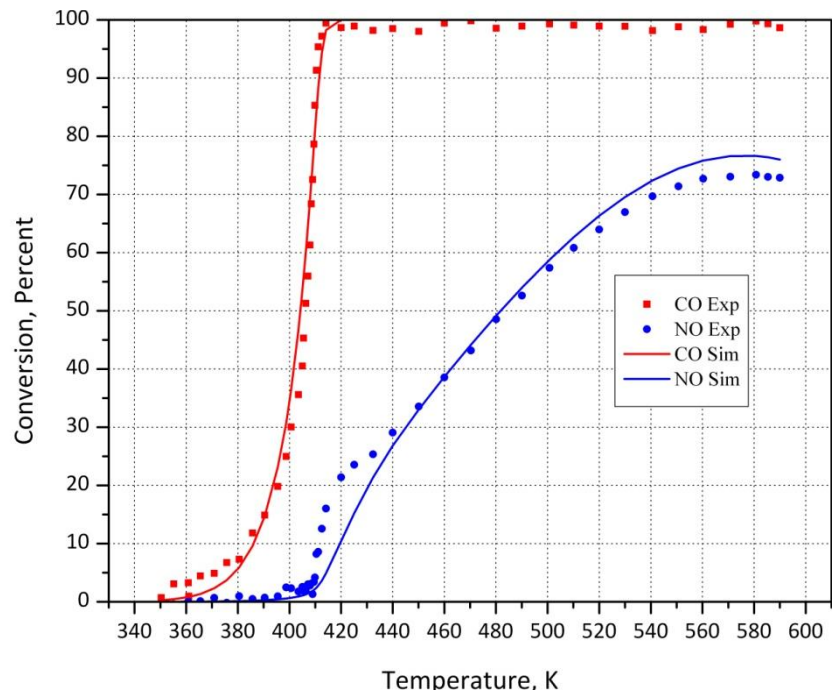


Figure 5-74: Simultaneous optimization result vs. Experimental data, Run 24, Model 1

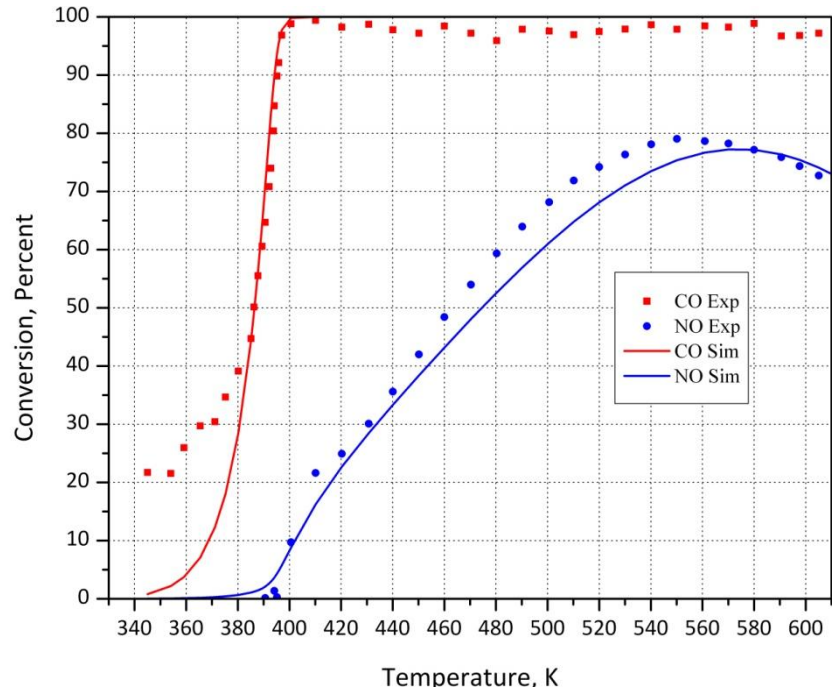


Figure 5-75: Simultaneous optimization result vs. Experimental data, Run 25, Model 1

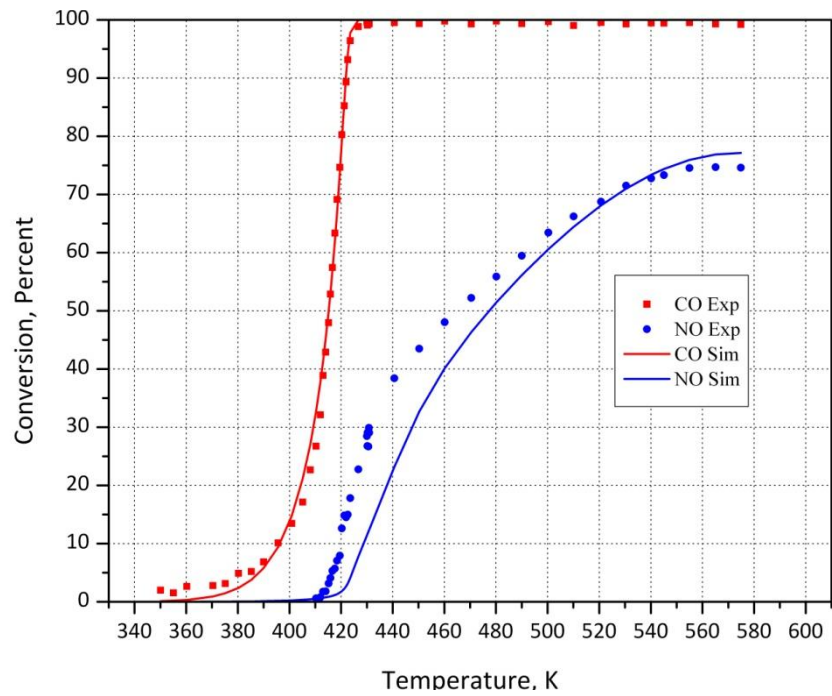


Figure 5-76: Simultaneous optimization result vs. Experimental data, Run 26, Model 1

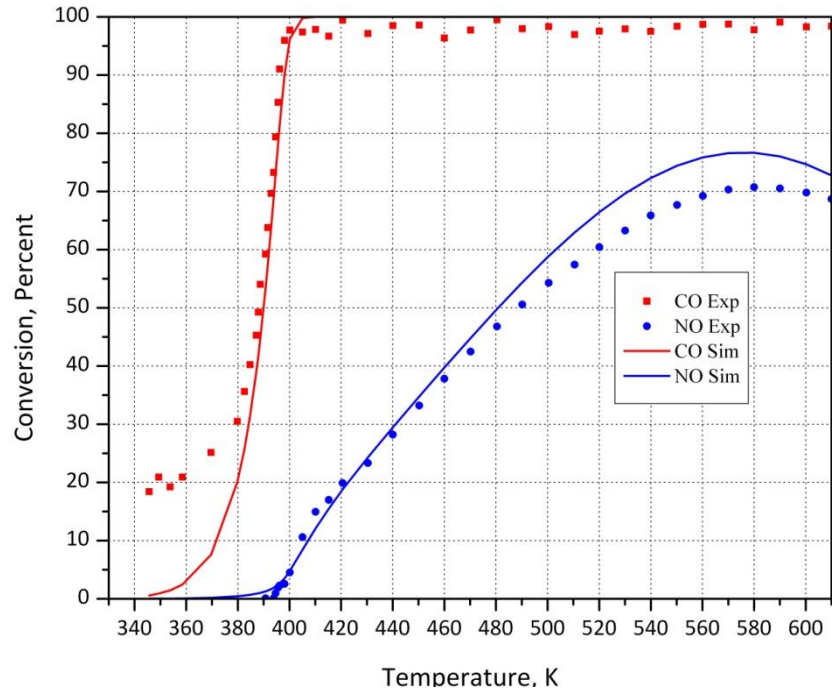


Figure 5-77: Simultaneous optimization result vs. Experimental data, Run 27, Model 1

Table 5-38: Runs 22-27 simultaneous optimization results, Model 2

Parameter	LB	HB	Run 22	Run 23	Run 24	Run 25	Run 26	Run 27
k ₁	A ₁	0	30	19.3				
	E ₁	20000	150000	23551				
k ₄	A ₄	0	30	7.64				
	E ₄	0	150000	25870				
K ₅	B ₅	0	30	6.79				
	H ₅	-150000	0	-43861				
K ₈	B ₈	0	30	5.82				
	H ₈	-150000	0	-34052				
K ₁₀	B ₁₀	0	30	0.86				
	H ₁₀	-150000	0	-22496				
Model 2	CO Residual		30	36	31.	70	8.0	52
	NO Residual		214	43	44	13	22	26
	Cumulative Residual		244	79	75	83	30	78

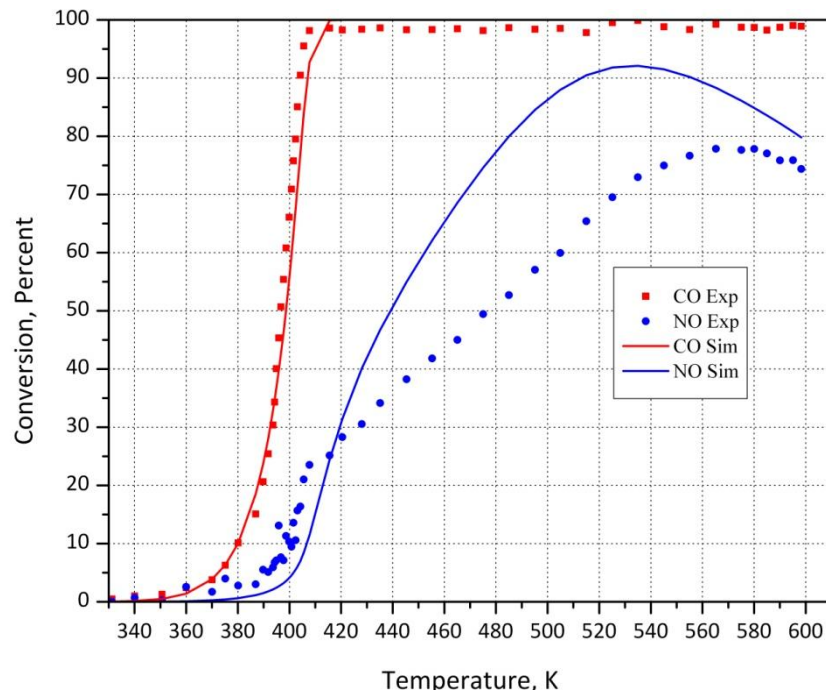


Figure 5-78: Simultaneous optimization result vs. Experimental data, Run 22, Model 2

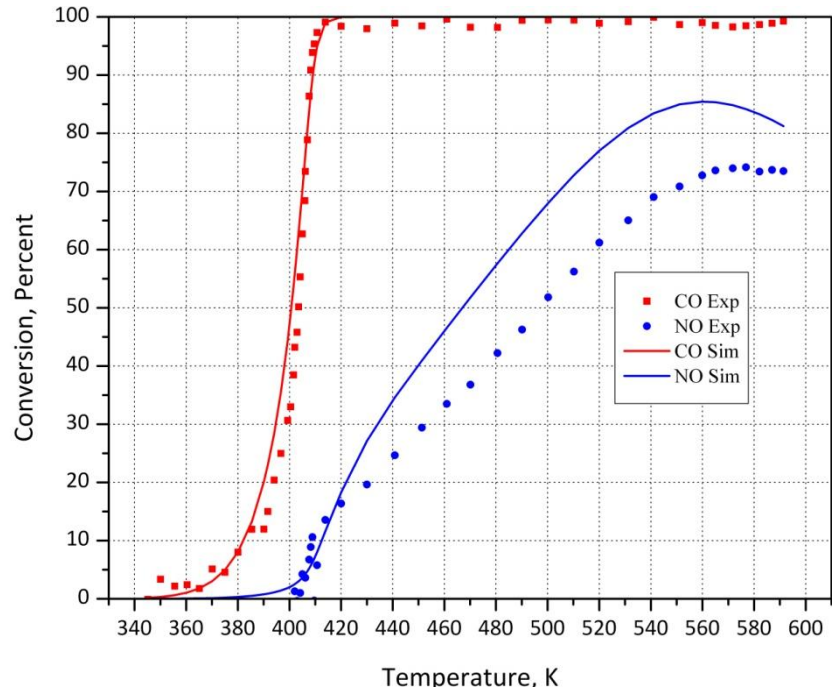


Figure 5-79: Simultaneous optimization result vs. Experimental data, Run 23, Model 2

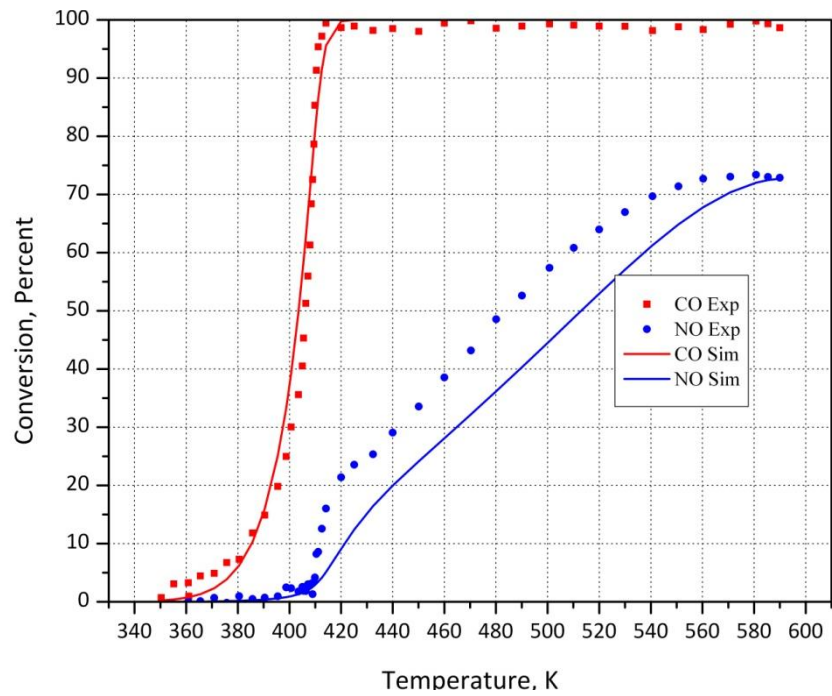


Figure 5-80: Simultaneous optimization result vs. Experimental data, Run 24, Model 2

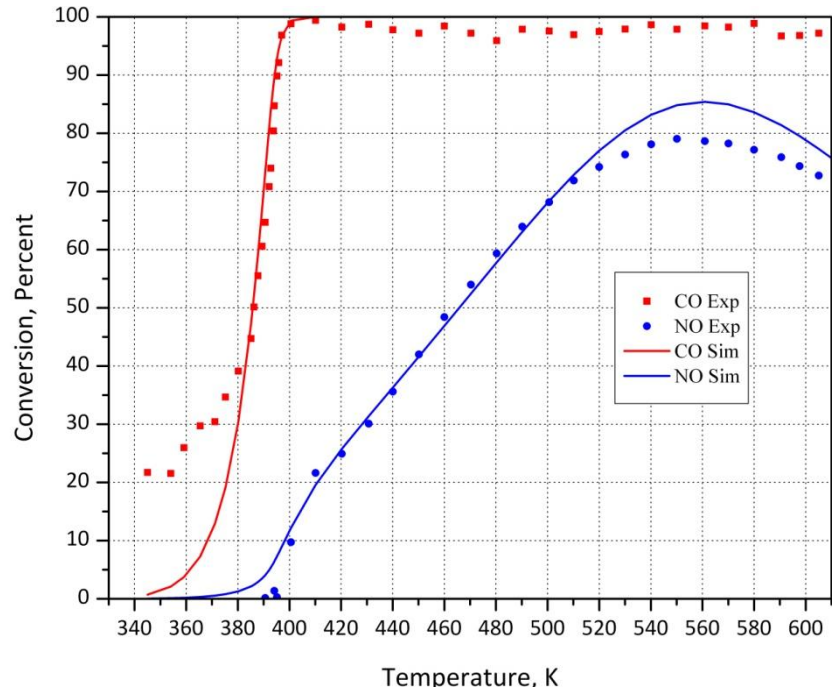


Figure 5-81: Simultaneous optimization result vs. Experimental data, Run 25, Model 2

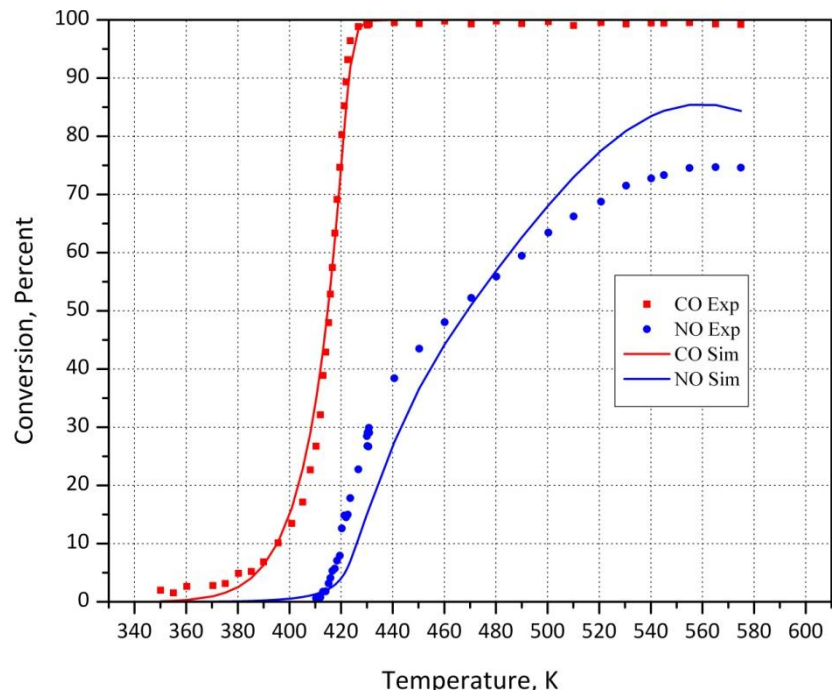


Figure 5-82: Simultaneous optimization result vs. Experimental data, Run 26, Model 2

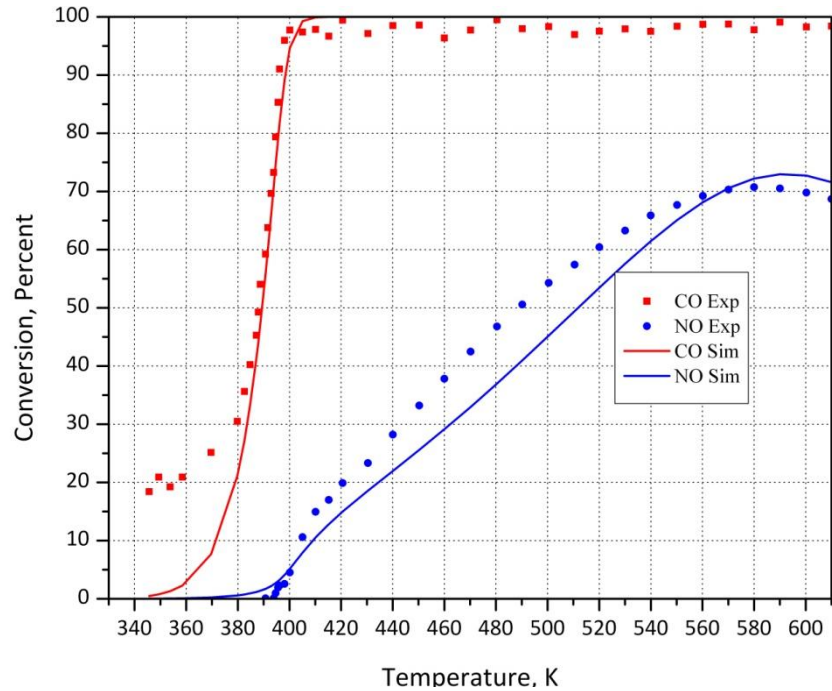


Figure 5-83: Simultaneous optimization result vs. Experimental data, Run 27, Model 2

Table 5-39: Runs 22-27 simultaneous optimization results, Model 3

Parameter	LB	HB	Run 22	Run 23	Run 24	Run 25	Run 26	Run 27
k_1	A_1	0	30	19.7				
	E_1	20000	150000	22971				
k_4	A_4	0	30	7.51				
	E_4	0	150000	27035				
K_5	B_5	0	30	7.04				
	H_5	-150000	0	-43610				
K_8	B_8	0	30	5.91				
	H_8	-150000	0	-36838				
K_{10}	B_{10}	0	30	2.77				
	H_{10}	-150000	0	-23803				
Model 3	CO Residual		29	27	20	84	4.8	59
	NO Residual		132	27	30	24	21	18
	Cumulative Residual		161	54	50	108	25.8	77

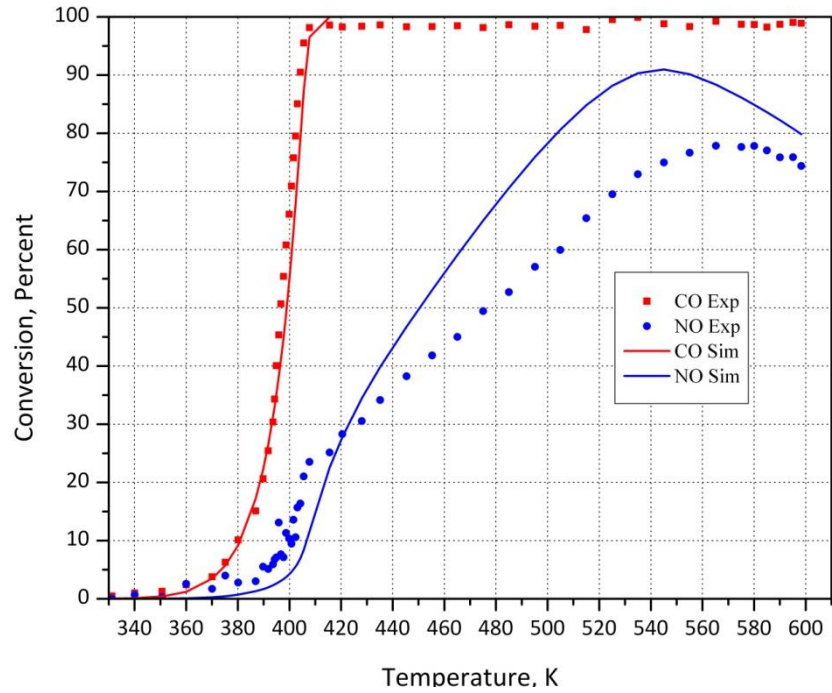


Figure 5-84: Simultaneous optimization result vs. Experimental data, Run 22, Model 3

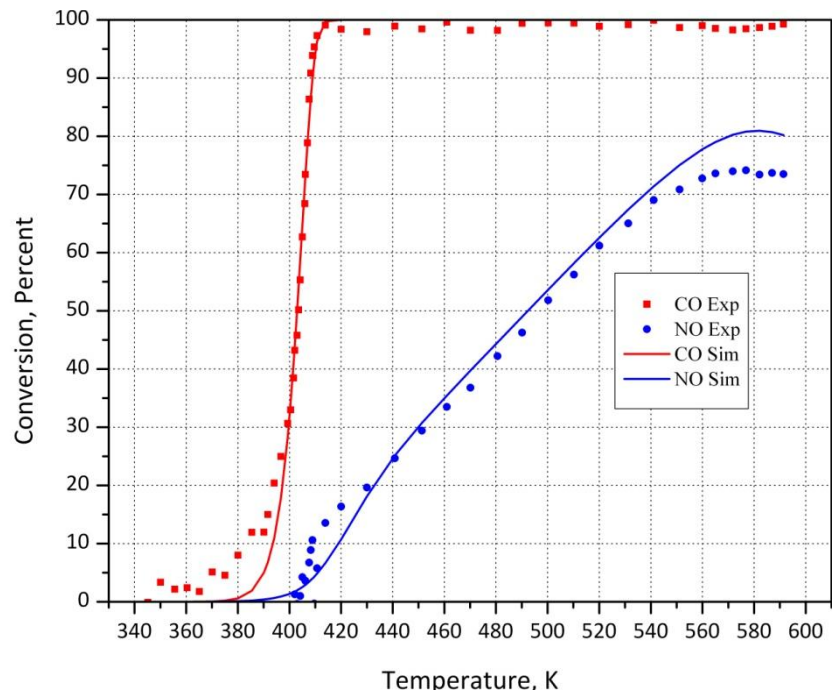


Figure 5-85: Simultaneous optimization result vs. Experimental data, Run 23, Model 3

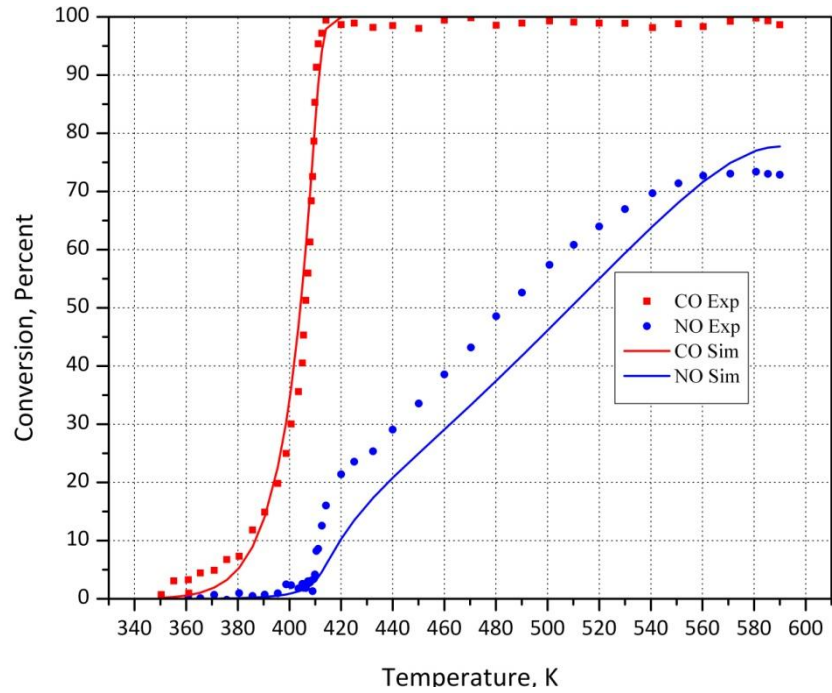


Figure 5-86: Simultaneous optimization result vs. Experimental data, Run 24, Model 3

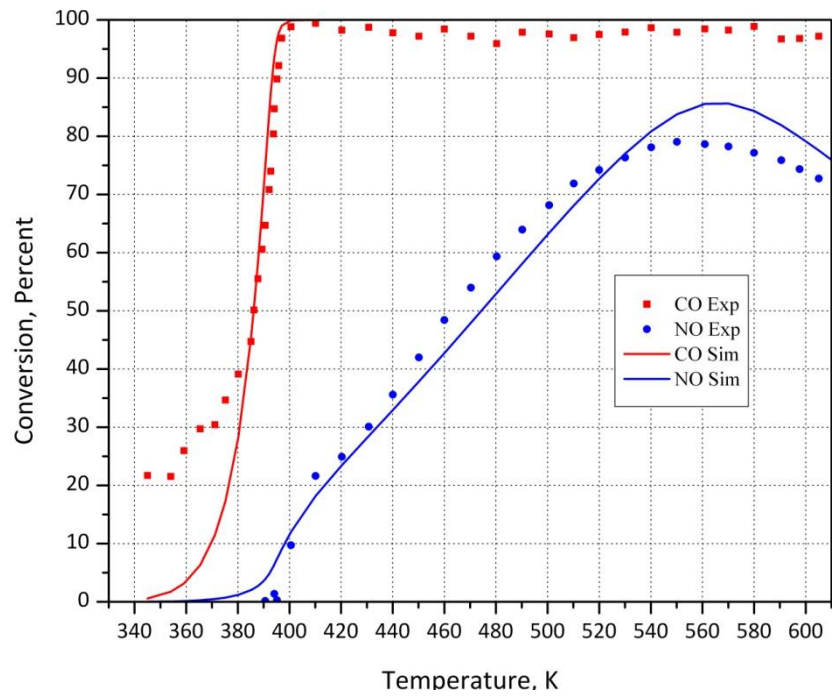


Figure 5-87: Simultaneous optimization result vs. Experimental data, Run 25, Model 3

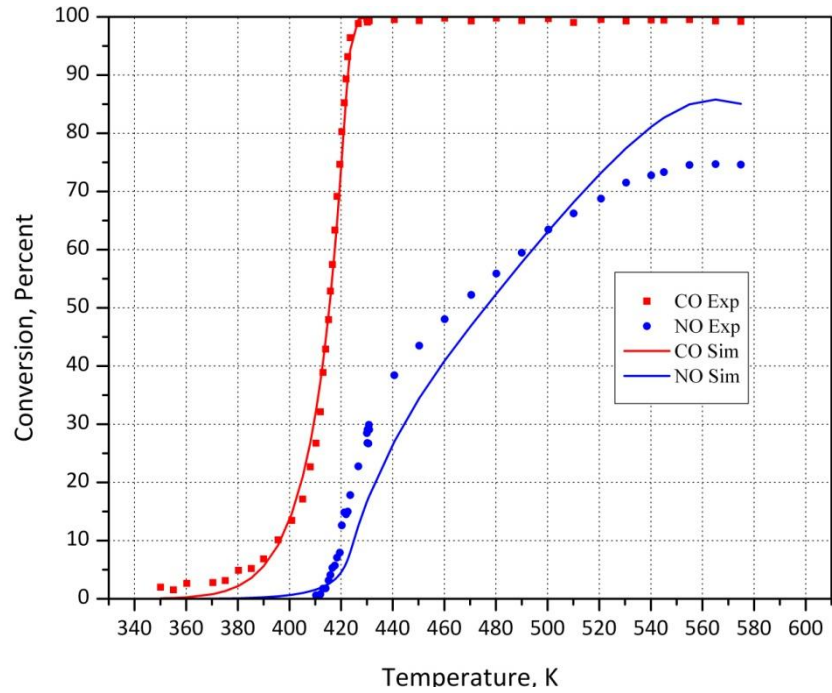


Figure 5-88: Simultaneous optimization result vs. Experimental data, Run 26, Model 3

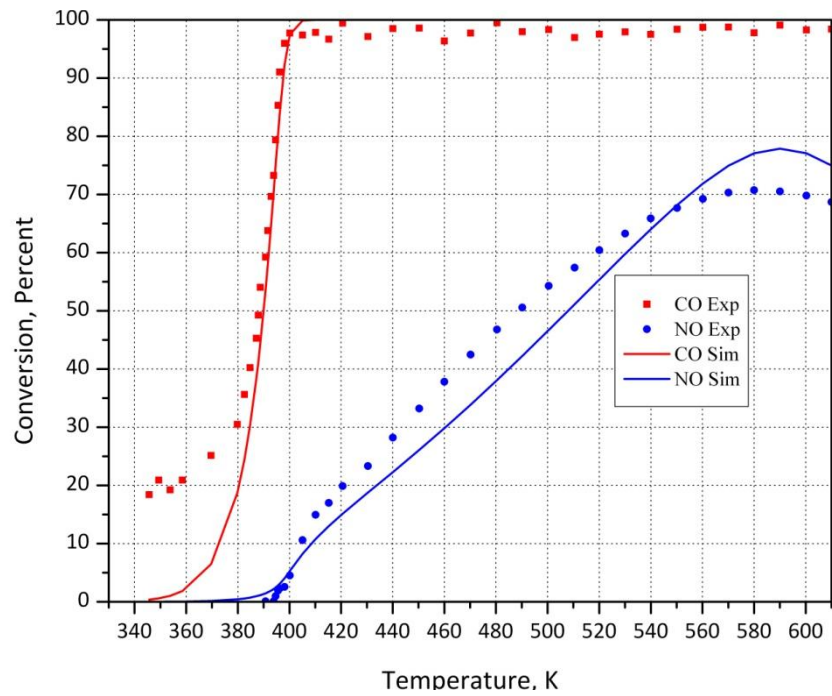


Figure 5-89: Simultaneous optimization result vs. Experimental data, Run 27, Model 3

Table 5-40: Runs 22-27 simultaneous optimization results, Model 4

Parameter	LB	HB	Run 22	Run 23	Run 24	Run 25	Run 26	Run 27
k_1	A_1	0	30	19.6				
	E_1	20000	150000	22955				
k_4	A_4	0	30	7.56				
	E_4	0	150000	26884				
K_5	B_5	0	30	7.03				
	H_5	-150000	0	-43496				
K_8	B_8	0	30	5.88				
	H_8	-150000	0	-36793				
K_{10}	B_{10}	0	30	2.72				
	H_{10}	-150000	0	-23780				
Model 4	CO Residual		33	25	20	81	6.1	59
	NO Residual		136	29	25	20	15	14
	Cumulative Residual		169	54	45	101	21.1	73

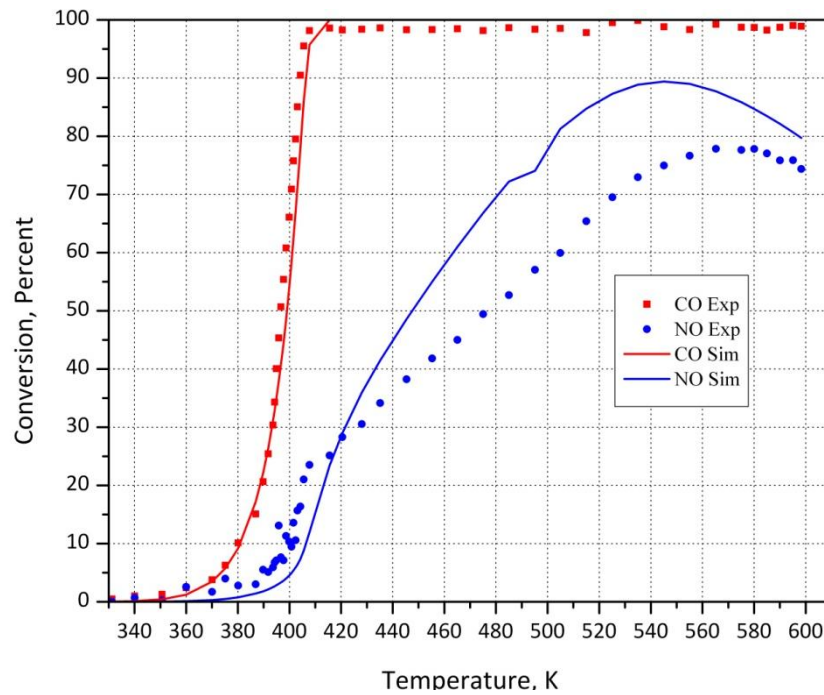


Figure 5-90: Simultaneous optimization result vs. Experimental data, Run 22, Model 4

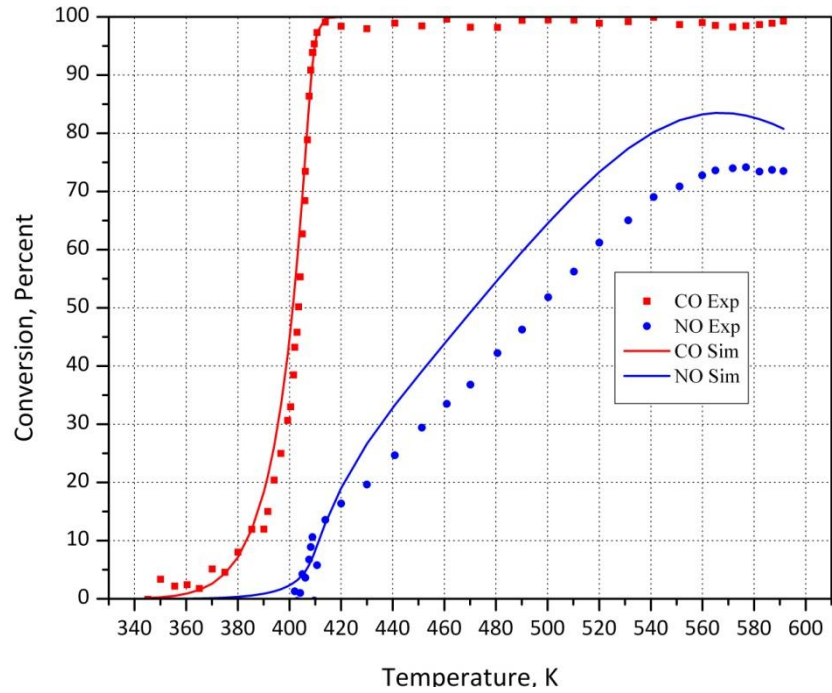


Figure 5-91: Simultaneous optimization result vs. Experimental data, Run 23, Model 4

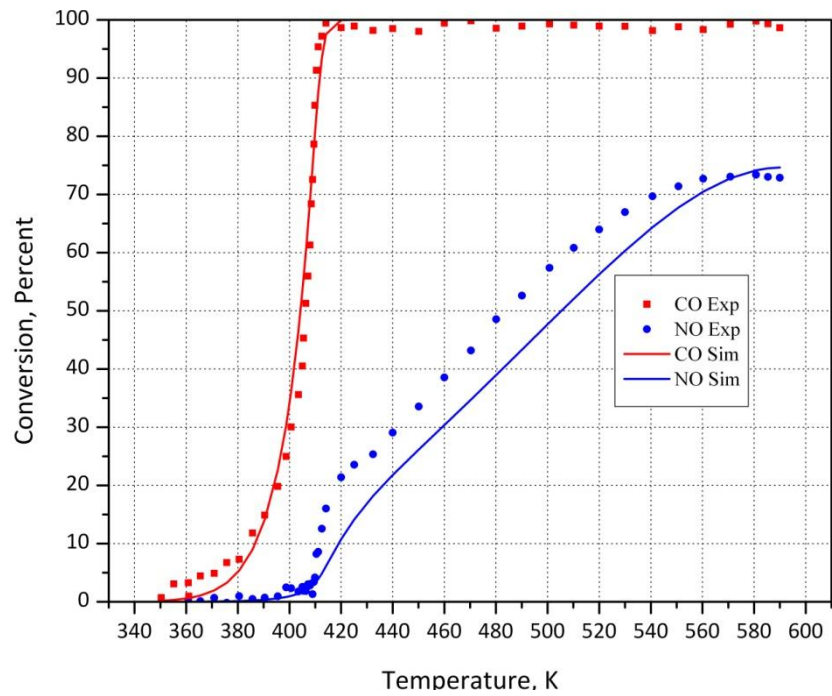


Figure 5-92: Simultaneous optimization result vs. Experimental data, Run 24, Model 4

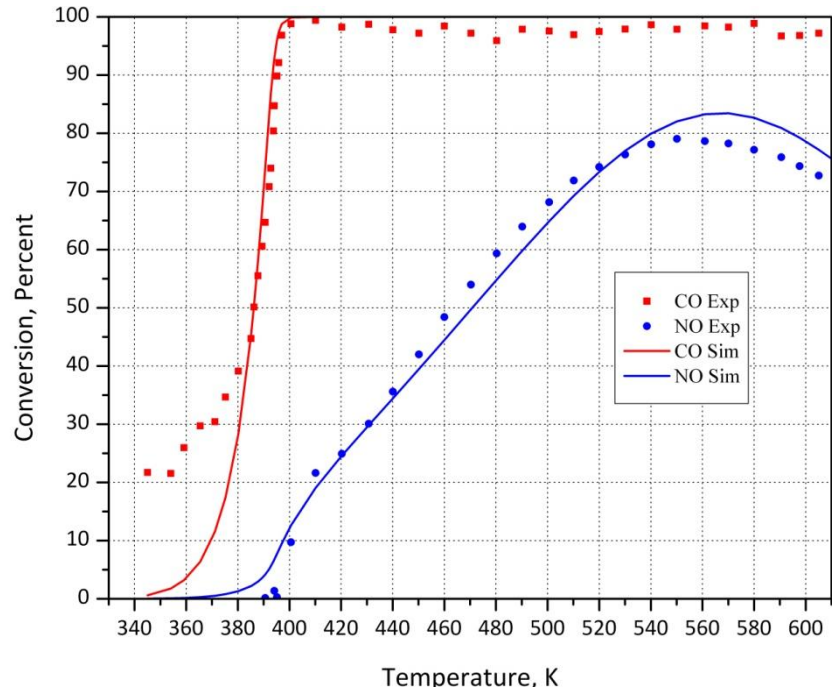


Figure 5-93: Simultaneous optimization result vs. Experimental data, Run 25, Model 4

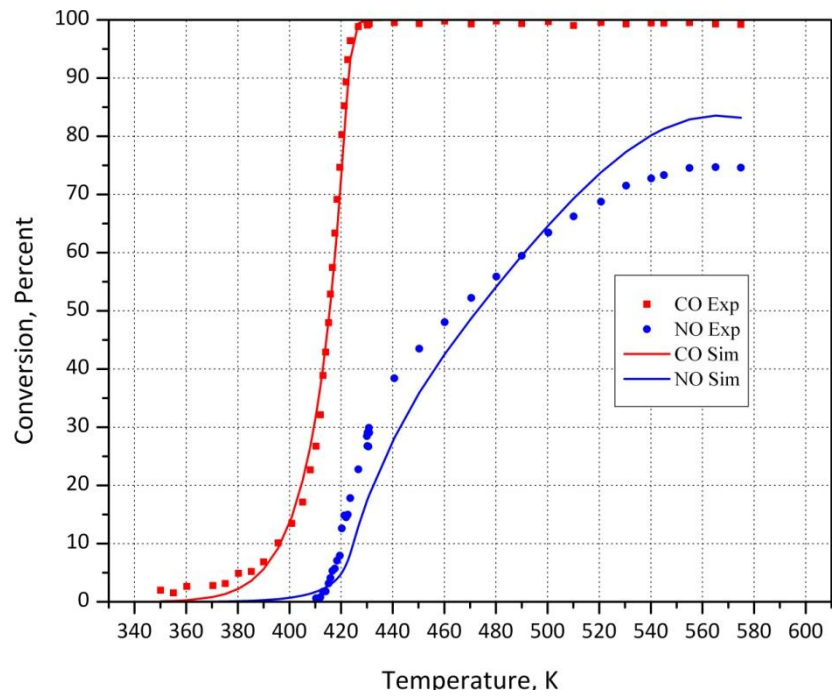


Figure 5-94: Simultaneous optimization result vs. Experimental data, Run 26, Model 4

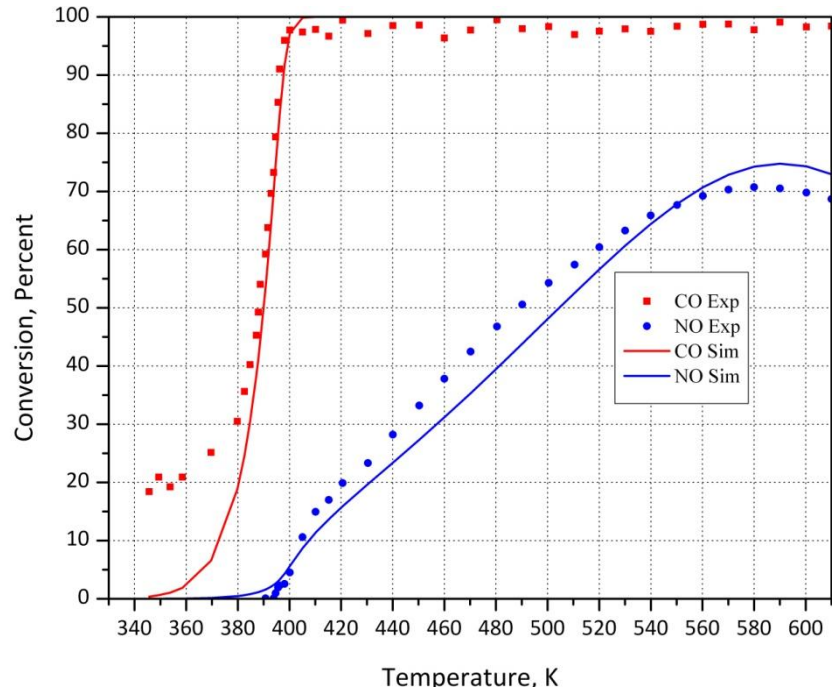


Figure 5-95: Simultaneous optimization result vs. Experimental data, Run 27, Model 4

Table 5-41: Runs 22-27 simultaneous optimization results, Model 5

Parameter	LB	HB	Run 22	Run 23	Run 24	Run 25	Run 26	Run 27
k ₁	A ₁	0	30	19.1				
	E ₁	20000	150000	20017				
k ₄	A ₄	0	30	14.1				
	E ₄	0	150000	33946				
K ₅	B ₅	0	30	6.72				
	H ₅	-150000	0	-47031				
K ₈	B ₈	0	30	3.37				
	H ₈	-150000	0	-85389				
K ₁₀	B ₁₀	0	30	3.99				
	H ₁₀	-150000	0	-149995				
Model 5	CO Residual		67	39	87	64	12	45
	NO Residual		24	10	9.1	30	63	13
	Cumulative Residual		91	49	96.1	94	75	58

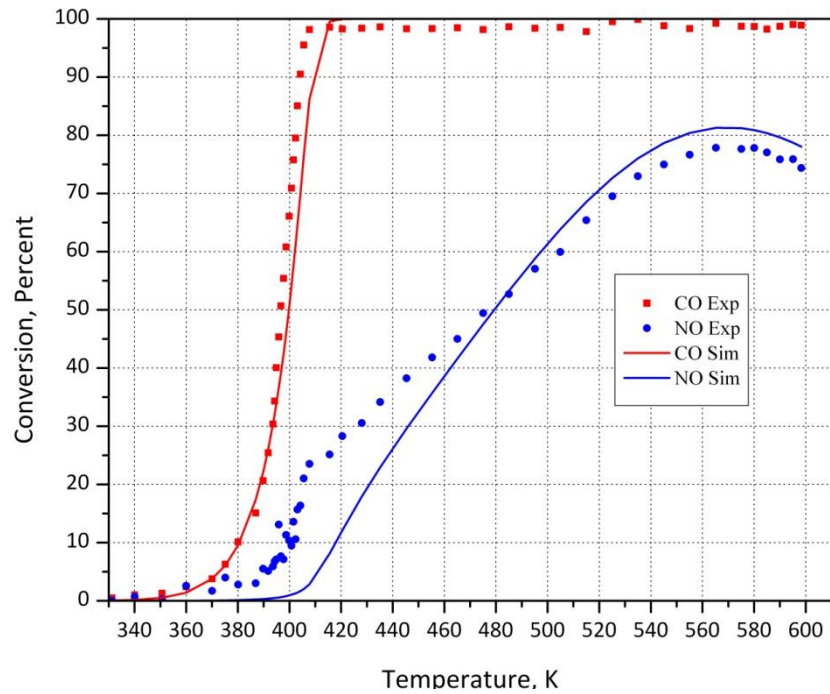


Figure 5-96: Simultaneous optimization result vs. Experimental data, Run 22, Model 5

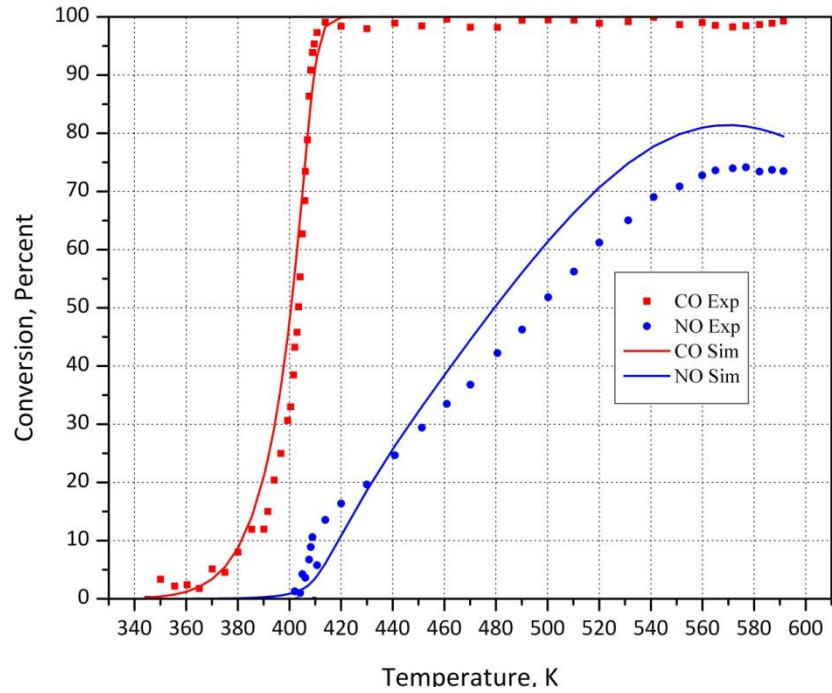


Figure 5-97: Simultaneous optimization result vs. Experimental data, Run 23, Model 5

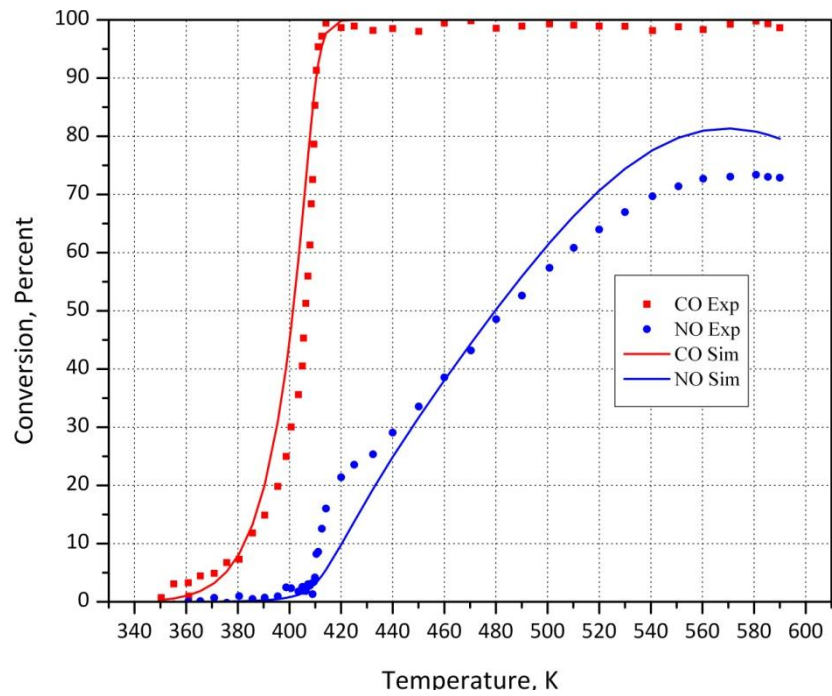


Figure 5-98: Simultaneous optimization result vs. Experimental data, Run 24, Model 5

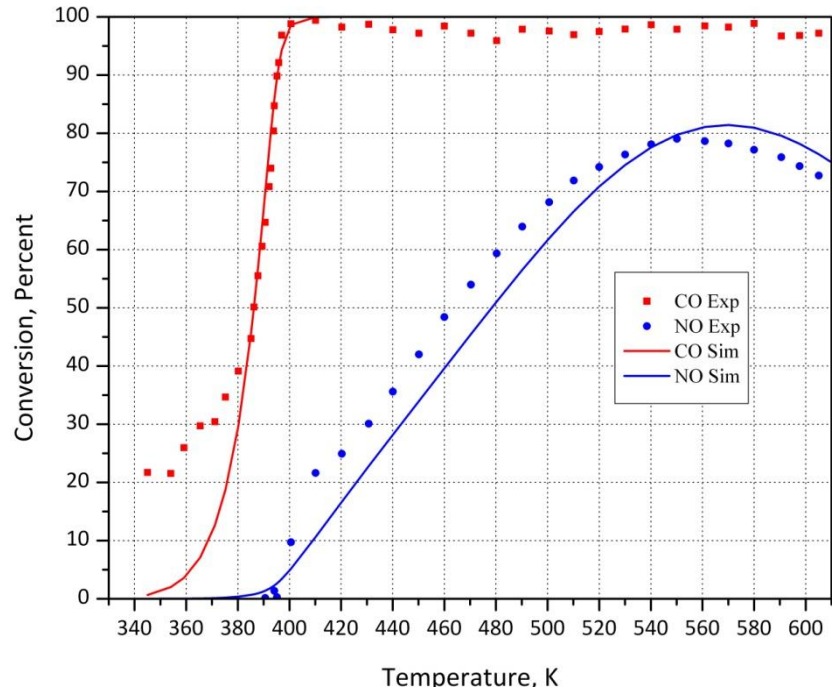


Figure 5-99: Simultaneous optimization result vs. Experimental data, Run 25, Model 5

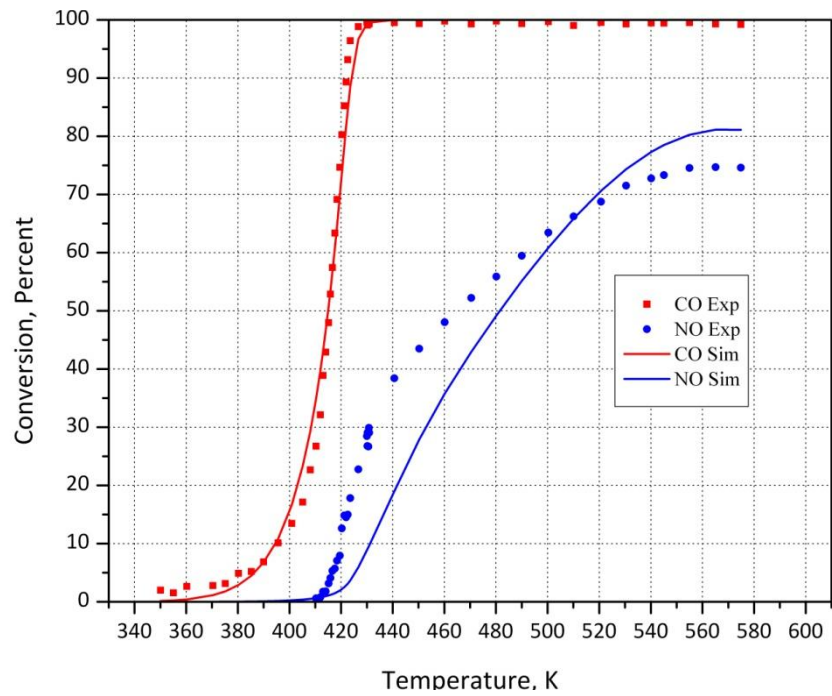


Figure 5-100: Simultaneous optimization result vs. Experimental data, Run 26, Model 5

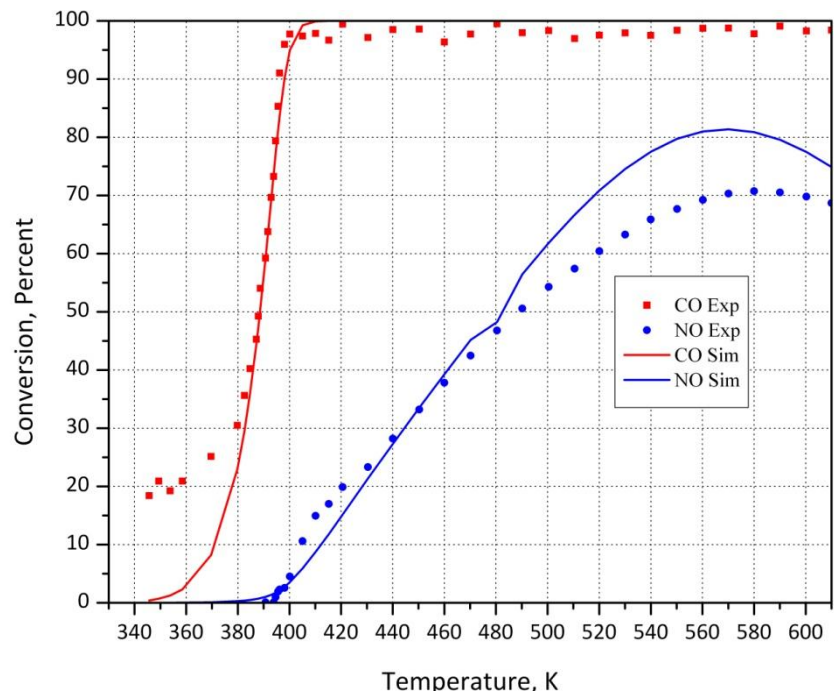


Figure 5-101: Simultaneous optimization result vs. Experimental data, Run 27, Model 5

From the results, it is observed that when CO/H₂ and NO are fed to the reactor, Model 1 is the best model to predict the behaviours of the system, followed by Model 5 and Model 4. It is interesting that the best model for CO/H₂ and NO system is the same as the best model for modelling of the NO only system.

5.6 Modelling of Mixture of C₃H₆ & NO

The only reactants in experiments 16 to 21 are C₃H₆ and NO. In these experiments, we have all reactions occurring except CO oxidation. It is first time that we have to consider NO_x reduction over catalyst by hydrocarbon. Table 5-42 contains the initial values of the experiments and the results for individual modelling of each experiment with different models are available in Table 5-43 to Table 5-47 and Figure 5-102 to Figure 5-126.

Table 5-42: NO & Propene experiments, initial concentrations

Run	Propene, ppm	NO, ppm
16	500	150
17	500	300
18	500	600
20	750	300
21	750	600

Model C₁, Oxidation of propene:

$$(-R_{C_3H_6}) = \frac{k_3 Y_{C_3H_6} Y_{O_2}}{T(1 + K_6 Y_{C_3H_6})^2 (1 + K_8 Y_{NO})} \quad (5-22)$$

Model C₁, Oxidation of NO:

$$(-R_{NO}) = \frac{k_4 Y_{NO} Y_{O_2}^{0.5} [1 - \beta]}{T(1 + K_6 Y_{C_3H_6})^2 (1 + K_8 Y_{NO})} \quad (5-23)$$

Model C₁, Reduction of NO to N₂:

$$(-R_{NO})_{r1} = \frac{(-R_{C_3H_6}) k_2 Y_{NO}}{(1 + K_9 Y_{O_2})} \quad (5-24)$$

Model C₁, Reduction of NO to N₂O:

$$(-R_{NO})_{r2} = \frac{(-R_{C_3H_6}) k_{11} Y_{NO}}{(1 + K_9 Y_{O_2})} \quad (5-25)$$

Model C₁, Reduction of NO₂:

$$(-R_{NO_2})_{r3} = \frac{(-R_{C_3H_6}) 10 k_2 Y_{NO_2}}{(1 + K_9 Y_{O_2})} \quad (5-26)$$

Table 5-43: Runs 16-21 individual optimization results, Model 1

Parameter	LB	HB	Run 16	Run 17	Run 18	Run 20	Run 21	
k ₂	A ₂	0	30	27.8	20.7	15.5	22.8	9.5
	E ₂	0	150000	58698	72779	101523	93344	131070
k ₃	A ₃	0	30	17.5	17.9	23.2	17.2	24.3
	E ₃	20000	150000	108141	62022	73316	100539	21482
k ₄	A ₄	0	30	12.4	12.1	19.3	13.1	13.9
	E ₄	0	150000	67693	83243	29950	50190	116410
K ₆	B ₆	0	30	5.79	7.18	6.47	6.09	7.44
	H ₆	-150000	0	-3884	-1.54	-3245	-0.451	-5290
K ₈	B ₈	0	30	6.07	8.40	14.1	7.82	14.7
	H ₈	-150000	0	-12998	-74088	-15176	-22071	-78827
K ₉	B ₉	0	30	23.8	16.2	12.2	18.8	7.27
	H ₉	-150000	150000	87407	104053	148413	130532	132113
k ₁₁	A ₁₁	0	30	28.4	21.4	16.1	23.2	11.1
	E ₁₁	0	150000	62856	75497	120409	100177	110331
Model 1	C ₃ H ₆ Residual			16	5.6	4.3	9.6	14
	NO _x Residual			1.7	2.0	2.3	2.9	19
	N ₂ O Residual			46	12	5.7	24	9.6
	NO ₂ Residual			3.8	13	10	4.3	73
	Cumulative Residual			67	33	22	41	116

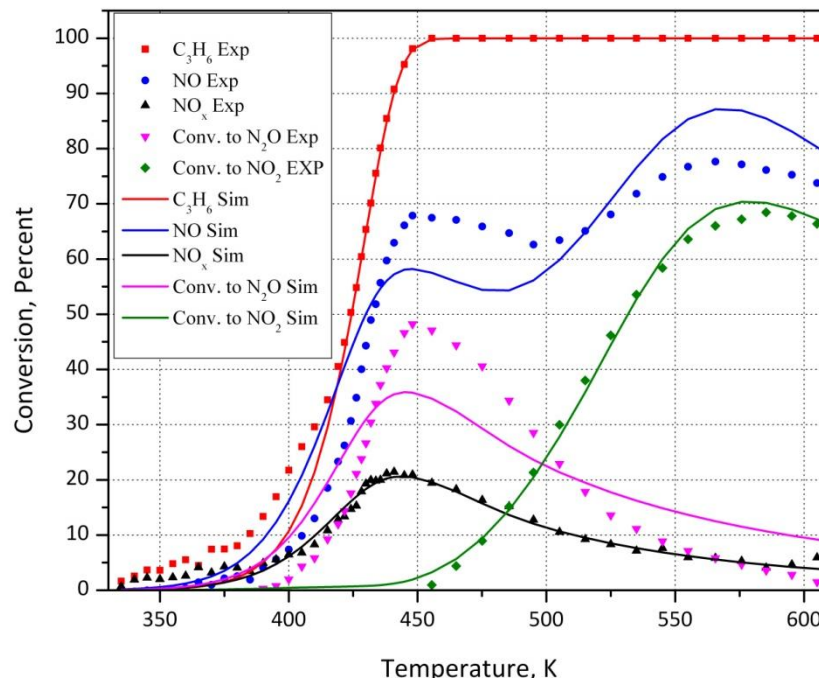


Figure 5-102: Individual optimization result vs. Experimental data, Run 16, Model 1

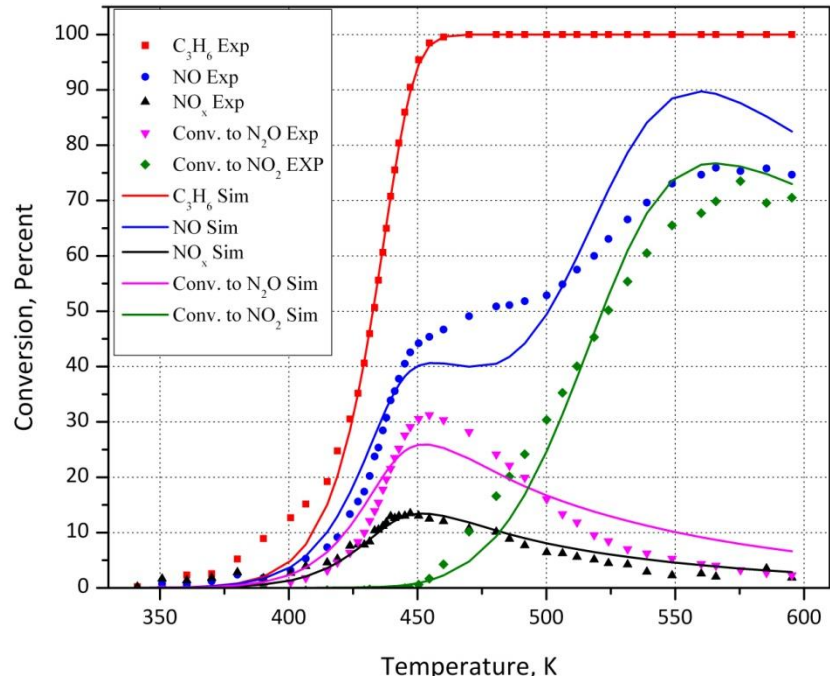


Figure 5-103: Individual optimization result vs. Experimental data, Run 17, Model 1

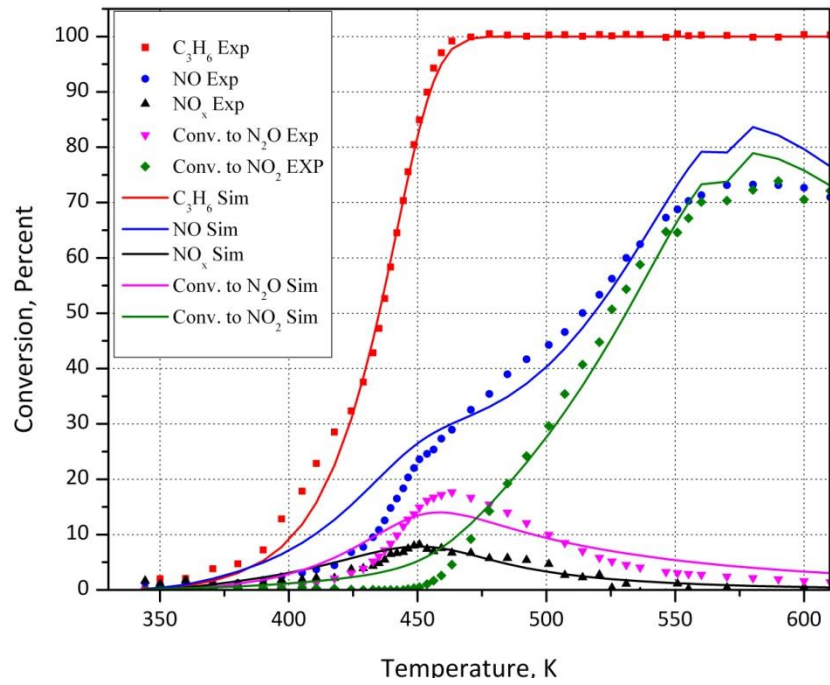


Figure 5-104: Individual optimization result vs. Experimental data, Run 18, Model 1

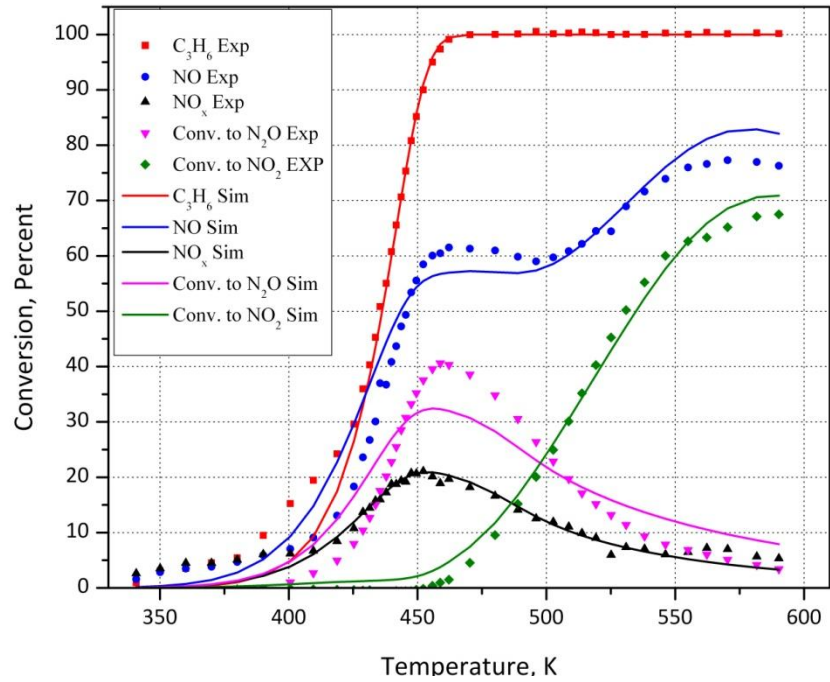


Figure 5-105: Individual optimization result vs. Experimental data, Run 20, Model 1

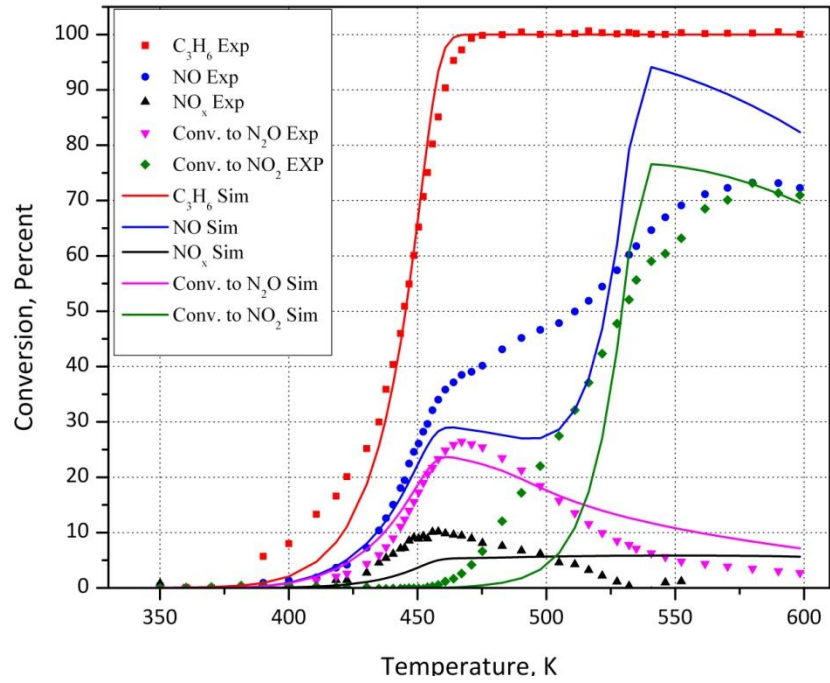


Figure 5-106: Individual optimization result vs. Experimental data, Run 21, Model 1

Model C₂, Oxidation of propene:

$$(-R_{C_3H_6}) = \frac{k_3 Y_{C_3H_6} Y_{O_2}}{T(1 + K_6 Y_{C_3H_6})^2 (1 + K_8 Y_{NO})} \quad (5-27)$$

Model C₂, Oxidation of NO:

$$(-R_{NO}) = \frac{k_4 Y_{NO} Y_{O_2} [1 - \beta]}{T(1 + K_6 Y_{C_3H_6})^2 (Y_{NO} + K_{10} Y_{NO_2})} \quad (5-28)$$

Model C₂, Reduction of NO to N₂:

$$(-R_{NO})_{r1} = \frac{(-R_{C_3H_6}) k_2 Y_{NO}}{(1 + K_9 Y_{O_2})} \quad (5-29)$$

Model C₂, Reduction of NO to N₂O:

$$(-R_{NO})_{r2} = \frac{(-R_{C_3H_6}) k_{11} Y_{NO}}{(1 + K_9 Y_{O_2})} \quad (5-30)$$

Model C₂, Reduction of NO₂:

$$(-R_{NO_2})_{r3} = \frac{(-R_{C_3H_6}) 10 k_2 Y_{NO_2}}{(1 + K_9 Y_{O_2})} \quad (5-31)$$

Table 5-44: Runs 16-21 individual optimization results, Model 2

Parameter	LB	HB	Run 16	Run 17	Run 18	Run 20	Run 21
k ₂	A ₂	0	28.1	27.0	20.4	24.8	25.0
	E ₂	0	63881	63840	38444	25572	51599
k ₃	A ₃	0	18.8	18.7	18.7	29.9	22.9
	E ₃	20000	20979	87773	29282	59137	34118
k ₄	A ₄	0	17.0	15.4	15.5	15.7	14.4
	E ₄	0	77146	89013	86083	4388	4072
K ₆	B ₆	0	3.44	8.49	9.03	14.3	7.97
	H ₆	-150000	-12962	-8693	-17340	-1319	-23788
K ₈	B ₈	0	10.6	8.74	3.93	7.1	12.9
	H ₈	-150000	-76511	-7796	-40823	-2879	-14562
K ₉	B ₉	0	24.0	22.4	17.2	20.9	21.7
	H ₉	-150000	81431	112026	74736	58730	96062
K ₁₀	B ₁₀	0	16.7	12.1	11.6	13.4	11.7
	H ₁₀	-150000	-87208	-12618	-6794	-112063	-113820
k ₁₁	A ₁₁	0	28.7	27.6	21.0	25.2	25.7
	E ₁₁	0	66031	76744	53086	33086	69956
Model 2	C ₃ H ₆ Residual		12	2.2	1.3	23	2.0
	NO _x Residual		2.7	0.96	2.1	1.3	2.6
	N ₂ O Residual		42	10	6.1	30	8.8
	NO ₂ Residual		6.7	7.0	5.0	5.6	6.5
	Cumulative Residual		64	20	14	61	20

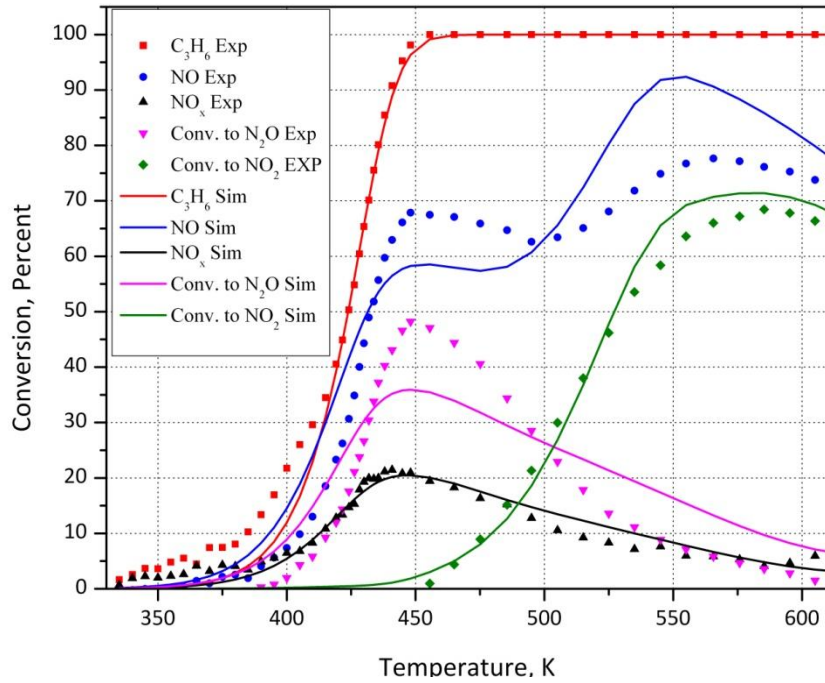


Figure 5-107: Individual optimization result vs. Experimental data, Run 16, Model 2

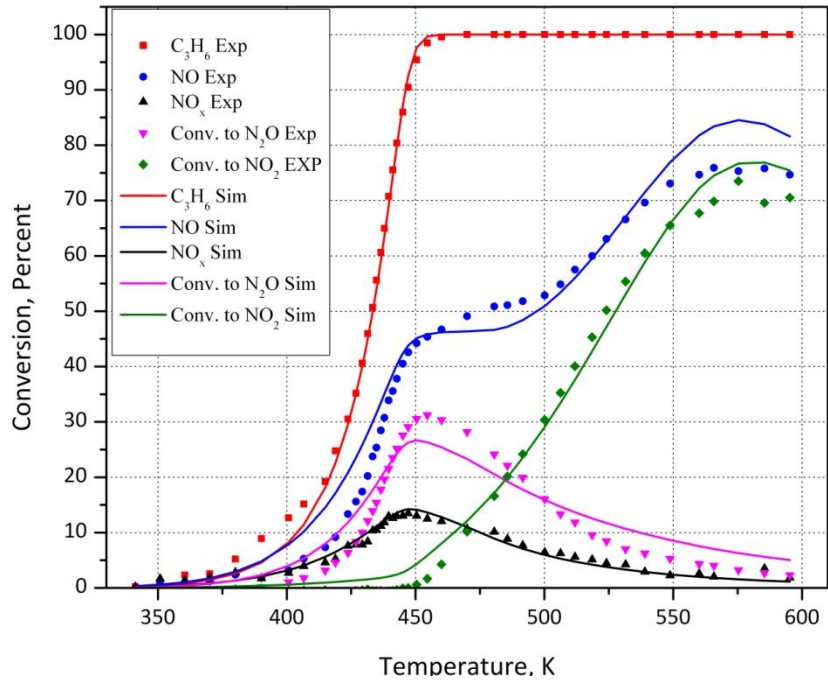


Figure 5-108: Individual optimization result vs. Experimental data, Run 17, Model 2

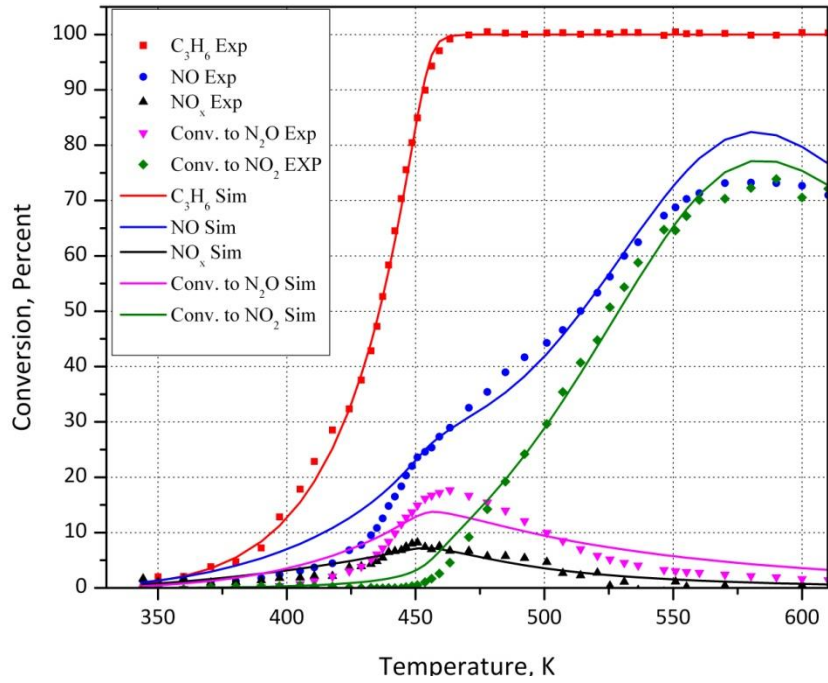


Figure 5-109: Individual optimization result vs. Experimental data, Run 18, Model 2

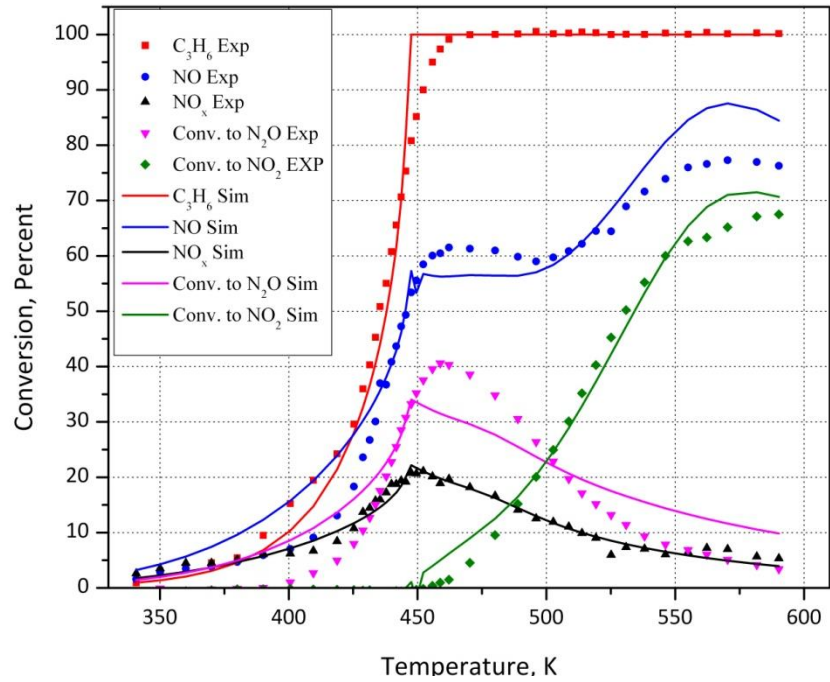


Figure 5-110: Individual optimization result vs. Experimental data, Run 20, Model 2

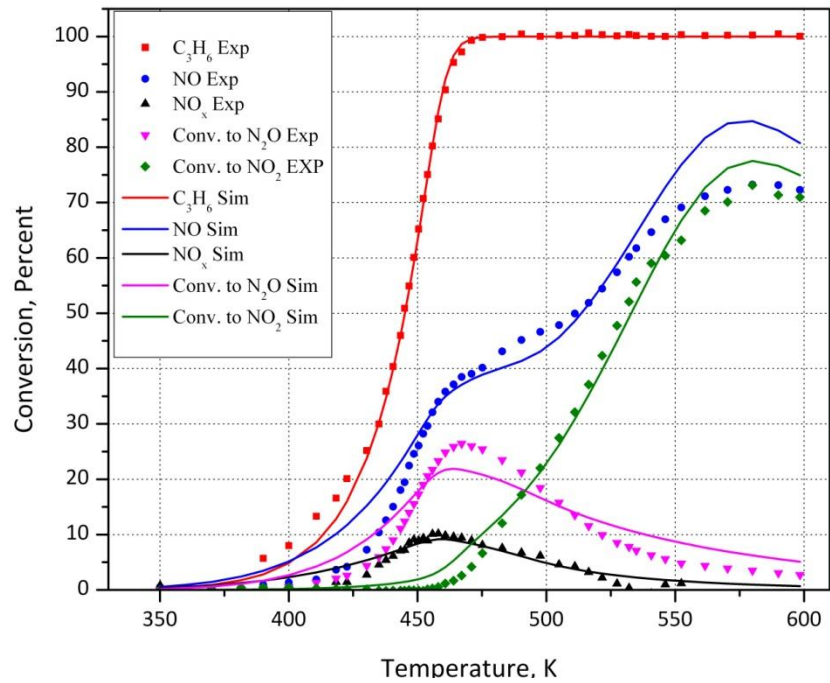


Figure 5-111: Individual optimization result vs. Experimental data, Run 21, Model 2

Model C₃, Oxidation of propene:

$$(-R_{C_3H_6}) = \frac{k_3 Y_{C_3H_6} Y_{O_2}}{T(1 + K_6 Y_{C_3H_6})^2 (1 + K_8 Y_{NO})} \quad (5-32)$$

Model C₃, Oxidation of NO:

$$(-R_{NO}) = \frac{k_4 Y_{O_2}^{0.5} [1 - \beta^2]}{T(1 + K_6 Y_{C_3H_6})^2 \left(1 + K_8 Y_{NO} + K_{10} \frac{Y_{NO_2}}{Y_{NO}}\right)} \quad (5-33)$$

Model C₃, Reduction of NO to N₂:

$$(-R_{NO})_{r1} = \frac{(-R_{C_3H_6}) k_2 Y_{NO}}{(1 + K_9 Y_{O_2})} \quad (5-34)$$

Model C₃, Reduction of NO to N₂O:

$$(-R_{NO})_{r2} = \frac{(-R_{C_3H_6}) k_{11} Y_{NO}}{(1 + K_9 Y_{O_2})} \quad (5-35)$$

Model C₃, Reduction of NO₂:

$$(-R_{NO_2})_{r3} = \frac{(-R_{C_3H_6}) 10 k_2 Y_{NO_2}}{(1 + K_9 Y_{O_2})} \quad (5-36)$$

Table 5-45: Runs 16-21 individual optimization results, Model 3

Parameter	LB	HB	Run 16	Run 17	Run 18	Run 20	Run 21	
k ₂	A ₂	0	30	8.30	17.9	21.8	29.6	22.8
	E ₂	0	150000	101988	51933	17892	77487	66891
k ₃	A ₃	0	30	27.2	21.1	24.8	29.0	18.8
	E ₃	20000	150000	39376	46324	26008	70934	32463
k ₄	A ₄	0	30	19.0	15.8	26.6	21.6	22.4
	E ₄	0	150000	21305	52942	6436	133355	40370
K ₆	B ₆	0	30	1.28	8.60	7.02	6.98	8.73
	H ₆	-150000	0	-37573	-4647	-79166	-2534	-16909
K ₈	B ₈	0	30	19.6	11.3	22.3	20.2	5.93
	H ₈	-150000	0	-21670	-47165	-88146	-7003	-63985
K ₉	B ₉	0	30	3.53	13.3	10.7	25.6	19.5
	H ₉	-150000	150000	146399	98618	149999	104983	111832
K ₁₀	B ₁₀	0	30	18.4	13.5	20.9	22.1	20.3
	H ₁₀	-150000	0	-86418	-43459	-34939	-26873	-63429
k ₁₁	A ₁₁	0	30	8.93	18.6	21.6	30.0	23.5
	E ₁₁	0	150000	105231	64067	21958	85254	85298
Model 3	C ₃ H ₆ Residual		2.2	2.0	43	4.4	2.5	
	NO _x Residual		8.6	0.86	85	2.5	2.7	
	N ₂ O Residual		5.1	10	18	32	9.3	
	NO ₂ Residual		13	8.5	70	7.9	7.0	
	Cumulative Residual		29	22	217	47	21	

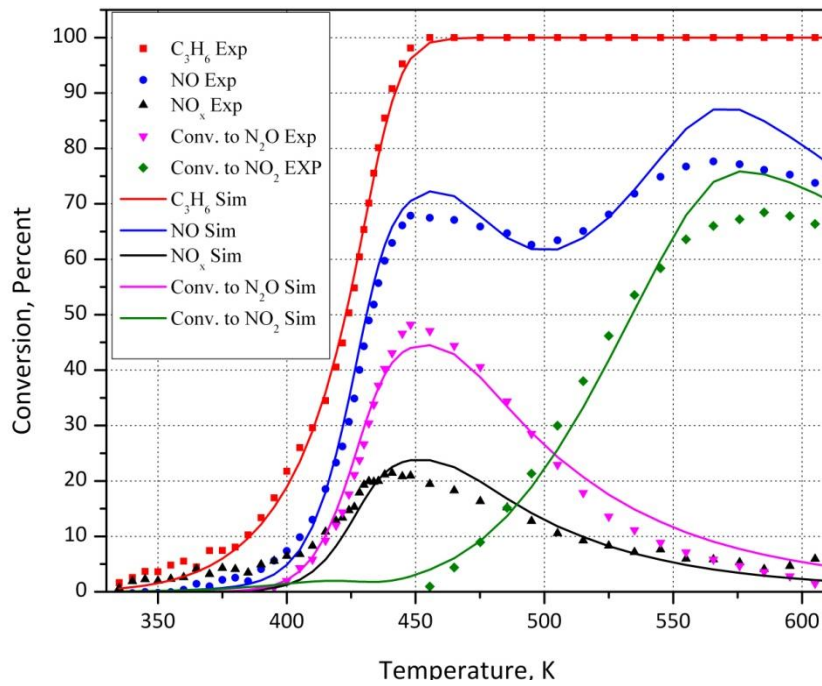


Figure 5-112: Individual optimization result vs. Experimental data, Run 16, Model 3

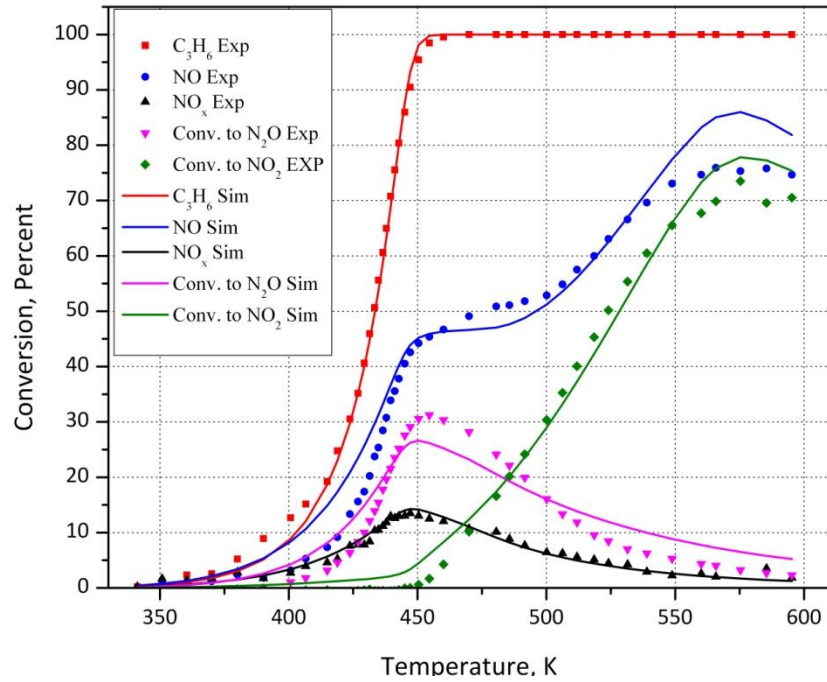


Figure 5-113: Individual optimization result vs. Experimental data, Run 17, Model 3

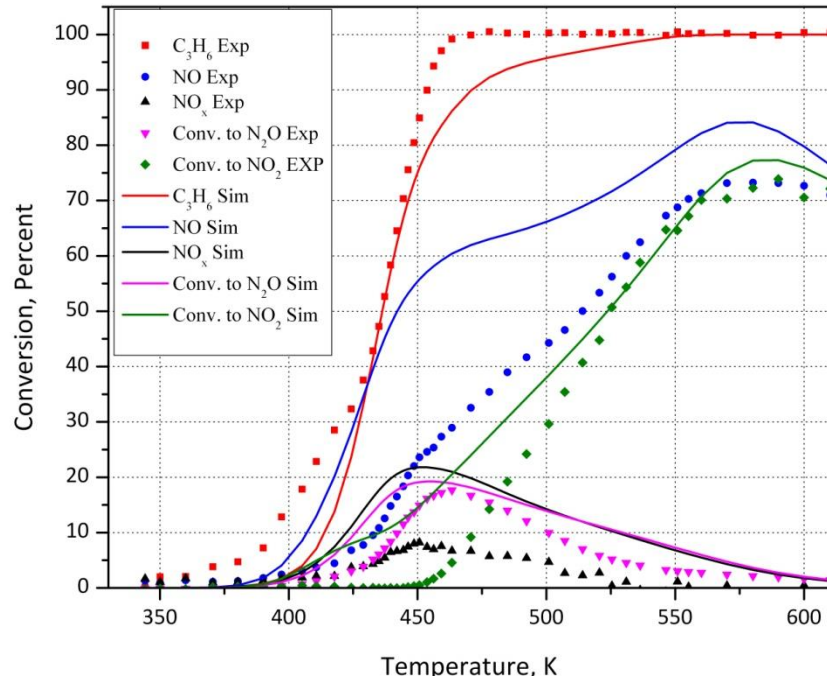


Figure 5-114: Individual optimization result vs. Experimental data, Run 18, Model 3

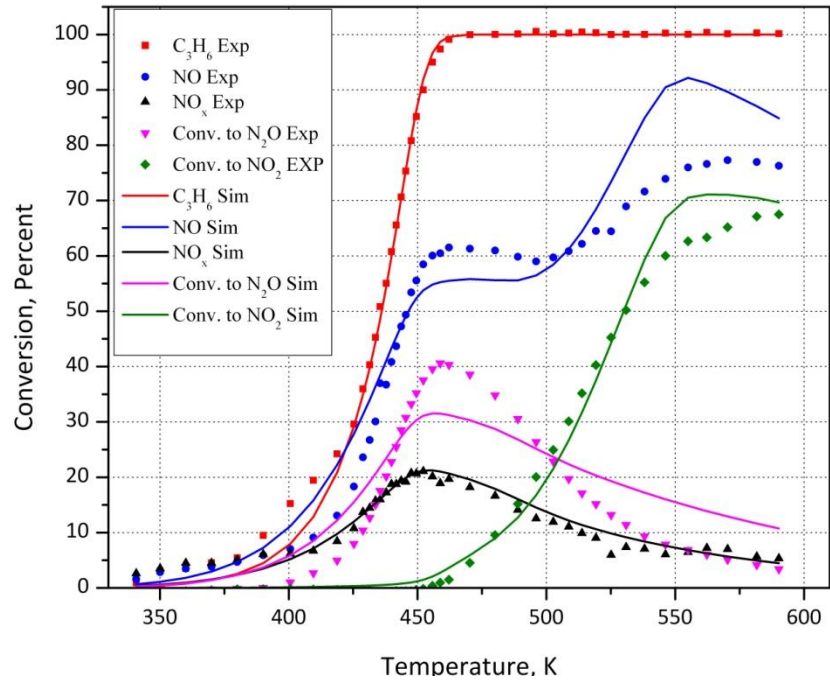


Figure 5-115: Individual optimization result vs. Experimental data, Run 20, Model 3

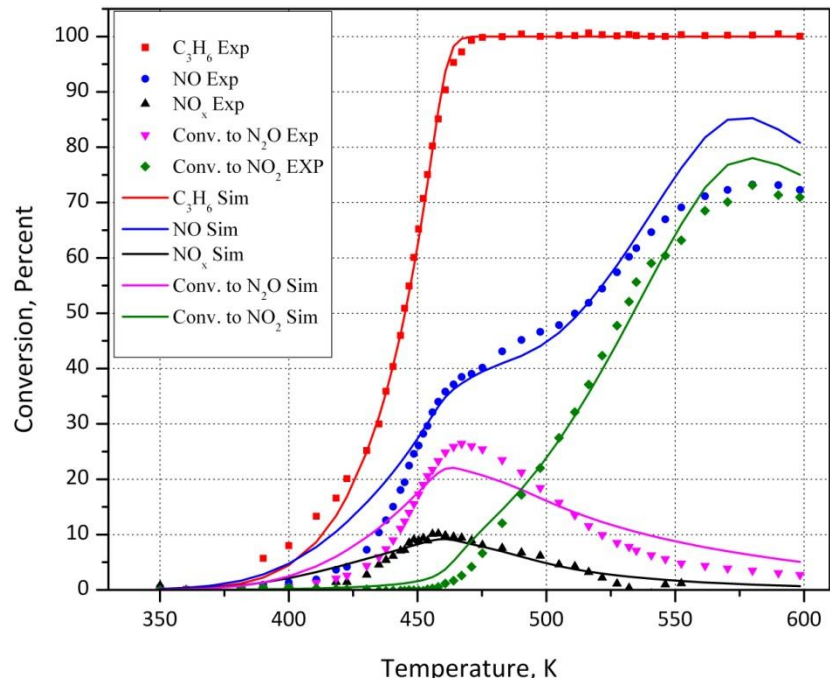


Figure 5-116: Individual optimization result vs. Experimental data, Run 21, Model 3

Model C₄, Oxidation of propene:

$$(-R_{C_3H_6}) = \frac{k_3 C_{C_3H_6} C_{O_2}}{T(1 + K_6 Y_{C_3H_6})^2 (1 + K_8 Y_{NO})} \quad (5-37)$$

Model C₄, Oxidation of NO:

$$(-R_{NO}) = \frac{k_4 Y_{O_2}^{0.5} [1 - \beta]}{T(1 + K_6 Y_{C_3H_6})^2 \left(1 + K_8 Y_{NO} + K_{10} \frac{Y_{NO_2}}{Y_{NO}}\right)} \quad (5-38)$$

Model C₄, Reduction of NO to N₂:

$$(-R_{NO})_{r1} = \frac{(-R_{C_3H_6}) k_2 Y_{NO}}{(1 + K_9 Y_{O_2})} \quad (5-39)$$

Model C₄, Reduction of NO to N₂O:

$$(-R_{NO})_{r2} = \frac{(-R_{C_3H_6}) k_{11} Y_{NO}}{(1 + K_9 Y_{O_2})} \quad (5-40)$$

Model C₄, Reduction of NO₂:

$$(-R_{NO_2})_{r3} = \frac{(-R_{C_3H_6}) 10 k_2 Y_{NO_2}}{(1 + K_9 Y_{O_2})} \quad (5-41)$$

Table 5-46: Runs 16-21 individual optimization results, Model 4

Parameter		LB	HB	Run 16	Run 17	Run 18	Run 20	Run 21
k ₂	A ₂	0	30	28.0	17.5	29.4	22.8	14.0
	E ₂	0	150000	32893	30386	119857	119709	59264
k ₃	A ₃	0	30	26.5	25.3	21.7	19.8	22.2
	E ₃	20000	150000	23596	37869	80483	74840	69793
k ₄	A ₄	0	30	11.5	13.5	25.8	9.69	17.3
	E ₄	0	150000	111535	27309	41509	123531	21055
K ₆	B ₆	0	30	5.94	13.1	5.41	4.82	7.24
	H ₆	-150000	0	-9356	-6575	-2.22	-0.274	-5860
K ₈	B ₈	0	30	18.3	5.97	12.7	11.6	12.9
	H ₈	-150000	0	-63127	-79016	-8868	-27097	-15759
K ₉	B ₉	0	30	23.9	13.0	26.2	18.8	10.8
	H ₉	-150000	150000	59045	75031	150000	149999	107068
K ₁₀	B ₁₀	0	30	10.9	10.8	24.9	9.34	15.9
	H ₁₀	-150000	0	-4950	-64742	-92842	-11660	-99299
k ₁₁	A ₁₁	0	30	28.6	18.1	30.0	23.2	14.8
	E ₁₁	0	150000	36830	41545	130270	124603	78846
Model 4	C₃H₆ Residual			12	10	5.1	7.3	2.4
	NO_x Residual			1.2	1.0	2.5	2.7	2.6
	N₂O Residual			47	11	6.8	27	8.7
	NO₂ Residual			2.9	5.0	11	7.0	7.4
	Cumulative Residual			64	27	26.	44	21

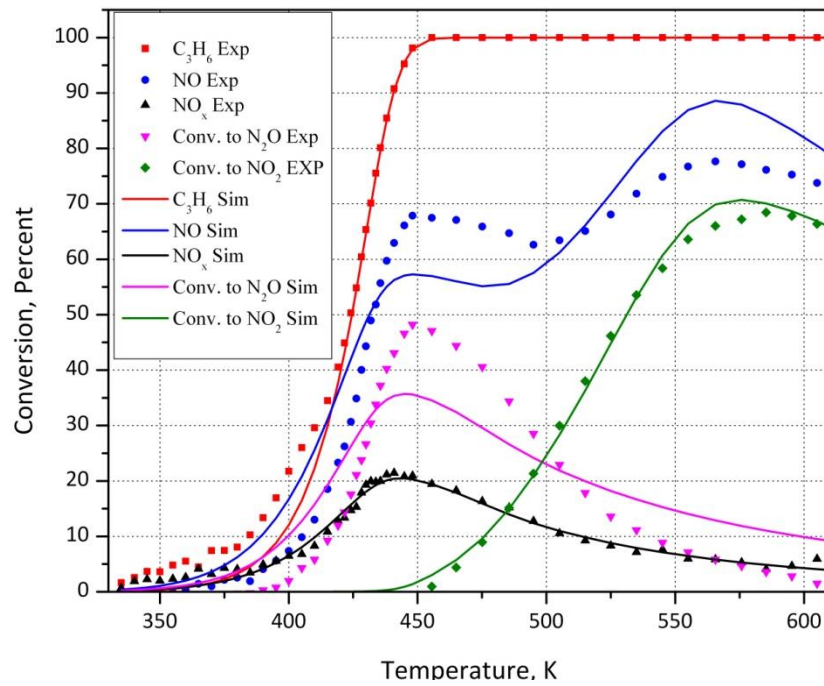


Figure 5-117: Individual optimization result vs. Experimental data, Run 16, Model 4

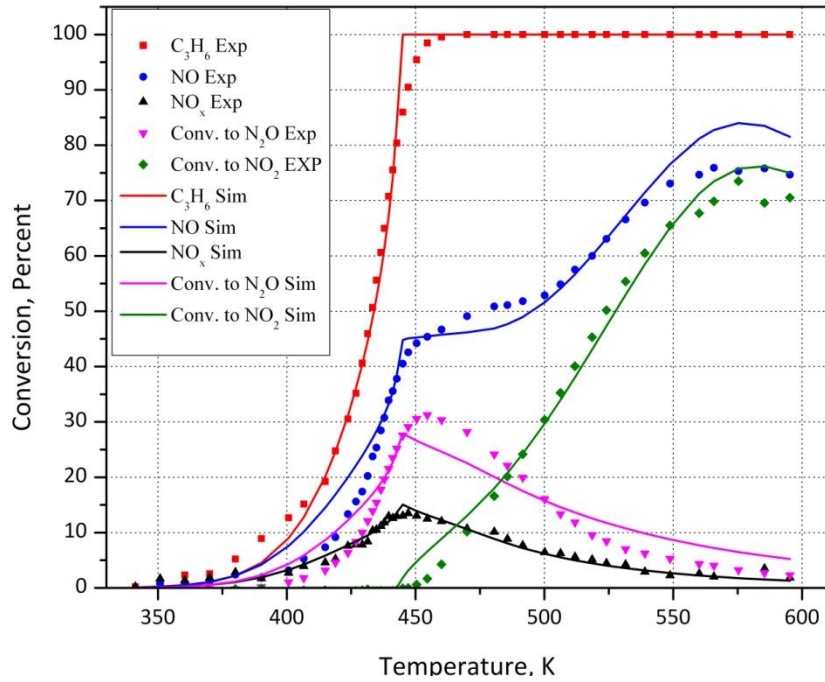


Figure 5-118: Individual optimization result vs. Experimental data, Run 17, Model 4

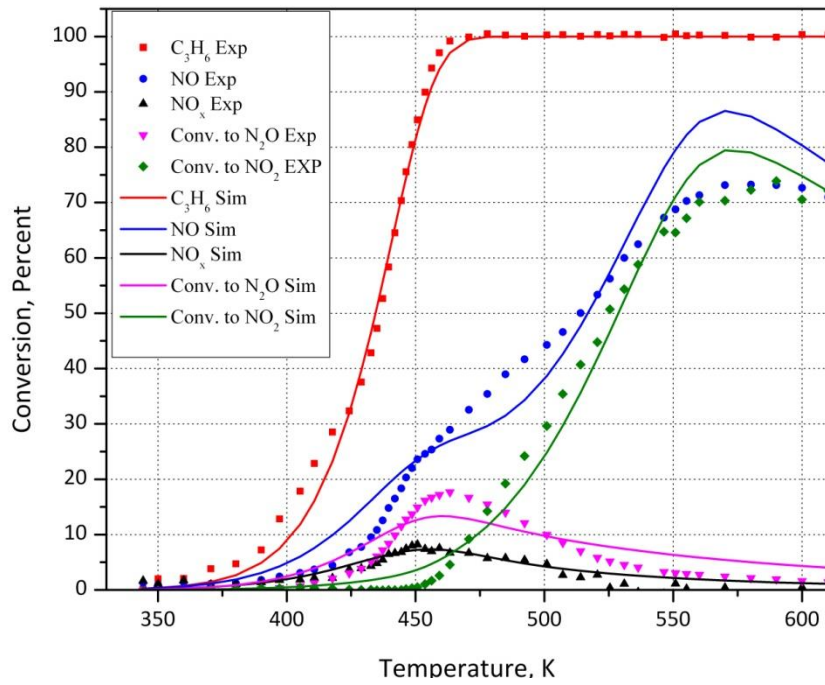


Figure 5-119: Individual optimization result vs. Experimental data, Run 18, Model 4

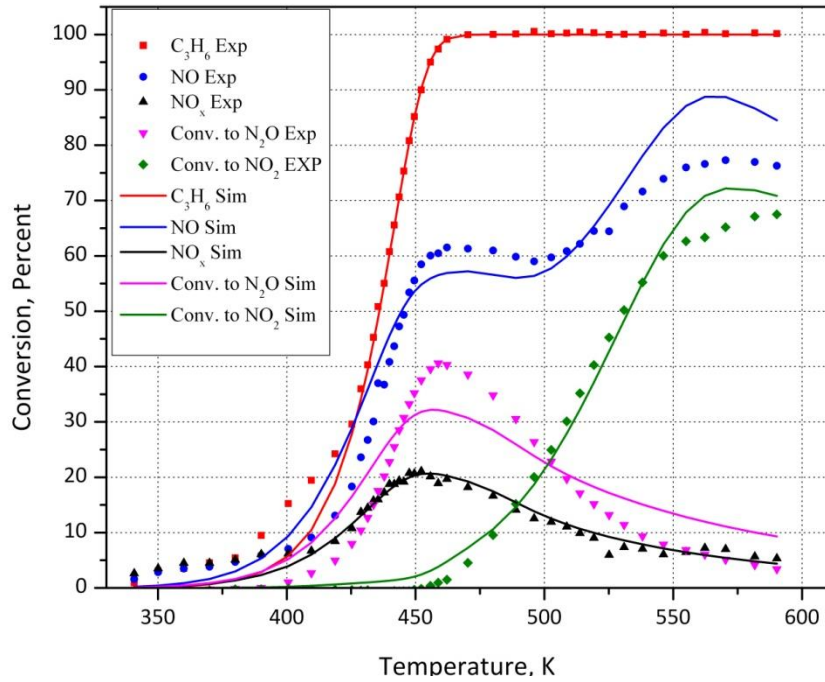


Figure 5-120: Individual optimization result vs. Experimental data, Run 20, Model 4

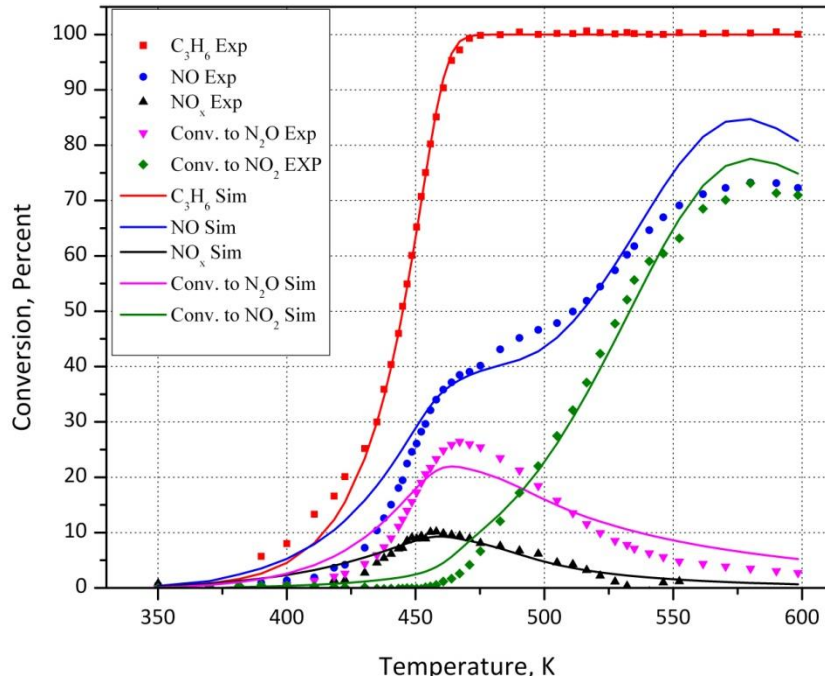


Figure 5-121: Individual optimization result vs. Experimental data, Run 21, Model 4

Model C₅, Oxidation of propene:

$$(-R_{C_3H_6}) = \frac{k_3 Y_{C_3H_6} Y_{O_2}}{T(1 + K_6 Y_{C_3H_6} + K_8 Y_{NO})^2} \quad (5-42)$$

Model C₅, Oxidation of NO:

$$(-R_{NO}) = \frac{k_4 Y_{NO} Y_{O_2}^{0.5} [1 - \beta]}{T(1 + K_6 Y_{C_3H_6} + K_8 Y_{NO} + K_{10} Y_{NO_2})^2} \quad (5-43)$$

Model C₅, Reduction of NO to N₂:

$$(-R_{NO})_{r1} = \frac{(-R_{C_3H_6}) k_2 Y_{NO}}{(1 + K_9 Y_{O_2})} \quad (5-44)$$

Model C₅, Reduction of NO to N₂O:

$$(-R_{NO})_{r2} = \frac{(-R_{C_3H_6}) k_{11} Y_{NO}}{(1 + K_9 Y_{O_2})} \quad (5-45)$$

Model C₅, Reduction of NO₂:

$$(-R_{NO_2})_{r3} = \frac{(-R_{C_3H_6}) 10 k_2 Y_{NO_2}}{(1 + K_9 Y_{O_2})} \quad (5-46)$$

Table 5-47: Runs 16-21 individual optimization results, Model 5

Parameter	LB	HB	Run 16	Run 17	Run 18	Run 20	Run 21	
k ₂	A ₂	0	30	18.1	28.9	8.76	29.1	29.2
	E ₂	0	150000	68458	66511	123600	55660	24772
k ₃	A ₃	0	30	17.3	29.0	29.3	24.4	20.2
	E ₃	20000	150000	99853	20586	93441	63285	102099
k ₄	A ₄	0	30	27.5	23.9	25.8	22.5	30
	E ₄	0	150000	71785	8790	82924	100282	97333
K ₆	B ₆	0	30	4.64	13.8	4.51	2.29	6.30
	H ₆	-150000	0	-2502	-38924	-10875	-71415	-1242
K ₈	B ₈	0	30	3.49	13.7	14.0	12.4	9.60
	H ₈	-150000	0	-86009	-47491	-424	-10941	-1298
K ₉	B ₉	0	30	14.0	24.4	5.65	25.2	26.0
	H ₉	-150000	150000	77363	120792	139419	73340	53231
K ₁₀	B ₁₀	0	30	22.3	14.0	18.7	19.6	21.9
	H ₁₀	-150000	0	-149187	-31044	-89429	-128531	-98760
k ₁₁	A ₁₁	0	30	18.7	29.6	9.59	29.6	30
	E ₁₁	0	150000	68522	84456	100564	57795	36719
Model 5	C₃H₆ Residual			14	2.3	9.0	5.3	3.6
	NO_x Residual			6.87	1.6	7.4	6.5	3.3
	N₂O Residual			38	9.4	6.3	28	10
	NO₂ Residual			12	1.8	37	19	21
	Cumulative Residual			71	15	60	59	39

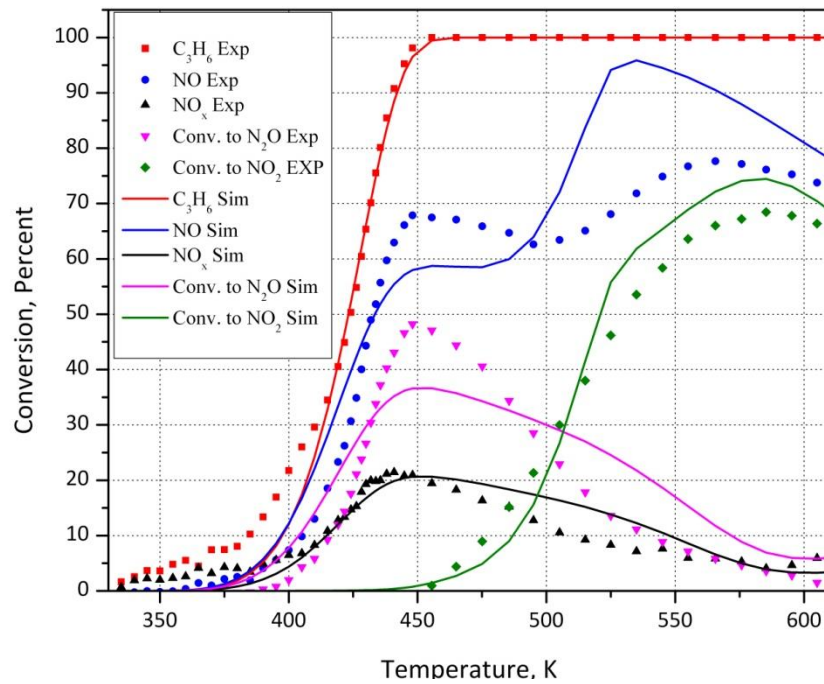


Figure 5-122: Individual optimization result vs. Experimental data, Run 16, Model 5

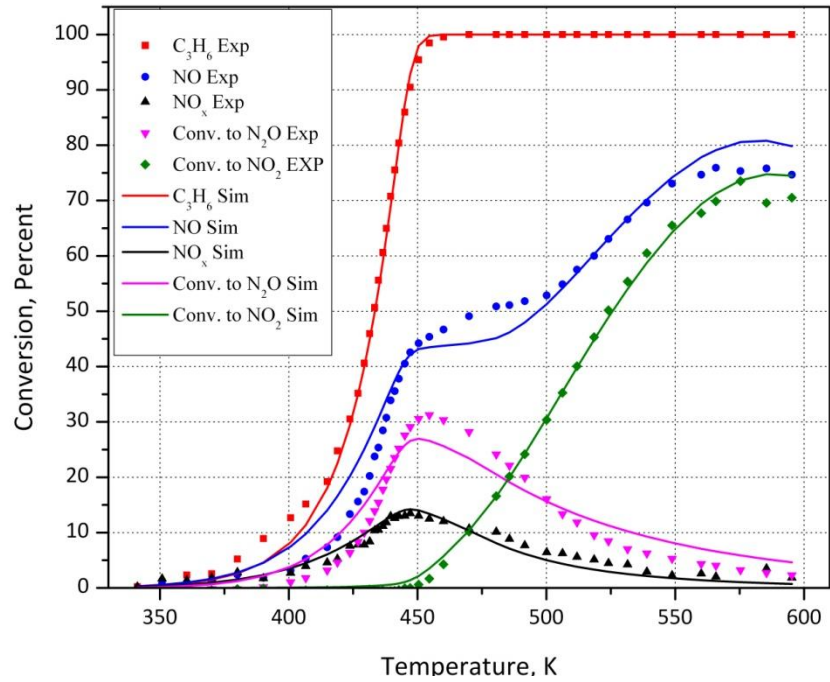


Figure 5-123: Individual optimization result vs. Experimental data, Run 17, Model 5

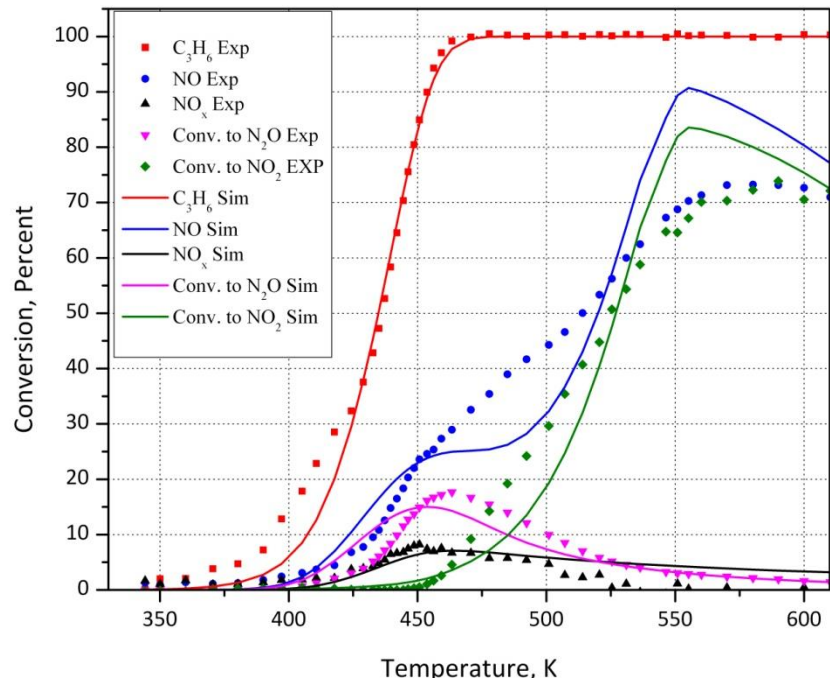


Figure 5-124: Individual optimization result vs. Experimental data, Run 18, Model 5

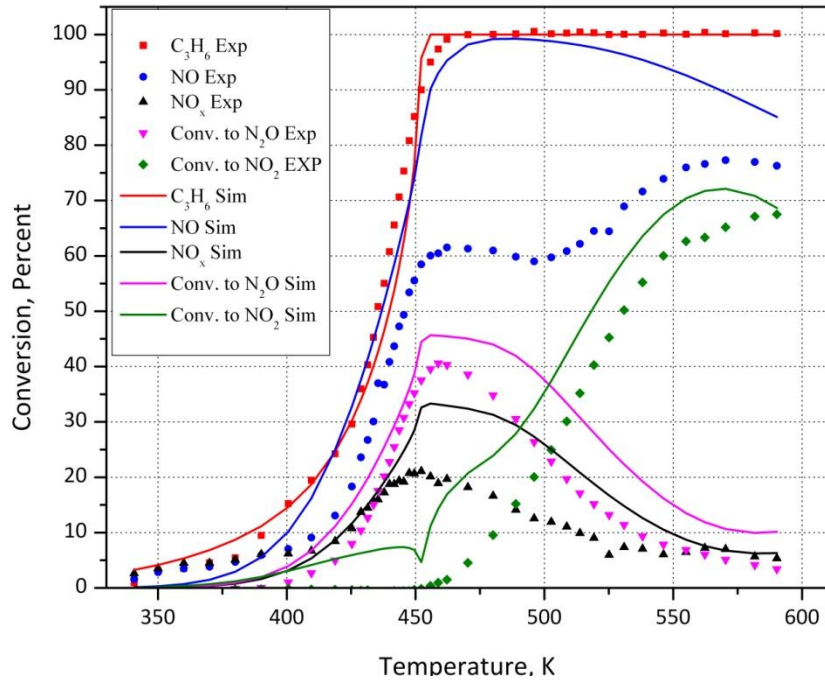


Figure 5-125: Individual optimization result vs. Experimental data, Run 20, Model 5

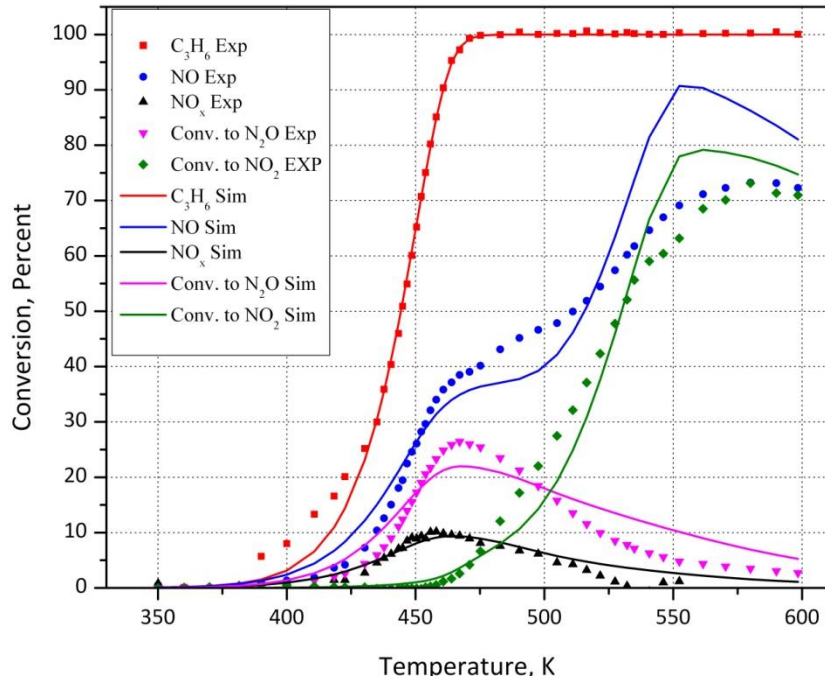


Figure 5-126: Individual optimization result vs. Experimental data, Run 21 Model 5

It is clear that our current model cannot predict NO_x reduction reactions sufficiently well, even when only one experiment at the time is optimized. The prediction of total NO_x conversion and conversion to N_2O not satisfactory, therefore an effort was made to improve the model.

5.6.1 Kinetic and Mechanism of the reduction of NO_x by C_3H_6

Many efforts have been made to understand the mechanism of NO_x reduction by hydrocarbons. Burch *et al.* showed that the reaction mechanism is strongly affected by reaction conditions such as gas composition, temperature and type of hydrocarbon [28-30]. They found that unsaturated hydrocarbons can adsorb on surface of Pt catalyst more strongly and irreversibly than their saturated counterparts [30]. Denton *et al.* proposed that oxygen main role is not to oxidize NO into NO_2 and NO acts as an intermediate during NO_x reduction [31]. In case which N_2O is the product, nitrosyl, dinitosyl species, nitrates and nitrites species could be considered as intermediate species during NO_x reduction [32].

It was observed that C_3H_6 conversion and NO_x reduction start at the same temperature, and increased with increasing temperature. Maximum NO_x conversion occurs at temperature that 100% hydrocarbon conversion is reached [33]. Comparing data for NO only experiments with NO, C_3H_6 showed that NO inhibited propene oxidation, which is in agreement with the results of Burch *et al.* [34]. Burch also showed that even with high presence of oxygen in lean condition, oxygen coverage on the Pt surface is too small while C_3H_6 coverage or at least hydrocarbon derived species coverage on catalyst site is at saturation. The double bond of propene make it possible to react strongly with Pt sites which results a high coverage of propene on the surface [33]. So there is no active site available for NO_x to react until adsorbed hydrocarbon species react, which means reduction of NO_x is secondary and dependent on reduction of the active sites by propene oxidation.

On the other hand, after reduction of the catalyst surface by hydrocarbon oxidation, NO will adsorb on the surface and will be reduced to N_2 or N_2O . After

decomposition of NO, O_{ads} would be built up on the catalyst surface and this will oxidize the surface, which can be interpreted as self poisoning effect of NO, because oxidized sites cannot adsorb and decompose further NO molecules[30].

In Figure 5-127 you can see briefly what occurs on the surface in the presence of NO and C_3H_6 :

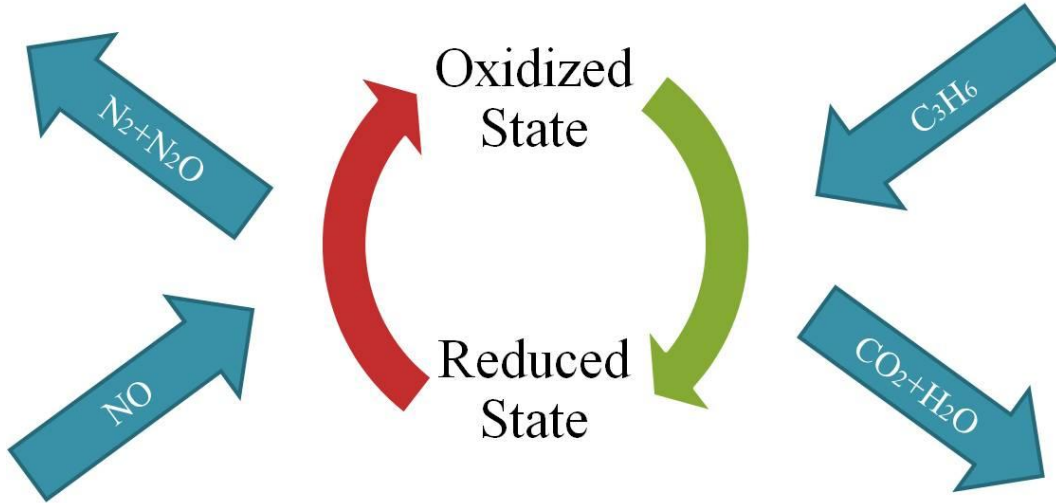


Figure 5-127: Oxidation and reduction of the catalyst surface

These two effects, hydrocarbon inhibition effect on NO_x reduction and NO self poisoning effect, should be considered to have a more realistic model. For the hydrocarbon inhibition effect, we suggest to add adsorption inhibition term into denominator of the rate equations for NO_x reduction. We also define here a new parameter, called K_{12} , which represents self poisoning effect of NO and we added this term to the denominator of the rate reaction as well. The modified rate models are as follow:

Reduction of NO to N_2 :

$$(-R_{NO})_{r1} = \frac{(-R_{C_3H_6})k_2 Y_{NO}}{(1 + K_9 Y_{O_2})(1 + K_6 Y_{C_3H_6})(1 + K_{12} Y_{NO})} \quad (5-47)$$

Reduction of NO to N₂O:

$$(-R_{\text{NO}})_{r2} = \frac{(-R_{\text{C}_3\text{H}_6})k_{11} Y_{\text{NO}}}{(1 + K_9 Y_{\text{O}_2})(1 + K_6 Y_{\text{C}_3\text{H}_6})(1 + K_{12} Y_{\text{NO}})} \quad (5-48)$$

Reduction of NO₂:

$$(-R_{\text{NO}_2})_{r3} = \frac{(-R_{\text{C}_3\text{H}_6})10k_2 Y_{\text{NO}_2}}{(1 + K_9 Y_{\text{O}_2})(1 + K_6 Y_{\text{C}_3\text{H}_6})(1 + K_{12} Y_{\text{NO}})} \quad (5-49)$$

It is clear that since oxidation of NO always happens after full conversion of hydrocarbon, we do not have to change NO oxidation rate equations.

To validate the new model, it was applied to experiments 16 to 21, both individually and simultaneously. Results for individual optimizations as well as simultaneous optimizations were very good, so here we report only simultaneous results. Table 5-48 to Table 5-52 and Figure 5-128 to Figure 5-152 are presenting the results for simultaneous optimization of experiments 16 to 21 with respect to different new models:

Table 5-48: Runs 16-21 simultaneous optimization results, Model 1

Parameter	LB	HB	Run 16	Run 17	Run 18	Run 20	Run 21	
k ₂	A ₂	0	30	8.24				
	E ₂	0	150000	43868				
k ₃	A ₃	0	30	17.9				
	E ₃	20000	150000	46743				
k ₄	A ₄	0	30	13.6				
	E ₄	0	150000	38150				
K ₆	B ₆	0	30	7.26				
	H ₆	-150000	0	-0.14				
K ₈	B ₈	0	30	8.20				
	H ₈	-150000	0	-44846				
K ₉	B ₉	0	30	2.63				
	H ₉	-150000	150000	103639				
k ₁₁	A ₁₁	0	30	8.84				
	E ₁₁	0	150000	57298				
K ₁₂	B ₁₂	0	30	8.16				
	H ₁₂	-150000	150000	10081				
Model 1	C₃H₆ Residual			8.1	14	14	5.8	3.3
	NO_x Residual			8.2	8.9	3.3	11	3.9
	N₂O Residual			3.9	41	4.7	4.1	1.5
	NO₂ Residual			5.7	5.4	3.4	3.3	2.2
	Cumulative Residual			26	71	25	24	11

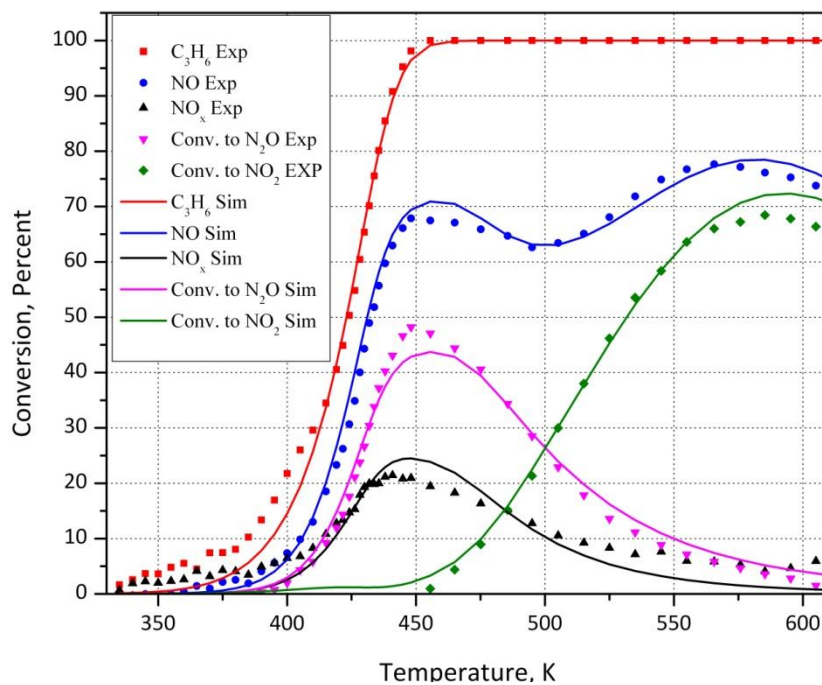


Figure 5-128: Simultaneous optimization result vs. Experimental data, Run 16, Model 1

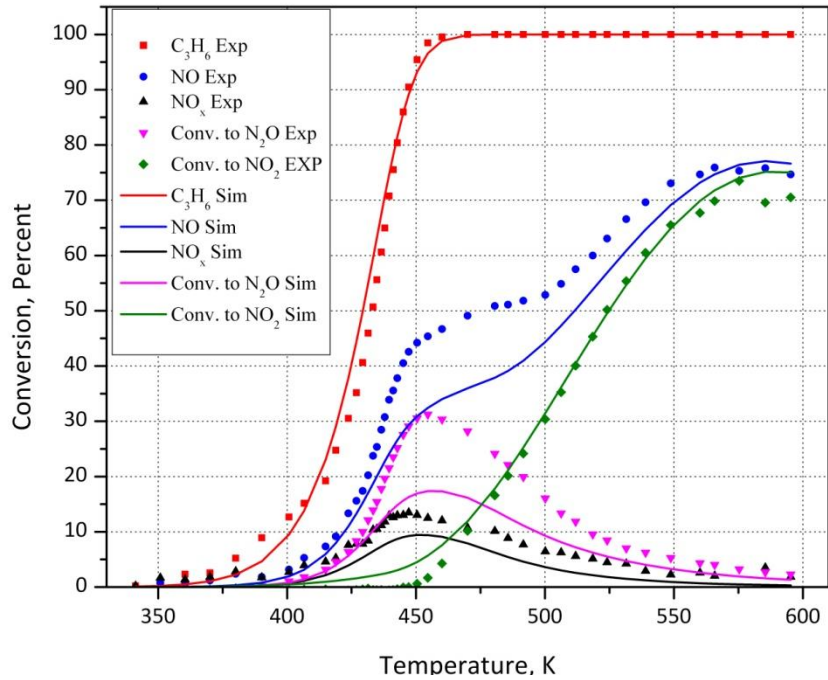


Figure 5-129: Simultaneous optimization result vs. Experimental data, Run 17, Model 1

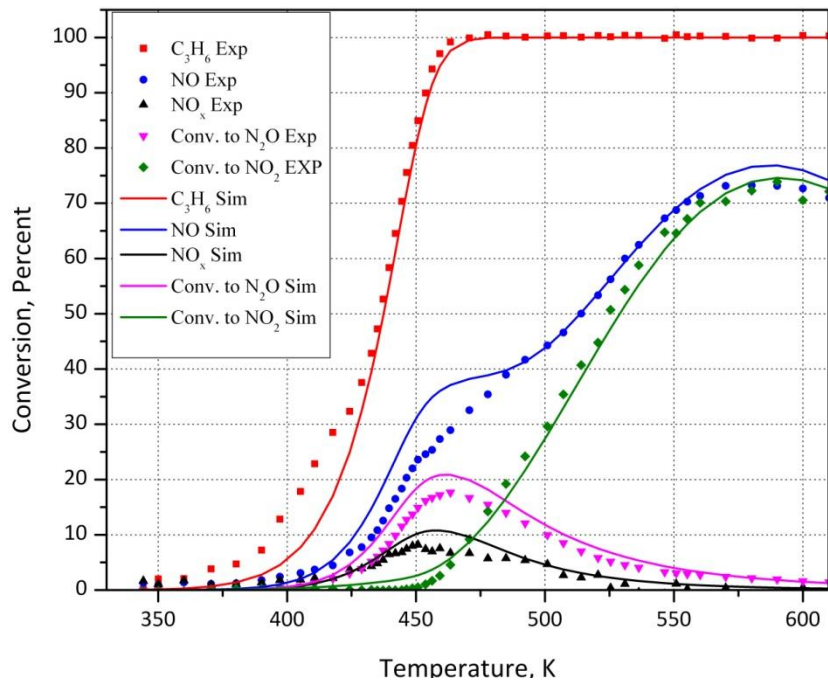


Figure 5-130: Simultaneous optimization result vs. Experimental data, Run 18, Model 1

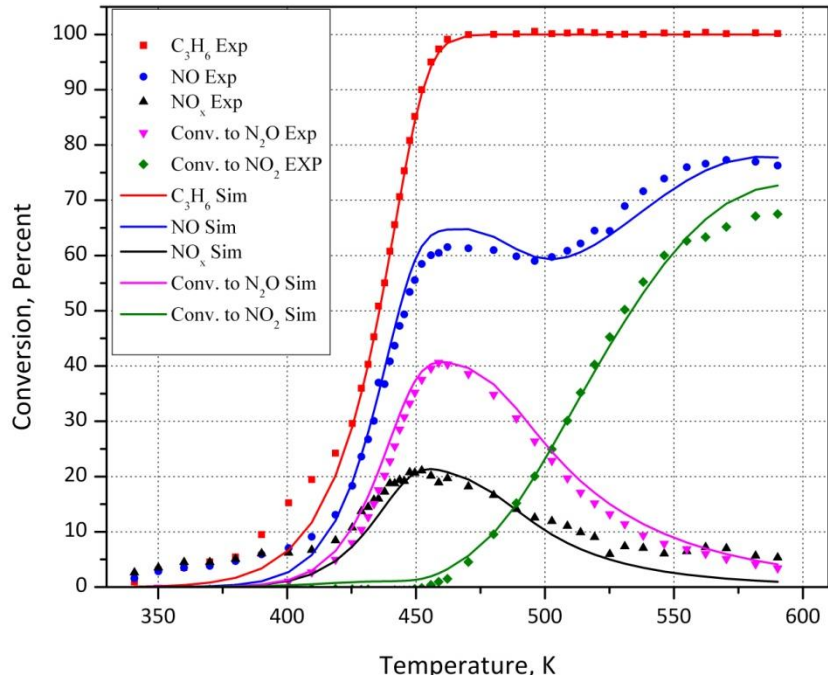


Figure 5-131: Simultaneous optimization result vs. Experimental data, Run 20, Model 1

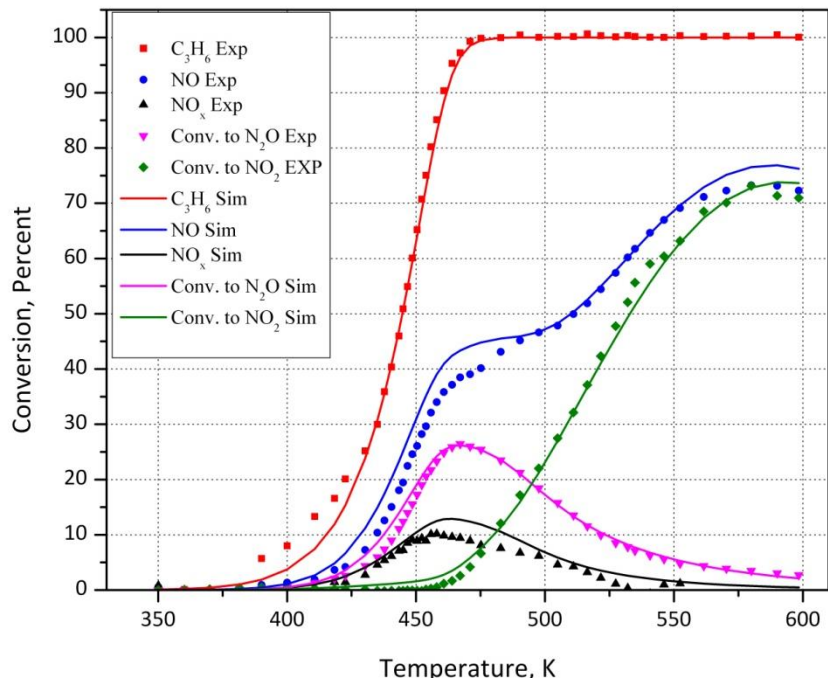


Figure 5-132: Simultaneous optimization result vs. Experimental data, Run 21, Model 1

Table 5-49: Runs 16-21 simultaneous optimization results, Model 2

Parameter	LB	HB	Run 16	Run 17	Run 18	Run 20	Run 21
k ₂	A ₂	0	30	28.1			
	E ₂	0	150000	93914			
k ₃	A ₃	0	30	18.0			
	E ₃	20000	150000	60601			
k ₄	A ₄	0	30	14.8			
	E ₄	0	150000	112693			
K ₆	B ₆	0	30	7.25			
	H ₆	-150000	0	-160			
K ₈	B ₈	0	30	8.46			
	H ₈	-150000	0	-28797			
K ₉	B ₉	0	30	23.1			
	H ₉	-150000	150000	87826			
K ₁₀	B ₁₀	0	30	12.2			
	H ₁₀	-150000	0	-2143			
k ₁₁	A ₁₁	0	30	28.7			
	E ₁₁	0	150000	99969			
K ₁₂	B ₁₂	0	30	8.04			
	H ₁₂	-150000	150000	59926			
Model 2	C ₃ H ₆ Residual		8.4	16	11	5.9	2.4
	NO _x Residual		5.2	7.3	3.7	7.5	5.8
	N ₂ O Residual		23	46	4.7	10	2.8
	NO ₂ Residual		15	15	14	16	9.5
	Cumulative Residual		52	85	35	39	20

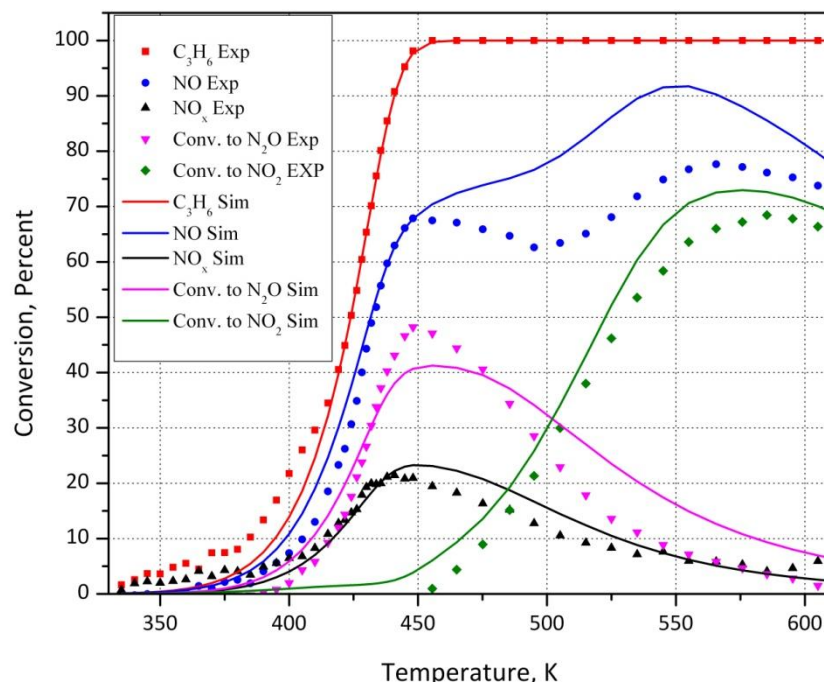


Figure 5-133: Simultaneous optimization result vs. Experimental data, Run 16, Model 2

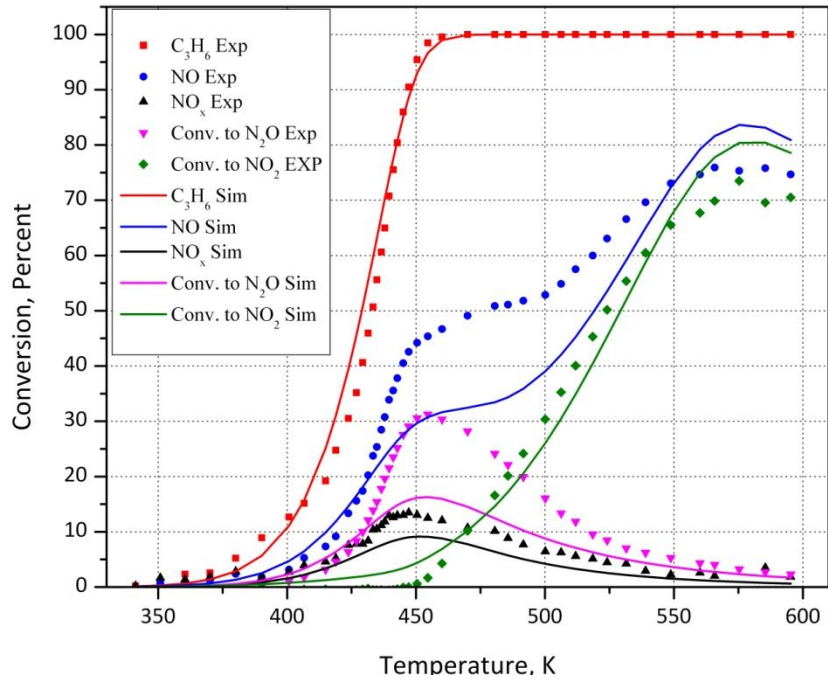


Figure 5-134: Simultaneous optimization result vs. Experimental data, Run 17, Model 2

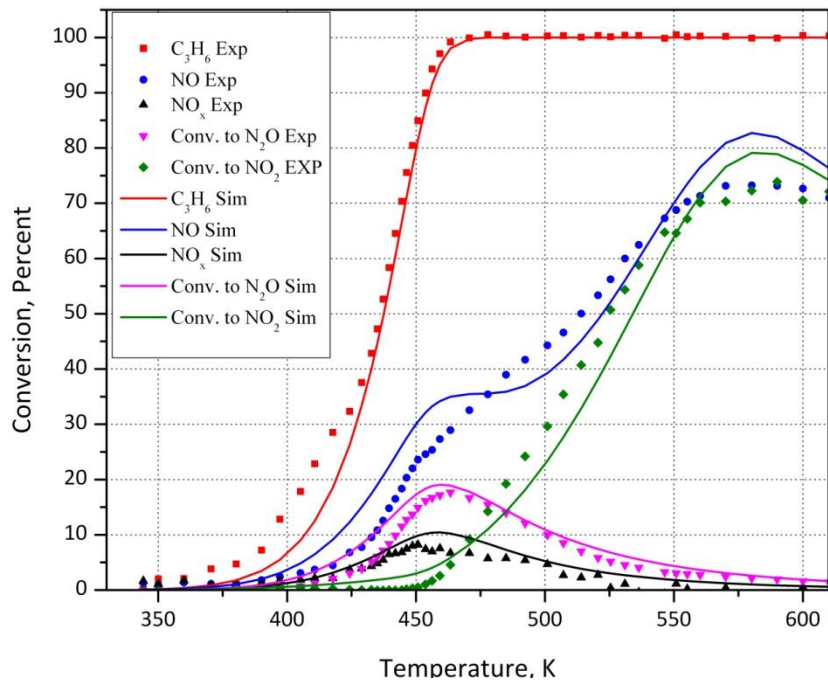


Figure 5-135: Simultaneous optimization result vs. Experimental data, Run 18, Model 2

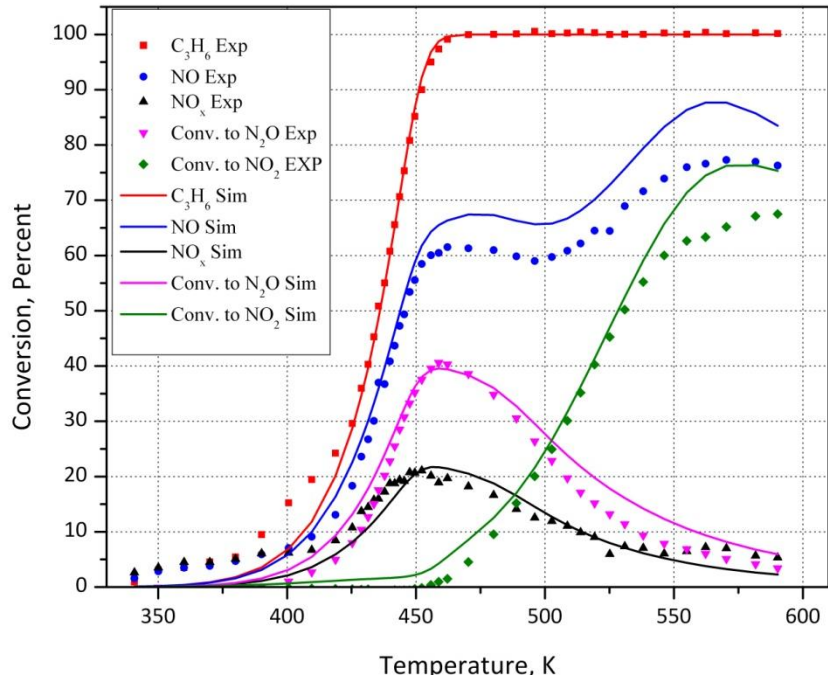


Figure 5-136: Simultaneous optimization result vs. Experimental data, Run 20, Model 2

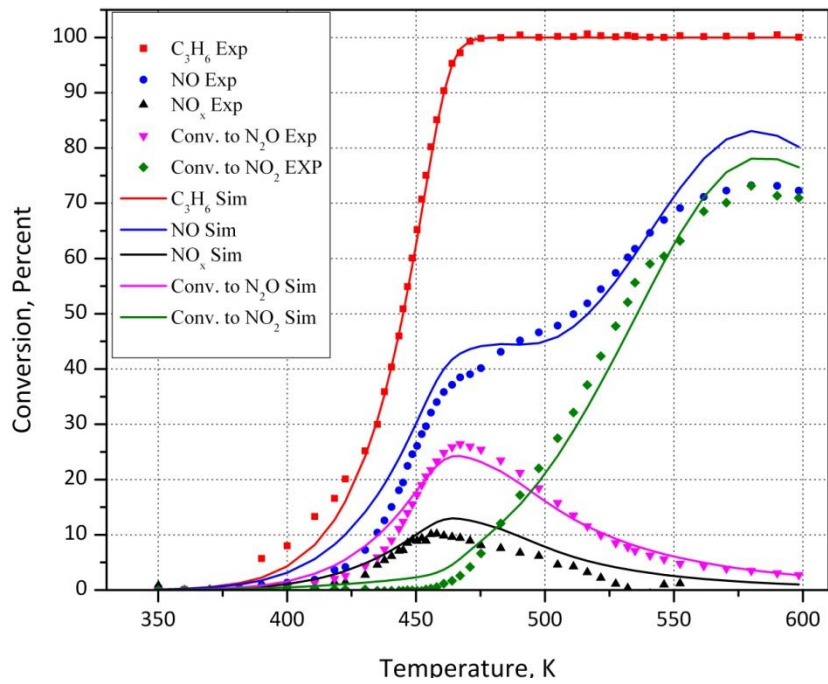


Figure 5-137: Simultaneous optimization result vs. Experimental data, Run 21, Model 2

Table 5-50: Runs 16-21 simultaneous optimization results, Model 3

Parameter	LB	HB	Run 16	Run 17	Run 18	Run 20	Run 21
k ₂	A ₂	0	30	29.3			
	E ₂	0	150000	78095			
k ₃	A ₃	0	30	18.0			
	E ₃	20000	150000	36563			
k ₄	A ₄	0	30	12.6			
	E ₄	0	150000	124405			
K ₆	B ₆	0	30	7.28			
	H ₆	-150000	0	-341			
K ₈	B ₈	0	30	8.24			
	H ₈	-150000	0	-69951			
K ₉	B ₉	0	30	24.5			
	H ₉	-150000	150000	85878			
K ₁₀	B ₁₀	0	30	14.4			
	H ₁₀	-150000	0	-86754			
k ₁₁	A ₁₁	0	30	29.8			
	E ₁₁	0	150000	81191			
K ₁₂	B ₁₂	0	30	7.85			
	H ₁₂	-150000	150000	25075			
Model 3	C₃H₆ Residual		14	10	17	8.0	3.8
	NO_x Residual		4.4	7.6	6.5	10	12.6
	N₂O Residual		29	43	8.4	22	7.1
	NO₂ Residual		14	47	42	16	25
	Cumulative Residual		62	108	75	57	49

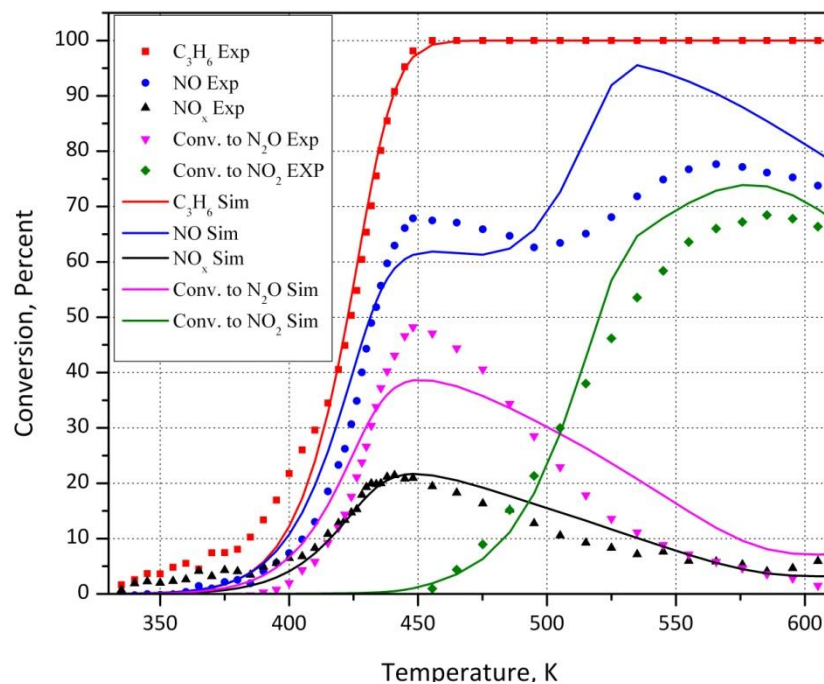


Figure 5-138: Simultaneous optimization result vs. Experimental data, Run 16, Model 3

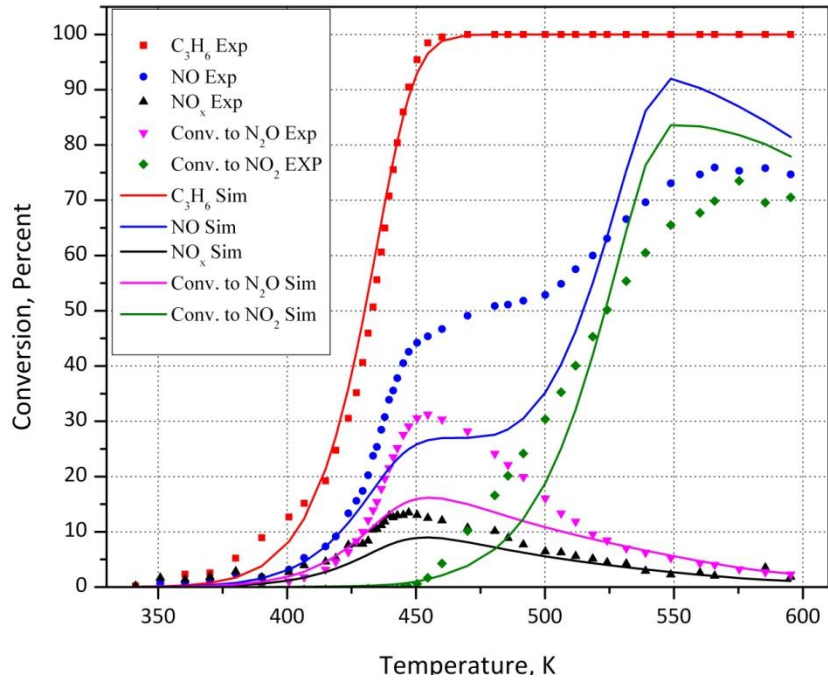


Figure 5-139: Simultaneous optimization result vs. Experimental data, Run 17, Model 3

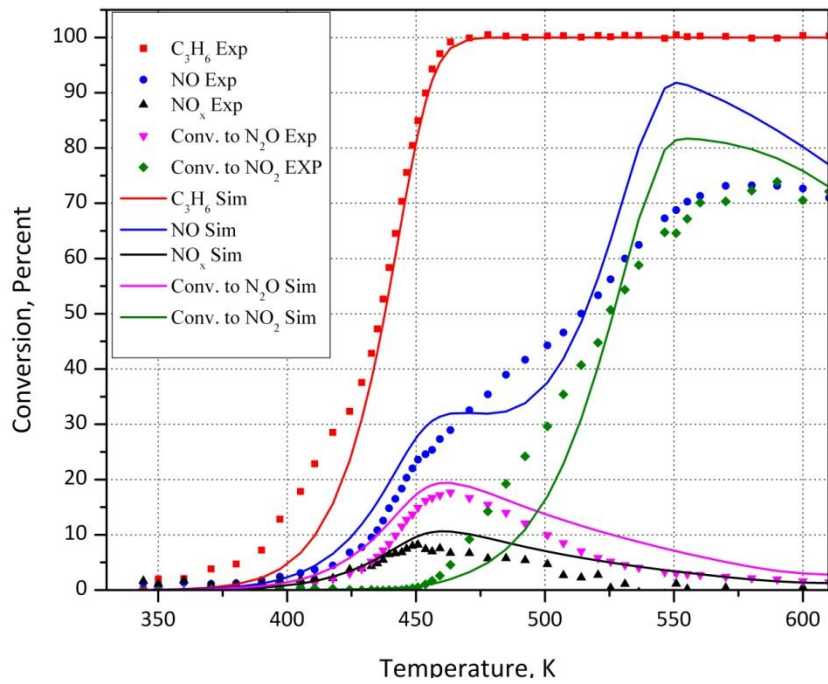


Figure 5-140: Simultaneous optimization result vs. Experimental data, Run 18, Model 3

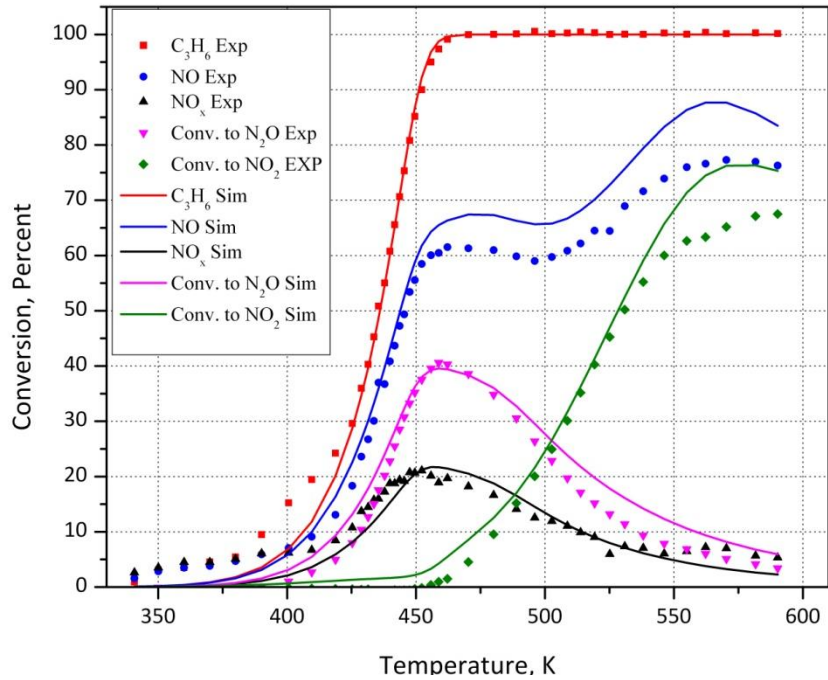


Figure 5-141: Simultaneous optimization result vs. Experimental data, Run 20, Model 3

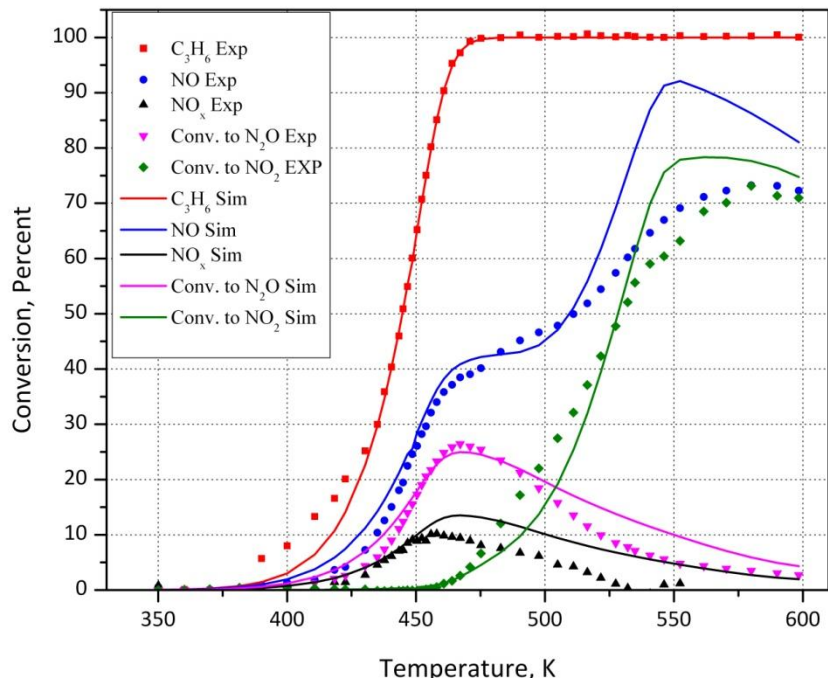


Figure 5-142: Simultaneous optimization result vs. Experimental data, Run 21, Model 3

Table 5-51: Runs 16-21 simultaneous optimization results, Model 4

Parameter	LB	HB	Run 16	Run 17	Run 18	Run 20	Run 21
k ₂	A ₂	0	30	29.1			
	E ₂	0	150000	119860			
k ₃	A ₃	0	30	17.9			
	E ₃	20000	150000	44959			
k ₄	A ₄	0	30	22.1			
	E ₄	0	150000	52279			
K ₆	B ₆	0	30	7.17			
	H ₆	-150000	0	-13945			
K ₈	B ₈	0	30	8.38			
	H ₈	-150000	0	-39215			
K ₉	B ₉	0	30	24.1			
	H ₉	-150000	150000	119165			
K ₁₀	B ₁₀	0	30	20.5			
	H ₁₀	-150000	0	-59398			
k ₁₁	A ₁₁	0	30	29.7			
	E ₁₁	0	150000	125450			
K ₁₂	B ₁₂	0	30	8.11			
	H ₁₂	-150000	150000	55263			
Model 4	C ₃ H ₆ Residual		11	19	14	8.1	3.4
	NO _x Residual		5.3	7.6	3.5	8.0	6.0
	N ₂ O Residual		22	48	4.3	10	2.8
	NO ₂ Residual		15	15	14	14	9.6
	Cumulative Residual		55	90	37	40	21

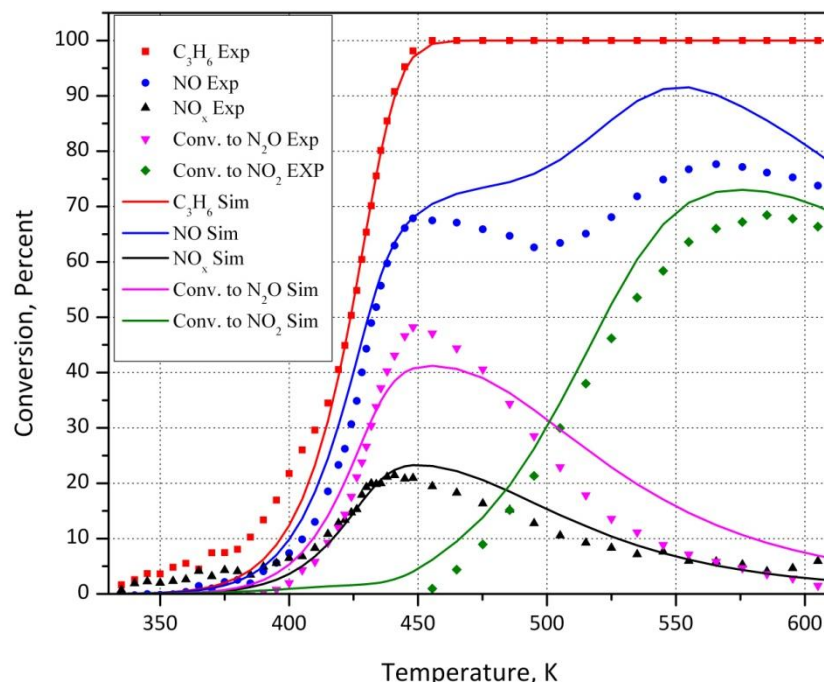


Figure 5-143: Simultaneous optimization result vs. Experimental data, Run 16, Model 4

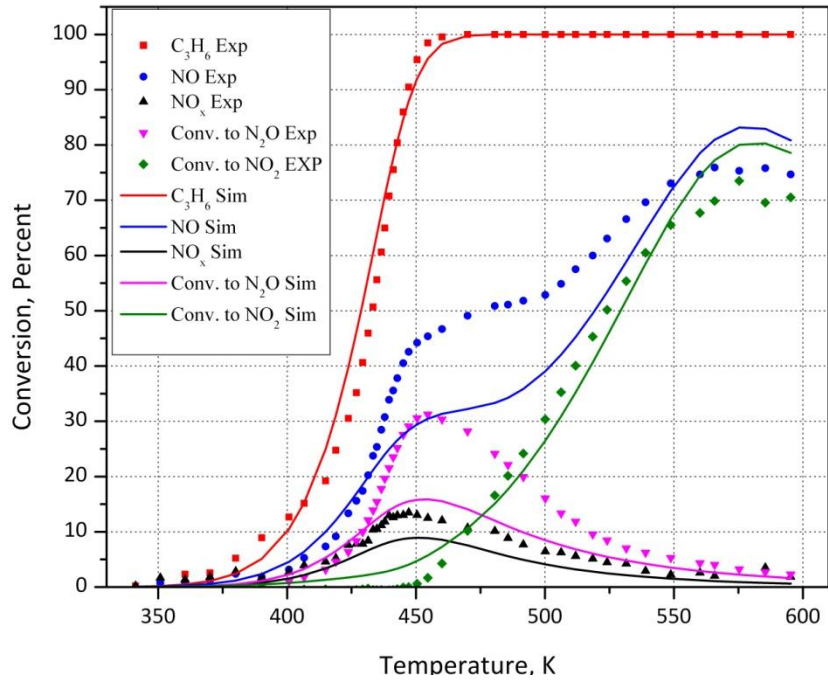


Figure 5-144: Simultaneous optimization result vs. Experimental data, Run 17, Model 4

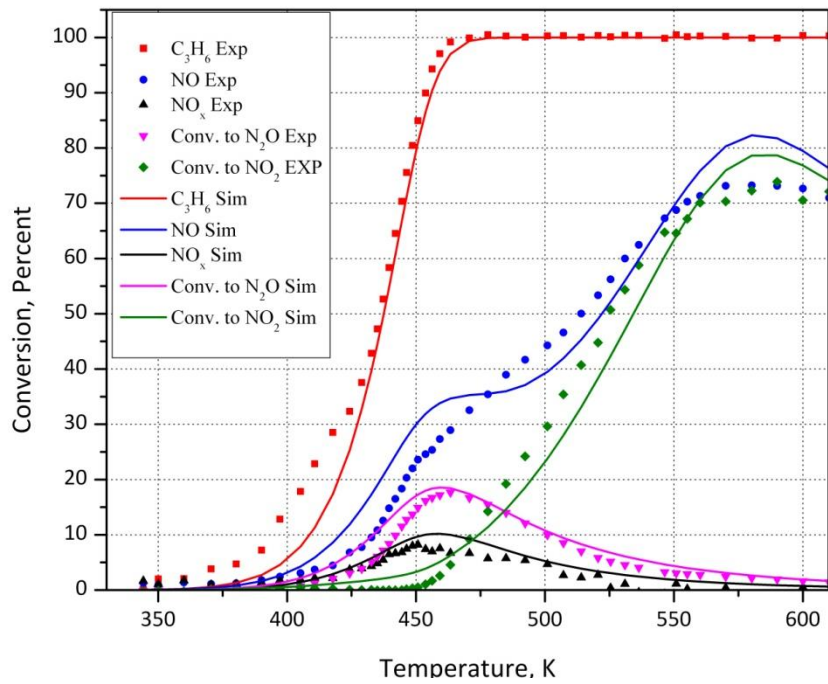


Figure 5-145: Simultaneous optimization result vs. Experimental data, Run 18, Model 4

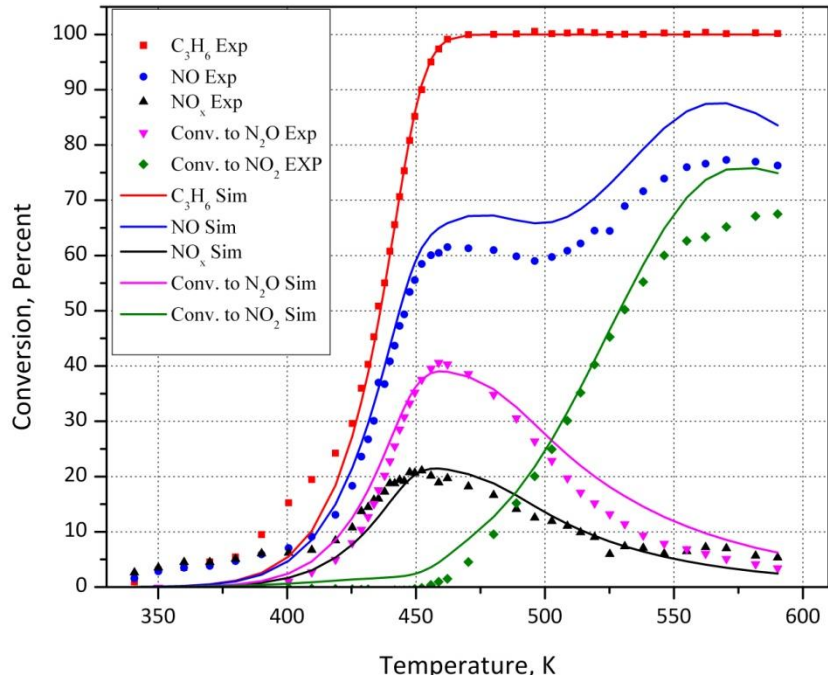


Figure 5-146: Simultaneous optimization result vs. Experimental data, Run 20, Model 4

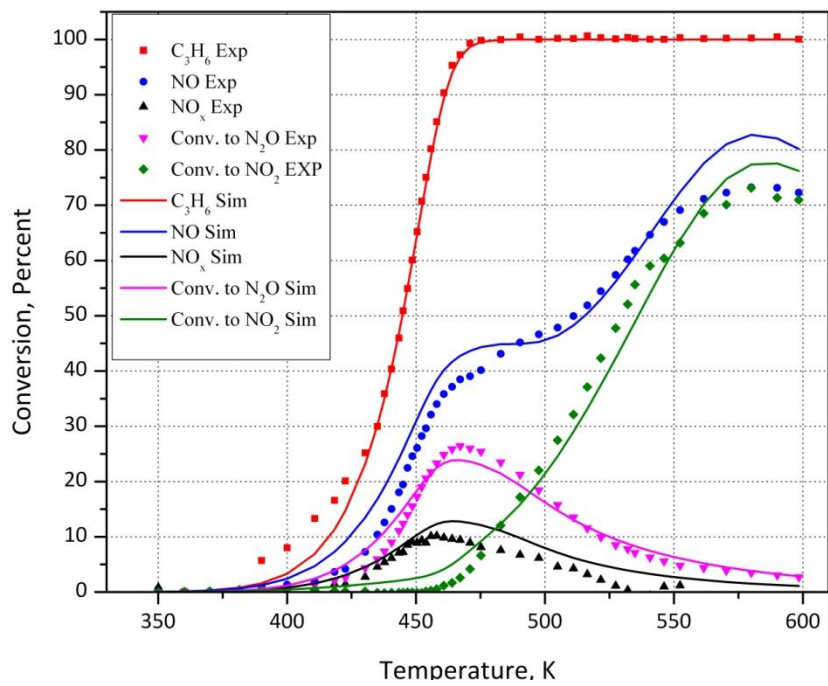


Figure 5-147: Simultaneous optimization result vs. Experimental data, Run 21, Model 4

Table 5-52: Runs 16-21 simultaneous optimization results, Model 5

Parameter	LB	HB	Run 16	Run 17	Run 18	Run 20	Run 21
k ₂	A ₂	0	30	22.9			
	E ₂	0	150000	40500			
k ₃	A ₃	0	30	18.4			
	E ₃	20000	150000	32530			
k ₄	A ₄	0	30	13.9			
	E ₄	0	150000	32185			
K ₆	B ₆	0	30	7.92			
	H ₆	-150000	0	-17868			
K ₈	B ₈	0	30	7.86			
	H ₈	-150000	0	-47612			
K ₉	B ₉	0	30	17.8			
	H ₉	-150000	150000	52536			
K ₁₀	B ₁₀	0	30	4.80			
	H ₁₀	-150000	0	-99990			
k ₁₁	A ₁₁	0	30	23.5			
	E ₁₁	0	150000	53977			
K ₁₂	B ₁₂	0	30	7.58			
	H ₁₂	-150000	150000	70273			
Model 5	C ₃ H ₆ Residual		9.9	12	19	6.5	3.2
	NO _x Residual		5.7	5.7	3.8	11	3.3
	N ₂ O Residual		10	33.	7.0	2.7	3.1
	NO ₂ Residual		5.2	3.0	2.8	2.9	1.5
	Cumulative Residual		31	55	32	23	11

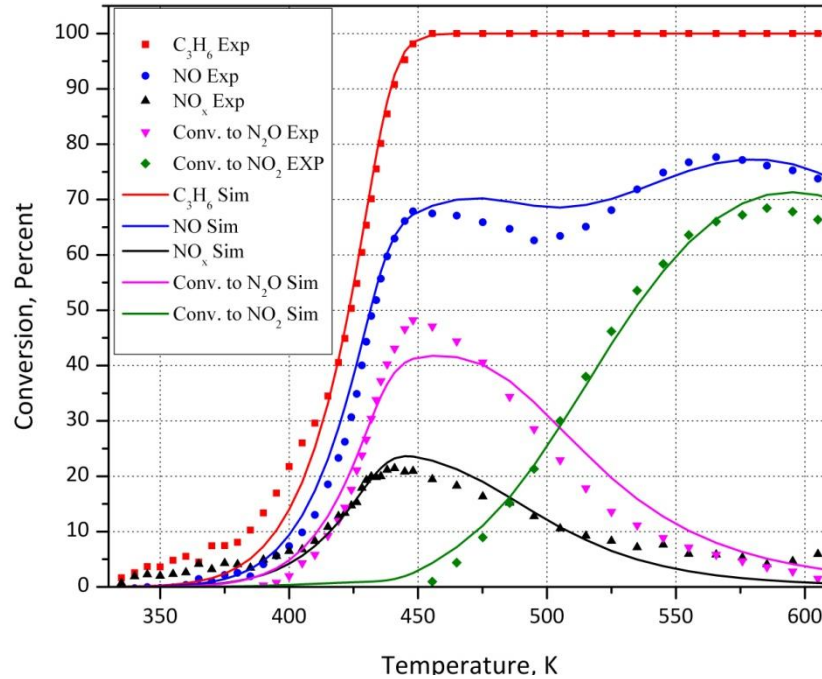


Figure 5-148: Simultaneous optimization result vs. Experimental data, Run 16, Model 5

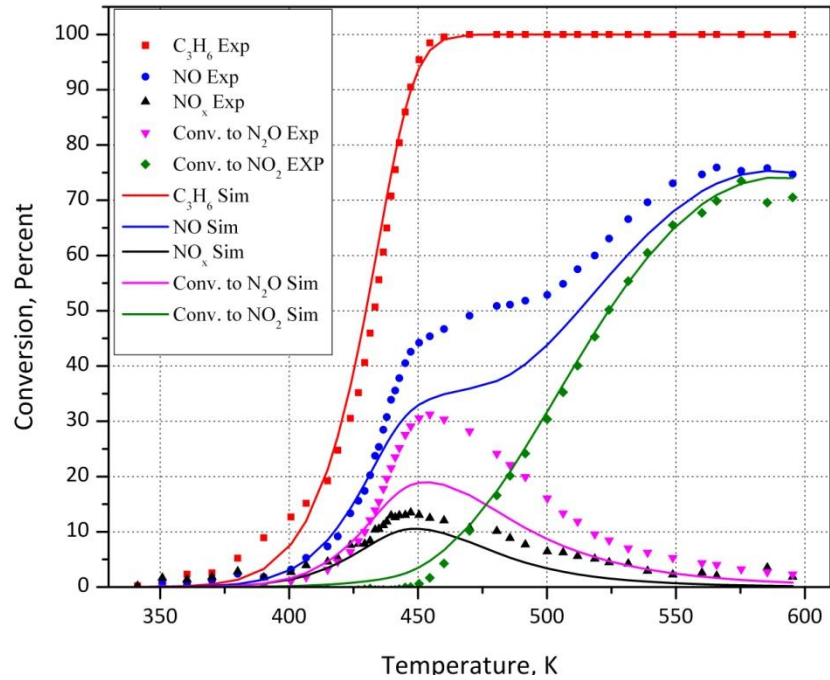


Figure 5-149: Simultaneous optimization result vs. Experimental data, Run 17, Model 5

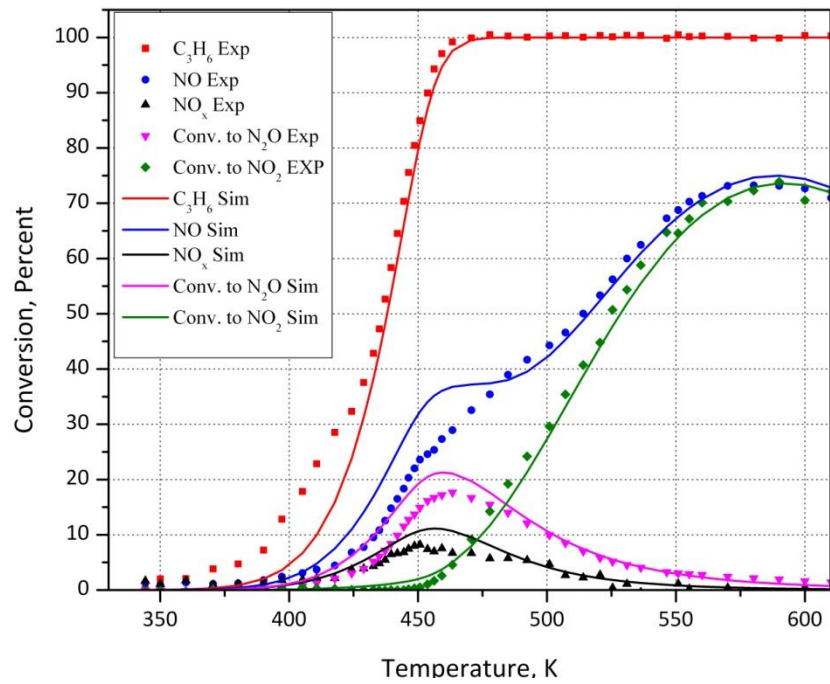


Figure 5-150: Simultaneous optimization result vs. Experimental data, Run 18, Model 5

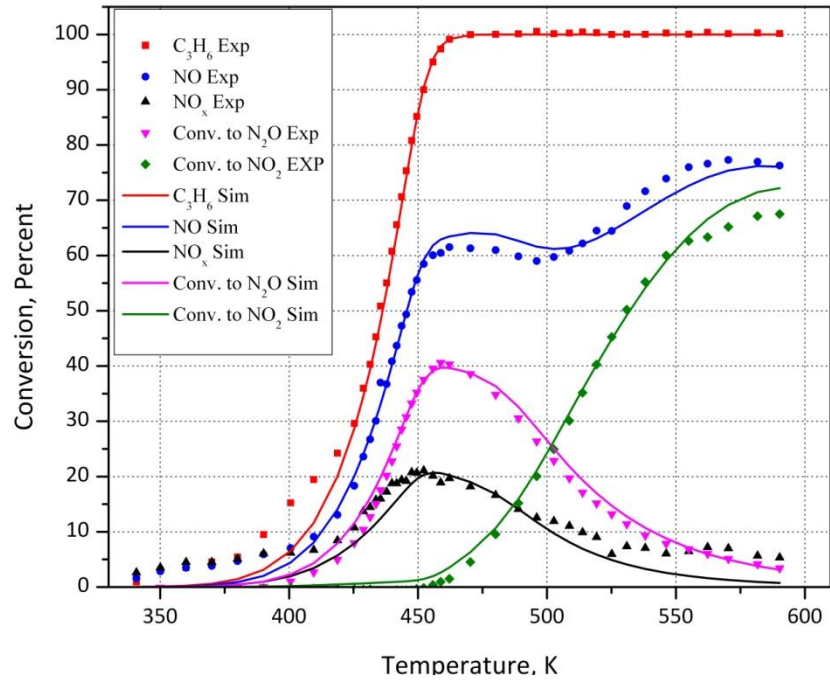


Figure 5-151: Simultaneous optimization result vs. Experimental data, Run 20, Model 5

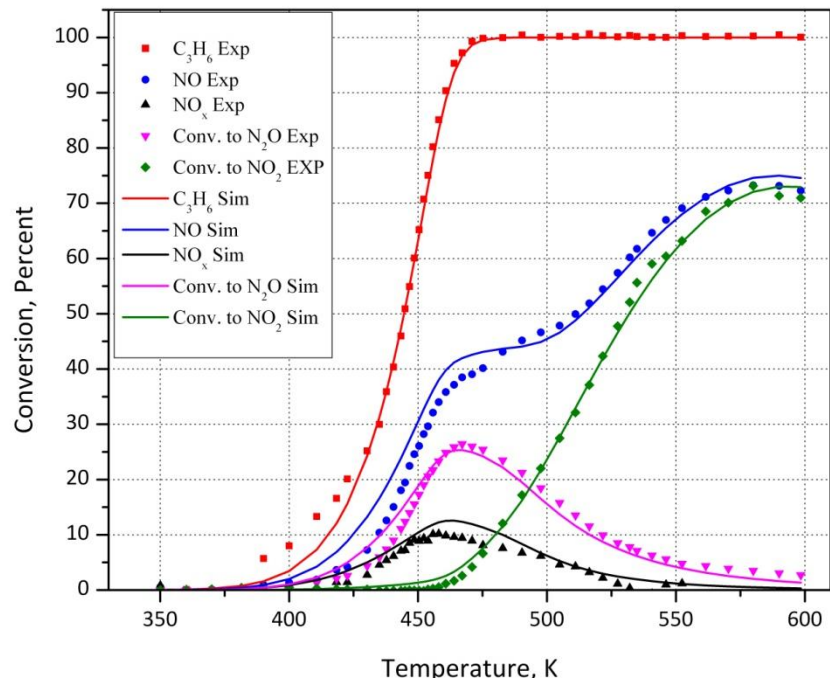


Figure 5-152: Simultaneous optimization result vs. Experimental data, Run 21, Model 5

It is seen that, although the low conversion portion of the CO oxidation curve is not captured very well by any of the models, Model 5 followed very close by Model 1, are the best models to predict behaviours of the system when C₃H₆ and NO are fed to the reactor.

5.7 Modelling of Mixture of CO, H₂, C₃H₆ & NO

This section presents modelling results obtained when all of the reactants (CO/H₂, NO and C₃H₆) were fed to the reactor. Initial concentrations for these experiments are shown in Table 5-53.

For these experiments, as it shown in Figure 5-153 and Figure 5-154, some unusual results were observed for the C₃H₆ ignition curves. Typical behaviour is shown in the next two figures, where a “Two Stage” ignition shape is observed. To the best of our knowledge, this type of behaviour has not previously been reported in the literature.

Table 5-53: CO, H₂, Propene & NO experiments, initial concentrations

Run	CO [ppm]	H ₂ [ppm]	Propene [ppm]	NO [ppm]
28	500	167	250	150
29	2000	666	250	150
30	500	167	750	150
31	2000	666	750	150
32	500	167	250	600
33	2000	666	250	600
34	500	167	750	600
35	2000	666	750	600
36	1000	333	250	150
37	1000	333	250	600
38	1000	333	750	150
39	1000	333	750	600
40	500	167	500	150
41	2000	666	500	150
42	500	167	500	600
43	2000	666	500	600
44	500	167	250	300
45	2000	666	250	300
46	500	167	750	300
47	2000	666	750	300
48	1000	333	500	150
49	1000	333	250	300
50	500	167	500	300
51	1000	333	500	300
52	2000	666	500	300
53	1000	333	750	300
54	1000	333	500	600

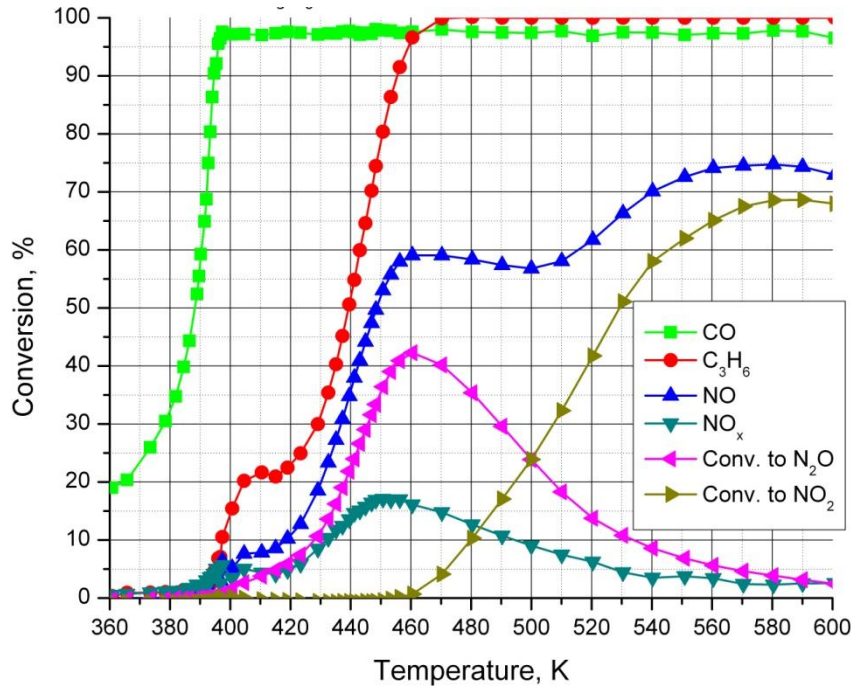


Figure 5-153: CO, C₃H₆, NO, NO_x, NO₂ & N₂O - Ignition curve Run 46

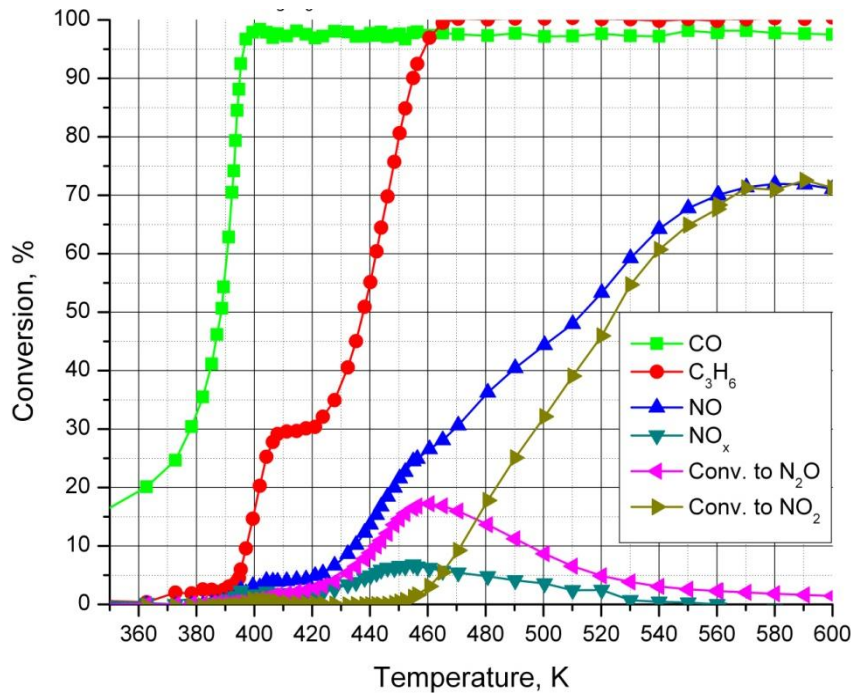


Figure 5-154: CO, C₃H₆, NO, NO_x, NO₂ & N₂O - Ignition curve Run 42

To find the cause for this deviation, we can compare different experimental results.

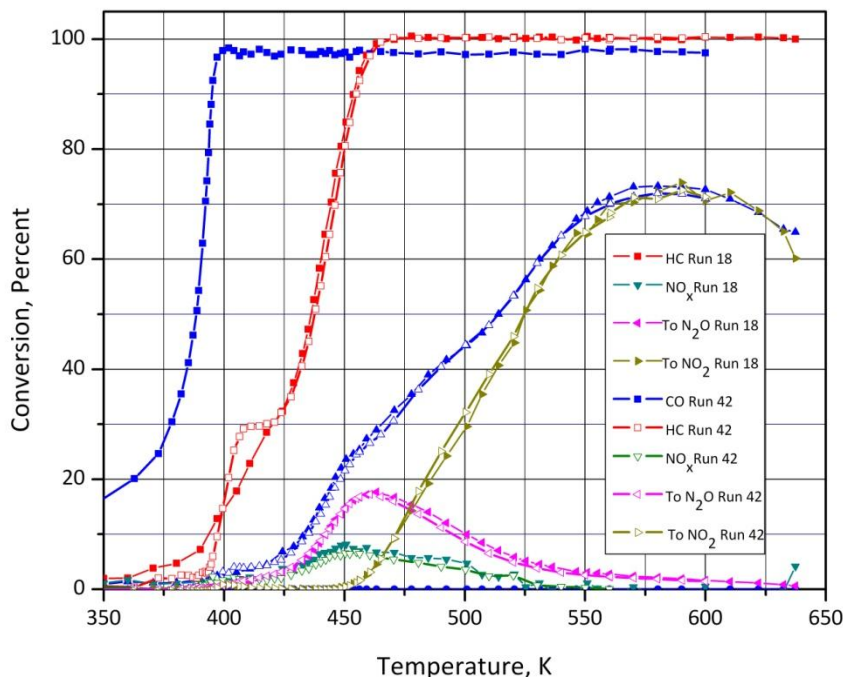


Figure 5-155: Ignition curves comparison, Run 18 vs. Run 42

Figure 5-155 compare runs 18 and 42. Both experiments used 500 ppm propene and 600 ppm NO; however run 42 included 500 ppm CO (with 167 ppm hydrogen).

As can be seen, all of the ignition curves are essentially the same for the two experiments, but the propene ignition curve shows an obvious deviation in comparison with the other experiment hydrocarbon ignition curve. The obvious conclusion is that this unusual behaviour in hydrocarbon oxidation is because of presence of CO. Since we did not see any major deviation in hydrocarbon ignition curves in experiments which we only had CO, H₂ & C₃H₆, it is clear that only presence of CO and H₂ with propene and NO have such an interesting effect on propene oxidation.

The shape of the propene ignition curve was observed to depend on feed concentrations. For example, Figure 5-156 shows a comparison of experiments 34

and 35. Both experiments used 750 ppm C_3H_6 and 600 ppm NO, but the CO concentrations were 500 and 2000 ppm for experiments 34 and 35 respectively.

As seen in Figure 5-156, increasing the CO concentration in the feed can smooth the deviation of the ignition curve, and increases the temperature at which deviation happens.

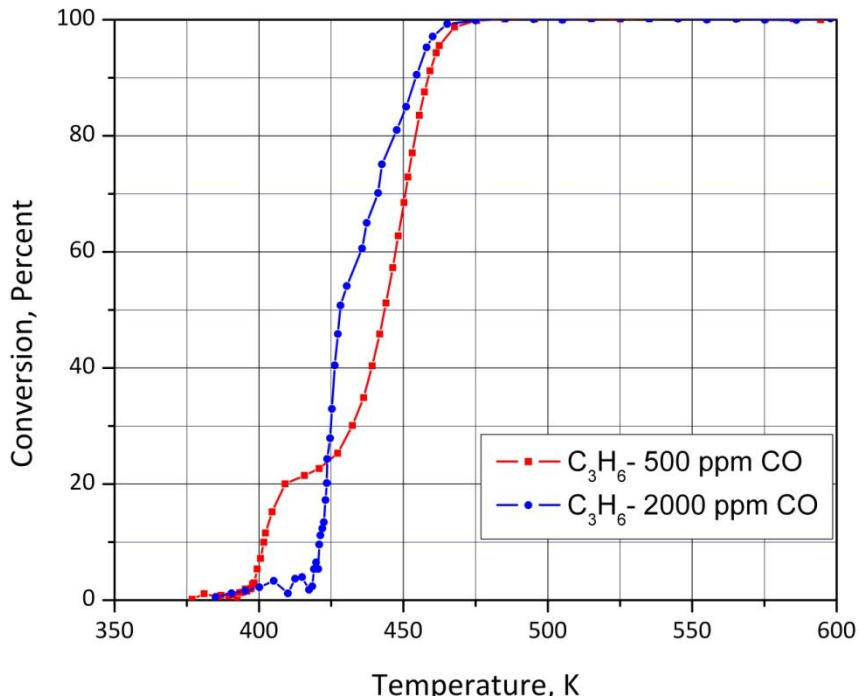


Figure 5-156: C_3H_6 Ignition curves comparison, Run 34 vs. Run 35

The shape of the deviation is also affected by the NO and C_3H_6 concentrations. Figure 5-157 compares the C_3H_6 ignition curves for experiments 28 and 30 (500 ppm CO and 150 ppm NO), two runs with different C_3H_6 concentration (250 ppm and 750 ppm). The run at 750 ppm C_3H_6 shows a sharper deviation with a longer “flat” section.

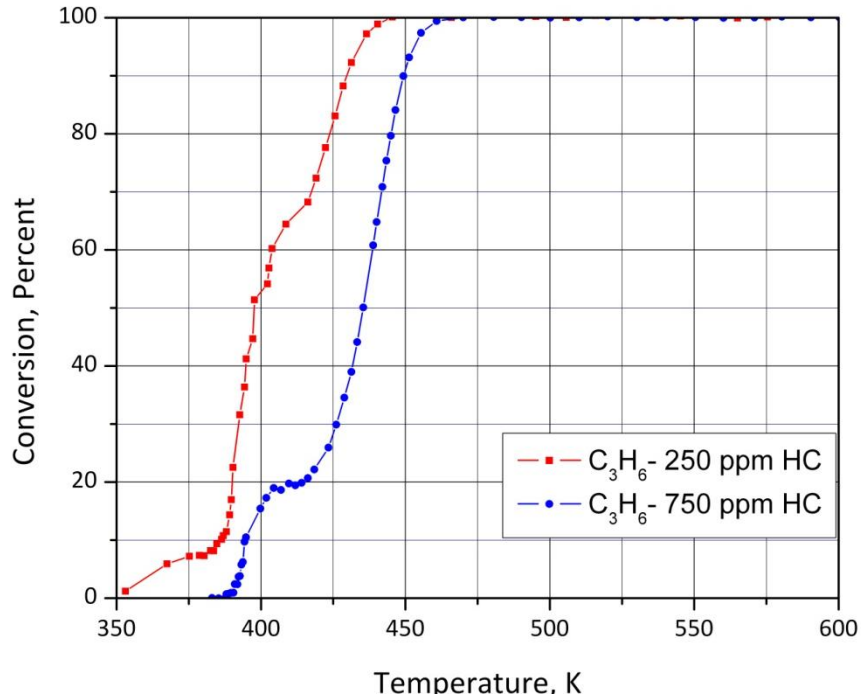


Figure 5-157: C₃H₆ Ignition curves comparison, Run 28 vs. Run 30

Figure 5-158 compares the C₃H₆ ignition curves for runs 28 and 32. Both these runs used 500 ppm CO and 250 ppm C₃H₆, but with NO concentrations of 150 and 600 ppm respectively. The higher NO concentration causes a sharper deviation with concomitant flat area.

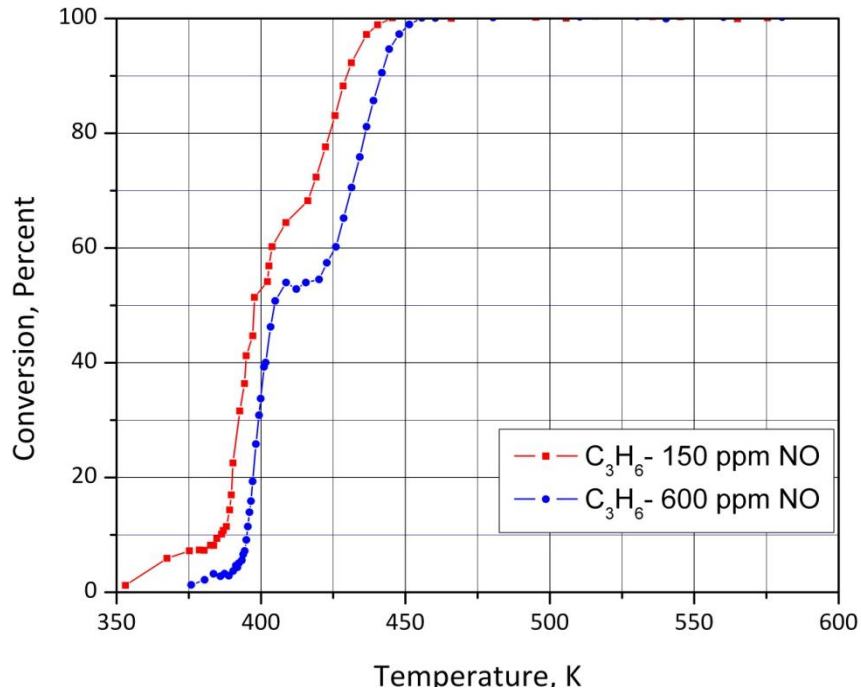


Figure 5-158: C₃H₆ Ignition curves comparison, Run 28 vs. Run 32

We now test the predictive ability of the modified model presented in the earlier sections. As a first step, the model was tested using individual experiments. The results for experiments 38, 39 and 53 are shown in Table 5-54 to Table 5-55 and Figure 5-159 to Figure 5-161 for model 5. The model equation can be found on the page 52.

Table 5-54: Runs 38, 39 & 53 individual optimization results, Model 5

Parameter		LB	HB	Run 38	Run 39	Run 53
k ₁	A ₁	0	30	26.8	26.8	26.8
	E ₁	20000	150000	140992	13469	146130
k ₂	A ₂	0	30	28.7	28.8	28.7
	E ₂	0	150000	69388	104726	103051
k ₃	A ₃	0	30	21.6	21.7	21.9
	E ₃	20000	150000	32836	34982	32613
k ₄	A ₄	0	30	16.6	16.7	17.5
	E ₄	0	150000	74984	87349	93096
K ₅	B ₅	0	30	4.44	5.46	4.41
	H ₅	-150000	0	-149995	-145256	-149991
K ₆	B ₆	0	30	7.35	7.27	6.93
	H ₆	-150000	0	-39388	-47548	-46624
K ₇	B ₈	0	30	15.3	15.7	13.2
	H ₈	-150000	0	-76646	-78896	-65622
K ₈	B ₈	0	30	11.5	10.3	10.9
	H ₈	-150000	0	-18934	-21712	-18353
K ₉	B ₉	0	30	23.9	25.0	24.5
	H ₉	-150000	150000	132602	148595	149282
K ₁₀	B ₁₀	0	30	11.9	11.0	12.1
	H ₁₀	-150000	0	-739	-922	-971.
k ₁₁	A ₁₁	0	30	29.5	29.5	29.4
	E ₁₁	0	150000	119684	117024	133958
K ₁₂	B ₁₂	0	30	7.75	5.79	5.55
	H ₁₂	-150000	150000	69790	19321	83681
Model 5	CO Residual			12	11	8.5
	C ₃ H ₆ Residual			43	14	18
	NO _x Residual			19	0.91	3.8
	N ₂ O Residual			8.0	4.0	7.3
	NO ₂ Residual			9.0	3.5	7.1
	Cumulative Residual			92	33	45

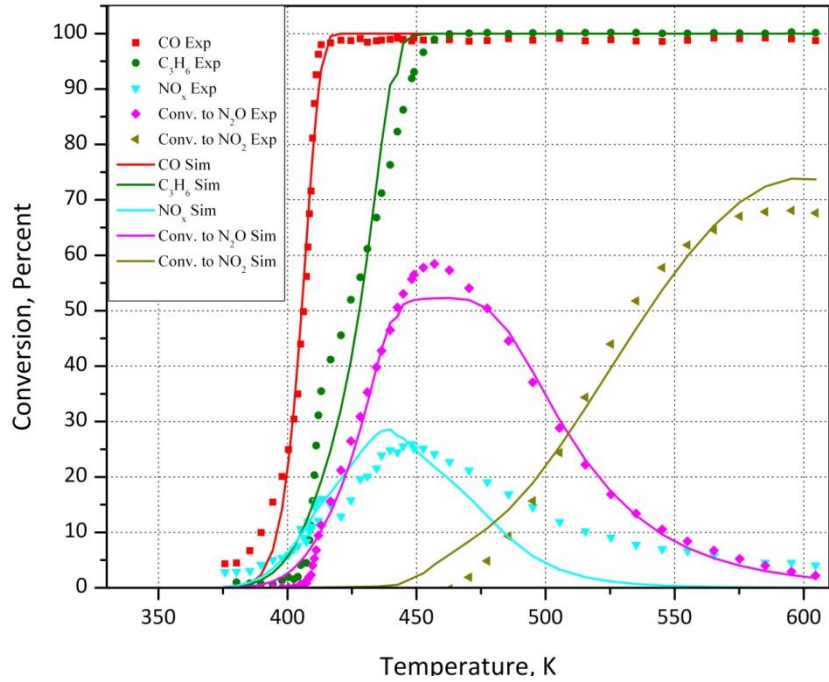


Figure 5-159: Individual optimization result vs. Experimental data, Run 38 Model 5

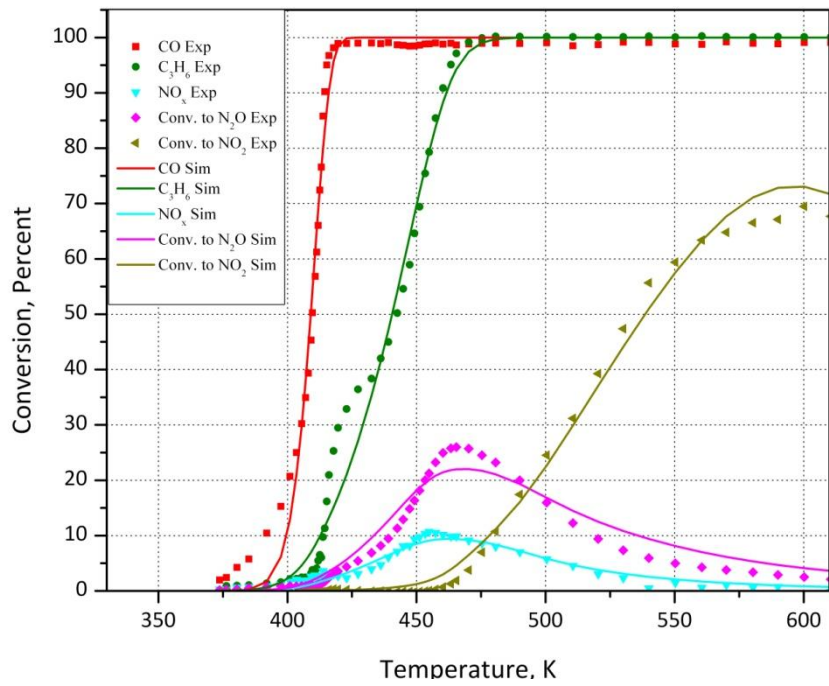


Figure 5-160: Individual optimization result vs. Experimental data, Run 39 Model 5

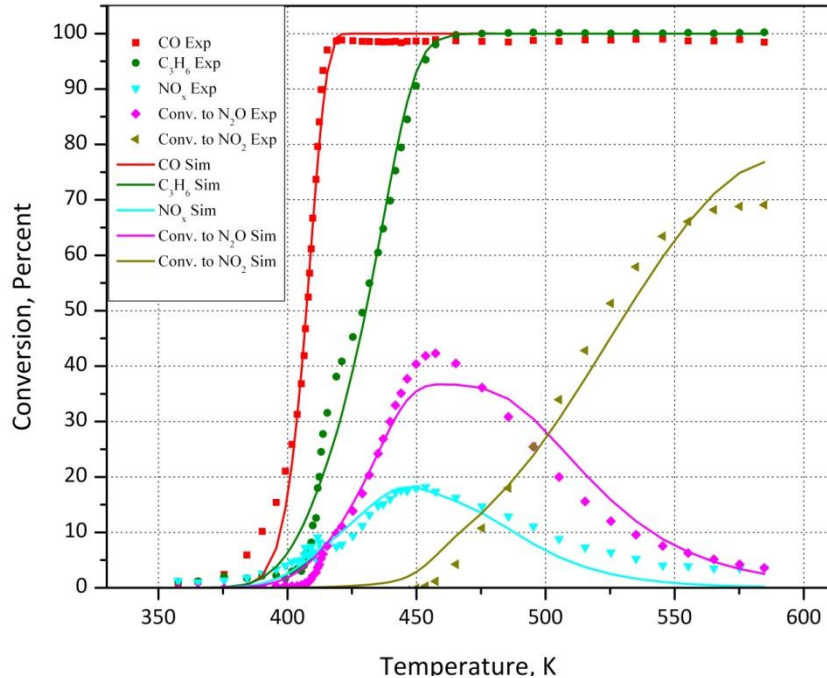


Figure 5-161: Individual optimization result vs. Experimental data, Run 53 Model 5

Our model can predict the behaviour of all of the ignition curves except the propene ignition curve. This observation is not surprising, because there is nothing in the model that would account for or predict this two stage C₃H₆ ignition shape. Furthermore, there are no literature results that offer clues as to the cause.

Based on experimental results, we hypothesize that this kind of behaviour could be caused by changing in mechanism during propene oxidation. It seems that we have two different mechanisms for propene oxidation, with switching between them a cause for this deviation. It is observed that this deviation started to happen when CO conversion was reaching 100%. So we can say that switching between two different mechanisms for propene oxidation which controls by CO conversion rate may cause this deviation in propene ignition curves.

Based on what we hypothesized previously, we proposed a new equation for hydrocarbon oxidation rate as follow. In these equations, we defined a new parameter, called K_{13} , which relate propene oxidation rate to CO oxidation rate with respect to hydrocarbon mole fraction.

Modified rate of propene oxidation, Models 1 to 4:

$$(-R_{C_3H_6}) = \frac{k_3 Y_{C_3H_6} Y_{O_2} + k_{13} Y_{C_3H_6} Y_{O_2} (-R_{CO})}{T(1 + K_5 Y_{CO} + K_6 Y_{C_3H_6})^2 (1 + K_7 (Y_{CO} Y_{C_3H_6})^2) (1 + K_8 Y_{NO})} \quad (5-50)$$

Modified rate of propene oxidation, Model 5:

$$(-R_{C_3H_6}) = \frac{k_3 Y_{C_3H_6} Y_{O_2} + k_{13} Y_{C_3H_6} Y_{O_2} (-R_{CO})}{T(1 + K_5 Y_{CO} + K_6 Y_{C_3H_6} + K_8 Y_{NO})^2} \quad (5-51)$$

As before, we apply these new models to our experimental data and see if they can successfully predict system behaviours. The results are presented in Table 5-55 and Figure 5-162 to Figure 5-164 for individual optimization tests.

Table 5-55: Runs 38, 39 & 53 individual optimization results, New Model 5

Parameter		LB	HB	Run 38	Run 39	Run 53
k ₁	A ₁	0	30	21.9	21.9	21.9
	E ₁	20000	150000	107923	109010	113770
k ₂	A ₂	0	30	22.1	22.2	22.2
	E ₂	0	150000	77495	86601	84672
k ₃	A ₃	0	30	16.7	16.0	16.7
	E ₃	20000	150000	106997	138331	118463
k ₄	A ₄	0	30	29.9	29.9	29.9
	E ₄	0	150000	98852	53295	56536
K ₅	B ₅	0	30	6.68	6.69	6.68
	H ₅	-150000	0	-44828	-52519	-40727
K ₆	B ₆	0	30	4.49	4.49	4.51
	H ₆	-150000	0	-93724	-93431	-98137
K ₇	B ₈	0	30	15.5	15.5	15.5
	H ₈	-150000	0	-75610	-75610	-75610
K ₈	B ₈	0	30	6.59	6.59	6.65
	H ₈	-150000	0	-65176	-40271	-49099
K ₉	B ₉	0	30	16.5	16.5	16.5
	H ₉	-150000	150000	49544	49110	49471
K ₁₀	B ₁₀	0	30	21.2	20.2	21.1
	H ₁₀	-150000	0	-41137	-69663	-90411
k ₁₁	A ₁₁	0	30	22.9	23.0	22.9
	E ₁₁	0	150000	89681	96334	88877
K ₁₂	B ₁₂	0	30	10.4	10.0	10.2
	H ₁₂	-150000	150000	77700	73699	69188
K ₁₃	B ₁₃	0	30	15.6	15.6	15.6
	H ₁₃	-150000	150000	-21896	-20582	-23965
Model 5	CO Residual			5.8	5.5	5.7
	C ₃ H ₆ Residual			3.6	5.1	2.4
	NO _x Residual			17	1.4	7.0
	N ₂ O Residual			9.5	5.0	7.9
	NO ₂ Residual			11	12	10
	Cumulative Residual			47	30	33

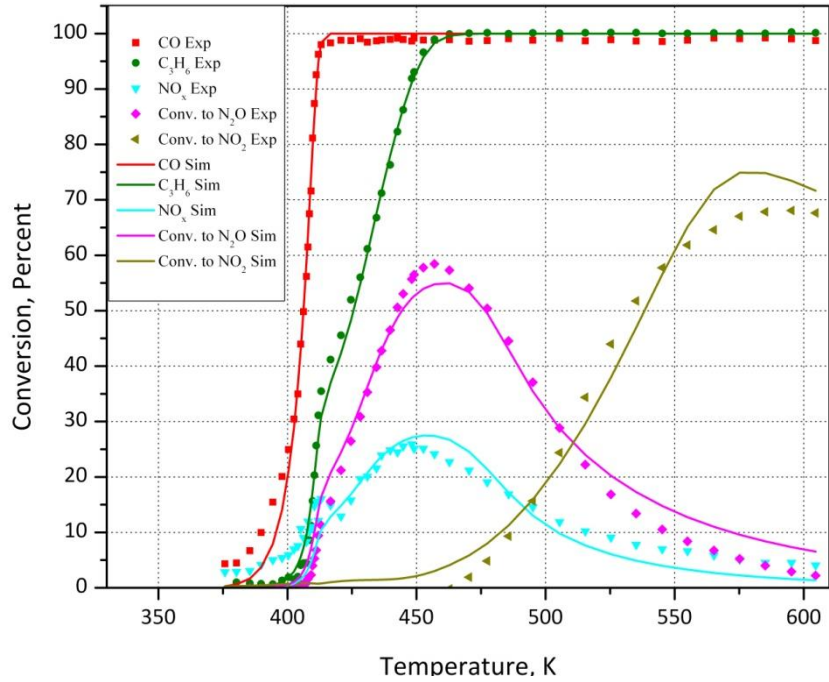


Figure 5-162: Individual optimization result vs. Experimental data, Run 38 New Model 5

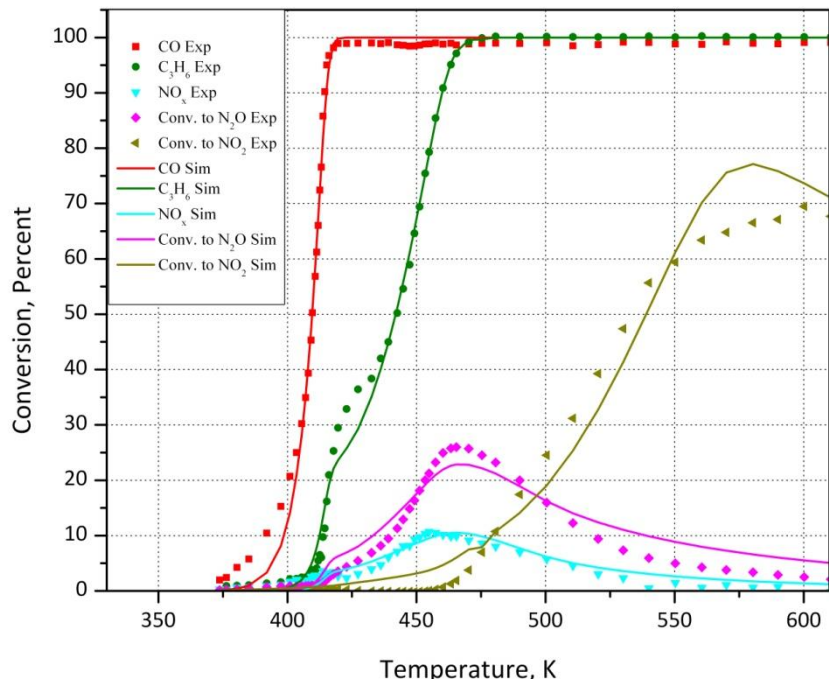


Figure 5-163: Individual optimization result vs. Experimental data, Run 39 New Model 5

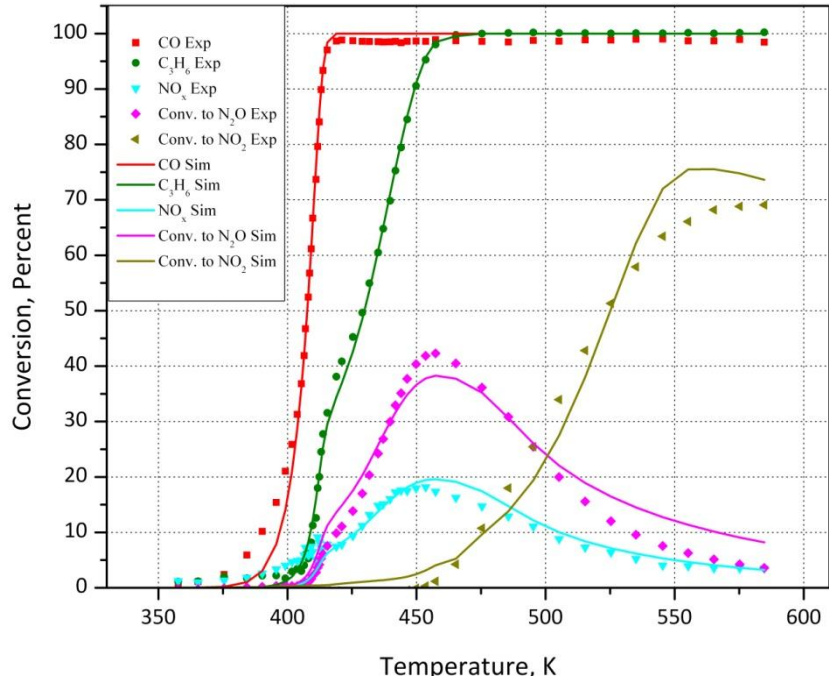


Figure 5-164: Individual optimization result vs. Experimental data, Run 53 New Model 5

It seems that the modified model, at least for single experiments, can predict the behaviour of the system reasonably well. The next step for validating this model is to apply it to several experiments at the same time, and see if we can have a good fit in this condition. Simultaneous optimization of experiments 38, 39 and 51 yielded the results shown in Table 5-56 and Figure 5-165 to Figure 5-167.

Table 5-56: Runs 38, 39 & 53 simultaneous optimization results, New Model 5

Parameter		LB	HB	Run 38	Run 39	Run 53
k ₁	A ₁	0	30	21.8		
	E ₁	20000	150000	107743		
k ₂	A ₂	0	30	22.2		
	E ₂	0	150000	86487		
k ₃	A ₃	0	30	16.5		
	E ₃	20000	150000	86954		
k ₄	A ₄	0	30	29.9		
	E ₄	0	150000	64623		
K ₅	B ₅	0	30	6.73		
	H ₅	-150000	0	-44814		
K ₆	B ₆	0	30	4.39		
	H ₆	-150000	0	-89642		
K ₇	B ₈	0	30	15.5		
	H ₈	-150000	0	-75610		
K ₈	B ₈	0	30	6.63		
	H ₈	-150000	0	-51685		
K ₉	B ₉	0	30	16.6		
	H ₉	-150000	150000	49836		
K ₁₀	B ₁₀	0	30	21.2		
	H ₁₀	-150000	0	-95706		
k ₁₁	A ₁₁	0	30	22.8		
	E ₁₁	0	150000	80123		
K ₁₂	B ₁₂	0	30	10.1		
	H ₁₂	-150000	150000	60755		
K ₁₃	B ₁₃	0	30	15.6		
	H ₁₃	-150000	150000	-16574		
Model 5	CO Residual			5.3	12	5.3
	C ₃ H ₆ Residual			4.3	13	5.1
	NO _x Residual			35	2.6	10
	N ₂ O Residual			26	11	10
	NO ₂ Residual			13	24	11
	Cumulative Residual			85	64	43

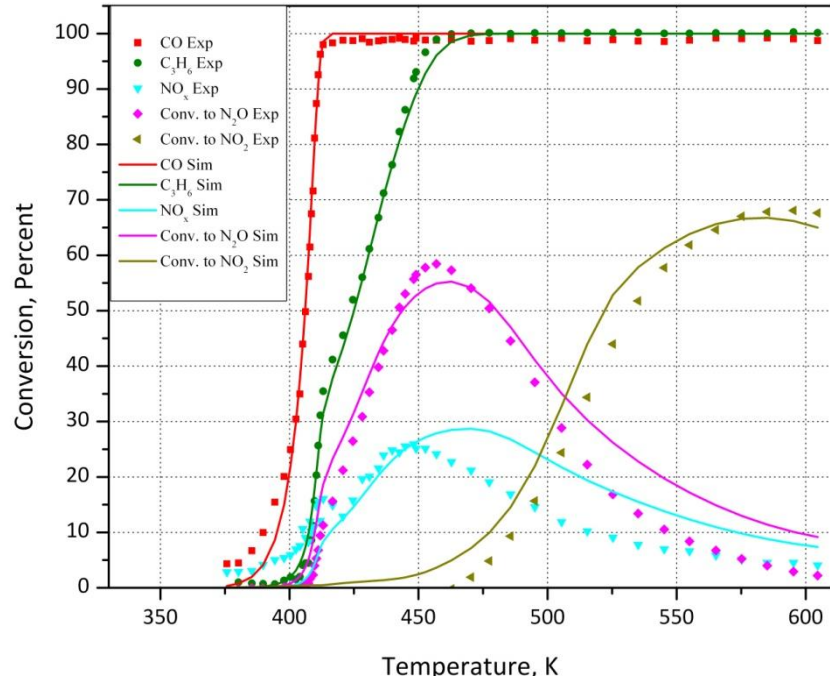


Figure 5-165: Simultaneous optimization result vs. Experimental data, Run 38, New Model 5

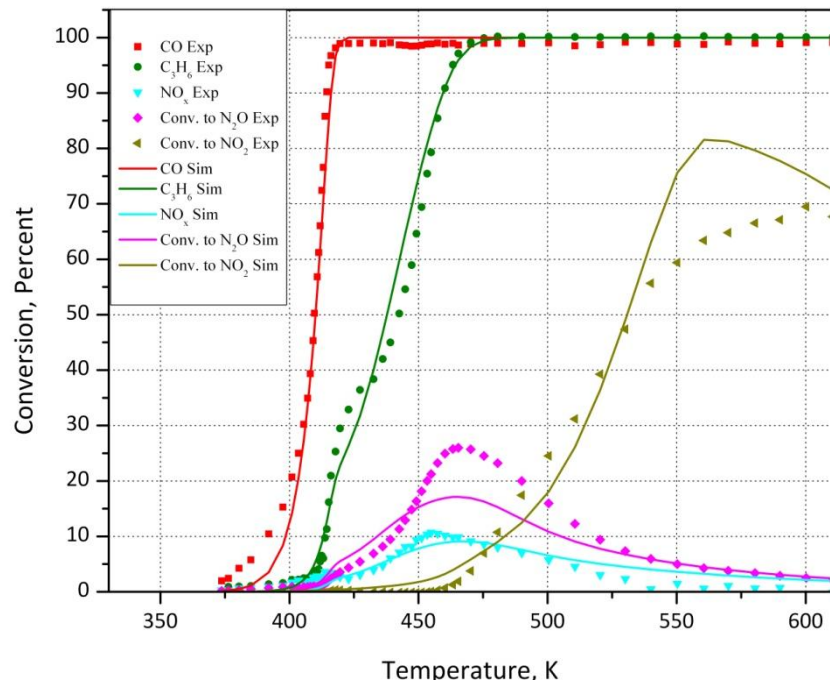


Figure 5-166: Simultaneous optimization result vs. Experimental data, Run 39, New Model 5

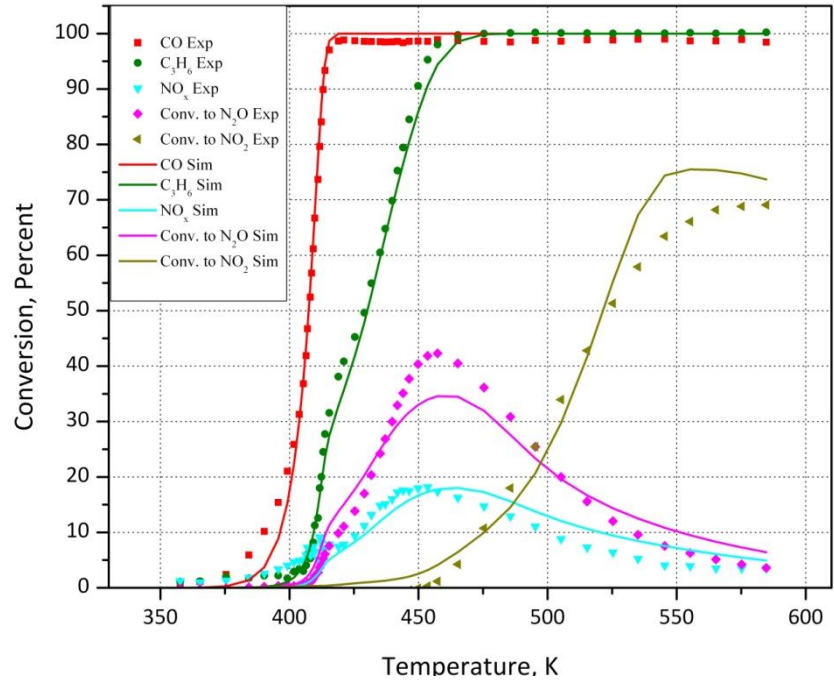


Figure 5-167: Simultaneous optimization result vs. Experimental data, Run 53, New Model 5

It is seen that at least for these three experiments, the new model is able to predict system behaviours reasonably well for multiple runs. We tried to use this set of parameters for other experiments but the results were not very good. So it seems that further investigation should be made into these models in order to find a global model which can be used in all these experiments successfully.

6 Conclusions and Future works

The Pt diesel oxidation catalyst kinetic model proposed by Sola was used as base to propose a global model which can simulate the results of the Pt-Pd diesel oxidation converters at various operating conditions. It was observed that this model could predict behaviours of the Pt-Pd system in simple cases, but for more complicated conditions like NO_x reduction with hydrocarbon, some modifications should be applied. Hydrocarbon adsorption inhibition and NO self poisoning effects were considered into modified models which improved the results a lot.

An interesting behaviour in hydrocarbon ignition curve has been detected in experiments which all three effective species (CO , NO & C_3H_6) were present. Effects of species concentration on sharpness of these deviations were surveyed. It was observed that the presence of CO was vital to see such behaviour.

We hypothesized that this deviation can be caused by switching between two different mechanisms for hydrocarbon oxidation. Based on this, we proposed a new model which could predict system behaviours in some cases but in other conditions, it did not work very well.

We suggest that, in future works, surface characterization experiments should be done to understand what is happening on the catalyst surface when CO is added to other species. Our knowledge about exact mechanism of hydrocarbon oxidation at presence of CO and NO_x is low so these experiments can help us understand mechanisms better and propose a better global model.

7 References

- [1] S. E. Voltz, C. R. Morgan, D. Liederman, and S. M. Jacob, "Kinetic Study of Carbon Monoxide and Propylene Oxidation on Platinum Catalysts," *Product R&D*, vol. 12, pp. 294-301, 1973/12/01 1973.
- [2] A. Pandya, J. Mmbaga, R. E. Hayes, W. Hauptmann, and M. Votsmeier, "Global Kinetic Model and Parameter Optimization for a Diesel Oxidation Catalyst," *Topics in Catalysis*, vol. 52, pp. 1929-1933, 2009/12/01 2009.
- [3] C. Sola Quiroz, "Kinetic Model for a Platinum Diesel Oxidation Catalyst," Master of Science, Department of Chemical and Materials Engineering, University of Alberta, Edmonton, AB, Canada, 2011.
- [4] G. J.C and F.-B. E., *Fuels and Engines: Technology, Energy, Environment*, , Technip ed. vol. 1. Paris, 1999.
- [5] J. Kaspar, P. Fornasiero, and N. Hickey, "Automotive catalytic converters: current status and some perspectives," *Catalysis Today*, vol. 77, pp. 419-449, Jan 2003.
- [6] G. o. Canada, "Regulatory Framework for Air Emissions," ed, 2007.
- [7] R. T. Park, "Air quality criteria for oxides of nitrogen.," US Environmental Protection Agency, NC1993.
- [8] R. T. Park, "Air quality criteria for ozone and related photochemical oxidants," US Environment Protection Agency, NC1995.
- [9] J. B. Heywood, "Motor Vehicle Emissions Control: Past Achievements, Future Prospects " in *Handbook of Air Pollution from Internal Combustion Engines: Pollutant Formation and Control* E. Sher, Ed., ed, 1998.
- [10] *Emission Standards (summary of worldwide emission standards)*. Available: <http://www.dieselnet.com/standards.html>
- [11] *Emission standards: Canada:On-road vehicles*. Available: <http://dieselnet.com/standards/ca/onroad.php>
- [12] R. Stone, *Introduction to Internal Combustion engines, Third Edition*: SAE publishing, 1999.
- [13] R. M. Heck, R. J. S. Farrauto, and S. T. Gulati, *Catalytic Air Pollution Control: Commercial Technology, 3rd edition*, 2009.
- [14] Tognum. Available: http://www.tognum.com/press/press-releases/presse-detail/news/mtu_showcases_future_engines_for_agricultural_machinery_at_agrit_echnica-1/news_smode/images/cHash/c8f20f13b7ae49c521bcddacc4f65e7f/

- [15] S. Henningsen, "Air Pollution from Large Two-Stroke Diesel Engines and Technologies to Control It " in *Handbook of Air Pollution from Internal Combustion Engines: Pollutant Formation and Control* E. Sher, Ed., ed, 1998.
- [16] M. Iwamoto and H. Hamada, "REMOVAL OF NITROGEN MONOXIDE FROM EXHAUST GASES THROUGH NOVEL CATALYTIC PROCESSES," *Catalysis Today*, vol. 10, pp. 57-71, Aug 1991.
- [17] Y. J. Li, P. J. Battavio, and J. N. Armor, "Effect of Water Vapor on the Selective Reduction of NO by Methane over Cobalt-Exchanged ZSM-5," *Journal of Catalysis*, vol. 142, pp. 561-571, 8// 1993.
- [18] J. N. Armor, "CATALYTIC REMOVAL OF NITROGEN-OXIDES - WHERE ARE THE OPPORTUNITIES," *Catalysis Today*, vol. 26, pp. 99-105, Nov 1995.
- [19] W. A. Majewski and M. K. Khair, *Diesel Emissions and Their Control*: SAE International, 2006.
- [20] M. S. Brogan, A. D. Clark, and R. J. Brisley, "Recent Progress in NO_x Trap Technology," 1998.
- [21] S. Erkkfeldt, M. Larsson, H. Hedblom, and M. Skoglundh, "Sulphur Poisoning and Regeneration of NO_x Trap Catalyst for Direct Injected Gasoline Engines," 1999.
- [22] A. Russell and W. S. Epling, "Diesel Oxidation Catalysts," *Catalysis Reviews- Science and Engineering*, vol. 53, pp. 337-423, 2011.
- [23] R. H. Heck, J. Wei, and J. R. Katzer, "MATHEMATICAL-MODELING OF MONOLITHIC CATALYSTS," *Aiche Journal*, vol. 22, pp. 477-484, 1976.
- [24] L. C. Young and B. A. Finlayson, " Mathematical models of the monolith catalytic converter: Part II. Application to automobile exhaust," *AICHE journal* vol. 22, pp. 343–353, 1976.
- [25] G. P. Ansell, P. S. Bennett, J. P. Cox, J. C. Frost, P. G. Gray, A. M. Jones, *et al.*, "The development of a model capable of predicting diesel lean NO_x catalyst performance under transient conditions," *Applied Catalysis B: Environmental*, vol. 10, pp. 183-201, 9/14/ 1996.
- [26] *fmincon* - *MathWorks*. Available:
<http://www.mathworks.com/help/optim/ug/fmincon.html>
- [27] *Genetic Algorithm* – *MATLAB*. Available:
<http://www.mathworks.com/discovery/genetic-algorithm.html>
- [28] R. Burch and T. C. Watling, "Kinetics of the reduction of NO by C₃H₆ and C₃H₈ over Pt based catalysts under lean-burn conditions," in *Studies in Surface*

- Science and Catalysis*. vol. Volume 116, A. F. a. J. M. B. N. Kruse, Ed., ed: Elsevier, 1998, pp. 199-211.
- [29] R. Burch, P. Fornasiero, and B. W. L. Southward, "An Investigation into the Reactivity, Deactivation, and in Situ Regeneration of Pt-Based Catalysts for the Selective Reduction of NO_x under Lean Burn Conditions," *Journal of Catalysis*, vol. 182, pp. 234-243, 2/15/ 1999.
- [30] J. A. Sullivan, R. Burch, and A. A. Shestov, "Transient Techniques in the Study of Lean-NO_x Reduction Over Supported Pt Catalysts," *Chemical Engineering Research and Design*, vol. 78, pp. 947-953, 10// 2000.
- [31] P. Denton, A. Giroir-Fendler, Y. Schuurman, H. Praliaud, C. Mirodatos, and M. Primet, "A redox pathway for selective NO_x reduction: stationary and transient experiments performed on a supported Pt catalyst," *Applied Catalysis A: General*, vol. 220, pp. 141-152, 10/25/ 2001.
- [32] P. Granger, J. P. Dacquin, F. Dhainaut, and C. Dujardin, "Chapter 10 The formation of N₂O during sNO_x conversion: fundamental approach and practical developments," in *Studies in Surface Science and Catalysis*. vol. Volume 171, P. G. a. V. I. Pârvulescu, Ed., ed: Elsevier, 2007, pp. 291-324.
- [33] R. Burch and T. C. Watling, "The difference between alkanes and alkenes in the reduction of NO by hydrocarbons over Pt catalysts under lean-burn conditions," *Catalysis Letters*, vol. 43, pp. 19-23, 1997/01/01 1997.
- [34] R. Burch and P. J. Millington, "Selective reduction of NO_x by hydrocarbons in excess oxygen by alumina- and silica-supported catalysts," *Catalysis Today*, vol. 29, pp. 37-42, 5/31/ 1996.